BROADBAND PIN DIODE SWITCHING AND PHASE SHIFTING

Desmond Hirson

A dissertation submitted to the Faculty of Engineering, University of Cape Town, in fulfilment of the requirements for the degree of Master of Science in Engineering.

Cape Town, 1986.

DECLARATION

I declare that this dissertation is my own, unaided work. It is being submitted for the degree of Master of Science in Engineering, at the University of Cape Town. It has not been submitted before for any degree or examination at any other University.

Signed

(Signature of candidate)

28th day of February 1986

ABSTRACT

Investigation into the limitations on the bandwidth of PIN diode switches in their different configurations is performed. The Single Pole Double Throw switch constructed with shunt mounted PIN diodes is shown to be bandlimited due to the line lengths involved in the operation. Series mounted diode switches have a wider bandwidth but the diodes cannot perform as power devices due to their physical construction. Radiation due to discontinuities were found to degrade the isolation but this was overcome by an evanescent waveguide structure.

The software program TOUCHSTONE (TM)/RF by EEsof is used extensively as a basic development tool. The characterisation of the PIN diodes which was used by the software, was carried out. A bias network had to be developed to allow for the biasing of the diodes before any test boards could be fabricated.

A literature survey was done on the different types of phase shifters available. A circuit which enables shifts in 45 degree increments was developed. The system consists of Reflection Phase Shifters which are made up of Quadrature Couplers that have different terminations switched in on two of their ports, a Wilkinson power splitter and a power combiner in the form of a 3 dB Quadrature Coupler. It was found that this configuration works well in theory but is too demanding on the practical components to allow for low phase shift errors to occur.

ACKNOWLEDGEMENT

The author wishes to express his gratitude to his supervisor Prof. B J Downing for his constant encouragement and guidance.

The work completed in this dissertation would not have been possible without the financial support and assistance of the Council for Scientific and Industrial Research. Thanks are especially due to Mr Johan Pretorius for his assistance and the supply of most of the hardware.

Thanks must also be extended to the following postgraduate students of the microwave laboratory; A.D. Hall, N.C. Martin, D.M. Rachman and T. Waardenburg.

Finally, the author's sincere thanks must go to Mrs Judith Wilson, for her careful typing of this manuscript.

CONTENTS

		Page
DECLARATION		ii
ABSTRACT		iii
ACKNOWLEDGEMENTS		iv
CONTENTS		v
LIST OF FIGURES		ix
LIST OF TABLES		xv
LIST OF SYMBOLS		xvi
1	INTRODUCTION	1
	1.1 Objectives	2
	1.2 The software program TOUCHSTONE TM/RF	2
	1.3 The test equipment that was used	3
2	THEORY	5
	2.1 Microwave circuit technology	6
	2.1.1 Waveguide	6
	2.1.2 Coaxial Line	8
	2.1.3 Microstrip	9
	2.1.4 Stripline	13
	2.2 Coupled Transmission Lines	14
	2.2.1 Coupled Transmission Line Characteristics	14
	2.2.2 The phase relationship of quad. couplers	16
	2.3 The Quadrature Coupler	18
3	BIAS NETWORKS	20
	3.1 Radial Stub	20
	3.2 High Impedance Low Impedance sections used in Bias Networks	23
	3.3 Bias networks using Elliptic Filters	25
	3.4 Pads that were tested as Bias Networks	30
	3.5 Ferrite cores used in Bias Lines	31
	3.6 Conclusions	33

CONTENTS (continued)

		Page
4	THE PIN DIODE	35
	4.1 PIN diode structures	36
	4.2 Transient Properties	39
	4.3 Power Handling	40
	4.4 Package Parasitics	40
	4.5 The HP3141 shunt mounted PIN diode	42
	4.6 The Beam Lead series mounted PIN diode	47
	4.7 Discussion	48
5	THE SINGLE POLE SWITCH USING SHUNT MOUNTED DIODES	49
	5.1 The first SPDT switch fabricated	51
	5.2 Development of the SPDT switch with the use of stub matching	54
	5.2.1 The design process that was followed	55
	5.3 The second SPDT switch fabricated	57
	5.4 The third SPDT switch fabricated	60
	5.5 The Single Pole Four Throw (SP4T) switch constructed with shunt PIN diodes	62
6	THE SINGLE POLE SWITCH USING SERIES MOUNTED DIODES	65
	6.1 Discussion	67
7	ISOLATION	68
	7.1 The investigation of the different diode combinations	68
	7.2 The SP4T switch that was built using series and shunt mounted PIN diodes	73
	7.3 The SP4T switch using three diodes in each branch	75
	7.3.1 Tests and discussion of the series mounted PIN diode switch	76
	7.4 The investigation of the isolation problem	79
	7.5 The microstrip circuit enclosed in a waveguide	81
	7.6 The SP4T switch enclosed in a waveguide	83
	7.7 Analysis of the results obtained	86

CONTENTS (continued)

		Page
8	PHASE SHIFTERS	89
	8.1 Switched-Line Phase Shifters	89
	8.1.1 The SPDT switch	91
	8.2 Loaded-Line Phase Shifters	93
	8.3 High-Pass Low-Pass Phase Shifters	96
	8.4 Reflection Phase Shifters	96
	8.5 The hybrid Coupler Phase-Shifter Circuit	98
	8.6 Discussion	102
9	THE PHASE SHIFTER CONSISTING OF REFLECTION PHASE SHIFTERS AND A POWER SPLITTER	104
	9.1 The Power Splitter	104
	9.2 The simulation of the Phase Shifter on TOUCHSTONE	106
	9.3 The realization of the Phase Shifter	108
	9.4 The investigation of a Single Section Overlay Coupler	113
	9.4.1 The single section Overlay coupler	116
	9.5 The Lange Coupler	118
	9.6 The investigation of the different parameters which effect the phase error	121
	9.6.1 Isolation	121
	9.6.2 Return loss of the terminated ports	123
	9.7 PIN diode switches for switching in the open circuit short circuit and 50 ohm matched load	124
	9.8 The effect of the imperfect components on the overall phase shifter	133
	9.9 Conclusion	136
10	CONCLUSION	137

CONTENTS (continued)

		Page
APPENDIX A :	Computer Programs	139
APPENDIX B :	Specifications and Characteristics of components	162
APPENDIX C :	Single Pole Double Throw Switch microstrip layouts and Microwave Capacitors	176
APPENDIX D :	Specifications and Measurements of the Enclosed SP4T Switch	184
APPENDIX E :	Specifications for the Overlay Couplers	189
APPENDIX F :	S-Parameter Measurements of the CSIR's Lange Coupler and the Termination Switch	192
REFERENCES		197
BIBLIOGRAPHY		200

LIST OF FIGURES

Figure		Page
1.1	The Test Equipment	3
1.2	The HP11608A Transistor test fixture	4
2.1	Variation of field components and field configurations for TE_{10} and TE_{20} modes in a hollow rectangular waveguide.	7
2.2	A coaxial line	8
2.3	The general geometry of a microstrip line	9
2.4	Changes in the distribution of the electric field as the thickness of the microstrip is altered	11
2.5	Cross-Section of shielded microstrip	12
2.6	A Stripline	13
2.7	Two parallel-coupled transmission lines	14
2.8	Schematic diagram of the directional coupler indicating the major parameters	16
2.9	The phase shift paths of the quadrature coupler	17
2.10	Cross-section dimensions of broadside-coupled strips parallel to the ground planes.	18
3.1	Required response for a bias network	20
3.2	The Radial Stub as a bias network	21
3.3	A semi-circular cavity resonator	21
3.4	The measured response of the radial stub circuits which were fabricated	22
3.5	A Microstrip circuit of High Impedance Low Impedance Sections	23
3.6	Microstrip circuit of broadened High Impedance Low Impedance Sections	24
3.7	Response using a) ideal transmission lines b) microstrip lines for the circuit shown in figure 3.6	24
3.8	Geometry of two types of filter elements with their equivalent circuit	25

LIST OF FIGURES (continued)

Figure		Page
3.9	The equivalent circuit that was programmed on SPICE	26
3.10	The response of the filter predicted by the SPICE program	28
3.11	Microstrip layouts with their accompanying predicted response	29
3.12	Theoretical and measured response of a square pad	30
3.13	Results of tests done with wire and ferrite beads	32
3.14	The bias system consisting of a capacitor and a short length of wire	33
3.15	Results of the capacitor and wire biasing system	34
4.1	The doping profile and electric field profile of a PIN diode	35
4.2	Passivated Mesa constructed PIN diode	36
4.3	Planar constructed PIN diode	37
4.4	Beam-lead constructed PIN diode	37
4.5	The equivalent circuit for a packaged PIN diode	38
4.6	Switching Transient of a PIN diode	39
4.7	Equivalent circuit ofa packaged PIN diode with external tuning.	41
4.8	An alternate theoretical model for the PIN diode	42
4.9	Phase response generated with a short and reference plane extension of 28.35 mm	43
4.10	Isolation versus bias current on the HP 3141 PIN diode	44
4.11	Insertion loss for the reverse biased HP 3141 PIN diode	45
4.12	The effect of moving the reference plane on the impedance	46
4.13	The Theoretical equivalent circuit of the HP 3141 PIN diode	47

LIST OF FIGURES (continued)

Figure		Page
5.1	A transmission line layout of the SPDT switch	49
5.2	The response of a broadbanded SPDT switch	49
5.3	The microstrip layout of the SPDT switch	50
5.4	The theoretical response of a Single Pole Three Throw switch using Shunt mounted diodes	50
5.5	The comparison of the measured and predicted SPDT switch with ideal components	51
5.6	The SPDT switch with ideal components and DC blocking capacitors	52
5.7	The SPDT switch with one forward biased PIN diode and no capacitors	53
5.8	The SPDT switch with one reverse biased PIN diode and a physical short	53
5.9	Responses obtained using different Stub matching configurations in the SPDT switch	56
5.10	The optimized SPDT microstrip circuit	57
5.11	The microstrip layout of the second SPDT switch	57
5.12	The measured response of the second SPDT switch using shunt mounted diodes	59
5.13	The theoretical response of the third SPDT switch	60
5.14	The layout of the third SPDT switch	61
5.15	The measured response of the third SPDT switch	61
5.16	The theoretical response of the SP4T switch	62
5.17	The microstrip layout of the SP4T switch	63
5.18	The measured response of the SP4T switch	63
6.1	The microstrip layout of the SP4T switch using series mounted diodes	65
6.2	The theoretical response of the SP4T switch using series mounted diodes	65
6.3	The measured response of the SP4T switch containing series mounted diodes	66

LIST OF FIGURES (continued)

Figure		Page
7.1	Isolation of two shunt mounted diodes	68
7.2	Series and shunt mounted diodes situated on a transmission line with a certain distance of separation	69
7.3	Two low impedances situated $\lambda/4$ apart on a transmission line	70
7.4	Response of the SP4T switch which consists of series mounted and shunt mounted diodes	72
7.5	Response of the SP4T switch which consists of two series mounted diodes in each branch	73
7.6	The SP4T switch that was fabricated using series and shunt mounted PIN diodes	73
7.7	The measured response of the SP4T switch containing series and shunt mounted PIN diodes	74
7.8	The theoretical response of the SP4T switch containing three diodes in each branch.	75
7.9	Microstrip layout for testing isolation of series mounted PIN diodes	76
7.10	The measured response of one, two and three diodes in a SPST switch	77
7.11	The isolation of the SPST switch without any bias circuitry	78
7.12	Tests carried out with the high dielectric board	80
7.13	Electric field distribution around a slot cut into a microstrip transmission line	80
7.14	The microstrip enclosed in waveguide	81
7.15	The microstrip circuit with and without the waveguide cover	82
7.16	The maximum measurable isolation	83
7.17	The SP4T switch built with waveguide system	84
7.18	The final measurements of the SP4T switch	85
7.19	The loss measured on a short circuited path of a SP4T switch	86

LIST OF FIGURES (continued)

Figure		Page
7.20	The effect of the bias current on insertion loss	87
8.1	Basic configuration of the Switched Line Phase Shifter	89
8.2	A network and the curves of the phase response (from reference [22])	90
8.3	A viable Shiffman phase shifter with the response (from reference [22])	91
8.4	a) The basic circuit b) An equivalent circuit c) One method of avoiding resonance problems	92
8.5	Loaded-Line phase shifters	94
8.6	Fractional bandwidth of the phase shifter using single lumped switched susceptances	95
8.7	Practical layout of a Low-Pass High-Pass phase shifter (from reference [21])	96
8.8	A reflection Phase Shifter with a shunt diode and a short length of transmission line	97
8.9	Terminated hybrid coupler for reflection phase shifting	97
8.10	Schematic diagram of the phase shifter which utilizes a Power Splitter and Reflection Phase Shifters.	99
8.11	The phase shifts which result in the 135 degree phase shift.	101
8.12	The phase shifts with the corresponding terminations applied to the couplers	102
9.1	The Power Splitter	104
9.2	The response of the Power Splitter	105
9.3	The influence of the Even and Odd Mode Impedances	107
9.4	The layout of the Phase Shifter that was fabricated	110
9.5	Measurements taken on D M Rachman's Overlay Coupler	112
9.6	The theoretical characteristics of the Single Section Overlay Coupler	115

LIST OF FIGURES (continued)

Figure		Page
9.7	The measured response of the Single Section Coupler	116
9.8	The Phase shift paths of an ideal coupler with the addition of the Isolation path	121
9.9	The effect of Isolation on the Open circuit and short circuit conditions	122
9.10	A simple switch configuration	124
9.11	The microstrip layout of the switch	126
9.12	The effect of increasing the distance between an open circuit and a bias line	127
9.13	The response of the 47 ohm resistor	127
9.14	Different switch configurations that were analysed	128
9.15	The Termination switch	129
9.16	The phase display of the open circuit and short circuit conditions	130
9.17	The Termination switch with two diodes connected directly to ground	130
9.18	Return loss for the two impedance states for the circuit shown in figure 9.17	131
9.19	The phase shift using the measured parameters of the termination switch	132
9.20	The phase shift using ideal terminations and a slightly improved Lange Coupler	133
9.21	The phase shifter using the real terminations and a slightly improved Lange Coupler	135

LIST OF TABLES

Table		Page
1	Resultant Phases for different terminations on a quadrature coupler	17
2	Conditions of the diodes for the different phase shifts	100
3	Phase Shift for D M Rachman's Overlay Coupler	113
4	Phase Shift for the Single Section Overlay Coupler	117
5	Phase Shift for the Lange Coupler	119
6 (a)	Phase Shift with the isolation angle set at zero degrees	123
6 (b)	Phase Shift with the isolation angle set at 90 degrees	123
7	Resulting terminations for the different diode conditions	125
8	The resulting terminations for the different bias voltage polarity	129
9	The phase difference between the open circuit and short circuit conditions	131
10	The phase difference between the open circuit and short circuit terminated coupler	134

LIST OF SYMBOLS

SPST	Single Pole Single Throw
SPDT	Single Pole Double Throw
SP4T	Single Pole Four Throw
Z_{IN}	Input Impedance to a transmission line
Z_o	Characteristic Impedance of a transmission line
Z_L	Load Impedance which terminates a transmission line
β	Phase-change coefficient in degrees or radians per metre
τ	Voltage reflection coefficient
SWR	Standing-wave ratio
F	Frequency
ε_{eff}	Effective microstrip permittivity
fc	Cutt-off frequency for waveguide
λ_o	Free-space wavelength
λ_{oc}	Cutoff wavelength for rectangular waveguide
Zoe	Even Mode Impedance in coupled lines
Zoo	Odd Mode Impedance in coupled lines
TEM	Tranverse Electric and Magnetic Field
TE	Transverse Electric Field
TM	Tranverse Magnetic Field
μ	Permeability
ε	Permittivity
ε_r	Relative permittivity
ρ	Reflection Coefficient
ϕ	Phase shift

1. INTRODUCTION

Extensive research and development of microwave integrated circuits (MIC's) using hard substates (Alumina) and soft substrates (RT DUROID and 3M) have been undertaken in recent years. Solid state microwave amplifiers and oscillators have appeared in the market place using MIC technology and other peripheral components and subsystems have to be compatible to allow this technology to be fully utilized. This thesis involves the development of Single Pole Multiple Throw switches and Phase Shifters which make use of the PIN diode. Development is carried out on microstrip and stripline softboard.

A large portion of the development process was done with the aid of the software package TOUCHSTONE TM/RF by EEsof. Certain techniques had to be developed to get the most from the software.

A switch can connect in one of any number of paths depending on the application. These switches can be developed using shunt or series mounted PIN diodes in different configurations all of which determines the frequency bandwidth.

The two principle means of providing electronic control of the phase of a microwave signal are realized by the diode and by the ferrite phase shifters [1]. Both of these circuit approaches have undergone extensive development since about 1960 when the major interest in electronically controlled phased array antennas began.

Phase shifting is also used in serrodyne techniques which are used in frequency shifting in microwave relay systems, electrical scanning of antennas, and doppler simulation for testing doppler radars [2]. The serrodyne frequency translation is theoretically obtained by a continuous phase modulation. It is possible to show that a continuously phase-modulated device can be replaced by a device that introduces quantized phase shifts.

In this dissertation the diode phase shifter in particular has been investigated. A unique method of phase shifting in 45° steps using hybrid couplers and PIN diodes is developed.

1.1 Objectives

The purpose of this study is twofold. Firstly to investigate circuit configurations which are suitable for wide band operation. A design technique is described which would enable the easy and reliable construction of any number of throws to be fabricated.

The specifications of more than 60dB of isolation on a switched off path and an insertion loss of less than 3dB for a transmit path in a four throw switch over a bandwidth of 2 GHz to 6 GHz was initially set.

Secondly, to design a phase shifter that switches in 45 degree steps depending on bias conditions of PIN diodes. The operating frequency is also from 2 GHz to 6 GHz.

1.2 The software program TOUCHSTONE (TM)

A brief overview of this software package is given.

The circuit file (as shown in Appendix A) is used to describe a circuit and specify the parameters to be measured. The following elements are available to use in the CKT blocks; active elements, device models, distributed elements, impedance converters, lumped passive components, s-parameters, special purpose elements and unilateral elements. TOUCHSTONE processes a circuit file when a frequency sweep is instituted or the circuit is tuned or optimization is performed.

The Tuner is a tool used to change parameter values of circuit elements which then allows another frequency sweep to be carried out. The new response is then overlayed on the previous response. The sensitivity of a single parameter can easily be seen as well as fine tuning of the overall response.

The Optimizer uses random exploration techniques to search for a global minimum of the error function. Only the selected parameters are optimized and it is always best to declare limits on the parameter values.

S-parameter files are used by TOUCHSTONE to obtain data for the circuit elements. These files contain values that are either measured or computed.

1.3 The test equipment that was used

The HP8410C Network Analyser, the HP8746B S-Parameter test set and the HP8350B sweep oscillator was used to analyze all the circuits built. The results could either be observed on a polar display or a linear frequency versus gain display.

An HP85 micro computer in conjunction with a HP11713A Attenuator/ switch driver and a HP59313A A/D converter was used to drive the system. A photograph of the complete test set up is shown in figure 1.1.

Figure 1.1 The test equipment

The HP 85 had an Accuracy Enhancement program which allowed print-outs to be obtained of the measurements. This program was also modified slightly to calculate the impedance of the circuit being measured at each frequency. It was found that the reference plane extension plays an important role in the accuracy of the results. There are two methods for adjusting the reference plane;

i) The physical adjustment on the S-parameter test set
ii) A software adjustment in the Accuracy Enhancement package.

The HP11608A transistor test fixture as shown in figure 1.2 is connected onto the ports of the S-parameter test set to facilitate the characterization of devices. The parameters measured can then be used by TOUCHSTONE.

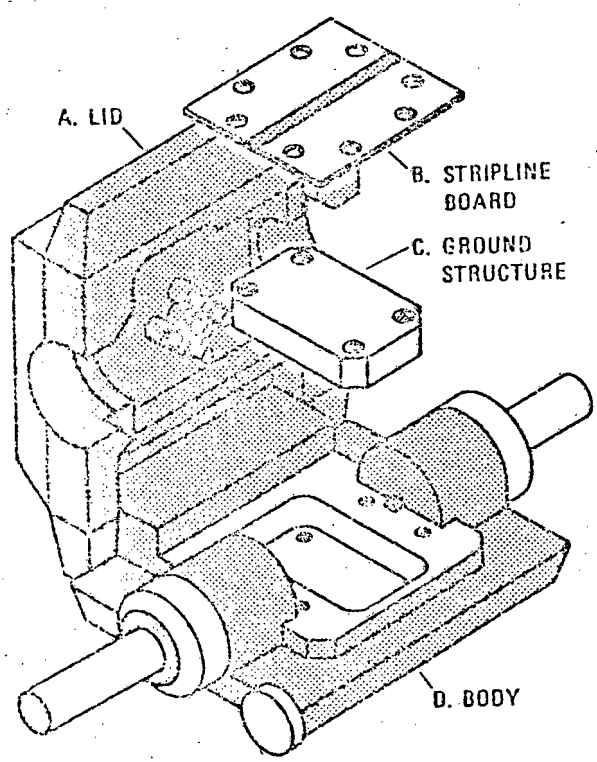

Figure 1.2 The HP11608A transistor test fixture

The stripline board and ground structure is machined and modified to allow the device to fit exactly into place. For active devices the biasing is applied through the biasing ports of the S-parameter test set. It is important that the reference plane is set at the terminals of the device for an accurate S-parameter representation.

2. THEORY

Once operating frequencies reach 1 GHz and above, the wavelength becomes comparable with lengths of connecting wires and strips and the use of lumped elements become expensive. As a result distributed circuits are more commonly used. It is therefore important to understand basic transmission line theory.

A transmission line may be defined as a device for transmitting or guiding energy from one point to another. [3] Transmission lines transmit energy in one of two main field configurations or modes. These are, the transverse electromagnetic (TEM) mode where both the electric and magnetic fields are entirely transverse to the direction of propagation, and higher-order modes where at least one field component is in the direction of transmission.

The input impedance to a transmission line varies with the distance progressed along the line. If the line is considered loss-free, which is valid if the line lengths are physically short, the following expression results;

$$Z_{IN} = Z_0 \left(\frac{Z_L + j\, Z_0 \tan B\ell}{Z_0 + j\, Z_L \tan B\ell} \right) \qquad (2.1)$$

where ℓ = length of line

$B = 2\pi/\lambda$

The input impedances for lines having short-circuited or open-circuited terminations follow from equation 2.1. By choosing different lengths of transmission lines either open-circuited or short-circuited inductive of capacitive circuit elements are realized which can readily be used in resonators, filters and matching networks.

It must be noted that these elements are dependant on B which in turn is dependant on frequency. For a short circuited quarter-wavelength line the standing wave has a voltage maximum which corresponds to an open circuit condition. Thus the short circuit is transformed to an open circuit. Consider the case when the operating frequency doubles. The quarter-wave length line now becomes a half wavelength line which means that the short circuit now is transferred to the point that was previously the open circuit. Only when the load impedance is equal to the characteristic impedance is there a match which is independant of frequency. This is important when broad-band work is undertaken.

Except in perfectly matched conditions the load termination reflects some of the energy sent down the line. Interference between the incident and reflected waves travelling at the same velocity but in opposite directions causes a Standing Wave field pattern to be set up. The ratio of reflected to incident voltage at the load is given by;

Voltage reflection coefficient:

$$\tau = \frac{Z_L - Z_0}{Z_L + Z_0} \qquad (2.2)$$

The ratio of maximum to minimum amplitude of the standing wave is given by;

$$\text{Voltage standing wave ratio} = \frac{1 + |\tau|}{1 - |\tau|} \qquad (2.3)$$

The basic transmission line can be implemented in various different physical constructions [4] p 19. Only the ones that are used will be further discussed.

2.1 Microwave circuit technology

2.1.1 Waveguide

Waveguide has been the traditional means of transporting microwave energy. From the Boundary conditions derived from Maxwells equations the electric field tangential to a perfect conductor must be zero [3] p 338. This leads to the field distribution as shown in Figure 2.1.

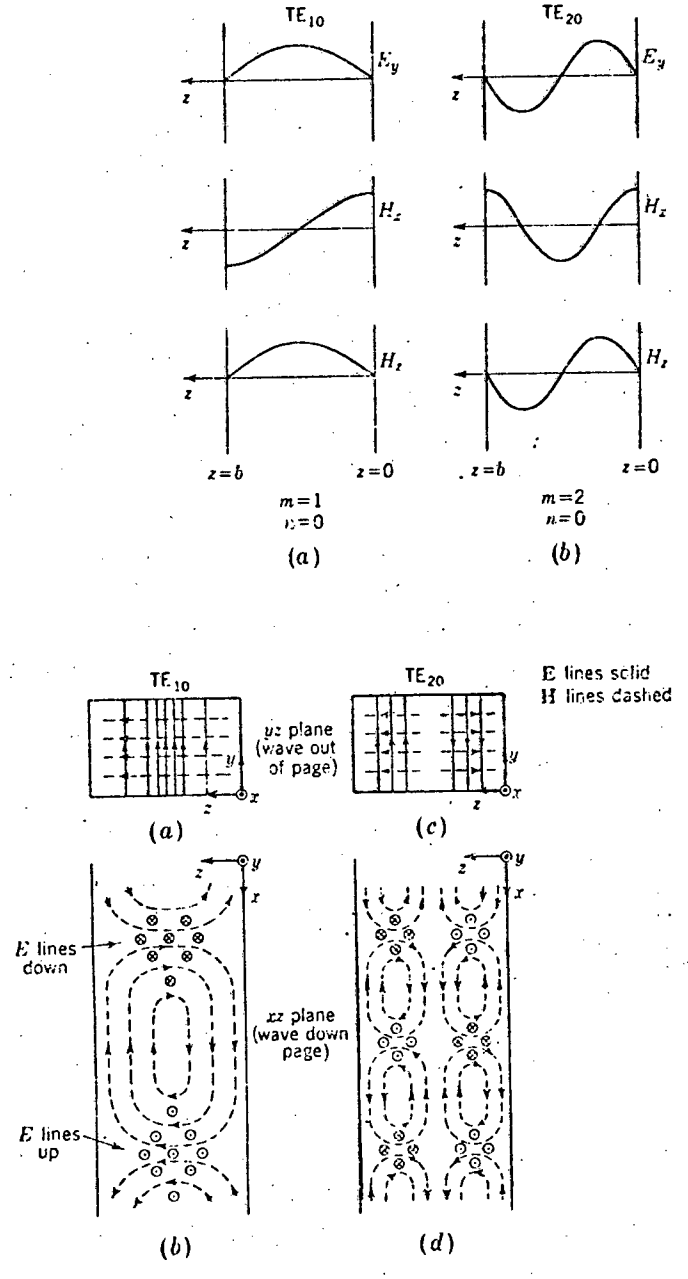

Figure 2.1 Variation of field components and field configurations for TE_{10} and TE_{20} modes in a hollow rectangular waveguide

The simplist mode is the TE_{10} which has the lowest cut off frequency given by equation 2.4:

$$\text{For } TE_{mn}: \quad fc = \frac{1}{2\sqrt{\mu\varepsilon}} \sqrt{\left(\frac{n}{Y_1}\right)^2 + \left(\frac{m}{Z_1}\right)^2} \qquad (2.4)$$

For frequencies below cutoff waves are not transmitted but are attenuated [3] p 561. The attenuation constant for a rectangular guide at frequencies below cut off is given by the equation below;

$$X = \sqrt{\left(\frac{n\pi}{Y}\right)^2 + \left(\frac{m\pi}{Z}\right)^2 - \left(\frac{2\pi}{\lambda_o}\right)^2} \quad \text{Np m}^{-1}$$

Alternatively

$$X = \frac{54.6}{\lambda_{oc}} \quad \text{dBm}^{-1}$$

2.1.2 Coaxial Line

The dominant mode of propagation in a coaxial transmission line as shown in figure 2.2 is the transverse electro-magnetic (TEM) mode. [5] page 49.

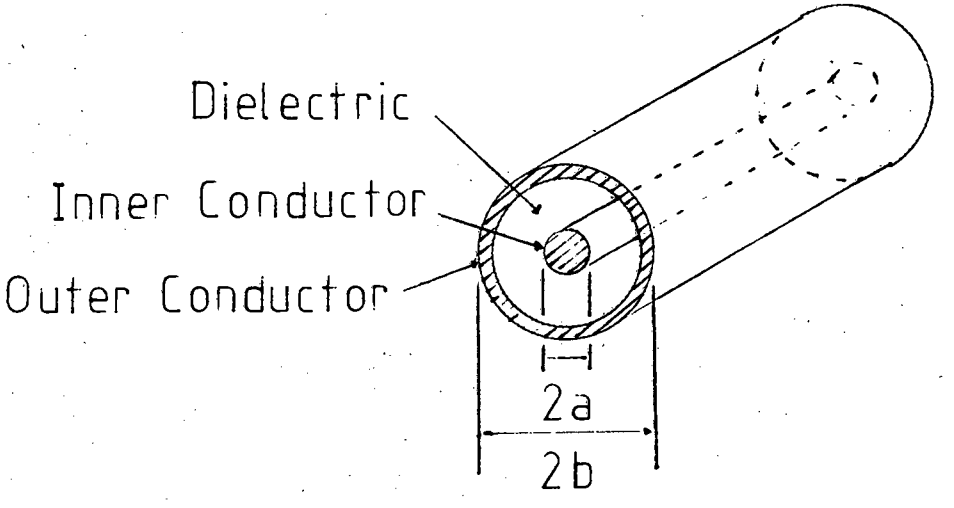

Figure 2.2 A coaxial line

For any lossless TEM mode structure the characteristic impedance is given by the following equation;

$$Z_o = \sqrt{L / C}$$

Where L and C denote the inductance and the capacitance per unit length of the structure and are defined in the following equations;

$$C = 2\pi\epsilon / \ell n\ (b/a)$$

and

$$L = \frac{\mu}{2\pi} \ell n\ (b/a)$$

Where ϵ and μ are the permittivity and the permeability of the dielectric medium. The cut-off wavelength of the lowest order TE_{01} mode of propagation is given by;

$$\lambda \approx 2\pi \left(\frac{b + a}{2}\right)$$

2.1.3 Microstrip

A microstrip transmission line as shown in figure 2.3 operates in a quasi - TEM mode because the conducting strip is not surrounded by a uniform dielectric.

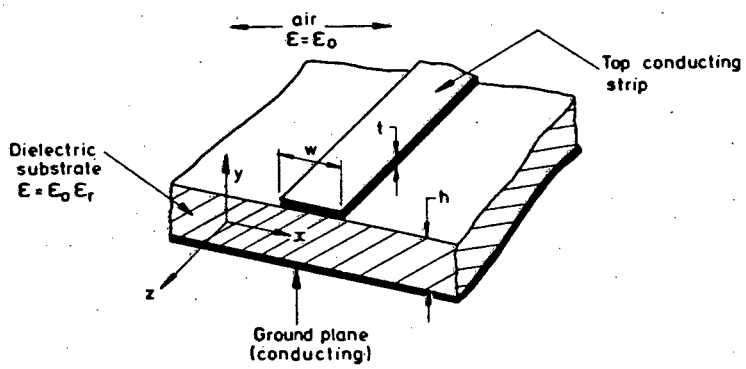

Figure 2.3 The general geometry of a microstrip line

The width of a microstrip line is principally a function of its characteristic impedance and the thickness of the substrate.

Some of the particularly useful characteristics of microstrip include the following: [4]

1) DC as well as AC signals may be transmitted.
2) Active devices, diodes and transistors may readily be incorporated (shunt connections are also possible).
3) In-circuit characterizations of devices is straightforward to implement.
4) Line wavelength is reduced considerably from its free space value, which leads to smaller circuits.
5) The structure is fairly rugged and can withstand moderately high voltages and power levels.

The following closed formulae were used to determine the width of the conducting strip when the dielectric constant and height of the dielectric are given.

For narrow strips $\left(Z_o > (44 - 2\varepsilon_r)\right)$

$$\frac{w}{h} = \left(\frac{\exp H'}{8} - \frac{1}{4\exp H'}\right)^{-1}$$

Where $$H' = \frac{Z_o\sqrt{2(\varepsilon_r + 1)}}{119.9} + \frac{1}{2}\left(\frac{\varepsilon_r - 1}{\varepsilon_r + 1}\right)\left(\ell n\frac{\pi}{2} + \frac{1}{\varepsilon_r}\ell n\frac{4}{\pi}\right)$$

For $Z_o < (44-2\varepsilon_r)$

$$\frac{w}{h} = \frac{z}{\pi}\left((d_\varepsilon - 1) - \ell n\,(2d - 1)\right) + \frac{\varepsilon_r - 1}{\pi\varepsilon_r}\left(\ell n\,(d - 1) + 0.293 - \frac{0.517}{\varepsilon_r}\right)$$

Where $$d = \frac{59.95\,\pi^2}{Z_o\sqrt{\varepsilon_r}}$$

With the formulae used accuracies of $\pm$ 1 per cent can be expected.

The wavelength at a given frequency on the microstrip is given by:

$$\lambda_g = \frac{300}{F\sqrt{eff}} \quad mm$$

Where

$$\varepsilon_{eff} = \frac{\varepsilon_r + 1}{2}\left(1 + \frac{29.98}{Z_o}\left(\frac{2}{\varepsilon_r+1}\right)^{\frac{1}{2}}\left(\frac{\varepsilon_r-1}{\varepsilon_r+1}\right)\left(\ell n\ \frac{\pi}{2} + \frac{1}{\varepsilon_r}\ \ell n\frac{4}{\pi}\right)\right)^2$$

For $Z_o > (63 - 2\varepsilon_r)$

$$\varepsilon_{eff} = \frac{\varepsilon_r}{0.96 + \varepsilon_r\ (0.109 - 0{,}004\ \varepsilon_r)\ (l_{o_g}\ (10 + Z_o) - 1)} \quad \text{For } Z_o < (63-2\ \varepsilon_r)$$

Accuracies of 0.5 per cent can be expected.

The literature shows [4] p 57 that the thickness of the conducting strip may be significant in that it influences the field distribution as shown in figure 2.4 which modifies the characteristic impedance.

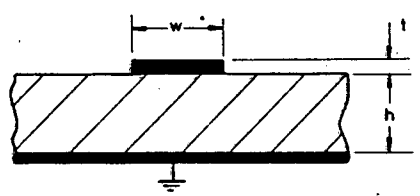

(a) Microstrip showing thickness t

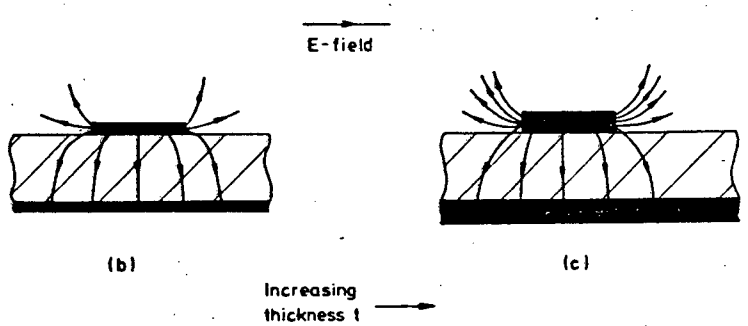

Figure 2.4 Changes in the distribution of the electric field as the thickness of the mictrostrip is altered.

Fifty ohm lines were constructed on Duroid 2.2 softboard and were found to present a good match which means that the equations used give a fair approximation.

In many practical applications the microstrip circuit is enclosed by a metal cover as shown in figure 2.5 .

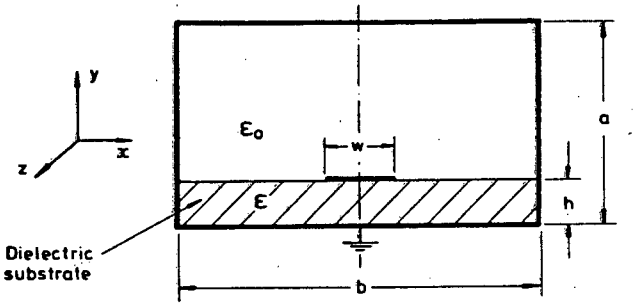

Figure 2.5 Cross-Section of shielded microstrip.

The presence of conducting top and side walls lowers both the characteristic impedance and the effective microstrip permittivity, which is due to the increased proportion of electric flux in the surrounding air. Closed formulae are available in the literature which predict the effects of the conducting walls [4] p 59.

The following equations show how the distance between a top cover and the microstrip (a-h) effects the characteristic impedance.

Where $w/h \leq 1.3$

$$Z_o \text{ (Shielded)} = Z_o \text{ (Unshielded)} - Z_{os1}$$

Where $w/h \geq 1.3$

$$Z_o \text{ (Shielded)} = Z_o \text{ (Unshielded)} - Z_{os2}$$

$$Z_{os1} = 270 \left(1-\tanh\left(0.28+1.2\sqrt{\frac{a-h}{h}}\right)\right)$$

$$Z_{os2} = Z_{os1} \left(1-\tanh\left(1+\frac{0.48\ (w/h)-1}{(1+(a-h)/h)^2}\right)\right)$$

The height of the conducting strip has been neglected because it has minimal overall effect in the above equations.

The losses that occur are due to losses in the dielectric, losses in the conducting strip and radiation losses. The conductor losses vary between $1X10^{-3}$ dB/mm at 1 GHz to $2.4x10^{-3}$ dB/mm at 7 GHz. The dielectric losses are usually far lower than the conductor losses depending on what substrate is used. If plastic substrates are used the two losses are comparible. [4] p 61.

2.1.4 Stripline

A stripline as shown in figure 2.6 operates in a TEM mode.

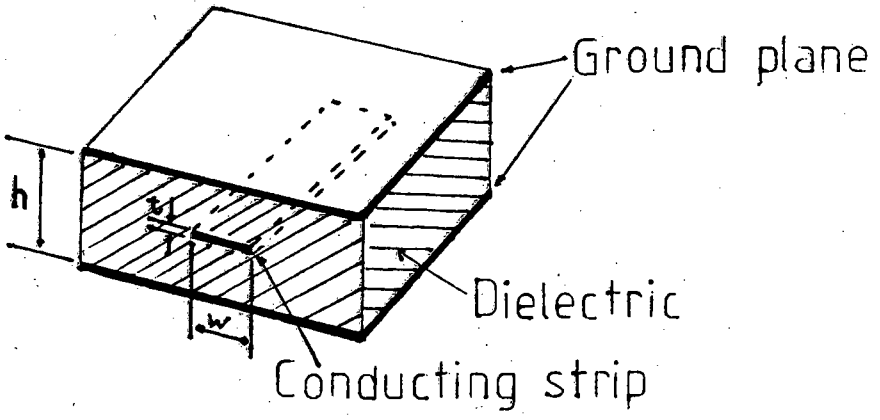

Figure 2.6 A stripline.

The analysis of stripline is considerably simplified when the thickness of the central strip is negligible. Design equations are found in [15] p 57 and [26]. The following equation is used.

$$\frac{w}{h} = \frac{16}{\pi} \frac{\sqrt{e^{\frac{\sqrt{KR}}{30}} + 0.568}}{e^{\frac{\sqrt{KR}}{30}} - 1}$$

Where R = characteric impedance
K = dielectric constant

2.2 Coupled Transmission Lines

Coupled transmission lines are used in a variety of circuit functions, namely directional couplers, filters, impedance matching networks and delay lines [5] page 76. They can be implemented in any of the microwave transmission line forms which include microstrip, stripline and coaxial line. They are of particular interest due to their unique phase shifting properties and can be fairly broad band. This allows them to be a viable solution for the Phase Shifters (see chapter 8).

Coupled lines are modelled on TOUCHSTONE which enables circuits to be designed in theory and be investigated fully before any fabrication process is performed. This is very important as some quadrature couplers (Lange couplers) have to undergo an expensive manufacturing process.

2.2.1 Coupled Transmission Line Characteristics

Any parallel-coupled pair of transmission lines may be described by the four-port configuration indicated in figure 2.7. The broken lines indicate mutual coupling.

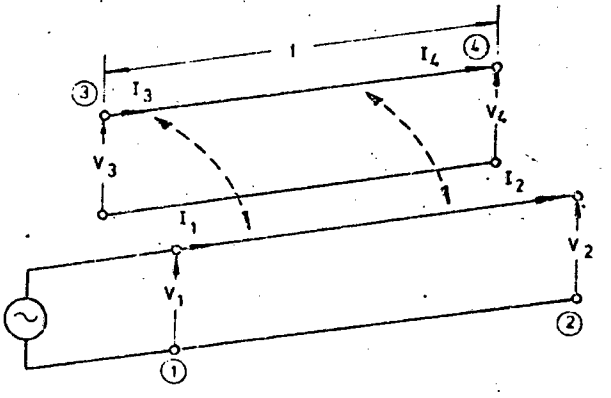

Figure 2.7 Two parallel-coupled transmission lines

These coupled lines yield contra-directional travelling waves. [4] p 12. At any instant the relative polarities of the voltages, taken at any specific plane along the structure will either be alike or opposite, which is referred to as the even mode and odd mode impedances respectively denoted by Zoe and Zoo. These characteristic impedances are major design parameters for any parallel-coupled transmission line configuration and are functions of the degree of coupling (C) and the single-line terminating characteristic impedance (Z_o). The important parameters are coupling factor C, transmission factor T, directivity D and isolation I. These quantities are defined when referring to figure 2.7 and figure 2.8.

$C = V_3 / V_1$ = voltage fraction transferred or coupled across to the opposite arm.

$T = V_2 / V_1$ = transmission directed through the "primary" arm of the structure.

$D = V_4 / V_3$ = measure of the undesireable coupling to port 4.

$I = V_4 / V_1$ = degree of isolation between port 4 and port 1.

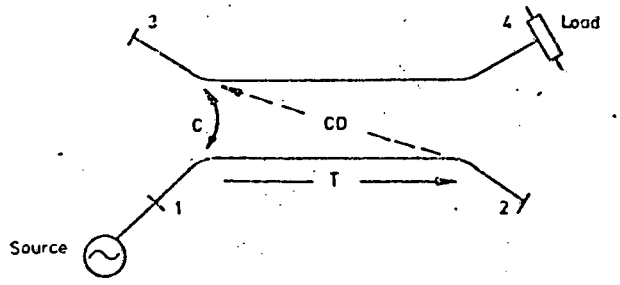

Figure 2.8 Schematic diagram of a directional coupler indicating the major parameters.

The following important equations are derived in [4].

$$C = 20 \log \frac{Zoe - Zoo}{Zoe + Zoo} \qquad (2.5)$$

and $$Z_o^2 = Zoe\ Zoo \qquad (2.6)$$

True TEM couplers yield equal phase velocities for each mode whereas quasi-TEM couplers yield differing phase velocities.

A coupler therefore has the following characteristics.

1) There is transfer of power from Port 1 to Port 2.
2) There is transfer of power from Port 1 to port 4.
3) There is no transfer of power from Port 1 to Port 3.
4) There is no reflected wave out of Port 1.

2.2.2 The phase relationship of quadrature couplers.

Refering to figure 2.9. When a signal is applied to Port 1 any reflections that occur on ports 2 and 3 due to mismatches are reflected back to Port 4 (or the isolation port). Therefore the reflection coefficient seen at Port 1 is theoretically minus infinity. Transmission from Port 1 to Port 3 (the direct path) has a constant phase delay of 90 degrees.

Transmission from Port 1 to Port 2 (the coupled path) has a constant phase shift of 180 degrees. The signals that reach port 4 are of the same frequency but shifted in phase which add vectorially.

If different terminations are applied to Port 2 and Port 3 a resultant phase shift is found at Port 4 as shown in Table 1 below.

Termination at Port 2	Termination at Port 3	Phase at 4 due to 2	Phase at 4 due to 3	Resultant Phase
Short Circuit	Short Circuit	90°	90°	90°
Matched Load	Matched Load	No Output	No Output	No Output
Open Circuit	Open Circuit	270°	270°	270°

Table 1 Resultant Phases for different terminations on a quadrature coupler

If open circuits are applied to Port 2 and Port 3 total reflections will occur at these ports. If short circuits are applied an additional 180° is added to each path.

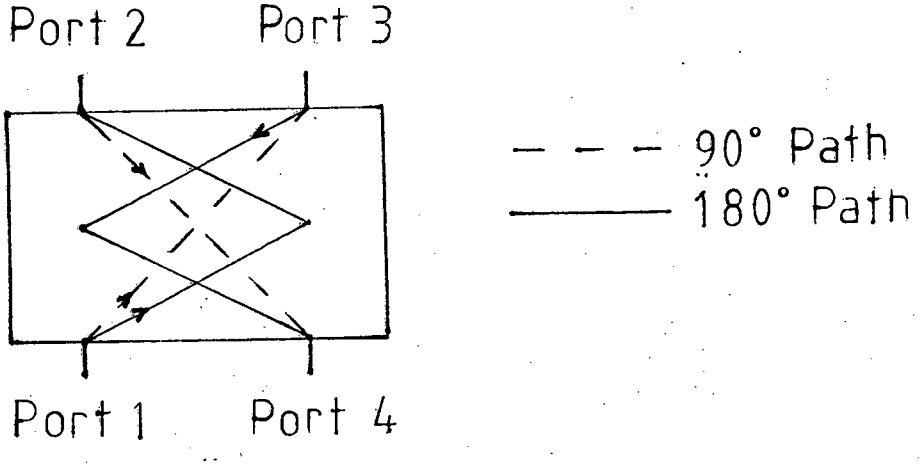

Figure 2.9 The phase shift paths of the quadrature coupler

2.3 The Quadrature Coupler

The couplers that were investigated were both of the microstrip and the stripline types. A microstrip coupler would have to take the form of a Lange coupler [7] [8] [9] because the gap between two straight coupled microstrip lines is too small to be physically realizable for a 3dB coupling. [5] p 130. Even the Lange couplers need very narrow gaps between the fingers which is not possible to fabricate with conventional etching techniques. A process which involves the copper sputtering of thin film Alumina is required.

Stripline couplers present much higher coupling for the same gap size as in coupled microstrip lines [10]. Formulae are available in [5] page 72 and [10] which enable the physical parameters to be calculated once the even and odd mode impedances are given. The gap sizes are still found to be very small.

An alternative to the stripline side-on coupler is the overlay coupler where a 3 dB coupling factor is feasible. The following formulae gives the even and odd mode impedances Zoe and Zoo [11] with respect to ground with the cross section as shown in figure 2.10.

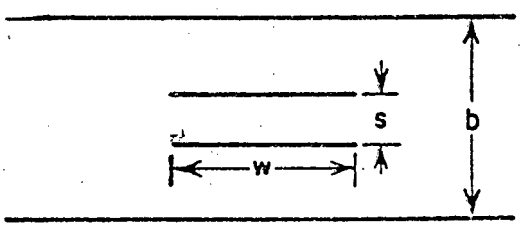

Figure 2.10 Cross-section dimensions of broadside-coupled strips parallel to the ground planes.

These formulae hold for any ratio of w/b and s/b as long as $w/s > 0.35$

$$Zoe = \frac{188.3}{\sqrt{\varepsilon_r}} \frac{K(K')}{K(K)} \qquad Zoo = \frac{296.1}{\sqrt{\varepsilon_r}\, {}^{b}/_{s} \tanh^{-1} K}$$

where K = a parameter

$K' = \sqrt{1 - k^2}$

K(K) amd K(K') = Complete integrals of the first kind.

An approximation is

$$K(K) = \frac{\pi}{2}\left(1 + (\tfrac{1}{2})^2 K^2 + (\frac{1.3}{2.4})^2 K^4 + (\frac{1.3.5}{2.4.6})^2 K^6 + \ldots\ldots\right)$$

The ratio $\frac{w}{b}$ is given by

$$\frac{w}{b} = \frac{2}{\pi}\left(\tanh^{-1}\sqrt{\frac{K\ \frac{b}{s} - 1}{\frac{1}{k}\ \frac{b}{s} - 1}} - \frac{s}{b}\ \tanh^{-1}\left[\frac{1}{k}\sqrt{\frac{K\ \frac{b}{s} - 1}{\frac{1}{k}\ \frac{b}{s} - 1}}\right]\right)$$

A basic program was developed (see program 20b) to calculate the width of the overlay once given the height of the dielectric (b), the height of the dielectric between the copper strips (s) and the even mode impedance. Equation 2.6 was always fulfilled. Program 20a is the flow chart for this program. It must be noted that all the conditions may not be satisfied for a given b and s.

3. BIAS NETWORKS

It is important that the circuitry used to bias the PIN diodes (or any other active device) does not interfere with the response of the overall circuit. Therefore the transmission line onto which the bias circuit is connected must still perform as a low loss line with the specified characteristic impedance.

It is also important that the bias network does not degrade the modulating signal in any way. A modulating frequency for the switch can be in the region of ten mega-hertz. Therefore the overall required response takes the form of a High Pass filter as shown in Figure 3.1.

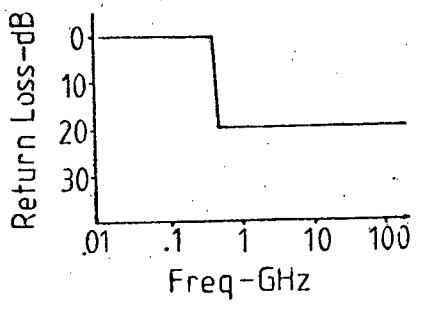

Figure 3.1 Required response for a bias network

A return loss of 20dB corresponds to one hundredth of the power being returned to the source which results in a SWR of 1.2.

A number of different biasing methods were investigated and developed as follows.

3.1 Radial Stub

The radial stub configuation as shown in figure 3.2 is a radial transmission line element [12] A magnetic wall model [13] can be employed for analysis where the radial element is considered as a cavity resonator with electric

walls on the top and bottom and magnetic walls on the side border.

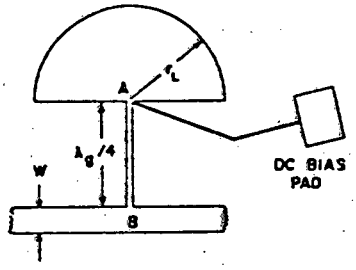

Figure 3.2 The Radial Stub as a bias network

A broad-band high frequency open-circuit is present at point B. The following design equations are given for a semi-circular cavity resonator[14] page 133, which was used to design a circuit.

For a TEnpq mode:

$$\text{Resonant freq.} = \frac{1}{2\pi a\sqrt{\mu\varepsilon}}\sqrt{(X'np)^2 + \left(\frac{q\pi a}{d}\right)^2}$$

where X'np = Kc a Bessel function

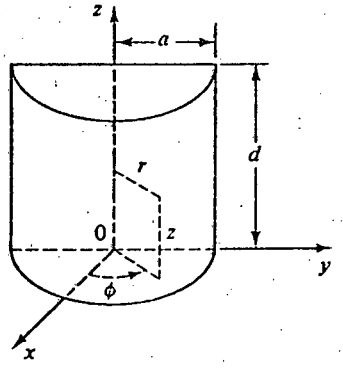

Figure 3.3 A semi-circular cavity resonator

For a frequency of 3.46 GHz and a TE$_{110}$ mode. From [14]p 116 $X'_{11} = 1.841$. A radius of 17.12mm is calculated. A feed line with an impedance of 110ohm was chosen. This results in a microstrip width of .57mm. Two circuits where fabricated.

One with a radius of 17.12 and another with a radius of 8.58mm. The measured response is shown in figure 3.4.

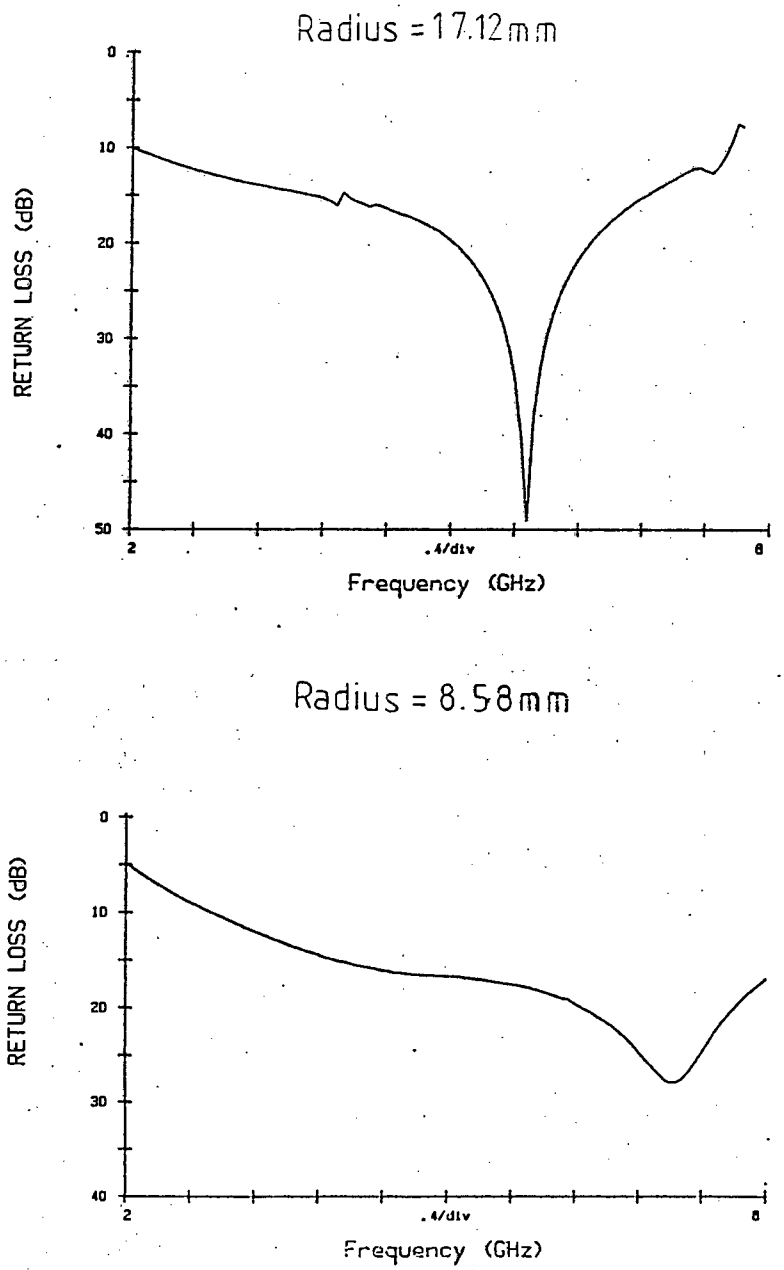

Figure 3.4 The measured response of the radial stub circuits which were fabricated.

The radial stub network is not broadband enough for the bandwidth in question. It can be easily noted that as the radius decreases the usable frequency response shifts up in frequency

which is to be expected. It was also found that the DC pad as shown in diagram 3.2 can be removed and replaced by a wire soldered to the centre of the radial stub. A major disadvantage with the radial stub is that it is physically very large compared to the other microwave circuitry and devices at the frequencies being delt with.

3.2 High Impedance Low Impedance sections used in Bias Networks

The property of the quarter wavelength impedance transformer can be used in a bias network. An open circuit at one end of a quarter wavelength section of transmission line is transformed to a short circuit at the other end and visa versa. If two quarter wavelength sections with different impedances follow one another as shown in figure 3.5 a broadening of the bandwidth occurs compared to one section. The low impedance (the wide section) has the influence of broadening the bandwidth of a single open circuited stub and ensures a low impedance point for the DC connection to be made. The high impedance is the thin line connected to the 50 ohm line.

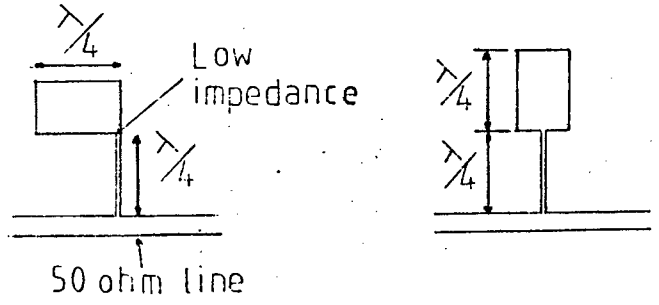

Figure 3.5 A Microstrip circuit of High Impedance Low Impedance Sections

A way of broadening the bandwidth even further would be to use multiple quarter wavelenth sections for different frequencies as shown in figure 3.6.

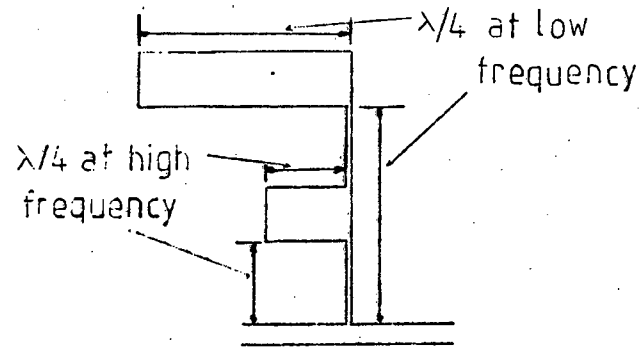

Figure 3.6 Microstrip circuit of broadened High Impedance Low Impedance Sections

The higher frequency is chosen to be double that of the lower frequency. When the circuit is operated at the higher frequency the long quarterwave section will support the shorter section because at this frequency it is half a wavelength. ie The open circuit at the extremity is transferred to the connection at the 50 ohm line.

This circuit was analysed on TOUCHSTONE using firstly ideal transmission lines. The circuit was optimized for the broadest bandwidth possible which resulted in the lengths not being exactly a quarter wavelength. See Program 1 Appendix A. The resulting response is shown in figure 3.7a.

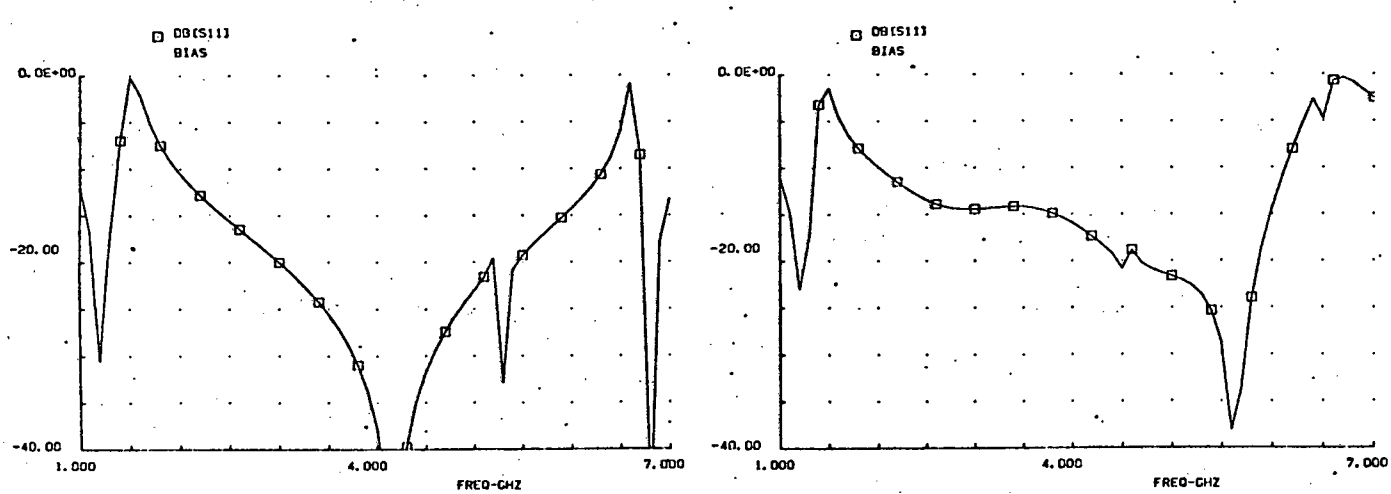

(a) (b)

Figure 3.7 Response using a) ideal transmission lines b) microstrip lines for the circuit shown in figure 3.6

A transformation from ideal transmission lines to microstrip was done where the MLIN and MLOC commands are used. See Program 2. It was found that the response did not follow the result shown in figure 3.7. This would be due to the open circuit stubs having finite widths. The circuit was again optimized to produce the response shown in figure 3.7b.

The software predicts that this system of biasing does not operate over the entire frequency range in question. A circuit was not produced to compare measured response to computed response.

3.3 Bias networks using Elliptic Filters

A means for constructing filters as rectangular pads on dielectric substrate is described in references [15], [16] and [17]. The merits of this construction is that the Bias network is constructed simultaneously with the rest of the circuit. A thin wire is then soldered to a low impedance point which injects the required bias signal. The pad has an equivalent LC circuit as shown in figure 3.8.

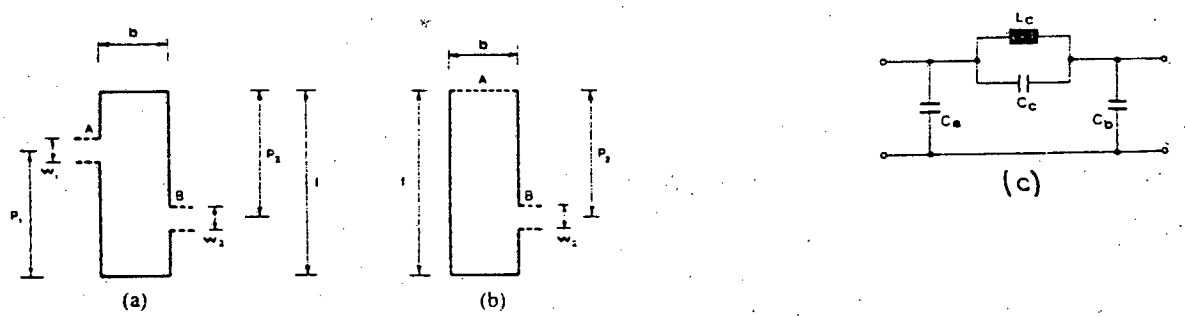

Figure 3.8 Geometry of two types of filter elements with their equivalent circuit.

The design equations used which relate component values to pad dimensions are given.

$$\ell = \frac{t\ (Ca + Cb)}{\varepsilon b}$$

$$q_1 = Cb/\sqrt{2\ (Ca\ Cb + Ca\ Cc + Cb\ Cc)}$$

$$q_2 = -Ca/\sqrt{2\ (Ca\ Cb + Ca\ Cc + Cb\ Cc)}$$

$$p_1 = (\ell/\pi)\ COS^{-1}\left(-q_1/Sn\ \left(\frac{\pi W_1}{2\ell}\right)\right)$$

$$p_2 = (\ell/\pi)\ COS^{-1}\left(q_2/Sn\ \left(\frac{\pi W_2}{2\ell}\right)\right)$$

Open circuit resonant frequency $= [Lc\ (Cc + \frac{Ca\ Cb}{Ca + Cb})]^{-1}$

For the circuit in figure 3.8a the following conditions have to be imposed.

$$Ca > \frac{Cb}{2}\ \left(\frac{Cb - 2Cc}{Cb + Cc}\right)$$

$$Cb > \frac{Ca}{2}\ \left(\frac{Ca - 2Cc}{Cb + Cc}\right)$$

For the circuit in figure 3.8b

$$Ca = \frac{Cb}{2}\ \frac{Cb - 2Cc}{Cb + Cc}$$

A Sharp PC I211 pocket computer was programmed to request component values and then to calculate the resonant frequency and pad dimensions. See Program 3 Appendix A for basic program. The SPICE program on the UNIVAC mainframe computer was then used to calculate the Return Loss of the equivalent circuit from 2GHz to 6GHz as shown in Figure 3.a. Ports 1 and 3 form the two port network.

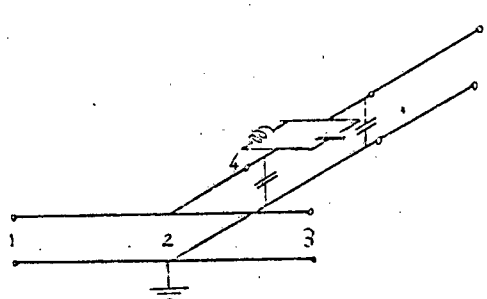

Figure 3.9 The equivalent circuit that was programmed on SPICE.

The following values were generated on the Sharp pocket computer.

Requested parameters:

L = 5.6 nH
Ca = 1pF
Cb = 1pF
Cc = .04fF
Width Port 1 = 0.57mm
Width Port 2 = 0.57mm
Width of pad = 5mm

Calculated values:

Resonant frequency = 3GHz
Length of pad = 16mm
P1 = 12mm
P2 = 12mm

These values were used in the configuration as shown in figure 3.1. It was found that if an open circuited quarter wavelength section was introduced between points 2 and 4 in figure 3.9 then the response was broadened. This configuration came about in an attempt to incorporate the High Impedance Low Impedance sections with an Elliptic filter pad. The program listing is shown in Appendix A (Program 4). The predicted response is shown in figure 3.10.

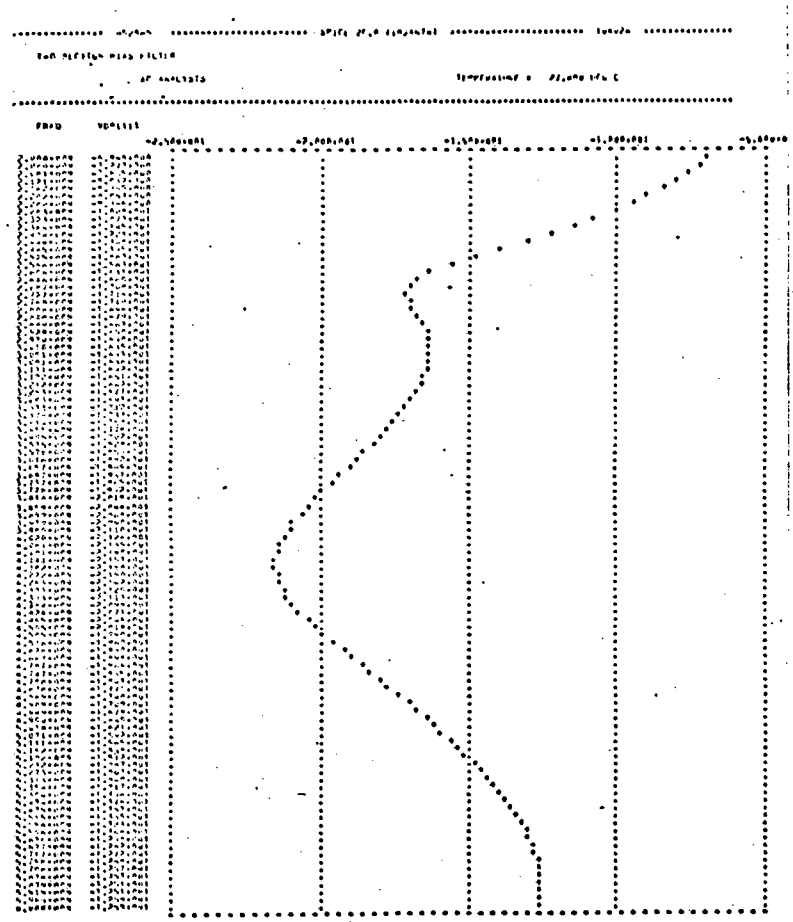

Figure 3.10 The response of the filter predicted by the SPICE Program

The ideal transmission line circuit that was developed on SPICE was simulated using the TOUCHSTONE program. Since TOUCHSTONE facilitates the entry of microstrip dimensions directly it was hoped that a higher degree of accuracy could be achieved. TOUCHSTONE predicts that the dimensions for the circuit that produced the response in figure 3.10 are far larger than those predicted by SPICE. Different configurations were tried where the optimization routine was used extensively. Some microstrip layouts with their accompanying predicted response is shown in figure 3.11. Their programs are shown in Appendix A. (Programs 5,6,7).

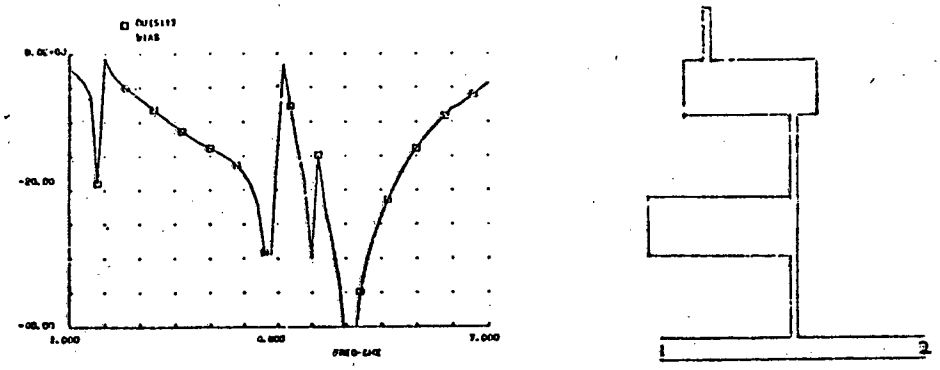

(a)

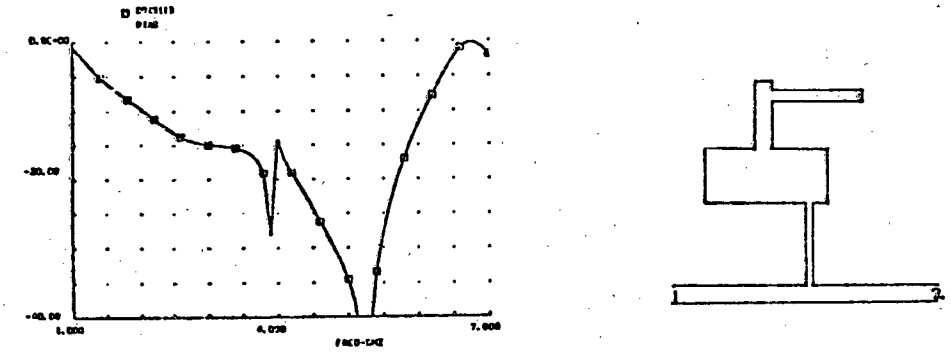

(b)

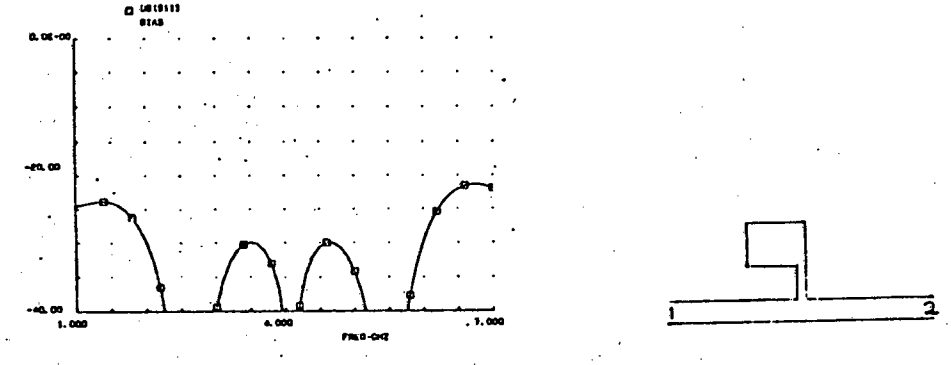

(c)

Figure 3.11 Microstrip layouts with their accompanying predicted response.

Figure 3.11c seems to give the required response but this is a prime example in which the program was allowed to optimize indefinitely without any limits provided. The stubs were reduced until the effect becomes negligible. A satisfactory frequency response was not obtained in software over at least two octaves of bandwidth and no circuits were fabricated as a result.

3.4 Pads that were tested as Bias networks

A number of simple circuits were built up using the 3M Microwave Design Aids. This design aid consists of thin copper strips with Low Loss glue on one side to facilitate the adhesion of pads and strips onto a dielectric substrate.

Pads of different sizes and shapes with thin copper wire connecting them to a 50 ohm line was constructed. The dimensions and shapes of the pads were easily altered by trimming off narrow strips of copper with a sharp knife. The change in the return loss on the display of the network analyser was then observed. The connection from the pad to the 50 ohm line is very important. It was found that the best results were obtained by using thin copper wire (diameter = .15mm) for this purpose.

TOUCHSTONE was used to model a pad with a thin connecting wire to a transmission line. It was then easy to construct the circuit using the design aid and then to compare the predicted response with the measured response. The predicted response is shown in figure 3.12a where a square pad was constructed with a 25mm length of .15mm copper wire connecting it to a 50 ohm transmission line. The measured response is shown in 3.12b.

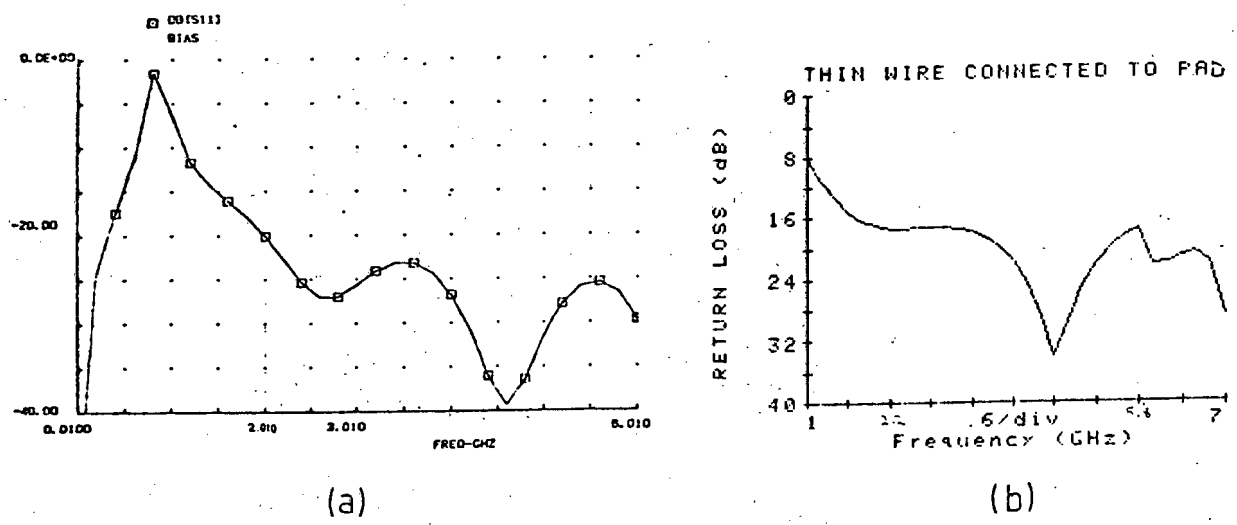

Figure 3.12 Theoretical and measured response of a square pad.

The pad can be considered as a capacitor when considering that there are two conducting plates separated by a dielectric slab. A 25mm length of connecting wire is a high impedance quarter wavelength at 3 GHz and the capacitor is a low impedance to ground at microwave frequencies. This is very similar to the High Impedance Low Impedance Sections as discussed in section 3.2, the difference being in the way the Low Impedance is implemented.

However the measured response is not better than 20 dB over the frequency range and forms a notch as in the radial stub case.

When the pad gets too large, the dimensions become comparable with that of the operating wavelength and uncertainty arises as to whether the pad is a capacitor or a resonant stub with quarterwavelength sections.

3.5 Ferrite cores used in Bias Lines

All the previous methods involved getting the bias circuit to present a high impedance to the 50 ohm line. This is to stop reflections occuring by minimizing any impedance mismatch.

It was thought that if all the microwave signal entering into the bias network was absorbed, then the bias connection would have minimal effect on the return loss. This would be implemented by using a ferrite material in the form of a bead which is very lossy at microwave frequencies. A thin wire fed through the ferrite bead would present a high impedance to the transmission line, therefore the amount of energy entering the bias line to be absorbed would be very little.

A wire (.15mm in diameter) was soldered onto a 50 ohm transmission line and a number of different cores were tested. The results were compared to that of the wire connected by itself. See figure 3.13.

Figure 3.13 a) displays the return loss of the 50 ohm transmission line on which all the tests were carried out. Figure 3.13 b) shows the response with only the thin wire. When the wire is touched or moved slightly the response changes. The three different traces are of three different wire positions.

Figure 3.13 c) and d) are the results of the same wire with different number of turns through a ferrite bead. The wire with two windings gives the best results. It is thought that the higher number of turns increase the inter-turn capacitance which degrades the response.

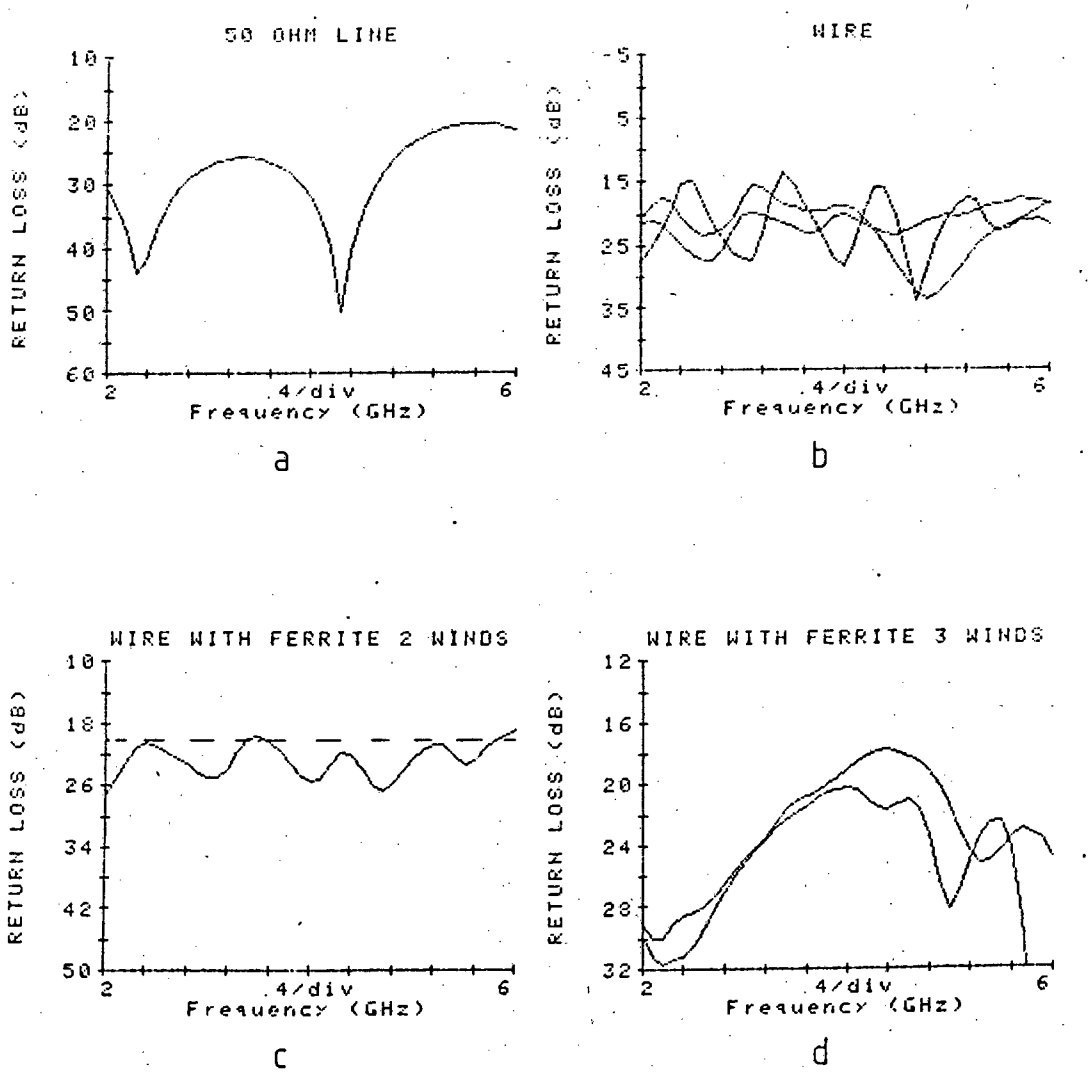

Figure 3.13 Results of tests done with wire and Ferrite beads

Many variations were tried and it was found that the ferrite bead must be placed as close to the 50 ohm line as possible for best results. An insertion loss test was also carried out to see if the ferrite material was not absorbing all the microwave energy present. This would not allow a transmitted or reflected signal resulting in a good return loss. In fact the additional insertion loss was negligible when compared to that of the 50 ohm line without any form of bias line attached.

3.6 Conclusions

Another method of biasing that was not fully investigated is to use a small wire wound inductance of approximately 100nH. If this inductance is placed close to the transmission line then a high impedance (approximately 1.2k ohm at 2 GHz) would be in shunt with the 50 ohm line resulting in a small mismatch. The problem is a very small coil with extremely thin wire which has to be constructed to keep the stray capacitance to a minimum.

The ideal bias network would be a small printed circuit that could be fabricated in the same process as the microstrip transmission lines and other microwave components. This type of circuit works well enough for small frequency bandwidths but alternatives had to be found for the frequency range in question.

The best solution was found to be a 22pF (ATC type A) capacitor with a short length of thin wire connected to the microstrip transmission line as illustrated in figure 3.14. (These ATC-A capacitors were used as DC blocking capacitors later).

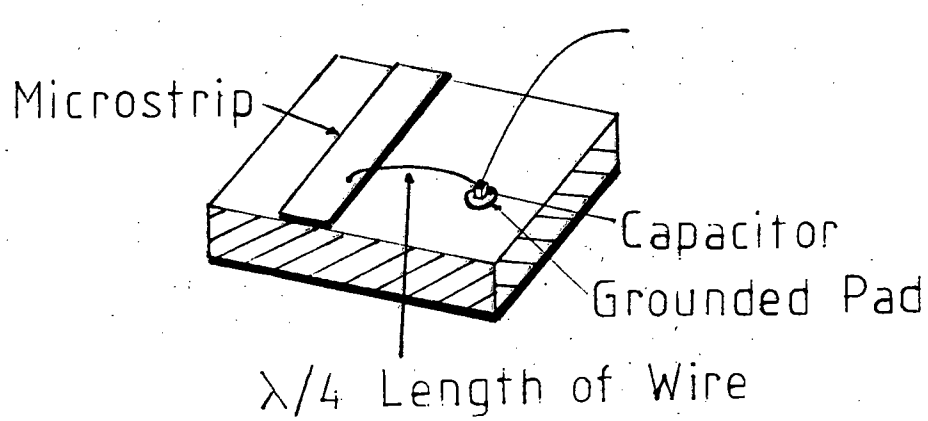

Figure 3.14 The bias system consisting of a capacitor and a short length of wire.

This again similar to the High Impedance Low Impedance system as in section 3.4. The capacitor has the advantage over the open circuited low impedance line in that as the frequency increases the impedance decreases and is not cyclical. The results of this method of biasing is shown in figure 3.15. A ferrite bead was also inserted which gives the best results overall.

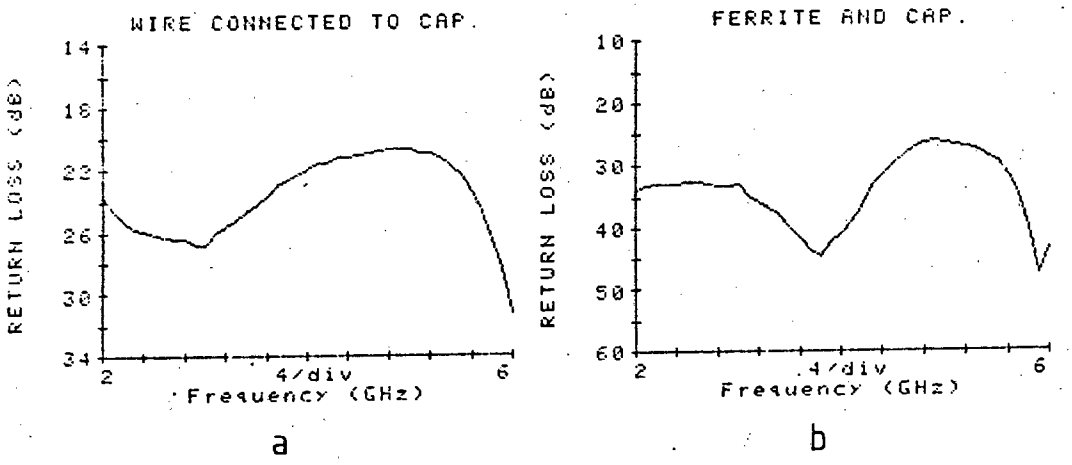

Figure 3.15 Results of the capacitor and wire biasing system.

4. THE PIN DIODE

PIN diodes can be used in variable-impedance elements to control microwave signals in applications which include switching, attenuating, modulating and phase shifting. The fundamentals for these silicon junction microwave diodes are found in the physics of the PN junction. [18]

The PIN diode consists of a P-type and a N-type layer and an Intrinsic (I) layer between them. In practice, it is impossible to obtain and maintain through processing, truly intrinsic material. Thus most PIN diodes have I layers which are slightly N-type or P-type. Consider a device with a very lightly doped N region. Figure 4.1 a) illustrates that there are in fact two junctions, a P^+ N^- junction and a N^- N^+ junction.

N_D is the donor doping density for the N material and N_A is the acceptor doping density for the P material. When zero biased a depletion region will form at the P^+N^- junction. If the doping in the N^- layer is sufficiently small, and the width is small, the zero bias depletion region may extend all the way to the N^+ region or a reverse bias might be required to obtain this condition. At this point, the depletion region will not increase further in width, figure 4.1 b) shows the electric field profile. The lower the doping level in the I region, the more constant the electric field is across the I region. [19]

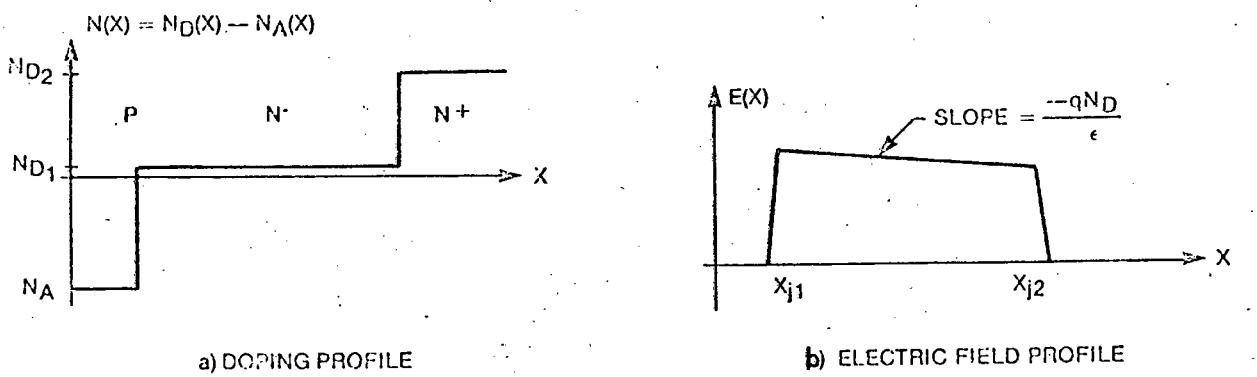

Figure 4.1 The doping profile and electric field profile of a PIN diode

At low frequencies the device behaves as a P-N junction rectifier, but at sufficiently high frequencies rectification ceases and the impedance becomes that of the I-region. This will be high when the P-N junction is reverse biased, but will become low when forward bias is applied to flood the I-region with injected carriers. For small signals no bias has to be applied to obtain the reverse bias condition. The frequency at which the device works must be such that its period is small compared to the effective lifetime of the charge carriers.

Since the electric field is almost uniform across the active region, and the voltage is the integral of the electric field across the junction, one can estimate the breakdown voltage of PIN diodes from a knowledge of the threshold field for avalanche breakdown. Typically the breakdown voltages range from 30 Volts to 1500 Volts.

4.1 PIN diode structures

i) The passivated mesa structure is shown in figure 4.2 where the active I-region resembles a parallel plate capacitor with minimum fringing capacitance to the sub-state. It also maximizes the surface breakdown voltage.

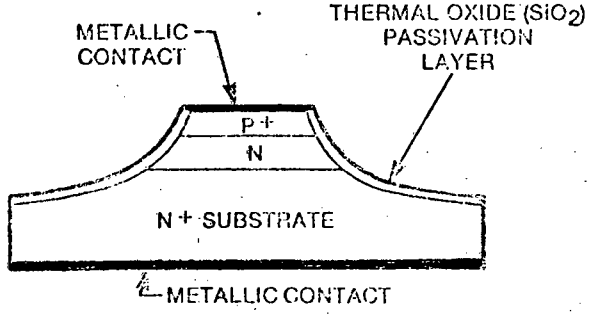

Figure 4.2 Passivated Mesa construction PIN diode

2) The planar PIN diode chip is shown in figure 4.3. For microwave purposes, planar devices have two major dis-advantages. First, the PN junction depletion region is shaped like a plane-parallel plate capacitor in the centre,

but is cylindrically shaped at the edges which reduces the voltage breakdown considerably from a mesa device with an I-region of the same thickness. Secondly, the inactive silicon surrounding the junction produces extra fringing capacitance. It also stores charge, thereby reducing switching speed. But the series resistance vs current characteristic is linear on a log-log plot over a wide dynamic range of forward-bias currents which make it useful for attenuator applications.

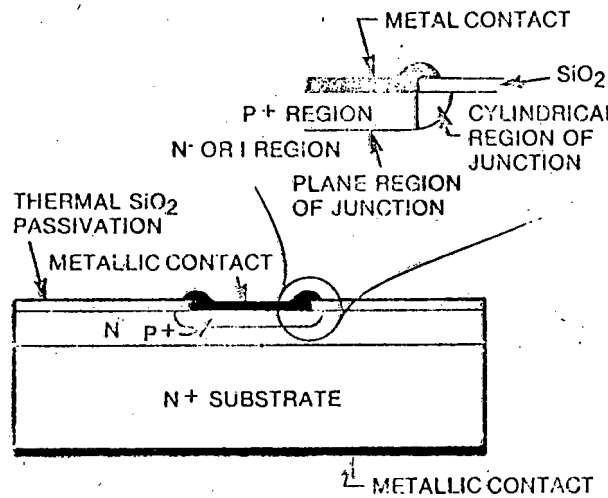

Figure 4.3 Planar constructed PIN diode

3) The beam-lead PIN diode as shown in figure 4.4 is a planar PIN diode with both contacts on the same side of the silicon wafer. This device is well suited for series mounting in hybrid IC circuits. The main advantages are that they can be made extremely small with very low junction capacitance, and that the mounting configuration results in a minimum of lead inductance.

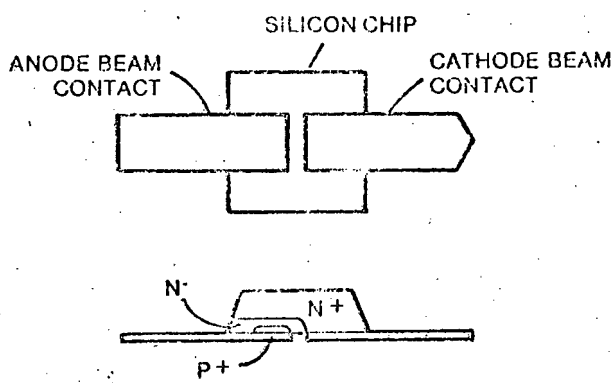

Figure 4.4 Beam-lead constructed PIN diode

These devices are generally used in high frequency applications in microstrip circuits.

PIN diodes are available as chip devices or mounted in a variety of microwave packages which provide a hermetically sealed environment for the chip which allows for mounting in coaxial, waveguide, stripline and microstrip circuit. The electrical effect of the package is to add a shunt package capacitance (Cp) across the junction and a lead inductance (Ls) in series with the junction. Both these effects limits bandwidth but if they are well defined they can be designed for in their respective circuits. Cp and Ls vary from package to package.

Figure 4.5 shows the equivalent circuit for a packaged PIN diode in the forward and reverse biased states.

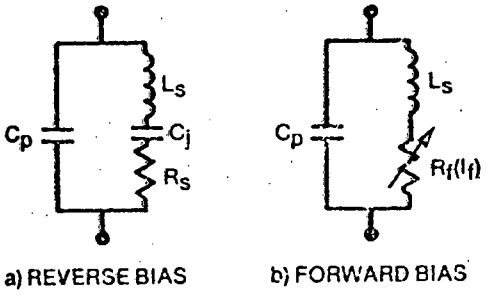

Figure 4.5 The equivalent circuit for a packaged PIN diode

It must be remembered that this is the simplest form of the model. The model changes according to the specific package. The capacitor Cj is given by:

$$Cj = \frac{\varepsilon A}{W_I}$$

ε = Dielectric constant
A = Area of Intrinsic layer
W_I = Width of I-layer

The diode series resistance (Rs) is the sum of all the resistances of the undepleted silicon regions and the contact resistance of both ohmic contacts. The reverse biased PIN diodes block RF transmission when placed in series with a transmission line, and permits RF transmission when placed in shunt with a transmission line.

4.2 Transient Properties

When a PIN diode is switched from the reverse biased state to the forward biased state the transient occurs rapidly. Carrier injection occurs almost immediately, and the carrier concentration in the intrinsic region grows to an equilibrium state. A finite amount of charge must be transferred in order for the junction to reach its equilibrium forward-bias value. The speed of the transient depends on the time constant of the PIN diode and bias network, with an almost negligible delay due to the diode's junction effects.

When a PIN diode is switched from a forward biased state to a reverse biased state, immediately after switching the diode can support a high value of reverse current from the charge that is stored in the I-region. The carrier concentration slope then adjusts itself to support a reverse current by diffusion from both edges of the I-region. The stored charge depletes itself by two mechanisms. The first is the charge removal caused by the reverse current and the second is the decay of the injected carriers by recombination in the I-region. This recombination proceeds with a time constant T_L, which is the average lifetime of a charge carrier in the I-region before it recombines. Figure 4.6 shows a typical switching transient of a PIN diode when switching from a forward current to a reverse current.

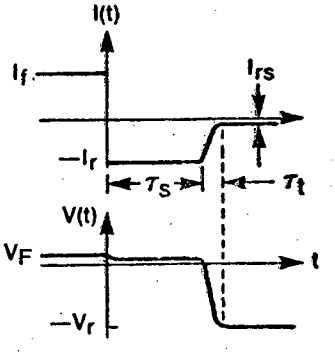

If = Current under forward biased condition
Irs = leakage current under reverse bias condition

Figure 4.6 Switching Transient of a PIN diode

The length of time the current Ir can be sustained is called the storage time Ts which is a function of both If and Ir since If determines the amount of stored charge and Ir determines its rate of removal. The transition time Tt is usually very much smaller that Ts.

The type of PIN diode driver determines the switching speed to a large extent. Drivers with high values of Ir or with spiked leading edges on their waveform are used to minimize reverse switching time. The limiting factor is the minimum time it takes for a carrier to transmit the I-region at maximum saturation voltage. The width of the I region determines the minimum speed with which the diode can be switched as well as the breakdown voltage. It should be noted that the switching speed of a diode decreases as its power handling capacity increases.

4.3 Power Handling

There are two factors which determine the power handling capability of any PIN diode. The first and most common is the maximum junction temperature at which the device can operate with full reliability. The second is the peak voltage that the device can be subjected to without causing damage to the junction.

4.4 Package Parasitics

Figure 4.7 shows the complete schematic for a PIN diode. The parasitic components can be tuned out by externally placed capacitance and inductance as shown in the figure below.

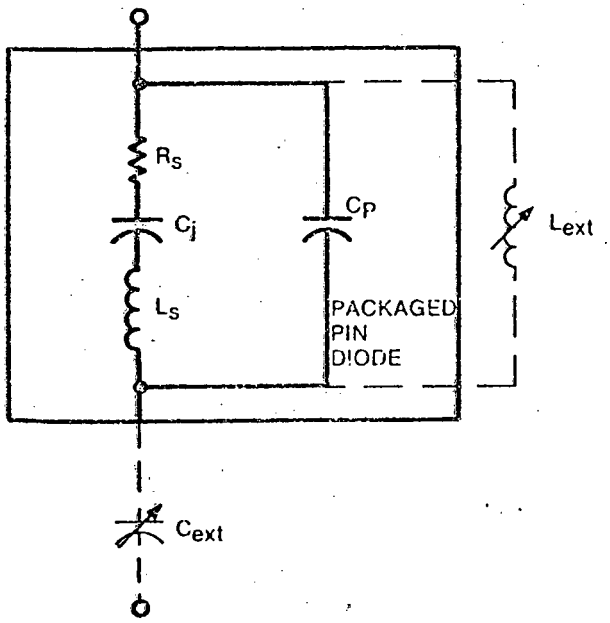

Rs = series resistance
Cj = junction capacitance
Ls = lead inductance
Cp = package capacitance

Figure 4.7 Equivalent circuit of a packaged PIN diode with external tuning.

If the case parasitics are not tuned out their effects become noticeable as the frequency increases. Lext is used to parallel-resonate the package capacitance and can be realised by a stub of critical length placed at a certain distance from the device. Cext is used to series-resonate the lead inductance.

In the design of circuits using PIN diodes the parasitic elements play a large role. A practised design technique is not to use the theoretical model of the packaged PIN diode but to characterise it in terms of the S-parameters measured on a S-parameter test set. Once this is done full use can be made of a software package such as TOUCHSTONE or COMPACT.

An alternative theoretical equivalent circuit for the PIN diode is shown in figure 4.8. The literature seemed to indicate that this is the preferred model.

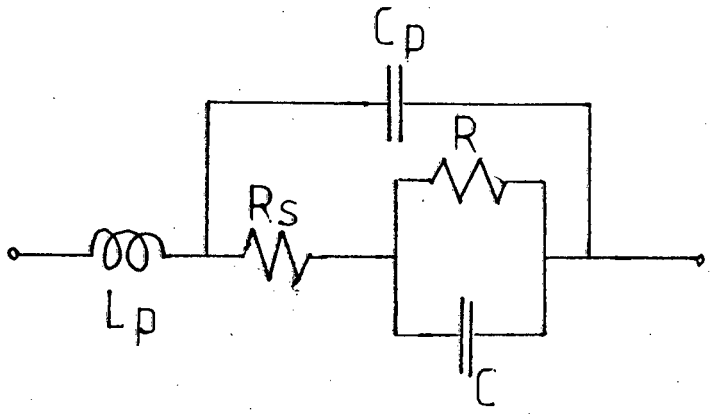

Figure 4.8 An alternate theoretical model for the PIN diode

4.5 The HP 3141 shunt mounted PIN diode

The HP 3141 PIN diode is of the oxide passivated mesa design which is enclosed in a package. See appendix B for specifications. The package is mounted directly onto the ground plane which facilitates the shunt operation.

The characteristics of the PIN diode that were investigated are as follows;

i) the effect of different biasing

ii) the impedance variation over the frequency range 2GHz to 6GHz

iii) the variation of characteristics from device to device.

All the tests made use of the transistor test fixture. A ground structure was machined from a brass plate as shown in Appendix B. A specially adapted microstrip board was also fabricated which allowed a diode to slot into place easily. The bias current was applied through the biasing ports of the s-parameter test set.

The reference plane was first set by placing a short in the diode slot. The mechanical slider which moves the reference plane was then adjusted to get a constant phase shift independant of frequency. The s-parameters measured with a diode inserted will be that of the device only without any small section of transmission line.

The Accuracy Enhancement package requires measurable open circuit, short circuit and 50 ohm through line terminations as well as the type of connector used in the calibration routine. The first three conditions can be met but the connector cannot be accommodated on the slotted micro-strip line.

A solution is to calibrate the system without the test fixture connected. This allows the APC-7 calibration kit to be used. The reference plane is then extended in software to obtain a constant phase shift which is displayed on the print-out. It is a matter of trial and error to reach the correct extension. A reference plane extension of 28.35cm was found to give the flattest phase response as shown in figure 4.9. The S-parameters that were generated were later used in creating an S-parameter file on the software package TOUCHSTONE. This is shown in Appendix B.

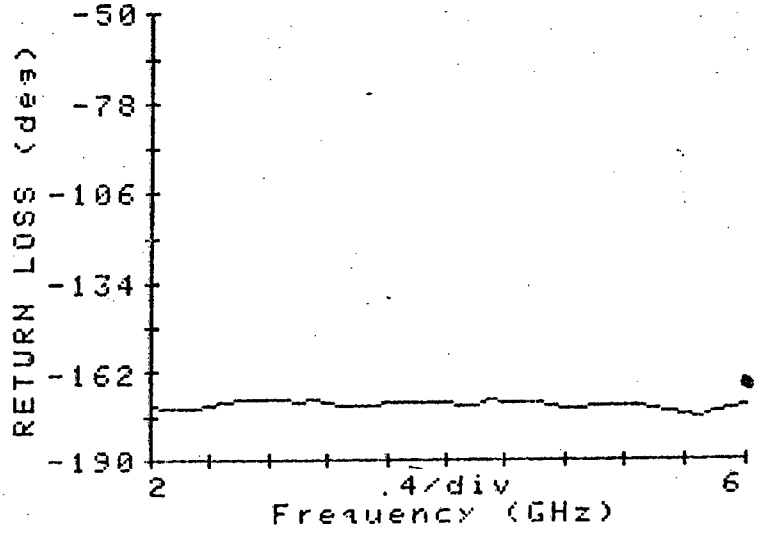

Figure 4.9 Phase response generated with a short and reference plane extension of 28.35 cm

Another method of getting around the problem is to adjust the reference plane on the s-parameter test set to half that of the software extension. The physical extension is half that of the software extension because return loss is being analysed where the signal has to travel to the device and back for a measurement to take place.

When the shunt mounted diode is forward biased it ideally presents a short circuit to ground. In practice a very low but finite impedance is realised. This implies that the signal is not transmitted from the input to the output of the microstrip circuit. A measure of how good the short circuit is, is determined by the isolation between the input and output ports or alternatively the insertion loss. This is determined by the bias current. The insertion loss changes as the forward bias current is varied between zero and ten milli-amps. Over ten milli-amps a diode can be considered to be switched on fully and a further increase in current has a very small but finite effect on the diode impedance. It was decided that an operating current of approximately fifteen milli-amps would suffice for all tests. Figure 4.10 shows the isolation that is presented from one diode when the current is changed in steps of ten milli-amps.

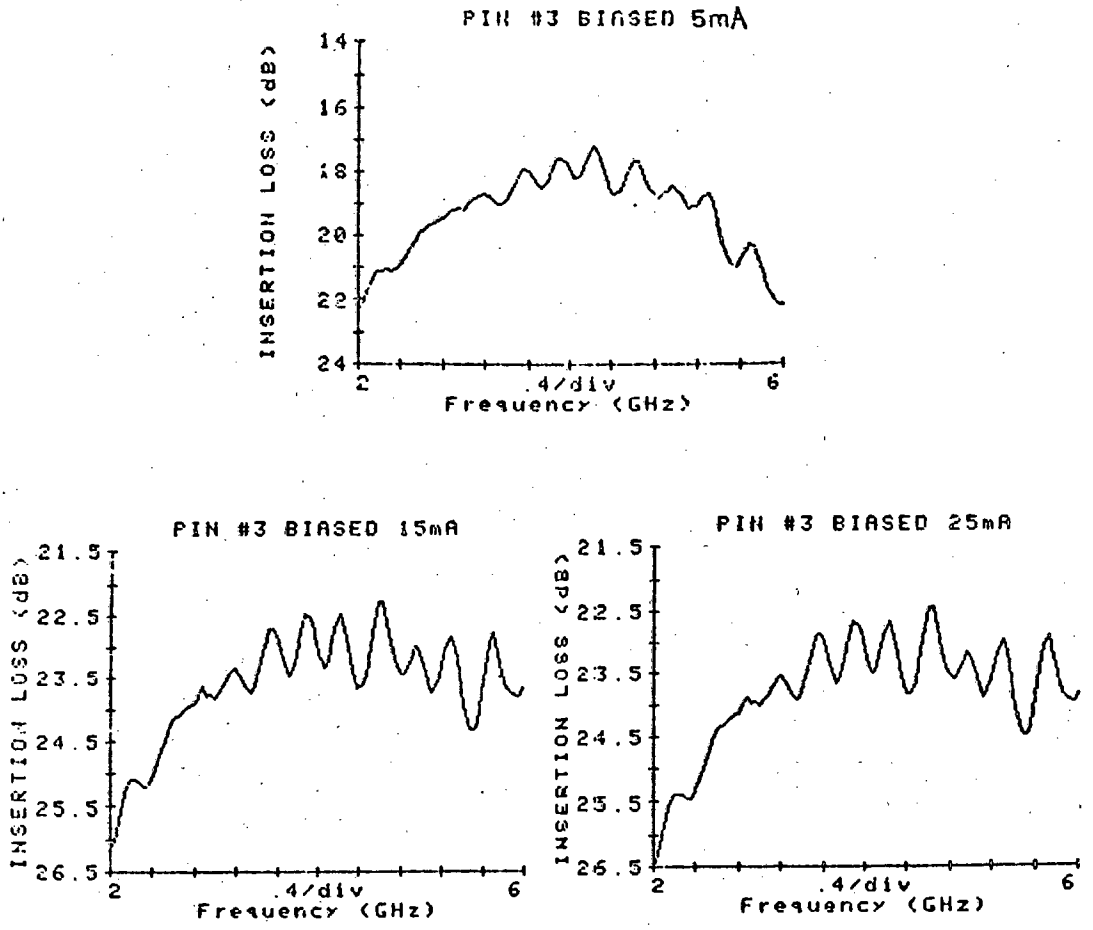

Figure 4.10 Isolation versus bias current on the HP 3141

In the reverse bias condition no difference in the response was observed as the reverse voltage was increased from zero volts. The insertion loss results as shown in figure 4.11 from which it can be concluded that very little signal is lost due to a mismatch in the 50 ohm line or attenuation through the PIN diode package.

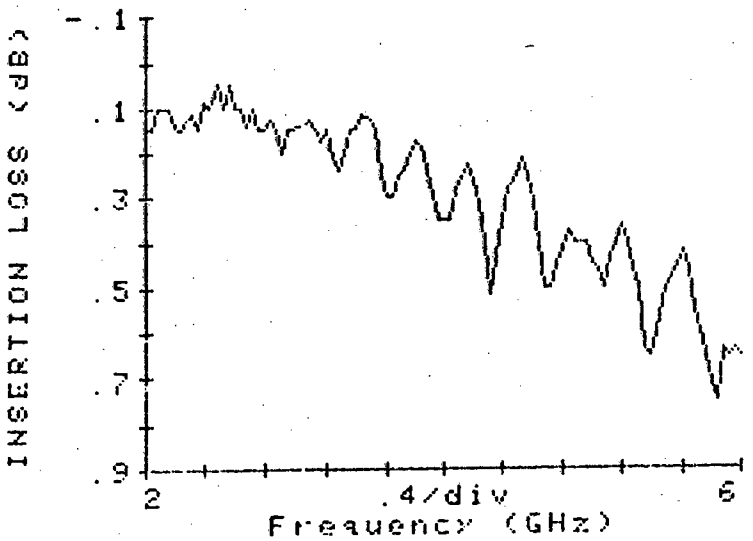

Figure 4.11 Insertion loss for the reverse biased HP 3141 PIN diode.

The reference plane extension is very critical when measurements of impedance are being performed which use the modified accuracy enhancement package. Figure 4.12 illustrates how the impedance varies when the extension is varied by .2cm in software.

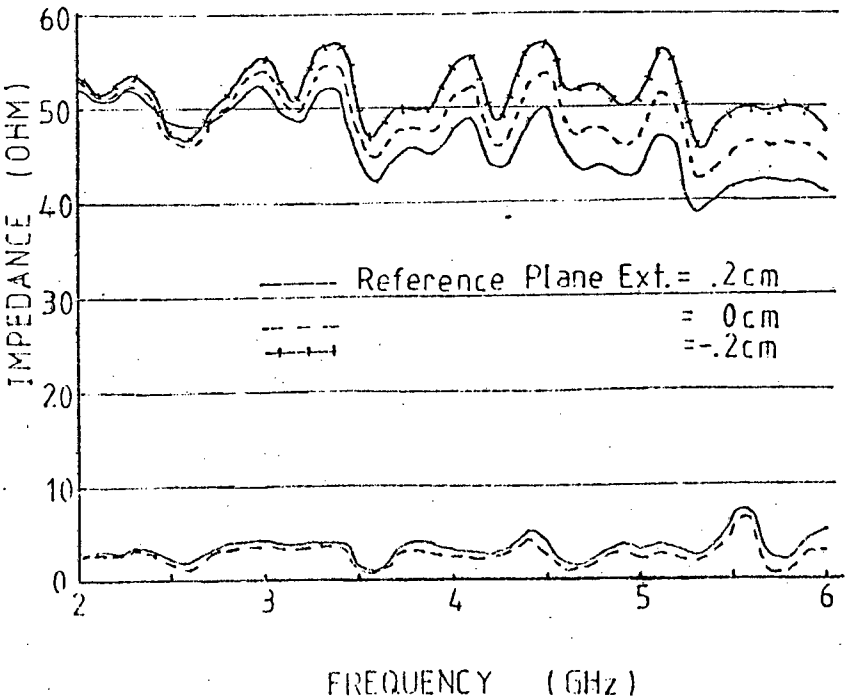

Figure 4.12 The effect of moving the reference plane on the impedance.

The trace of -.2cm gives the flattest impedance response and the reverse biased diode has an impedance of 50 ohms with a 5 ohm variation. The forward biased diode has a maximum resistance of approximately six ohms.

Six diodes were tested and they were found to give the same response with a variation of not more than one ohm variation from diode to diode over the frequency range. (See Appendix B for the listings of the impedances)

The theoretical equivalent circuit as shown in the data sheet is shown in figure 4.13

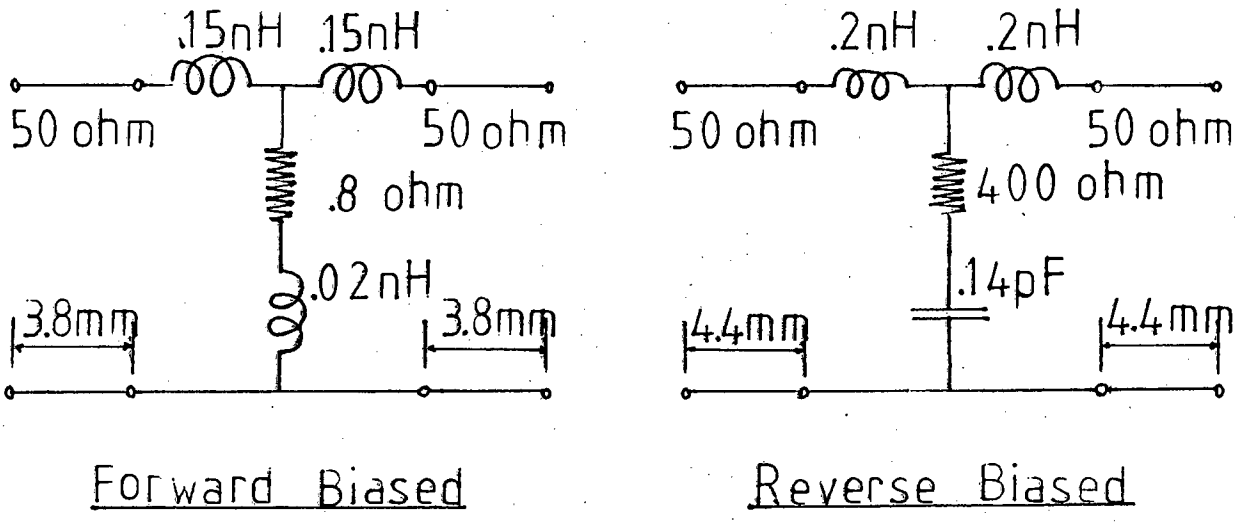

Figure 4.13 The Theoretical equivalent circuit of the HP 3141 PIN diode

4.6 The Beam lead series mounted PIN diode

Two slightly different beam lead devices were available; 1) ALPHA INDUSTRIES DSG6474 silicon oxide passivated beam lead and 2) MA-47301 which is a silicon nitride passivated beam lead. See Appendix B for specifications.

These devices are extremely small as can be seen on the specification sheets. This leads to the small parasitic components but the handling of these devices are difficult and great care has to be taken in fixing them into position. A few different methods were tried with low temperature solder and a hot plate, however the best system is to use ordinary solder with a very small temperature controlled soldering iron. The soldering was done under a microscope.

The S-parameters were not measured for design purposes. The theoretical model as shown in figure 4.5 was used to generate the S-parameter files for the reverse and forward biased cases.

Program 8 as shown in Appendix A was used for this purpose. The component values used are not exactly the same as those stated in the specification sheets. The worst case values were used which still resulted in the measured response looking like the predicted response as shown in chapter 6 for the SP4T switch.

4.7 Discussion

The series mounted diode operates in a reverse manner to the shunt mounted diode regarding the biasing. For forward biased conditions there is a transmission of microwave signal from the input to the output. This becomes significant when the series mounted diodes are used together with shunt mounted diodes.

The power handling capacity of the series mounted diode is far lower than that of the shunt mounted type. (Power dissipation for the HP 3141 is 1 Watt and for the series mounted type is 250 MilliWatts). Isolation is generally better for the shunt mounted diode. Switching times vary depending on the diode construction but no tests were carried out on switching speeds.

It must be noted that only small signals are being tested thus the reverse biased condition on all the diodes discussed can be achieved by applying zero bias.

5. THE SINGLE POLE SWITCH USING SHUNT MOUNTED DIODES

A single pole double throw (SPDT) switch was initially of main interest. A transmission line layout of the switch is shown in figure 5.1.

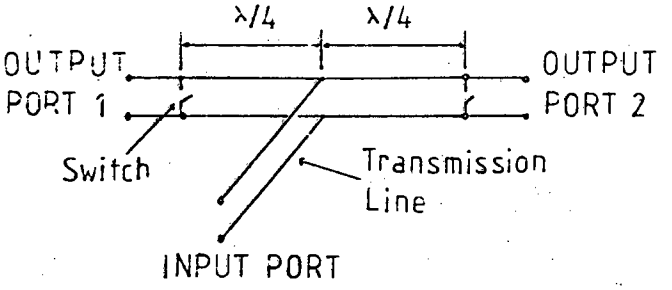

Figure 5.1 A transmission line layout of the SPDT switch

When one switch is closed (ie the transmission line is short circuited) the quarter wavelength section transforms the short circuit to an open circuit at the junction. This causes all the signal at the input port to travel through to the output port which has the open switch. The major problem is that the quarter wavelength sections are only quarter wavelengths at one particular frequency, but if the impedances were altered and an impedance matching section was inserted in the input port line, then a broadening of the bandwidth results. [20]. Figure 5.2 shows the response of a SPDT switch with 35 ohm quarter wavelength sections as shown in figure 5.1 with an additional 35 ohm quarter wavelength section in the input port line connected directly onto the junction.

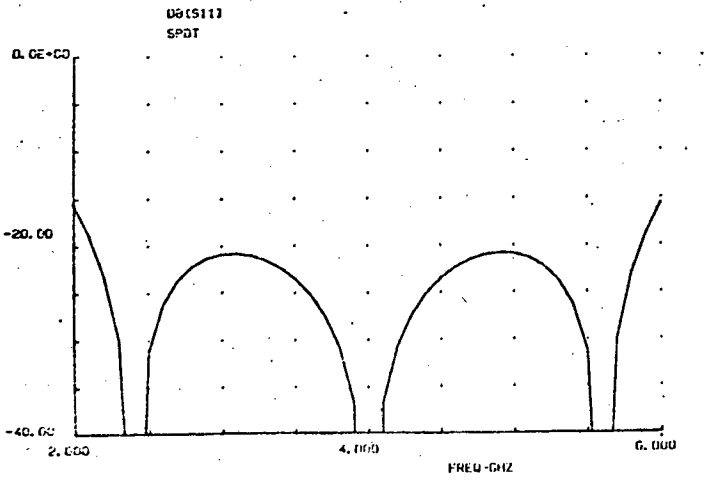

Figure 5.2 The response of a broadbanded SPDT switch

The microstrip layout is shown in figure 5.3 where the 3 5 ohm sections are 4mm wide and 13.3mm long. (A quarter wavelength at 4GHz). The notch at the junction is to improve the response [4] page 111.

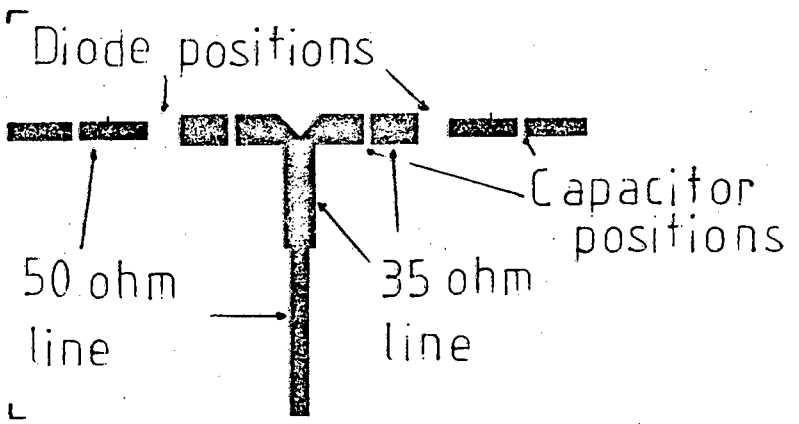

Figure 5.3 The microstrip layout of the SPDT switch

When one PIN diode is forward biased the circuit can be considered as a length of 35 ohm line section terminated on both sides by a 50 ohm line with a 35 ohm short circuited stub situated midway along the lower impedance line.

A single Pole three throw switch was investigated in software and it was found that, even after optimization, the frequency bandwidth never reached that of the SPDT configuration. The best response that was obtained is shown in figure 5.4.

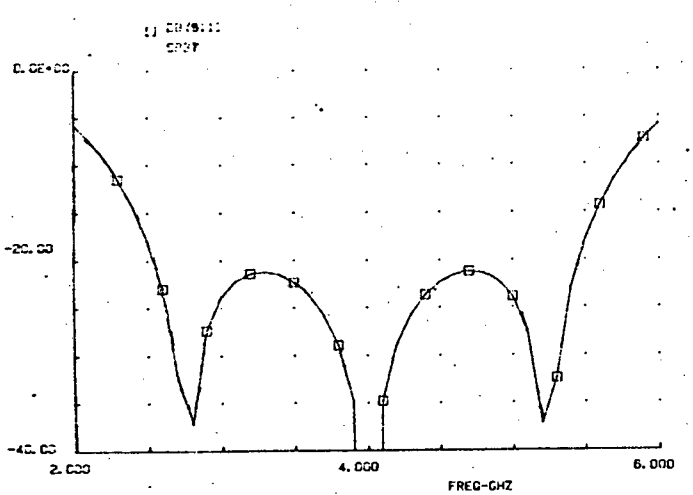

Figure 5.4 The theoretical response of a single Pole three throw switch using Shunt mounted diodes

Also the quarterwavelength lines did not remain at 35 ohms. The drawback of this is that multiple throw switches cannot be built up as required using lengths and impedances previously defined.

A possibility is to use the SPDT switch as a building block for multiple throw switches. See SP4T switch constructed with shunt PIN diodes.

5.1 The first SPDT switch fabricated

A SPDT switch as shown in figure 5.3 was fabricated. (Figure 5.3 is the artwork used in the manufacturing process) The exact dimensions are shown in Appendix C.

The SPDT switch with ideal components ie a physical short, 50 ohm through line and no capacitors, was tested to see how the response compares with the theoretical response. The two plots are shown in figure 5.5.

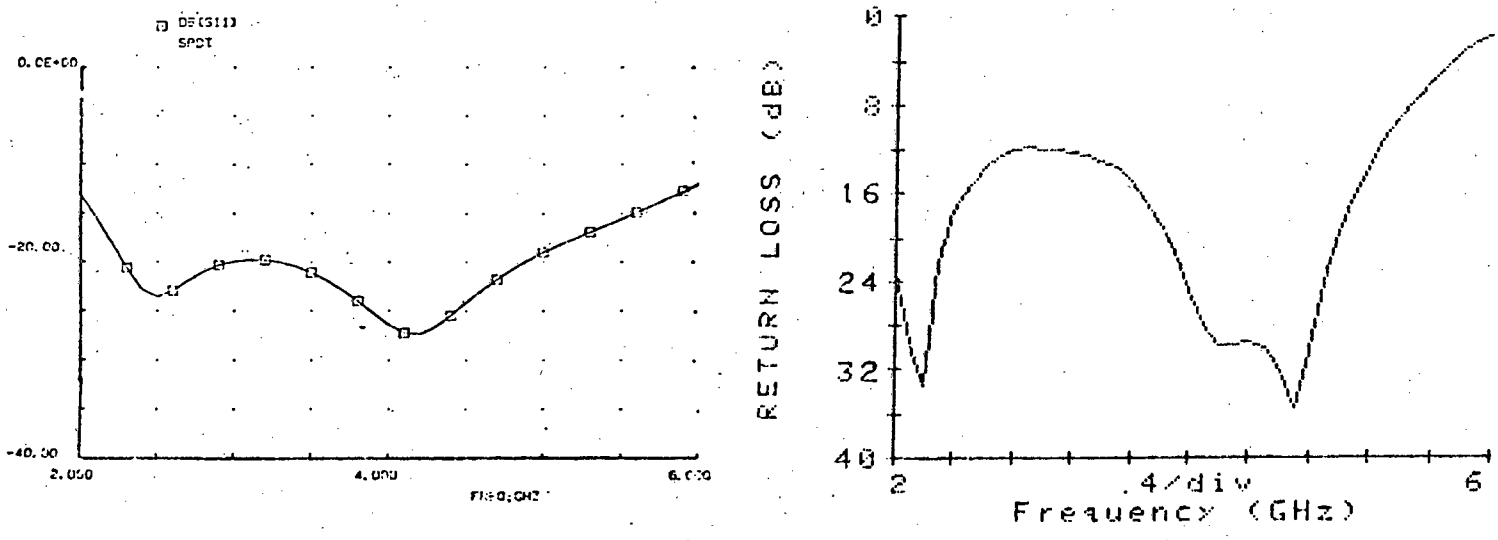

Figure 5.5 The comparison of the measured and predicted SPDT switch with ideal components

The theoretical response generated on TOUCHSTONE is shown on the left, the plot on the right is the measured response.

The TOUCHSTONE program is shown in Appendix A Program 9. The measured response agrees with the predicted response in shape but not in magnitude. The return loss drops to approximately 12dB in the middle of the range. Also the entire frequency response is shifted down by about .6GHz. When 22pF DC blocking capacitors are soldered into place over 1mm gaps in the 35 ohm transmission lines the response is substantially worsened as shown in figure 5.6.

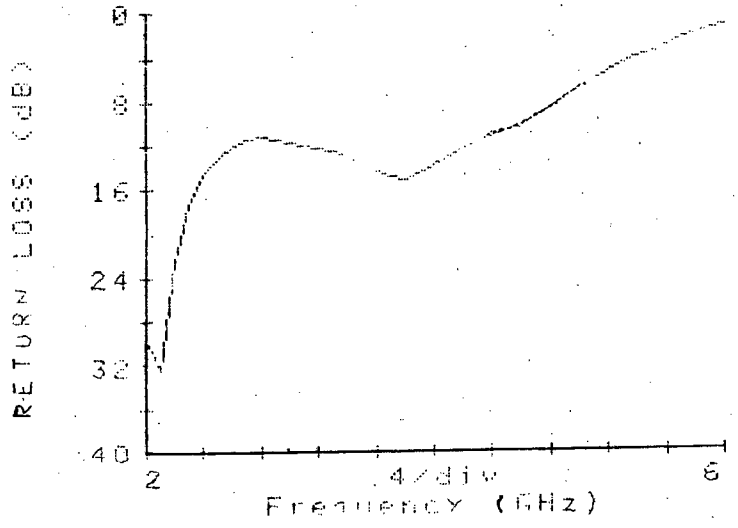

Figure 5.6 The SPDT switch with ideal components and DC blocking capacitors.

This could be due to the capacitors themselves or the size of the microstrip gaps over which they are soldered or the soldering techniques used. Also the notch at the junction has an effect on the response. It was found that by removing the notch when the capacitors were inserted improved the response slightly.

One PIN diode was inserted in the place of the physical short. This allowed forward biasing to take place through the biasing ports of the s-parameter test set, which results in no capacitors being mounted. Program 10 (Appendix A) predicts this response where the measured s-parameters of the forward biased PIN diode are used. Figure 5.7 displays the predicted and the measured response respectively.

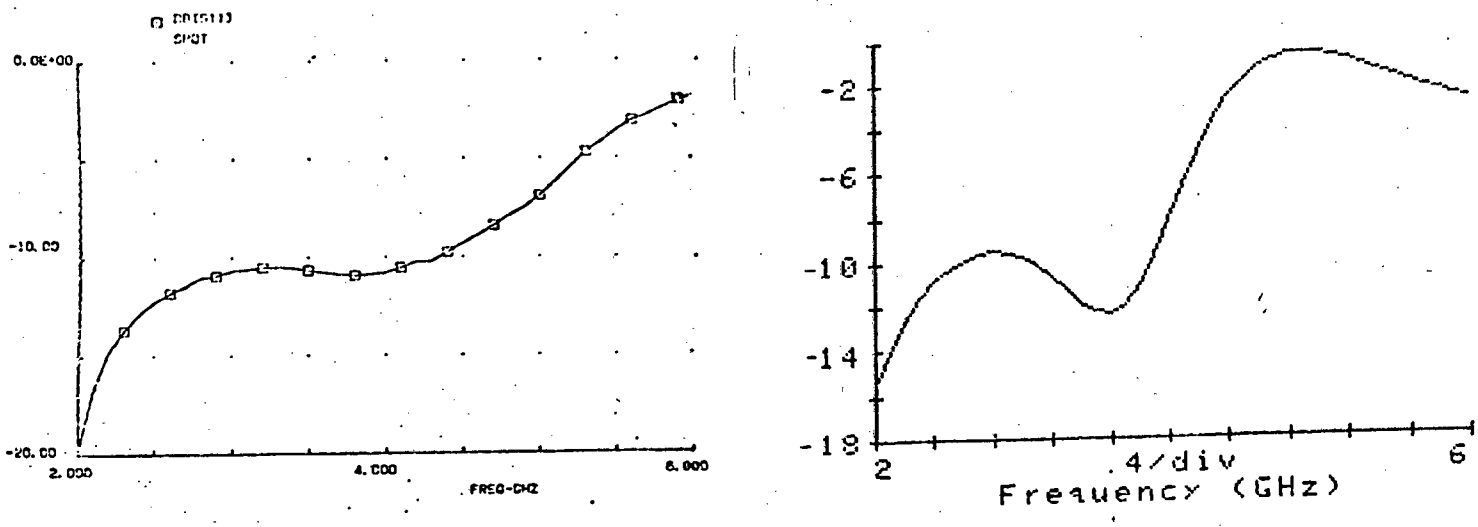

Figure 5.7 The SPDT switch with one forward biased PIN diode and no capacitors

Figure 5.8 shows the measured response of one reverse biased PIN diode and a physical short. In actual fact the diode had zero bias applied, because the sweep generator only supplies 10 dBm of power.

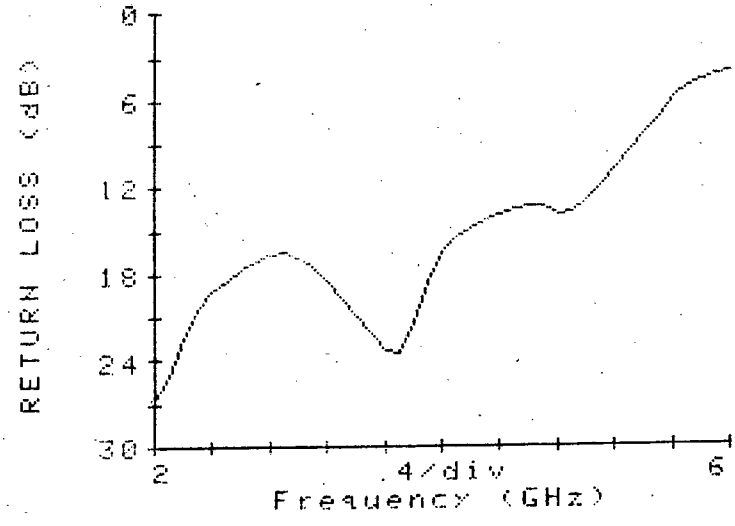

Figure 5.8 The SPDT switch with one reverse biased PIN diode and a physical short.

The theoretical models of the HP3141 diode as shown in figure 4.13 was inserted into the programs to replace the measured s-parameters to see if the predicted response would follow the measured response more closely. It was found that the

difference between the theoretical response generated with the use of the PIN diode model was very similar to that predicted, using the measured s-parameters of the diodes.

The conclusion that was made is that TOUCHSTONE can be used to develop circuits but the theoretical results generated only give an approximation to the real response. This allows a computer analysis of circuit configurations to be optimised and will show which circuits offer wider bandwidths. However, the exact bandwidth of the insertion loss, return loss and isolation cannot be predicted.

The response of the SPDT switch with ideal components as shown in figure 5.5 does not have the required bandwidth. The basic circuit has to be developed further.

5.2 Development of the SPDT switch with the use of stub matching.

The PIN diodes are not perfect short circuits and open circuits. This is mainly due to the parasitic components. It is thought that stub matching can be used to match out the parasitic components of the diodes as well as to broaden the bandwidth of the basic circuit.

The equivalent impedances for the forward and reverse biased HP3141 PIN diode calculated directly from the model is:

For the forward biased case

$$ZIN = 0.865 + j\ 4.248$$

For the reverse biased case

$$ZIN = 46.53 + j\ 6.73$$

To match out a reactance of j 4.248 a reactance of - j 4.248 must be added in the form of an open circuit stub.

From the open circuit stub equation

$$ZIN = - jZ_o \cot 2\pi\ell$$

For Z_o = 84 ohms $\ell = .242\lambda$

The problem is that a stub required for the forward biased case is not the same as that required for the reverse biased case. Therefore the easiest and simplest way of designing is to use a software program such as TOUCHSTONE where extensive use is made of the optimization routine.

5.2.1 The design process that was followed

Ideal lossless transmission lines were initially used to give an indication of the best configuration to develop further with the microstrip software commands.

The basic SPDT switch with the theoretical PIN diode models was first optimized as shown in Program 11. A fairly broadband response was obtained as illustrated in figure 5.9(a). The line lengths between the diodes and the junction are decreased from the quarter wavelength due to the PIN diodes having a small section of 50 ohm line as shown in figure 4.13.

The 50 ohm transmission line in the model is approximately 26 degrees in the forward biased case and 30 degrees in the reverse biased case at 4GHz. Therefore a 60 degrees length is required to make up a quarter wavelength section. The TOUCHSTONE program verified this.

Open circuit stubs were introduced at the point next to the PIN diodes on the 35 ohm line. Program 12 illustrates this. The response shown in figure 5.9b resulted. The trace shown with squares is that of the response using the measured s-parameters of the PIN diodes. Other stubs were then introduced on the other side of the diodes resulting in the plot shown in figure 5.9c. Program 13 was used to generate this response.

Program 14 was used to optimize the response of a SPDT switch with a stepped impedance change in the quarter wavelength sections between the junction and the diodes. The response is shown in figure 5.9(d).

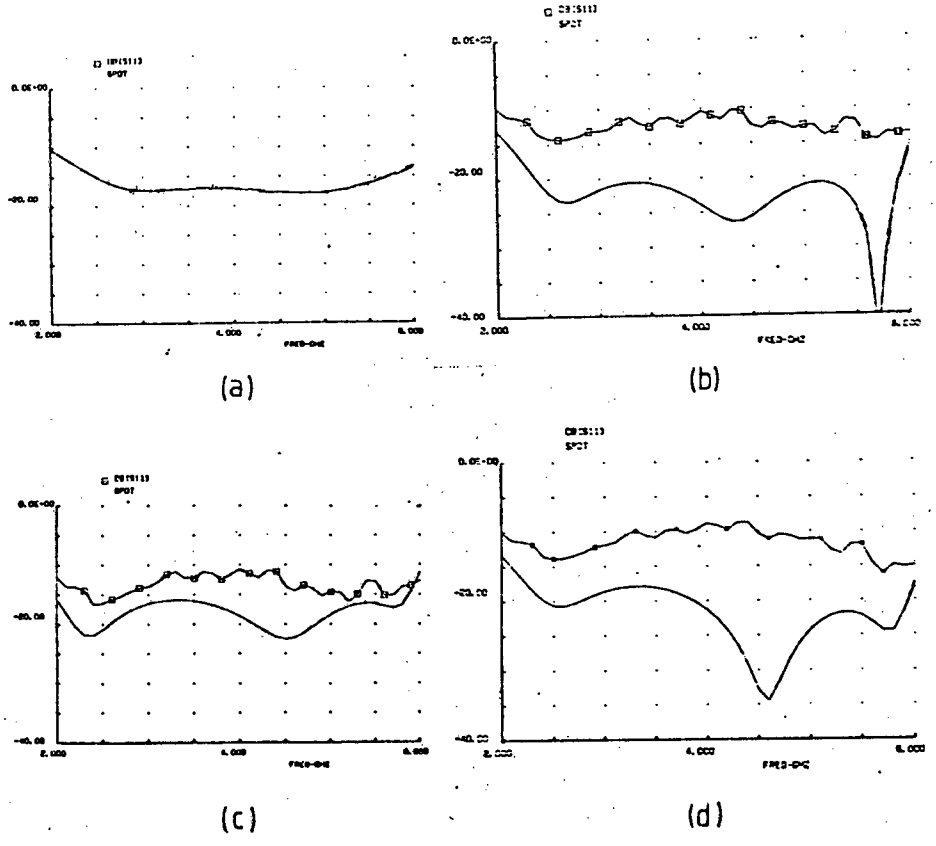

—□— Response obtained by using the measured s-parameters of the PIN diodes

——— Response obtained using the PIN diode theoretical model

Figure 5.9 Responses obtained using different Stub matching configurations in the SPDT switch.

Different combinations were tried, and it was decided that the SPDT switch with open circuit stubs on the low impedance side of the PIN diodes held the most promise for further development. Figure 5.9b displays a large discrepancy between the responses using the PIN diode models and the measured s-parameters for the diodes, but it was hoped that the real response lies somewhere between the two.

5.3 The second SPDT switch fabricated

The circuit described in Program 12 (response shown in figure 5.9b) was transformed into a microstrip circuit, as shown in Program 15, to obtain higher accuracies. Extensive optimization was employed to obtain the results shown in figure 5.10.

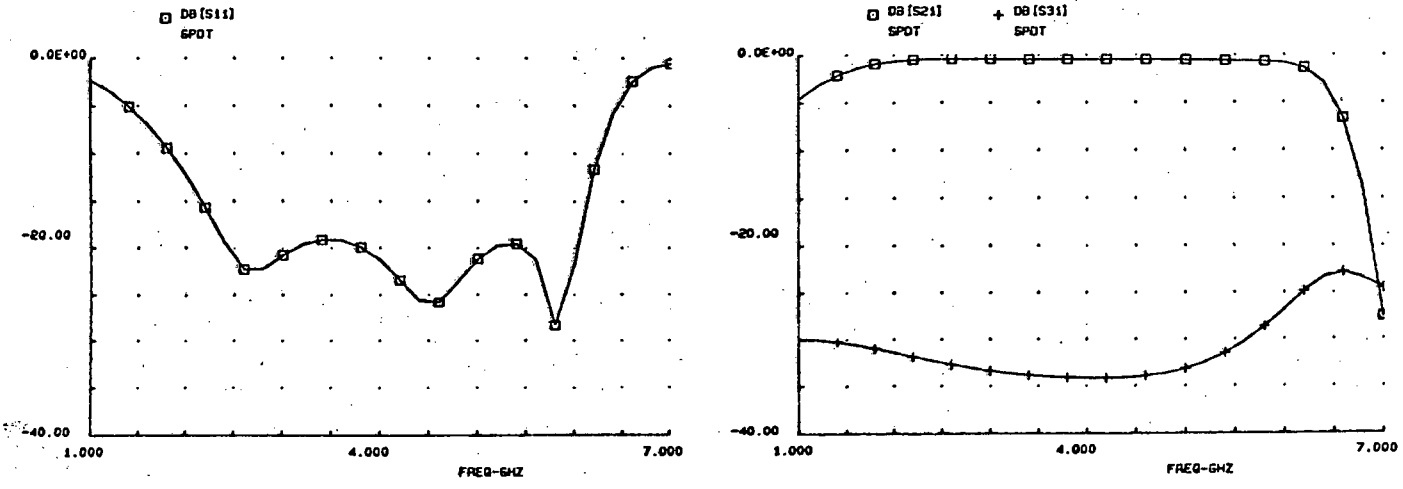

Figure 5.10 The optimized SPDT microstrip circuit

The autoCAD software which is a draftsmans package was used to draw the microstrip circuit to the highest possible accuracy. The drawing was photo-reduced by a factor of four to increase the accuracy further. The microstrip layout is shown in figure 5.11. The matching stubs were angled to keep them clear from the machined grooves which facilitates the mounting of the PIN diodes. The exact dimensions are shown in Appendix C.

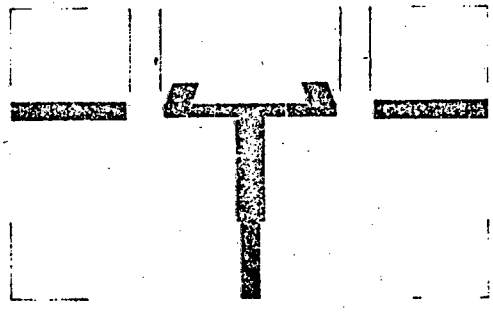

Figure 5.11 The microstrip layout of the second SPDT switch

After optimization the resulting branch impedances are higher than 35 ohms. Due to the nature of the optimization process there is no logical impedance matching process that can be followed on a Smith Chart or any other means. The results generated is based on a trial and error process which obtains the best response for the given configuration and constraints. It does this by systematically changing the length and impedance of the transmission line elements and checking the resulting response until the required constraints are achieved. This is not a fool proof method because it might not be physically possible to obtain the desired response for a given circuit.

The entire circuit was fabricated with the DC blocking capacitors (ATC-A 22pf) as well as the bias circuits. The ferrite cores with lengths of thin wire was used for biasing. The measured response is shown in figure 5.12. The traces in the return loss plot was generated by each of the two channels biased in turn for transmission. Figure 5.12 b and 5.12 c illustrates the measured isolation and transmission respectively.

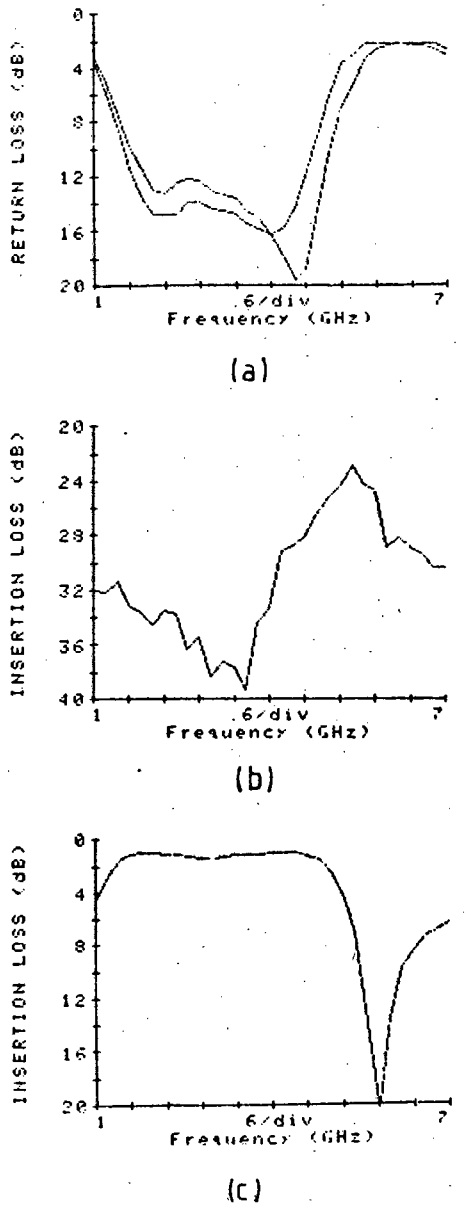

Figure 5.12 The measured response of the second SPDT switch using shunt mounted diodes

When a comparison is performed between the predicted response (as shown in Figure 5.10) and the measured response it can be seen that the measured response is shifted down in frequency and does not obtain the return loss predicted. The frequency bandwidth of one and a half octaves is reached if the bandwidth is defined as the return loss beter than 10dB in the measured case.

TOUCHSTONE predicted that the response should not be degraded by the DC blocking capacitor as shown in figure 5.6. Different capacitors were tried in different positions along the quarter wavelength. It was found that the 22pF capacitors gave the best results and the exact position and orientation did not have a marked effect on the overall response.

The soldering process seemed to have the largest influence on the results. If the measured response looked totally different to the predicted response then the capacitors were removed and resoldered, which would usually improve the result. Also different gap widths, over which the capacitors were soldered, were tried. It was concluded that the actual soldering was more important than the gap size and the capacitors must be soldered so that there is minimal gap between the capacitor and the dielectric substrate. The best capacitors for this purpose would be the Gapcaps as shown in Appendix C but none were available for testing.

5.4 The third SPDT switch fabricated

The measured response of the previous SPDT switch is shifted down in frequency when compared to that of the designed circuit. It was thought that if the circuit was designed with a frequency offset then the required response would be obtained. TOUCHSTONE was used to optimize the bandwidth from 2.25 GHz to 7.5 GHz to generate the response shown in figure 5.13.

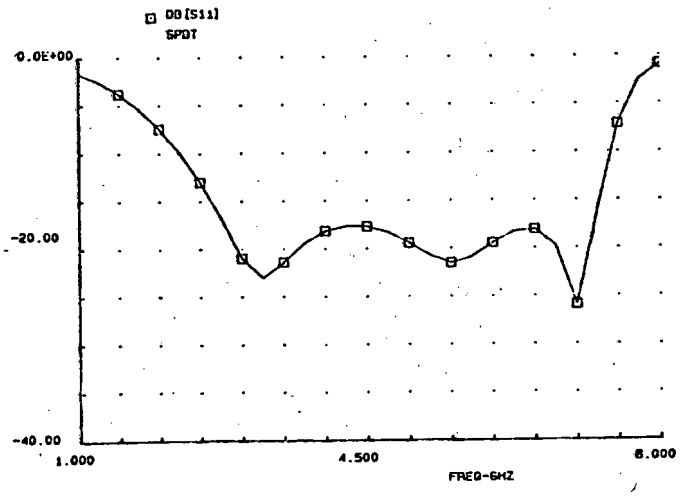

Figure 5.13 The theoretical response of the third SPDT switch

The microstrip layout is shown in figure 5.14, the exact dimensions of which are shown in Appendix C.

The measured response is shown in figure 5.15.

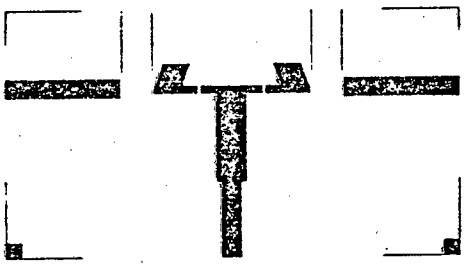

Figure 5.14 The layout of the third SPDT switch

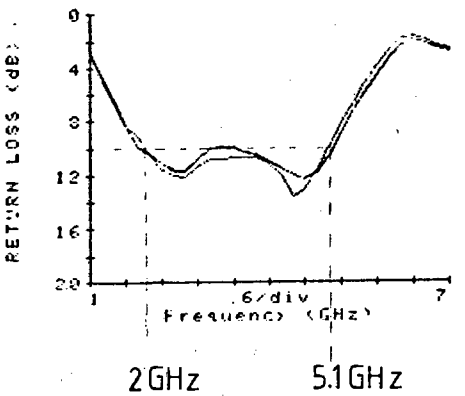

(a)

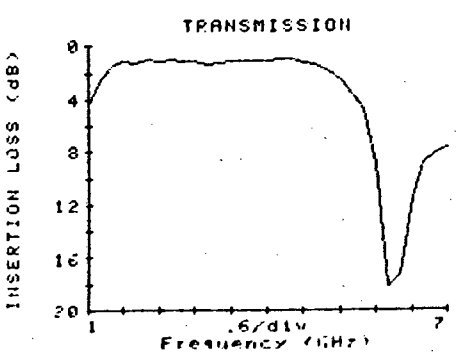

(b)

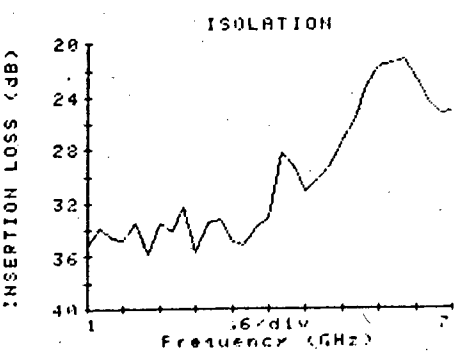

(c)

Figure 5.15 The measured response of the third SPDT switch

The response of the third SPDT switch has no improvement over the second switch. The reasons for this are thought to be;

1) The DC blocking capacitors used do not operate above 5GHz.
2) The PIN diode models and s-parameters are inaccurate.
3) Inaccuracies were introduced in the fabrication process.
4) Inaccuracies in the software package for T-junction and open circuit stub corrections.

5.5 The Single Pole Four Throw (SP4T) switch constructed with shunt PIN diodes.

The microstrip branches are different for different numbers of throws in a switch as discussed previously. A means of using SPDT switches for building up multiple pole switches which have an even number of output ports are considered.

The SPDT switch is used as a building block and in the software development the theoretical s-parameters of the third SPDT switch was used. (See Program 16). Additional matching stubs were placed between the building blocks to try and improve the response further. The theoretical response is shown in figure 5.16, the microstrip layout is shown in figure 5.17 and the measured response in figure 5.18.

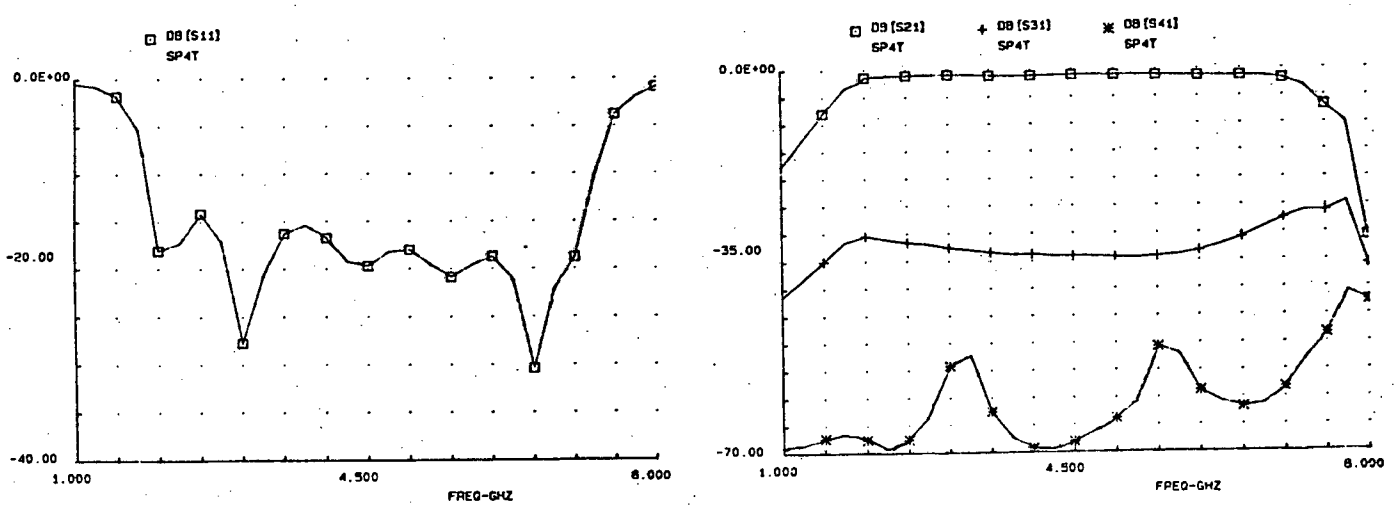

Figure 5.16 The theoretical response of the SP4T switch

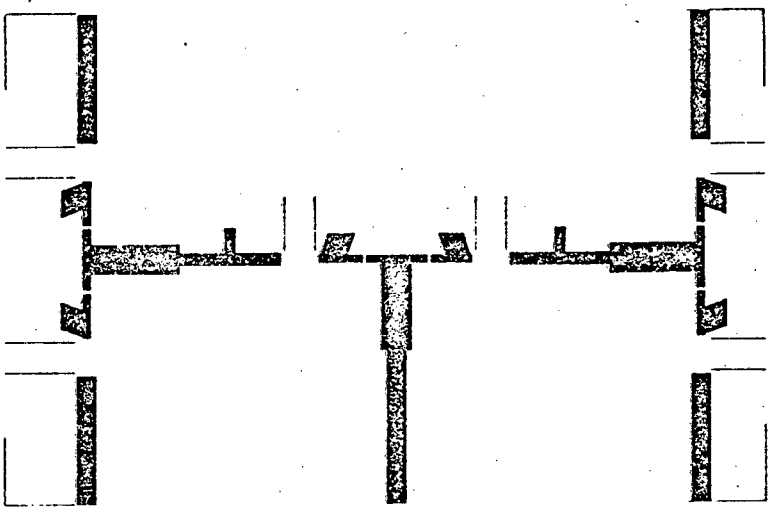

Figure 5.17 The microstrip layout of the SP4T switch

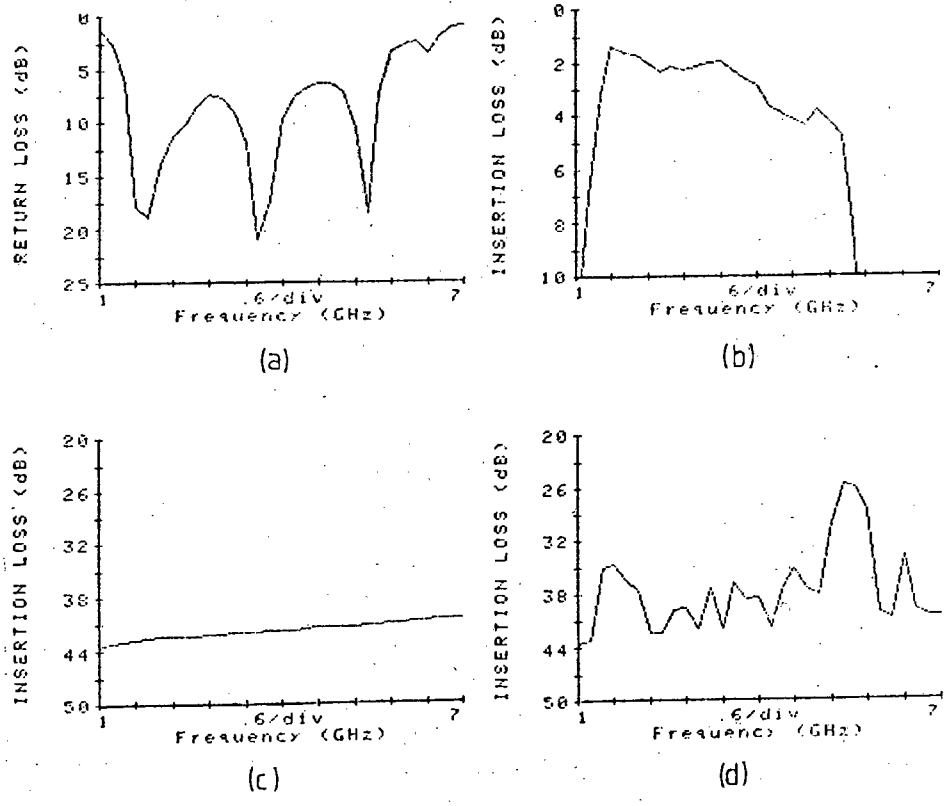

Figure 5.18 The measured response of the SP4T switch

The measured response is poor. The return loss extends below 10dB (ie a VSWR worse than 2:1). The responses from all ports switched on in turn are very similar therefore it is not necessary to display all of them. The isolation does not follow the predicted curves. The reasons could include those as mentioned in section 5.4 as well as the bias lines do not perform as required.

The major disadvantage of this system is that the isolation of the switched off ports are not all the same. ie The isolation for a port on the same SPDT switch that has the ON path is lower than for the port that have two forward biased diodes in their path.

6. THE SINGLE POLE SWITCH USING SERIES MOUNTED DIODES

The basic switch using series mounted diodes is inherently broader in bandwidth compared to the shunt mounted case due to the fact that there are no line lengths that determine their operation. The only frequency dependant components are the parasitic components of the PIN diodes, which are much smaller than in the packaged shunt diode, but which still degrade the response as the frequency increases.

The theoretical model of the series PIN diode, as described in chaper 4, is used in the TOUCHSTONE program (number 17) to generate the response of a SP4T switch. The number of throws of a switch alters the response slightly if at all. The only limiting factor is how close together the microstrip lines can be placed at the junction. The layout of a SP4T switch with 50 ohm lines is shown in figure 6.1, the theoretical response of which is shown in figure 6.2.

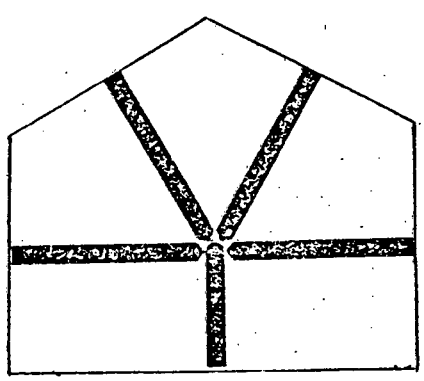

Figure 6.1 The microstrip layout of a SP4T switch using series mounted diodes

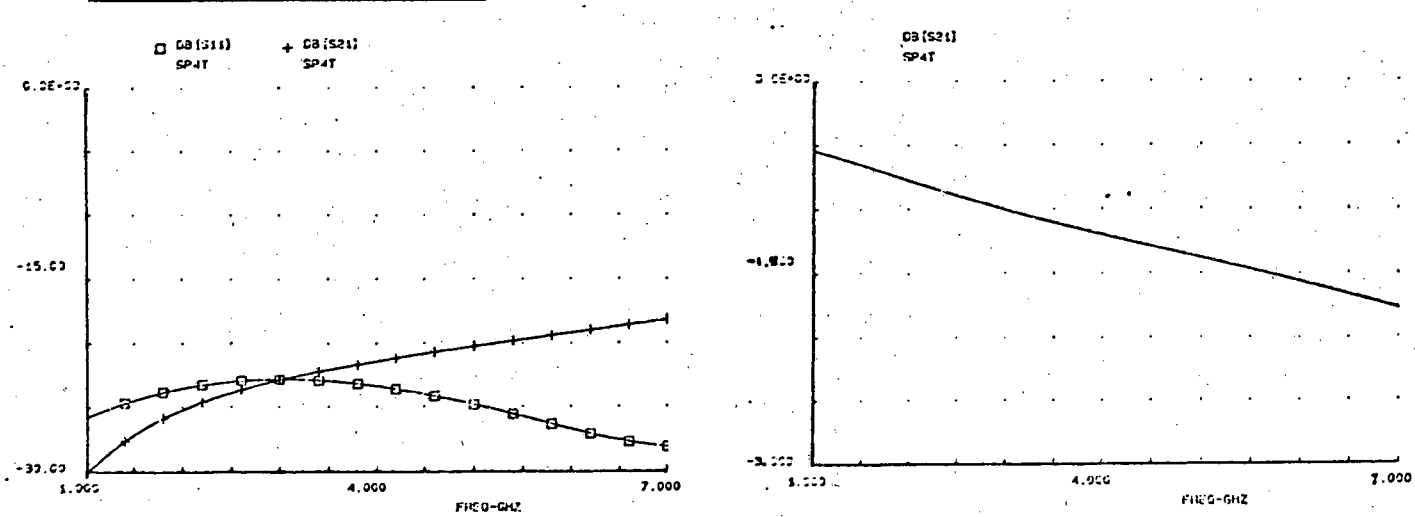

Figure 6.2 The theoretical response of the SP4T switch using series mounted diodes

Both the Alpha 6474 and the MA47301 were tested. Firstly one diode was soldered into place to make up a single pole single throw switch. The tests were run to give the results shown in figure 6.3. The forward bias current was set at 12mA. Figure 6.3b illustrates the isolation of an OFF path and figure 6.3c shows the insertion loss of an ON path when the second, third and fourth diodes were inserted. The responses did not change noticeably when more paths were added to the switch. This is true for both types of diodes.

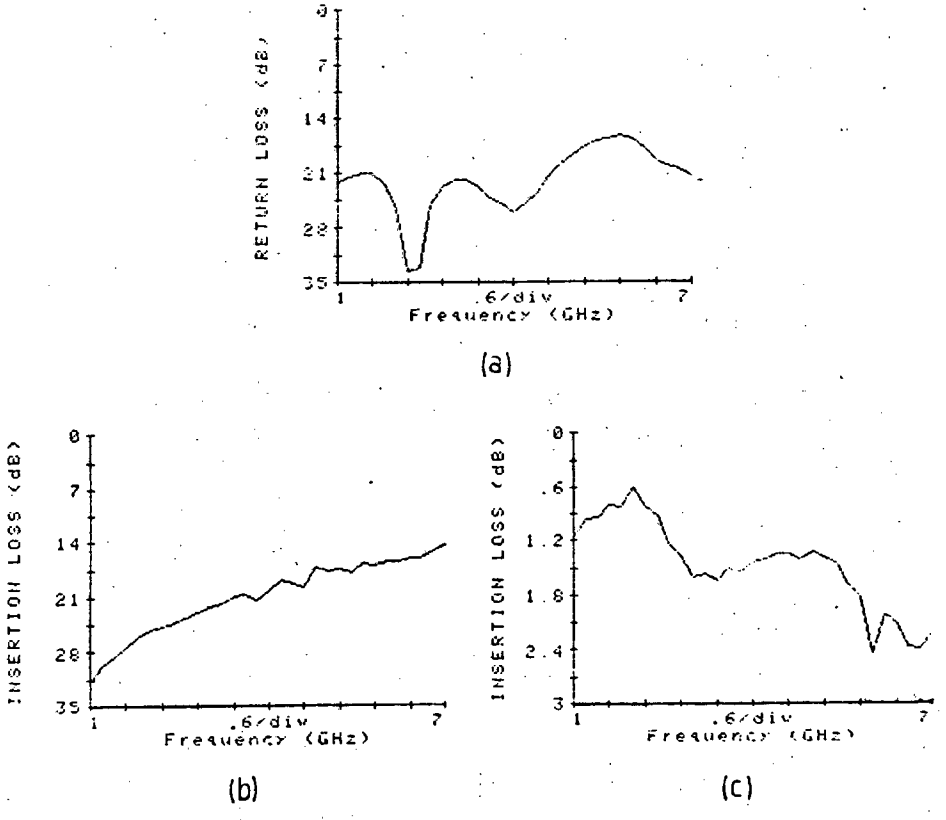

Figure 6.3 The measured response of the SP4T switch containing series mounted diodes.

The measured response is similar to the predicted response which implies that the model used for the series mounted PIN diode is accurate enough to develop other circuits. The return loss plots do not follow one another exactly but they are both better than 15dB.

6.1 Discussion

The switches containing the series mounted diodes are advantageous in that they are simpler in construction and broader in bandwidth. The isolation for an off path in the shunt mounted diode switch is higher than in the series mounted case. The optimum bandwidth that was obtained in the shunt mounted case was just over one octave (2GHz to 5.1 GHz). In the series mounted case a bandwidth of 1 GHz to 7 GHz is easily obtainable with the isolation ranging from 32 dB to 15 dB respectively.

The major disadvantage with series mounted diodes is the limited power handling capacity due to the poor heat sinking. The maximum power rating is in the order of 250 milli-Watts. However the shunt mounted diodes are mounted directly onto a heatsink which enables them to handle powers in the region of Watts. (The MA-4P505 shunt diode is rated at a maximum power capability of 10 Watts but has slower switching speeds compared to lower power shunt mounted diodes).

7. ISOLATION

A major constraint of the multiple pole switch is to present an isolation of more than 60 dB for a switched off path. The isolation of an OFF path in the shunt mounted diode switches varies between 34 dB and 20 dB and in the series mounted case between 32 dB and 15 dB. It is therefore a common problem in both these circuits.

To achieve the required isolation more than one diode in each branch is necessary. Diodes can be connected together in microstripin various series and shunt combinations. There are numerous configurations all of which must be fully investigated, therefore there is a separate chapter on isolation.

7.1. The investigation of the different diode combinations

A simplification is made to the analysis by considering the diodes as resistors. Consider two small resistors situated a certain fraction of a wavelength apart on a 50 ohm transmission line. Reference [19] page 24 shows that for shunt mounted diodes, a quarter wavelength separation gives the highest possible isolation. Even though quarter wavelengths are involved the isolation is fairly broad in bandwidth as shown in figure 7.1 where not more than a ten percent fluctuation occurs over two octaves.

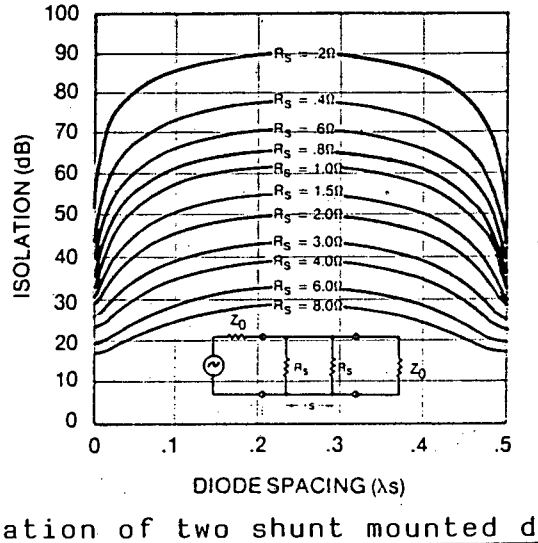

Figure 7.1 Isolation of two shunt mounted diodes (from [19] page 24).

When a series mounted reverse biased diode is followed by a shunt mounted diode as shown in figure 7.2 the isolation varies between 31 dB and 55 dB when the separation is varied between a quarter wavelength and a half a wavelength respectively. A frequency analysis with the full diode model is performed later where the separation is set to zero.

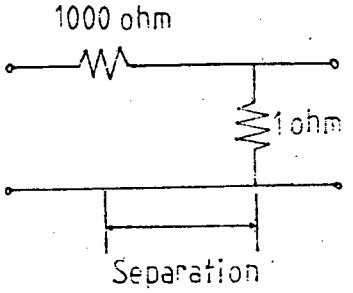

Figure 7.2 Series and shunt mounted diodes situated on a transmission line with a certain distance of separation.

If a series mounted diode is placed a quarter wavelength from another series mounted diode then an isolation of 47 dB results which drops to 26 dB if the separation is increased to half a wavelength.

The method of how these isolations are calculated is illustrated in the following example. Two low impedances situated a quarter wavelength apart are connected onto a 50 ohm transmission line as shown in figure 7.3 a.

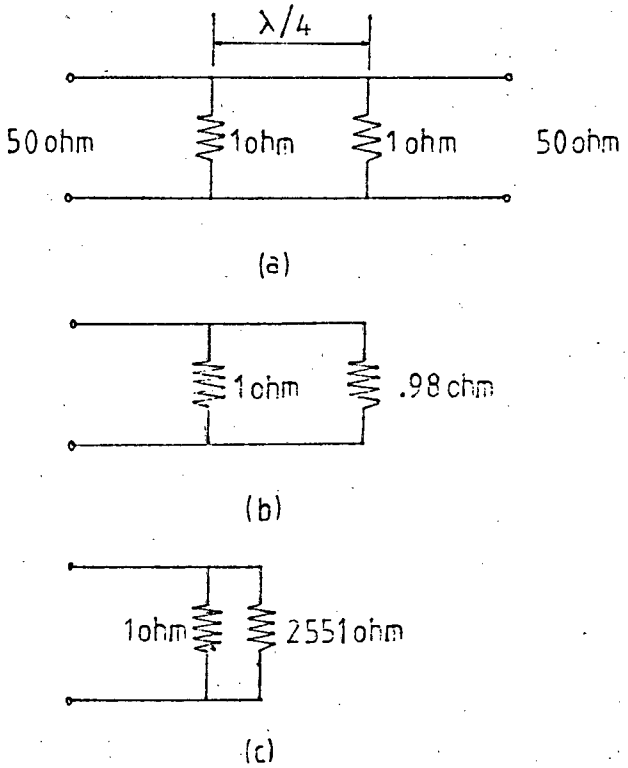

Figure 7.3 Two low impedances situated λ/4 apart on a transmission line.

In figure 7.3 a) the 1 ohm and the 50 ohm resistances are in parallel. Figure 7.3 b) results where a 1 ohm and a .98 ohm resistance are spaced a quarter wavelength apart. When the quarter wavelength transformation is done figure 7.3 c) results. Therefore the effective resistance seen at the termination is 0.9996 ohms. This results in a reflection coefficient of 0.9608.

$$\text{Power reflected} = \rho^2 = .923 \text{ Watts.}$$

If 1 Watt of power is applied at the input then .076 Watts is transmitted onto the resistances. This transmitted power is distributed to the 1 ohm and the 2551 ohm resistors in the ratios 2551/2552 and 1/2552 respectively. The power is then distributed again onto the 1 ohm and the 50 ohm resistors in the ratio 50/51 and 1/51 respectively. Therefore the power transmitted onto the 50 ohm line after the two 1 ohm resistors is .58 micro-Watts which results in 62 dB of isolation, which is more than double the isolation presented by one 1 ohm resistor.

TOUCHSTONE was used to investigate the frequency response. The theoretical s-parameter files for the series mounted diodes were used and optimization of the diode separation was performed.

Program 18 analysed the series mounted diode followed by a shunt mounted diode in a SP4T configuration. The best isolation was obtained when there was no separation between the diodes, as shown in figure 7.4a. In practice the shunt mounted PIN diode package does not allow this to be physically realizable. When the distance was set at half a wavelength a separation of 16.24mm was found to be optimum. This response is shown in figure 7.4b. When this separation is added to the parasitic line length in the shunt mounted diodes the total length is approximately 2/5 of a wavelength.

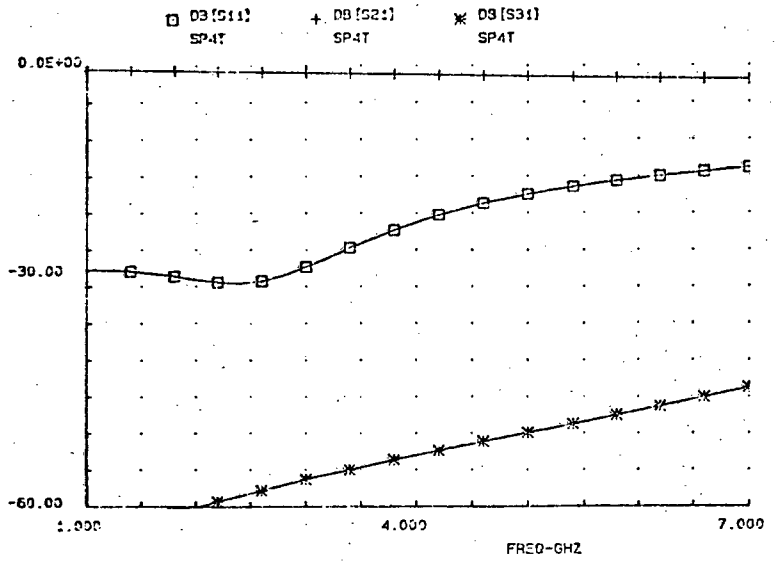

(a)

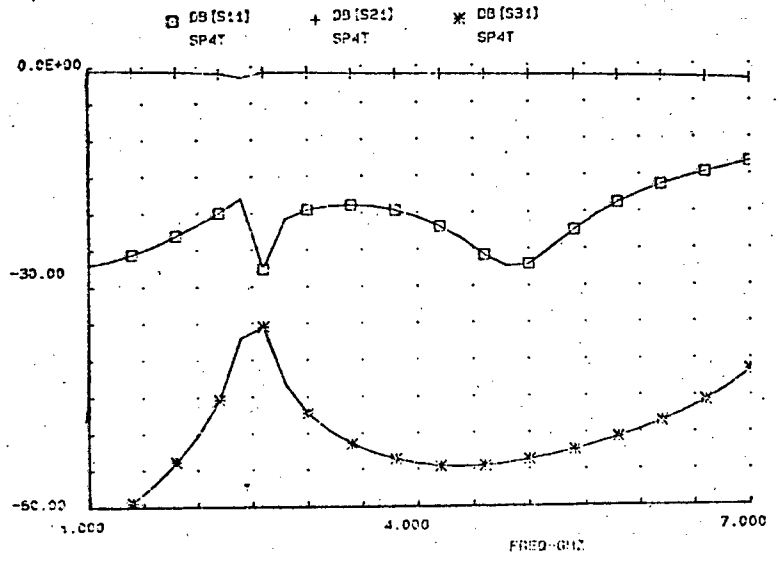

(b)

Figure 7.4 Response of the SP4T switch which consists of series mounted and shunt mounted diodes.

The TOUCHSTONE response with two series mounted diodes following one another in each branch of a SP4T switch is shown in figure 7.5. A separation distance of 10mm was found to give the broadest response. This is shorter than the quarter wavelength used in the previous analysis. The difference in length is due to adjustments made to accommodate the parasitic components.

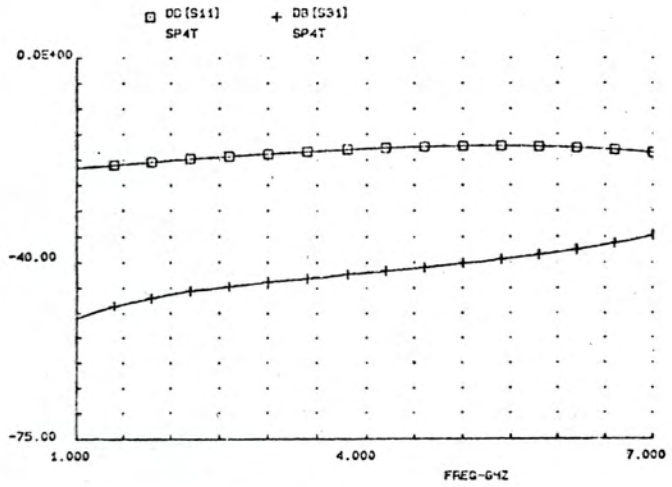

Figure 7.5 Response of the SP4T switch which consists of two series mounted diodes in each branch

7.2 The SP4T switch that was built using series and shunt mounted PIN diodes

A SP4T switch using MA 47301 and HP 3141 PIN diodes was fabricated as shown in figure 7.6. Ferrite beads were used for the bias circuitry. The shunt mounted diodes are screwed down into the machined slots.

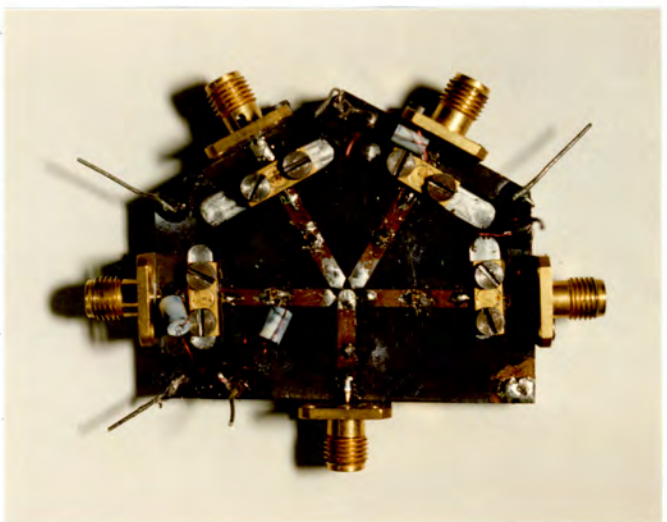

Figure 7.6 The SP4T switch that was fabricated using series and shunt mounted PIN diodes.

Only three ports were tested and transmission and isolation tests were carried out on each port in turn. Each diode was biased individually where the series PIN diodes were biased with approximately 15mA and the shunt PIN diodes with 40mA. The biasing currents were set higher than normally practised (usually set at 10mA) in order to obtain a low insertion loss for a transmission path and high isolation for a switched off path. With the correct orientation of the diodes all the diodes in one branch can be switched for either isolation or transmission simultaneously, in this case DC blocking capacitors were placed between the diodes to facilitate individual biasing.

The measured responses are shown in figure 7.7. The return loss does not follow the predicted response exactly but it is almost better than 10dB over the range. The plots for all the ports are similar except for the isolation. Figure 7.7c and 7.7d show the measured isolation for two different ports. All the other ports with different branches in the transmission mode are similar to one or the other.

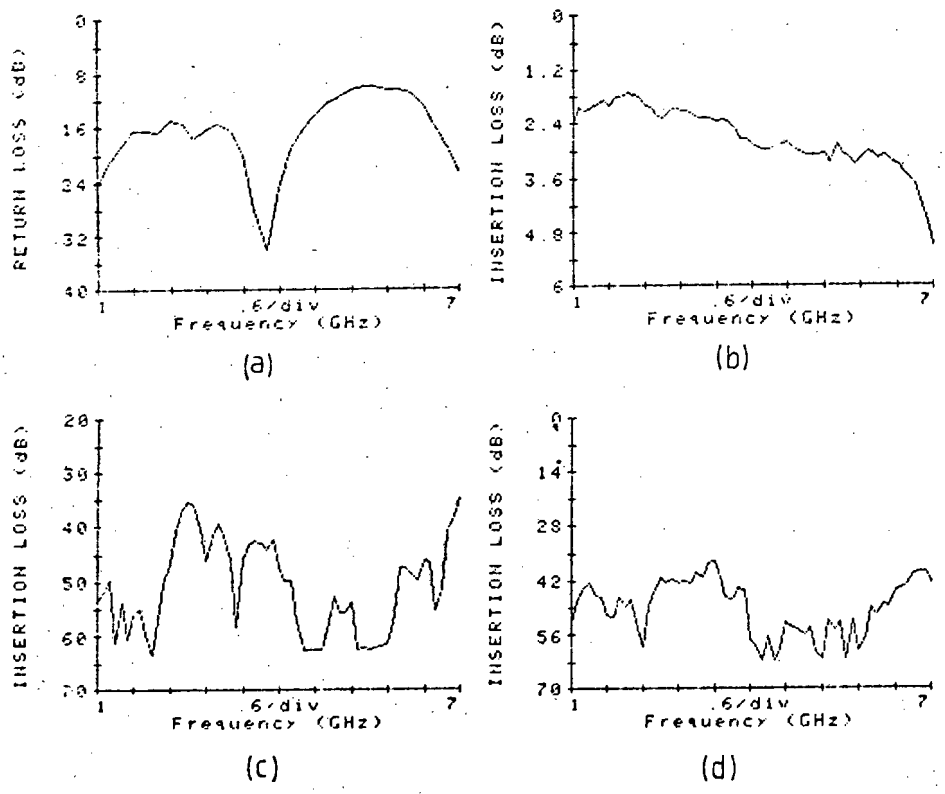

Figure 7.7 The measured response of the SP4T switch containing series and shunt mounted PIN diodes.

The measured isolation follows the trends predicted but there may be a number of reasons for the sharp dips and jumps in the curves.

7.3 The SP4T switch using three diodes in each branch

The isolation encountered thus far only approaches 60dB over part of the range. For the isolation criterion to be fulfilled a third diode has to be added to each path. The simplest switch configuration as far as construction and biasing is concerned, when dealing with the basic series mounted diode switch, is when only series mounted diodes are added.

When three series diodes mounted on a transmission line is analysed an isolation of 73dB is obtained. A TOUCHSTONE program (program number 19) generated the response for a SP4T configuration using three series mounted diodes in each branch. Figure 7.8 demonstrates that slightly better isolation is obtained over the range if the diode seperation is less than a quarter wavelength. (ie 10mm instead of 13.4mm)

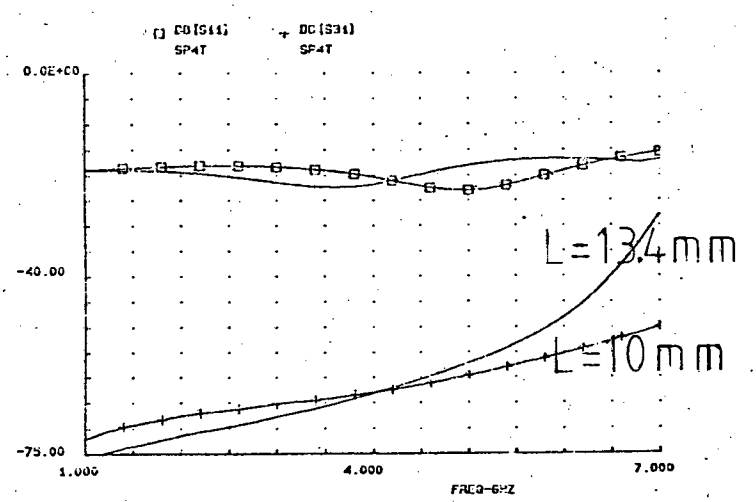

Figure 7.8 The theoretical response of the SP4T switch containing three diodes in each branch

The TOUCHSTONE program does not show an isolation of 73dB as predicted previously. This could be due to the parasitic components in the diodes as well as the interaction of the different paths in the switch.

7.3.1 Tests and discussion of the series mounted PIN diode switch

Diodes were mounted in only one branch of the SP4T layout as shown in figure 7.9. This was done because firstly, the diodes could be tested with minimal interaction or interference from other branches and secondly, to conserve the number of diodes used in the development process. The problem with the series mounted diodes is that once they are soldered into a circuit they are too small and fragile to be removed and used again. Three of the four paths of the SP4T switch were removed but the junction configuration was still maintained as shown.

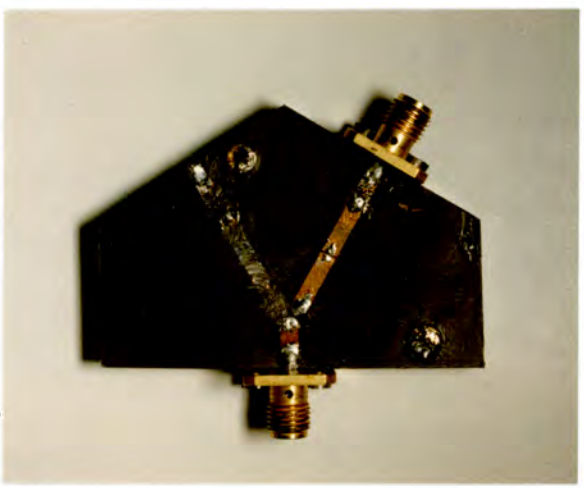

Figure 7.9 Microstrip layout for testing isolation of series mounted PIN diodes.

Figure 7.10 shows the measured response with one, two and then three diodes soldered into place to form a Single Pole Single Throw (SPST) switch. The insertion loss through the diodes increase by approximately .8dB as the number of diodes increase. The isolation increases from one to two diodes reverse biased but there is no improvement from two to three diodes over the range.

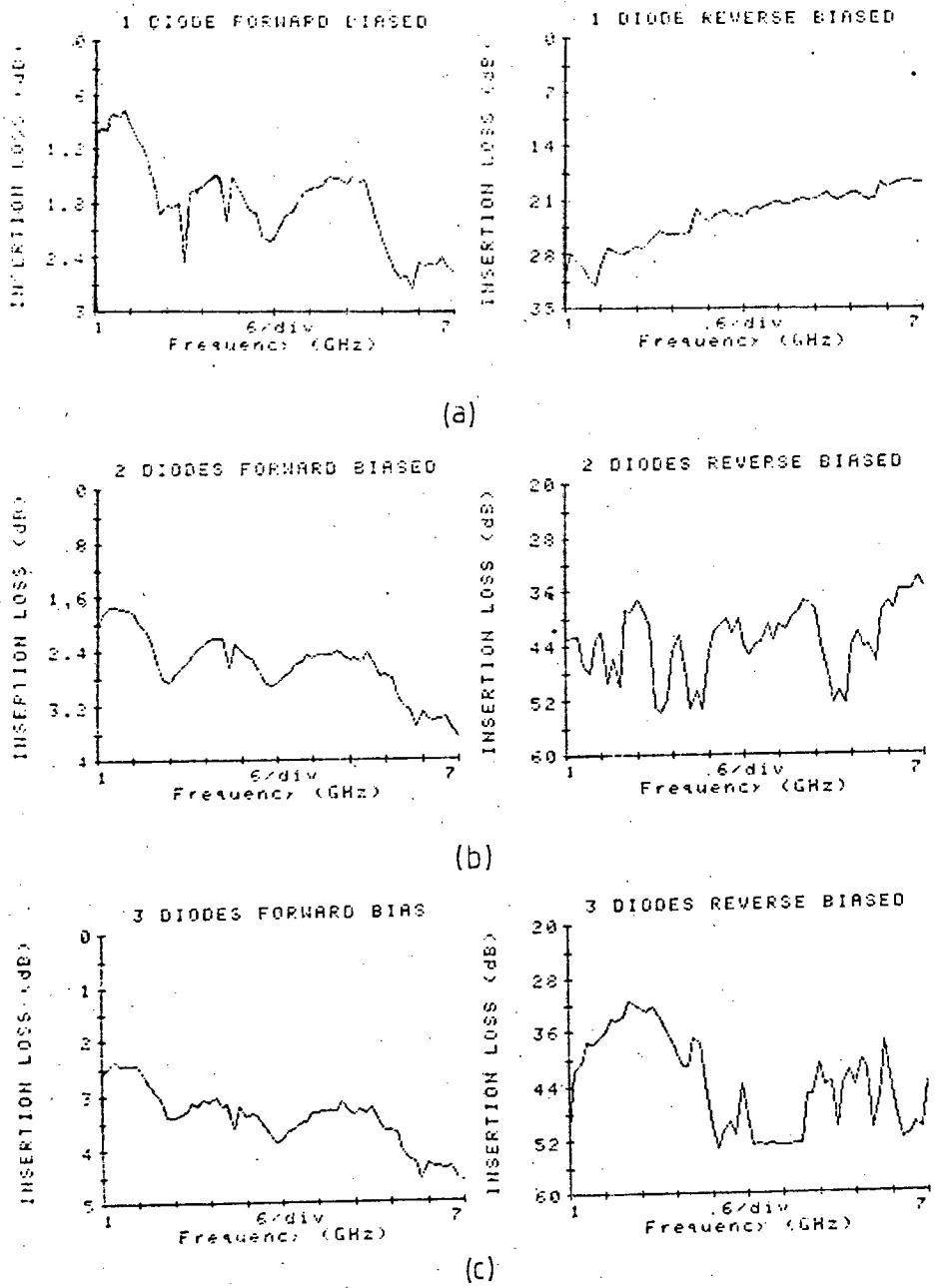

Figure 7.10 The measured response of one, two and three diodes in a SPST switch.

The bias circuitry (the ferrite bead with thin wire) was removed to cause the diodes to be in reverse bias. This increased the isolation considerably as shown in figure 7.11.

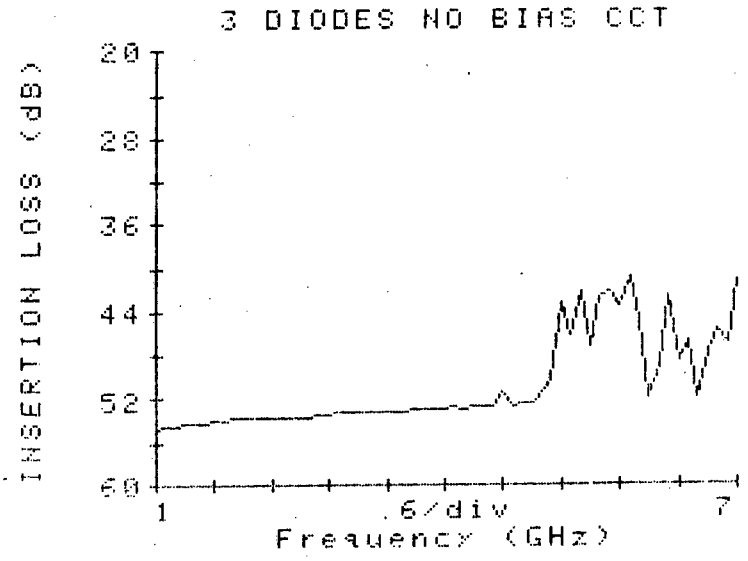

Figure 7.11 The isolation of the SPST switch without any bias circuitry.

It is concluded that even though the bias circuits presents a high impedance to the 50 ohm line they still couple to one another to transfer a small amount of energy from input to output. When considering isolations of 40dB and more the signal strength is small enough for any coupling to be critical. This was occuring in section 7.2 which caused the isolations to be different.

Above 5.2 GHz the isolation without the bias circuitry is degraded to approximately 42dB. It is thought that this is due to electromagnetic coupling between the input and output ports. An experiment to support this theory was to place an Aluminum reflecting plate a few centimeters above the microstrip board. As the distance between the Aluminum and the board was changed, so the isolation changed which illustrates the different degrees of coupling. When microwave absorbing material was placed above the microstrip the isolation improved. Transmission characteristics were examined and they were found to be altered negligibly with the absorbing material and the reflecting material. This implies that the discontinuity of the open circuits cause energy to be launched into free space.

7.4 The investigation of the isolation problem

For all the previous tests the bias lines were situated approximately 30 millimeters apart. It was initially thought that if the biasing wires were soldered onto the 50 ohm line at a greater distance from each other then the isolation will be improved.

A straight 50 ohm line 68 millimeters long was constructed on board with a dielectric constant of 2.2 to make a SPST switch. The diode slots were set at 10mm apart. It must be noted that for isolation investigations no diodes were soldered into the slots that were cut.

Tests were run at all the intermediate stages of construction. Isolation increased from one slot to two, but there was no vast improvement with three slots. The influence of the bias lines were clearly seen. The microwave absorbing material has the effect of flattening out the isolation curve but it does not improve the overall result. The distance between the slots were changed as well as the slot sizes were increased and made into "Vees" in the microstrip line. None of which improved the isolation noticeably.

It was thought that surface current existed on the low dielectric board (dielectric constant = 2.2) which degrade the isolation. Also if the field lines were more concentrated then not as much radiation would occur to couple between input and output ports.

A 50 ohm line was constructed on high dielectric board (dielectric constant = 10). The overall isolation does improve but there are still spikes and humps in the curve. Figure 7.12 shows the isolation of one slot (7.12a) then two slots (7.12b) and finally three slots (7.12c) where this is clearly seen.

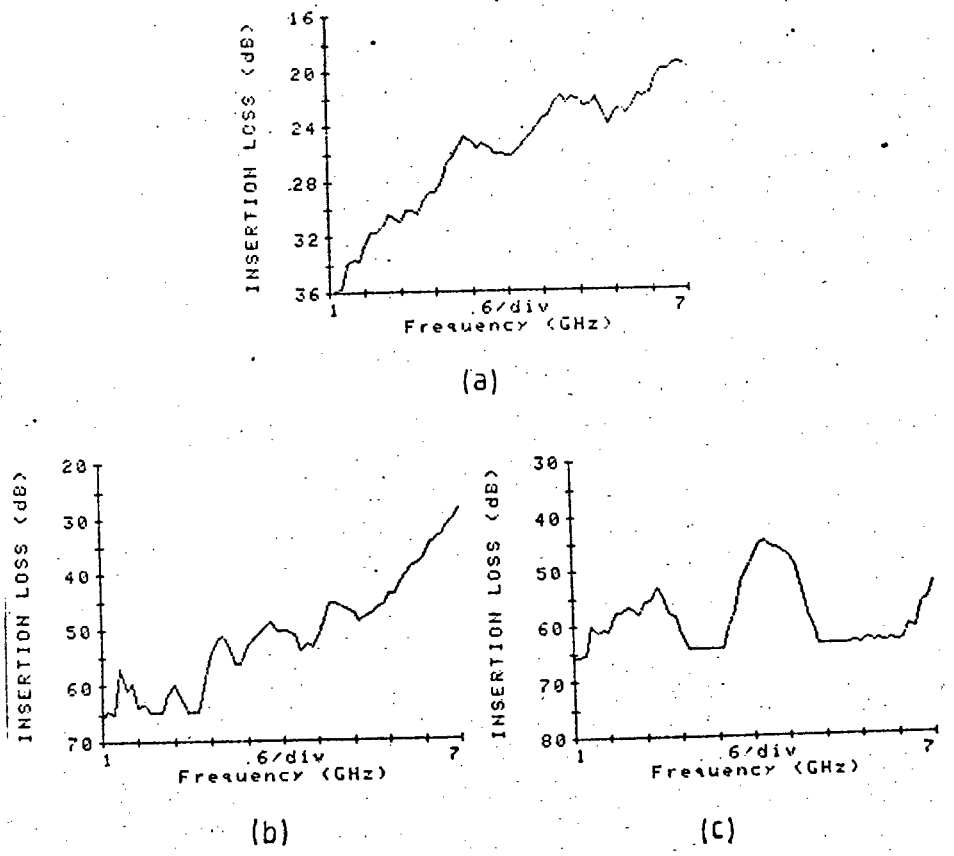

Figure 7.12 Tests carried out with the high dielectric board

The isolation still does not extend beyond 40dB to 45dB. It can thus be concluded that the discontinuity launches the electromagnetic wave to allow it to couple with the 50 ohm line further down its length. It is visualized as shown in figure 7.13. Only the electric field lines are shown.

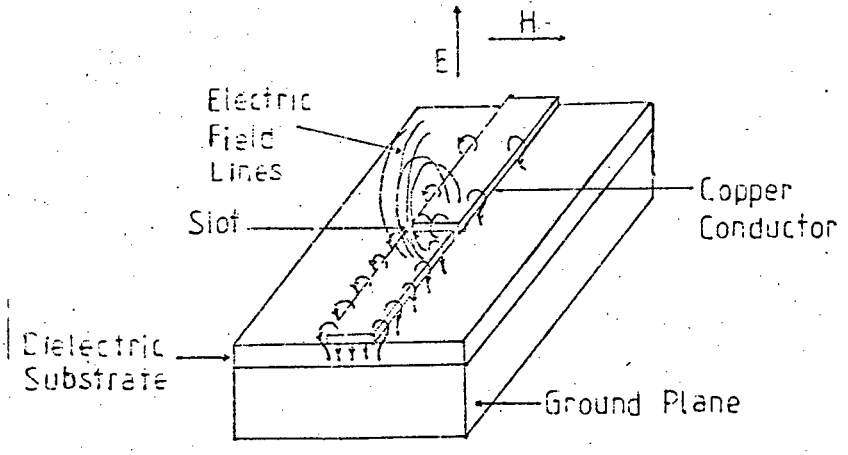

Figure 7.13 Electric field distribution around a slot cut into a microstrip transmission line

A ground plane placed around the microstrip board causes the electric field lines to couple directly to it and not to any transmission line beyond the slot. This can be considered as a waveguide operating in the TEM mode below the cut-off frequency.

7.5 The microstrip circuit enclosed in a waveguide

The TE_{10} mode of transmission gives the lowest possible propogation frequency for a given waveguide structure. Figure 7.14 illustrates the two possible orientations of the microstrip in the waveguide.

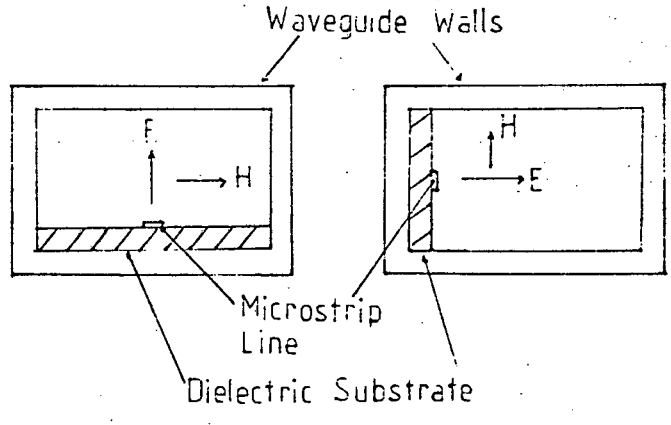

Figure 7.14 The microstrip enclosed in a waveguide

A waveguide width of 20 millimeters gives a cut off frequency of 7.5 GHz. A microstrip line was constructed on low dielectric board with three slots spaced a quarter wavelength apart. An aluminium cover was fitted in such a way as to allow the height between the top of the dielectric board and the cover to change. Figure 7.15 shows the isolation measured with a) no cover and b) with the cover set to a height of 15 millimeters. The width was set at 20 millimeters.

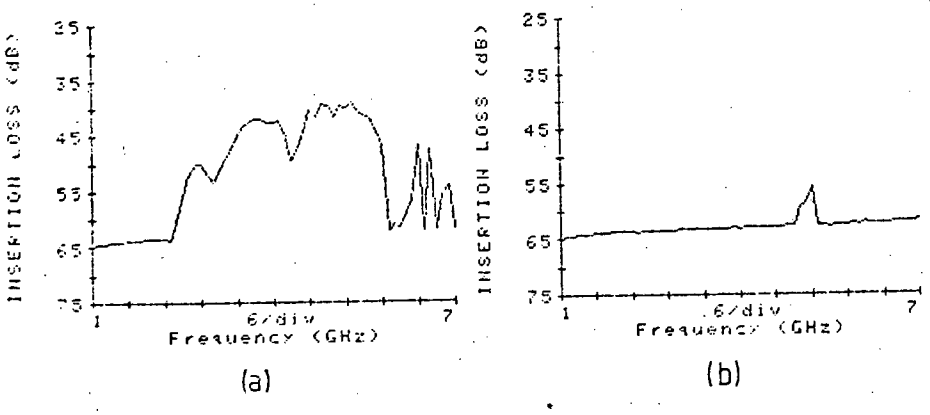

Figure 7.15 The microstrip circuit with and without the waveguide cover

The isolation did not change much when the height of the cover was changed from 10 millimeters through to 20 millimeters. The results seem to suggest that the waveguide cutoff frequency is enforced by the width of the guide and not the height. This is supported by the results obtained by a 27mm wide board with a waveguide cover. These results have not been shown. Bias lines were soldered into place in the waveguide. Their overall effect was minimal which suggests that the waveguide suppressors any radiation that is not a TEM wave operating above the cutoff frequency.

It must be kept in mind that the maximum measurable isolation varies between 60dB and 65dB. This is illustrated in figure 7.16 where the two ports of the s-parameter test set were totally disconnected and measurements were taken.

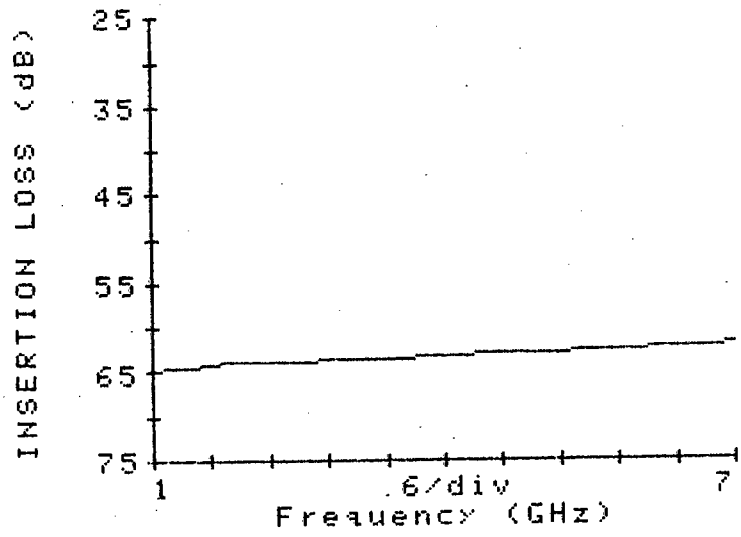

Figure 7.16 The maximum measurable isolation

The microstrip circuit enclosed in a waveguide enables the isolation criterion to be met. The waveguide does not alter the characteristic impedance of the microstrip transmission line and does not increase the insertion loss.

7.6 The SP4T switch enclosed in a waveguide

A SP4T switch which using only series mounted diodes was constructed on low dielectric board. PIN diodes were not initially soldered into place but slots a quarter wavelength apart were cut. A waveguide system was constructed where the ground-plane connection was made along the outside of the dielectric board as shown in figure 7.17. This resulted in a dielectric sheet between the bottom of the wall and the ground plane.

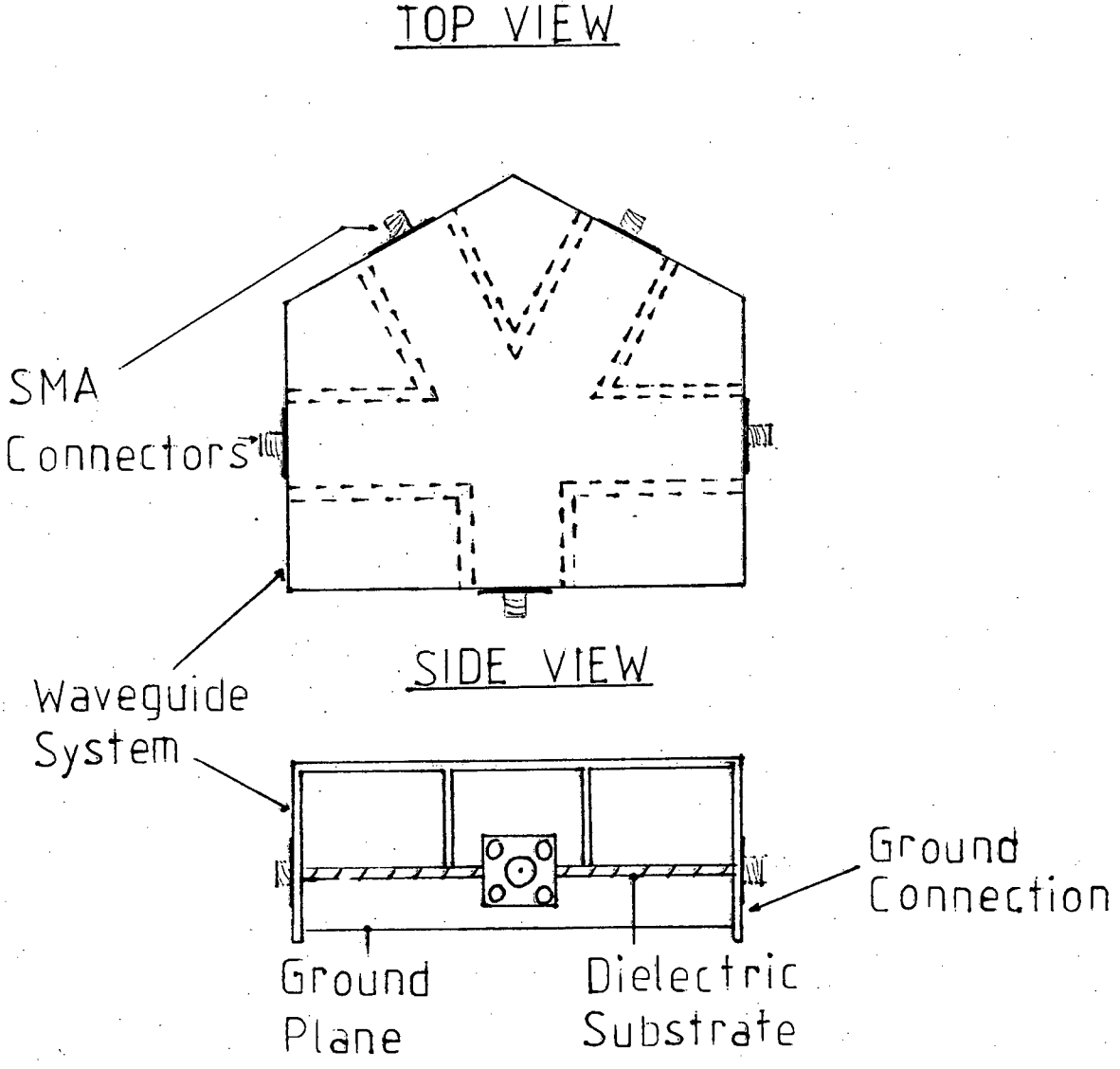

Figure 7.17 The SP4T switch built with waveguide system

The measured isolation is shown in figure 7.18. The response changes from port to port. Only when good ground plane connections were made at the waveguide immediately next to the microstrip did the isolation improve to something like that shown in figure 7.15.

Two channels had PIN diodes soldered into place. Figure 7.18 shows the final measurements that were taken. The tabulated measurements are shown in Appendix D. together with the exact dimensions of the SP4T switch with waveguide.

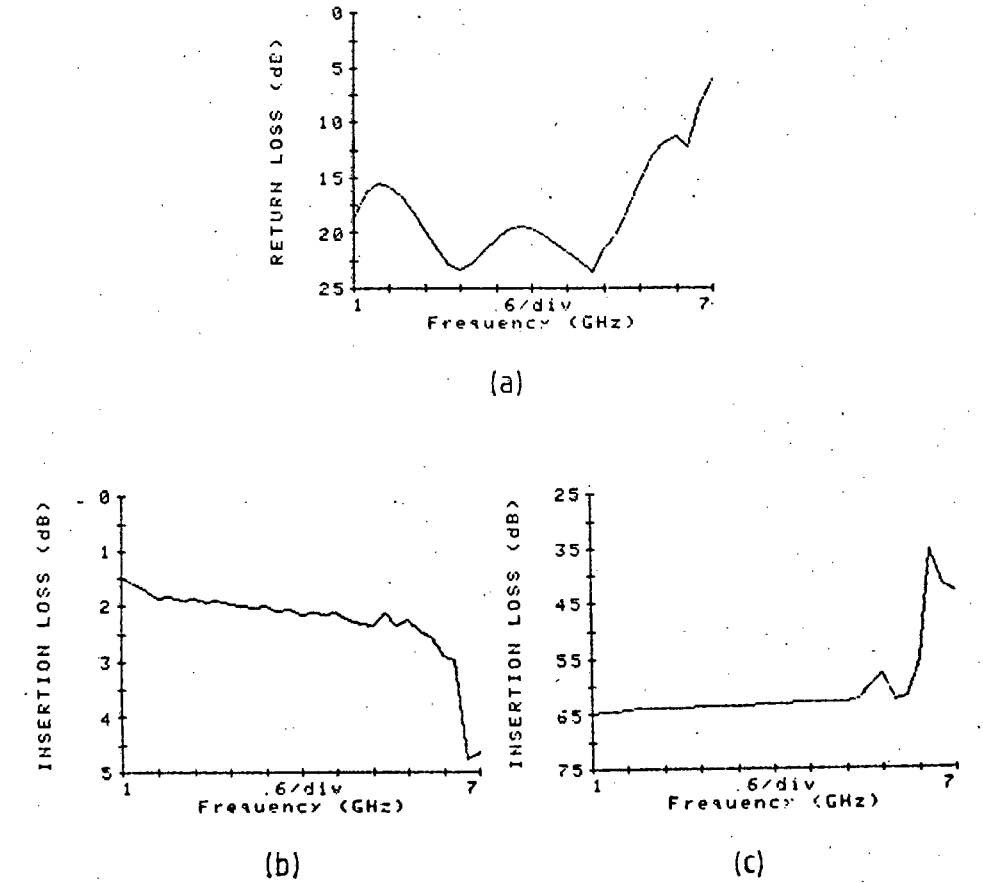

Figure 7.18 The final measurements of the SP4T switch

The return loss is better than 15dB over the range 2GHz to 6GHz. Transmission losses do not amount to more than 2.5dB and isolation of just better than 60dB over the range is obtained. The bias current was set slightly over 10mA (approximately 15mA) and a thin quarter wavelength of wire shorted to ground via a capacitor is used for biasing. Above 6.2 GHz the isolation falls to 35dB and the transmission loss increases considerably. This is due to other waveguide modes being propagated.

7.7 Analysis of the results obtained

The insertion loss of 2dB to 2.5dB on a transmission path of a switch is due to:

i) Reflection loss
ii) Absorption loss
iii) Radiation loss

These losses can be attributed to the loss in the microstrip transmission line which are made up of conductor losses and dielectric losses [15]. Also the PIN diodes, bias networks and the capacitors will contain all three losses.

The HP3141 are rated at 1dB maximum insertion loss. The series mounted diodes specify an insertion loss of between .5dB and 1.5dB depending on biasing.

The measured insertion loss over one path of the SP4T switch that has been short circuited by a thin wire is shown in figure 7.19. The theoretical loss of this 40 millimeter length of microstrip is .2dB over the frequency range in question. The reason for the spike occuring at 6.5GHz is due to the configuration at the junction.

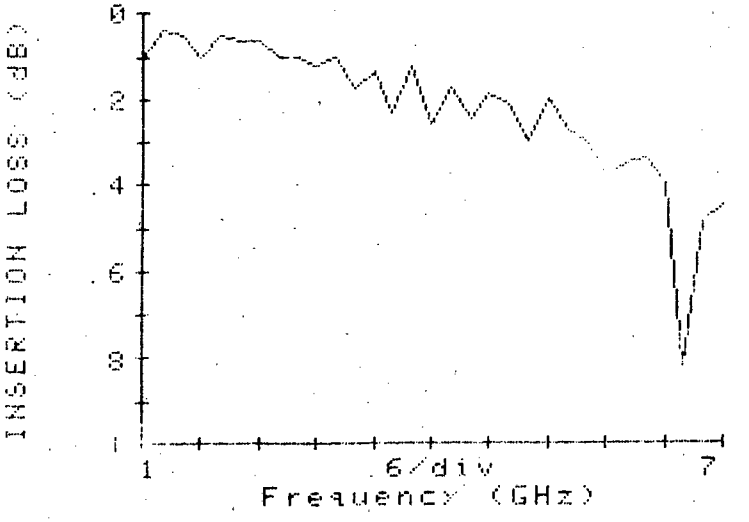

Figure 7.19 The loss measured on a short circuited path of a SP4T switch.

The return loss measured was better than 20dB which means that less than one hundredth of the power is returned to the source due to mismatches in the configuration. When the Ferrite bead bias lines were soldered on, the insertion loss increased by up to one dB and the return loss was degraded slightly.

The insertion loss with three series diodes soldered into place is shown in figure 7.20. The dependance on the bias current is clearly seen. When the bias current was increased to 40 milli-amps almost a one dB improvement can be obtained.

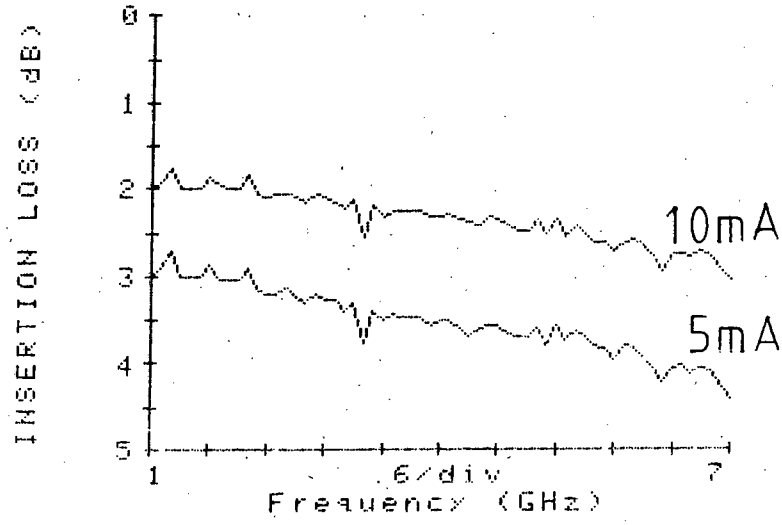

Figure 7.20 The effect of the bias current on insertion loss

This previous test was carried out with the bias current being applied through the biasing port of the network analyser. The only components that could contribute to the loss is the microstrip line and the diodes. From this it can be seen that the loss due to the microstrip transmission line is negligible compared to that of the diodes.

The reason for the poor results obtained from the SP4T switch containing series and shunt mounted diodes (figure 7.7) is that the bias lines used in that case (the ferrite beads) were

not performing as required. Their close proximity caused microwave coupling and interference from path to path because there was one bias system for each diode. The insertion loss amounted to approximately 0.6dB for the series mounted diode and .7dB for the shunt mounted diode.

8. PHASE SHIFTERS

A number of different types of phase shifters were found in the literature which are all investigated. A bandwidth of at least an octave and a half is required for many applications. The different types are investigated, all of which can utilize PIN diodes mounted in either a shunt or series configuration.

8.1 Switched-Line Phase Shifters

The switched line Phase Shifters [21] uses two SPDT switches as shown in figure 8.1.

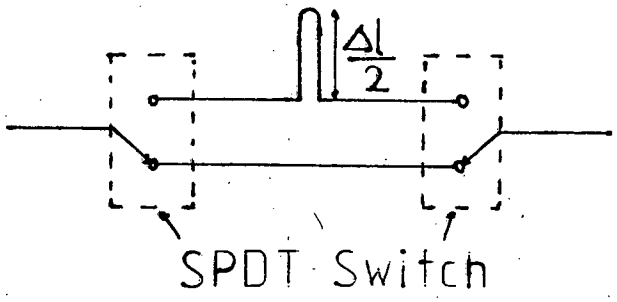

Figure 8.1 Basic configuration of the Switched Line Phase Shifter

The one path has transmission length ℓ, while the other has transmission length $\ell + \Delta\ell$

$$\text{Therefore } \Delta\phi = 2\pi\Delta\ell/\lambda$$

It can be shown that large errors occur when the effective length of the OFF path is $\lambda/2$ or multiples thereof. The effective length is the electrical length plus the equivalent length of the Capacitive OFF diode switches. This method of phase shifting is a time delay device. Phase shift will be proportional to frequency. If a Schiffman phase shifter [22] is inserted into one of the transmission paths then a relatively constant phase shift will occur over a significant bandwidth. The phase shift is then a linear function of frequency plus a sinusoidal function of frequency.

The Schiffman phase shifter employs sections of coupled strip transmission lines operating in the TEM mode. Essentially this shifter consists of two parallel coupled lines of equal length connected at one end with a zero length strap. The equations for the image impedance Z_I, and the phase constant in terms of the even and odd mode characteristic impedances of the lines and their length,

$$Z_I = \sqrt{Zoo \cdot Zoe}$$

and

$$\cos \phi = \frac{\frac{Zoe}{Zoo} - \tan^2 \theta}{\frac{Zoe}{Zoo} + \tan^2 \theta}$$

where $\theta = B\ell$ (the electrical length of a uniform line of length ℓ and phase constant B)

A desirable differential phase response can be obtained by connecting in parallel a coupled line network and a suitable length of uniform transmission line. The simplest form is shown in figure 8.2.

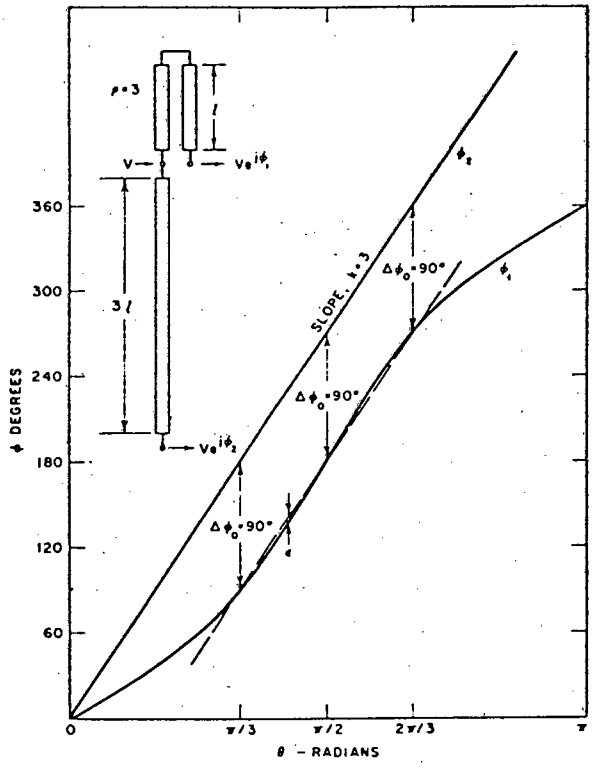

Figure 8.2 A network and the curves of the phase response (from reference [22]).

Input impedance of the network is $Z_I/2$, a constant impedance of frequency. The phase shift through the uniform transmission line is ϕ_2 which is represented by the straight line of slope k through the origin, where k is the ratio of the length of the uniform line to that of the coupled lines. The phase shift through the coupled line portion (ϕ_1) has odd symmetry about $\Theta = n\pi/2$. It can be seen that $\Delta\phi = \phi_2 - \phi_1$ can be made equal to the same angle for three desired values of Θ. ($\pi/3$, $\pi/2$, $2\pi/3$). At other points in the interval $\pi/3 < \theta < 2\pi/3$ and for a small distance outside this interval, the phase difference, $\Delta\phi$ will vary from $\Delta\phi_0$ by some small amount which is the phase error. It is possible to reduce the maximum phase error of this network by connecting another differential phase shift network in tandem. The optimum option of interconnections is shown in figure 8.3 with its phase response.

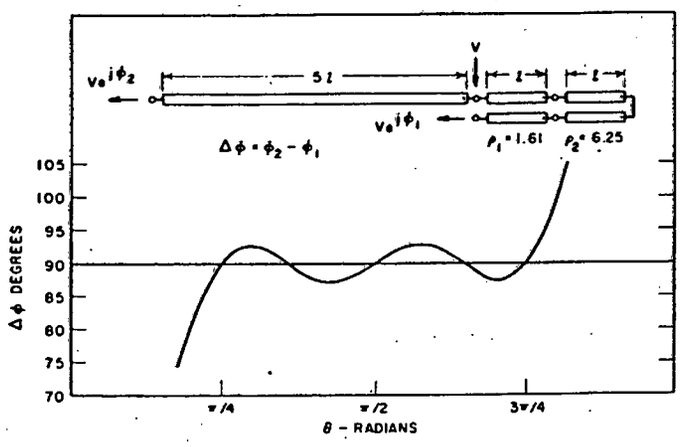

Figure 8.3 A viable Schiffman phase shifter with the response from reference [22].

8.1.1 The SPDT switch

The SPDT switch as shown in figure 8.1 can utilize either shunt or series PIN diodes. The configuration utilizing series switches may initially be thought to be the most desirable [23] because the position of the diodes relative to the input and

output junction does not impose a potential bandwidth limitation as it does in the shunt-diode switch case. However, analysis of a mathematical model of the configuration utilizing series switches revealed that it has operating points in the octave band, at which the isolation between switching paths become very low. At these points, the phase-shifted insertion loss becomes high and the phase error large. The configuration employing shunt diode switches was not found to have the same problem.

Bandwidths and maximum phase shifts have been limited by resonance effects which cause notches in the amplitude response and large errors in the phase response. [24]. (This is true for all types of phase shifters). By eliminating the resonance effects, ultra broad-band phase shifters with large amounts of phase shift become possible.

By using two transfer switches in place of the two single-pole double throw switches the switched out line may be terminated on both ends in its characteristic impedances which disallows any resonance to occur. See figure 8.4.

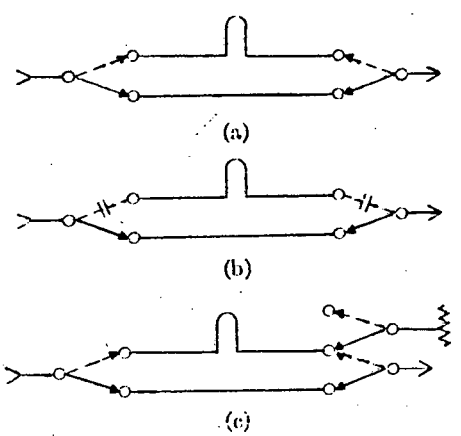

Figure 8.4 a) The basic circuit. b) An equivalent circuit. c) One method of avoiding resonance problems.

In the basic circuit the problem is that when either of the two lines has an electrical length of $\frac{n\lambda}{2}$ it forms a high Q

resonator when it is the 'switched out' line. The open contacts of the pin diode switches are lightly coupled to this resonant line which causes a sharp insertion loss notch in amplitude at the resonant frequency, and large phase errors near resonance. The alternative circuit shown in figure 8.4 c) eliminates this problem by terminating the "switched out" line in its characteristic impedance.

The advantages of the switch-line phase shifter are [1] :

1) The diode contribution to insertion loss is practically constant in the forward and reverse bias cases.

2) The circuit can be fabricated in one plane.

3) The circuit is compact, especially for small bits.

The disadvantages are:

1) Four diodes per bit are required

2) Complimentary bias signals are needed for each bit (on and off paths).

3) Phase shift is proportional to frequency unless a Schiffman circuit is used.

4) All bits have as much diode loss as the 180° bit while in other types of phase shifters the diode losses decrease with phase shift.

8.2 Loaded-Line Phase Shifters

The loaded-line phase shifter circuit can be realized using three types of loading configurations [25];

a) Main line mounting type

b) Stub mounting type

c) Switchable stub length type as shown in figure 8.5.

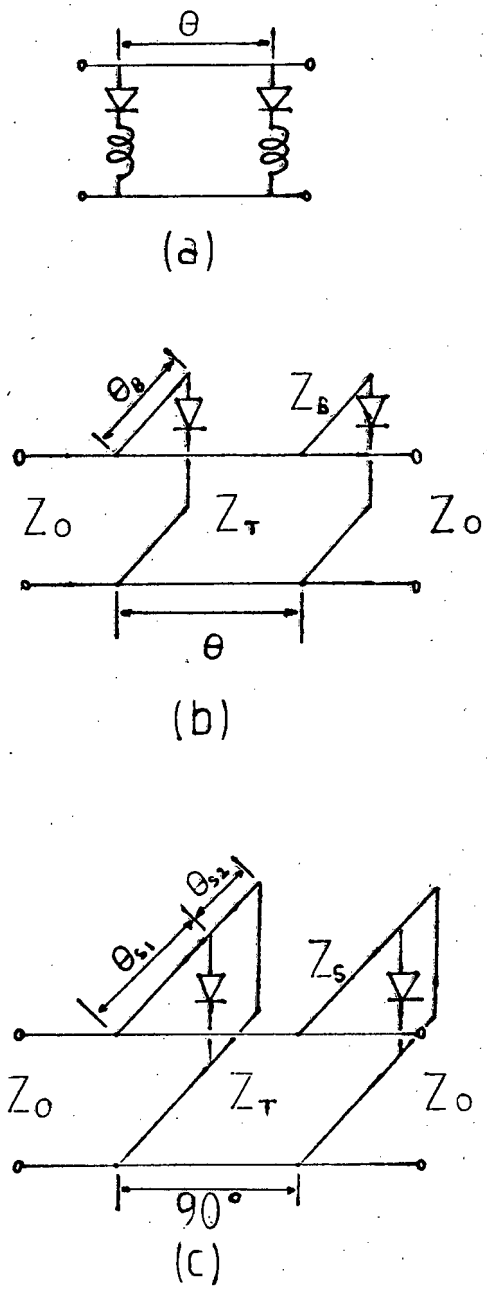

Figure 8.5 Loaded-Line phase shifters

In the main line mounting lumped reactances are added to the diodes. The Loaded-Line phase shifters use two admittances $Y_i = G_i + j\,B_i$ approximately a quarter wavelength apart along a transmission line of characteristic impedance Z_T.

The differential phase shift $\Delta\phi$ for $G_i = 0$ is given by;

$$\Delta\phi = \cos^{-1}\left(\cos\theta - \frac{B_1}{Y_T}\sin\theta\right) - \cos^{-1}\left(\cos\theta - \frac{B_2}{Y_T}\sin\theta\right)$$

The subscripts "1" and "2" denotes the ON and OFF states of the diode when the circuit is matched at its centre frequency. θ is the distance between the stubs. Equations for insertion loss and reflection coefficient can be found in the literature. [25].

The bandwidth for the three different types of circuits is defined as the frequency range over which the phase error is less than $\pm$ 2° and the maximum VSWR is <1.2. In the main line mounted case the bandwidth is 9.1% for 45° phase shift. The switchable stub type circuit has a bandwidth which is a function of X_R, X_F and θ_{s1} and will reach a bandwidth of 20% at best. The stub mounted type will also reach 20%. The bandwidth increases if the phase shift is lower. Figure 8.6 compares the bandwidth of a 22.5° phase shifter to a 45° phase shifter. [26].

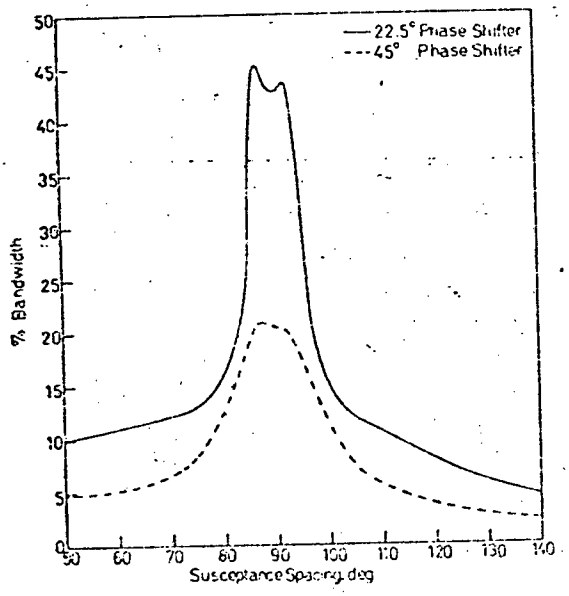

Figure 8.6 Fractional bandwidth of the phase shifter using single lumped switched susceptances.
(from reference 26)

8.3 High-Pass Low-Pass Phase Shifters

A Low-Pass filter comprising of series inductors and shunt capacitors provides phase delays to signals passing through it, and a High-Pass filter comprising of series capacitors and shunt inductors provides phase advance [21]. By arranging diode switches to permit switching between low pass and high pass filters it is possible to make a phase shifter that is smaller than the other types and with a bandwidth almost as good as the lumped element reflection phase shifter. A practical layout of the circuit is shown in figure 8.7.

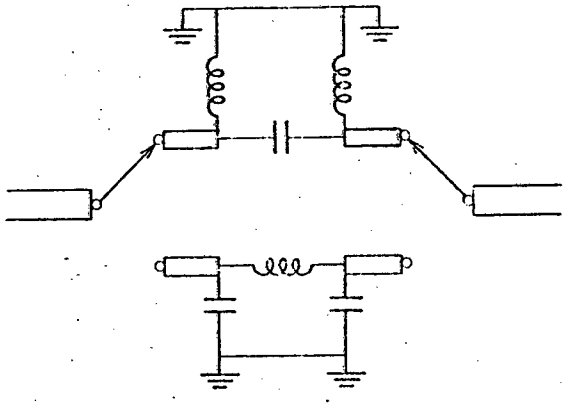

Figure 8.7 Practical layout of a Low-Pass High-Pass phase shifter. (from reference [21]).

8.4 Reflection Phase Shifters

A reflection type Phase Shifter can take the form of a shunt diode with a short circuit behind it, a series diode with an open circuit behind it, or a lumped circuit including diode parasitics terminating the line. [21]. An example is shown in figure 8.8.

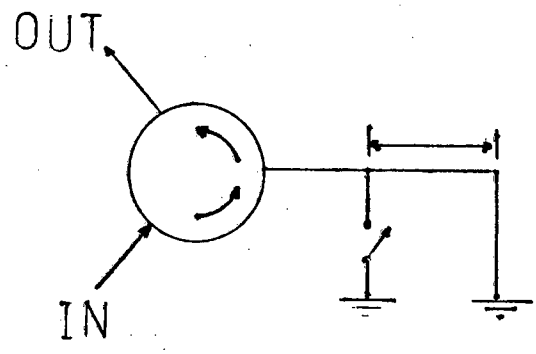

Figure 8.8 A Reflection Phase Shifter with a shunt diode and a shorted length of transmission line.

The switches backed up by lengths of transmission line have the advantage that they are time delay devices giving wide instantaneous bandwidth while the lumped circuit versions can be made to give constant phase shift over octave or wider bandwidths. However mismatches occur between the terminating impedance and the perfect circulator or 3dB coupler which result in large phase errors.

For wide-band phase shifting, the diodes are connected to the circulator without a length of transmission line behind them, the "on" and "off" states result in a 180° phase shift.

Another form of the Reflection Phase Shifter is shown in figure 8.9, [27] where a Branch Arm Coupler is used.

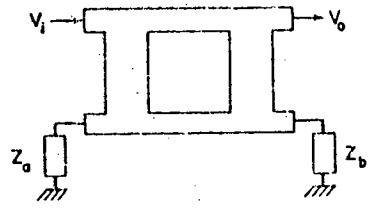

Figure 8.9 Terminated hybrid coupler for reflection phase shifting.

8.5 The Hybrid Coupler Phase-Shifter Circuit

An extension to the idea of the terminated hybrid coupler for reflection phase shifting as shown in figure 8.9 is further investigated. The advantage of this method is that it uses the least number of diodes per bit. [1]

The requirements for the couplers are;

i) They must provide a 3 dB power split for the two output arms.

ii) There must be a 90° phase difference in its output signals.

The 3 dB 90° properties of the coupler can be realized in TEM transmission lines with at least three different types of circuits. ie The Branch-arm coupler as shown in figure 8.9, the Rat Race coupler [1] and the Backward-wave coupler.

The reflection properties are achieved by the use of an impedance transforming two-part network, which consists of switchable impedance elements Za and Zb terminating two ports of a 3 dB coupler. The output signal from the hybrid is:

$$V_o = j\frac{Vi}{z}\left[\tau a\,(Za) + \tau b\,(Zb)\right]$$

$\tau(z)$: reflection coefficients of termination Z. If Za = Zb there is no reflection at the input. Z contains a semiconductor element which may be biased to its "off" or "on" state producing impedances Z_1 and Z_2 respectively.

The output of the phase shifter will have constant signal amplitude with phase angle change ϕ. If $\tau_1(Z_1) = e^{j\phi}\tau_2(Z_2)$ Then a 180° phase shift is achieved by switching between an open circuit and a short circuit. Tuning elements and circuits may be introduced in order to adjust the amount of phase shift or improve the uniformity of the reflected signal in amplitude.

The series inductance, shunt capacitance and resistances associated with PIN diodes all effect the performance of the Phase Shifter [28]. It is found that shunt capacitance is the most dominant reactance influencing the phase shift and it increases the phase shift value. The series inductance reduces the phase-shift value. The bandwidth is determined by the bandwidth of the hybrid coupler or circulator.

The branch line hybrid coupler can be built on microstrip but it is limited to 5 to 10% bandwidth. The Rat Race has its 3 dB output ports 180° out of phase. However the required phases are obtained by extending the reference plane on one port by 90°. The backward wave hybrid coupler gives the broadest bandwidth of the three just mentioned.

A phase shifter which utilizesa power splitter and three Reflection phase shifters [29] holds the most promise in terms of bandwidth. The different phases are switched with the use of PIN diode circuits which switch in either a short circuit, an open circuit or a matched load. A schematic diagram of this phase shifter is shown in figure 8.10. The Reflection phase shifters consist of Quadrature couplers and PIN diode switches.

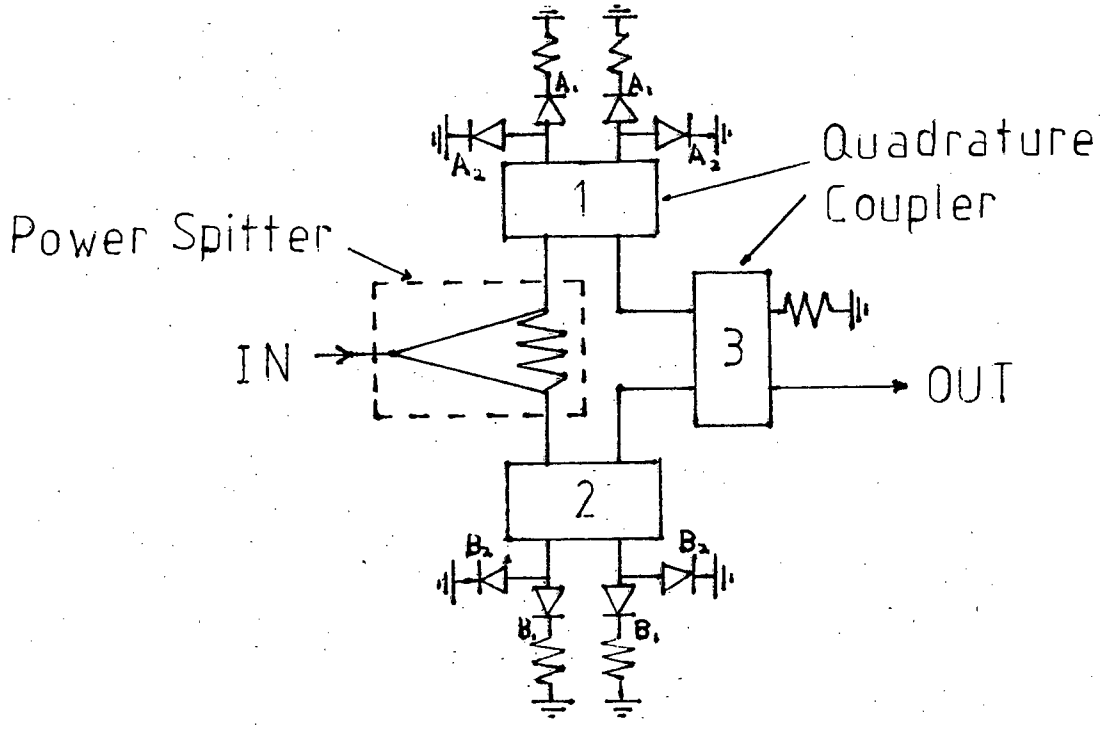

Figure 8.10 Schematic diagram of the phase shifter which utilizes a Power splitter and Reflection phase shifters.

The following table illustrates the resultant phase on the output port for the different states of the diodes.

Condition of diodes A	Condition of diodes A_2	Condition of diodes B_1	Condition of diodes B_2	Resultant Phase (degrees)
Open circuit	Open circuit	Short circuit	Open circuit	0
Open circuit	Open circuit	Open circuit	Open circuit	45
Short circuit	Open circuit	Open circuit	Open circuit	90
Open circuit	Short circuit	Open circuit	Open circuit	135
Open circuit	Short circuit	Short circuit	Open circuit	180
Open circuit	Short circuit	Open circuit	Short circuit	225
Short circuit	Open circuit	Open circuit	Short circuit	270
Open circuit	Open circuit	Open circuit	Short circuit	335

Table 2 Conditions of the diodes for the different phase shifts.

The operation is based on the fact that, in this particular configuration, a quadrature coupler which has grounded terminations has a 90° leading phase shift. An open circuit terminated coupler has a 90° lagging phase shift and matched load terminations result in no output as described in section 2.2.2. For one particular coupler the terminations are always the same.

Coupler 3 (as shown in figure 5.10) adds the two phases from 1 and 2 vectorially, but still adds 90° and 180° in the internal paths of the coupler.

Take for example the 135 degree resultant phase shift. If diode A_1 is open circuited and A_2 is short circuited then short circuit terminations are applied to Coupler 1 which results in a positive 90 degree phase shift. If diodes B_1 and B_2 are open circuited then open circuit terminations are applied to Coupler 2 resulting in a minus 90 degree phase shift, this is illustrated in figure 8.11 (a). The signal out of Coupler 1 then travels through the direct path of coupler 3 which advances the phase by an additional 90 degrees. The signal out of coupler

2 goes through the coupled path of Coupler 3 which advances the phase by 180 degrees. The two signals are added vectorially at the OUT port as shown in figure 8.11 (b).

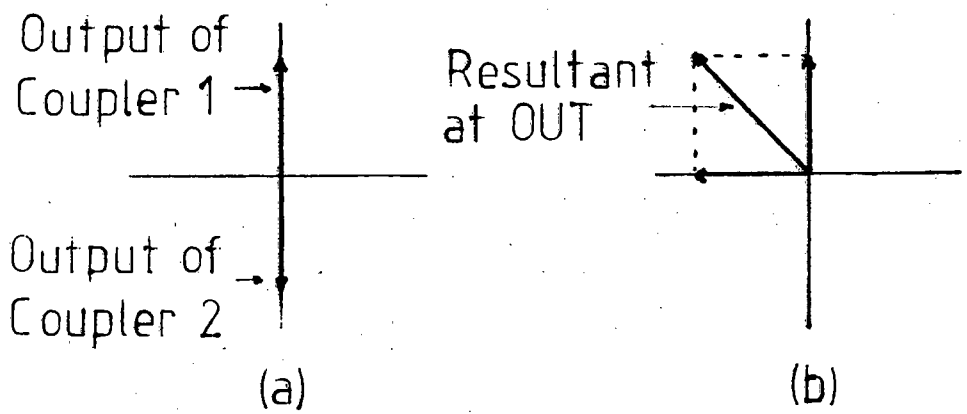

Figure 8.11 The phase shifts which result in the 135 degree phase shift.

When 50 ohms (or matched loads) are applied to Coupler 1 or Coupler 2 then no output results from that coupler. (There is never a condition when both couplers have matched terminations). The resultant phase at the OUT port is then only the phase shift through the coupler that has no matched terminations plus the phase shift through either the coupled path (180 degree shift) or the direct path (90 degree shift).

The phase shifts through 360 degrees with the respective terminations on the couplers are shown in figure 8.12. For each vector the condition on the left is for Coupler 1 and on the right for Coupler 2. (SC is short circuit, OC is open circuit and 50 is matched load).

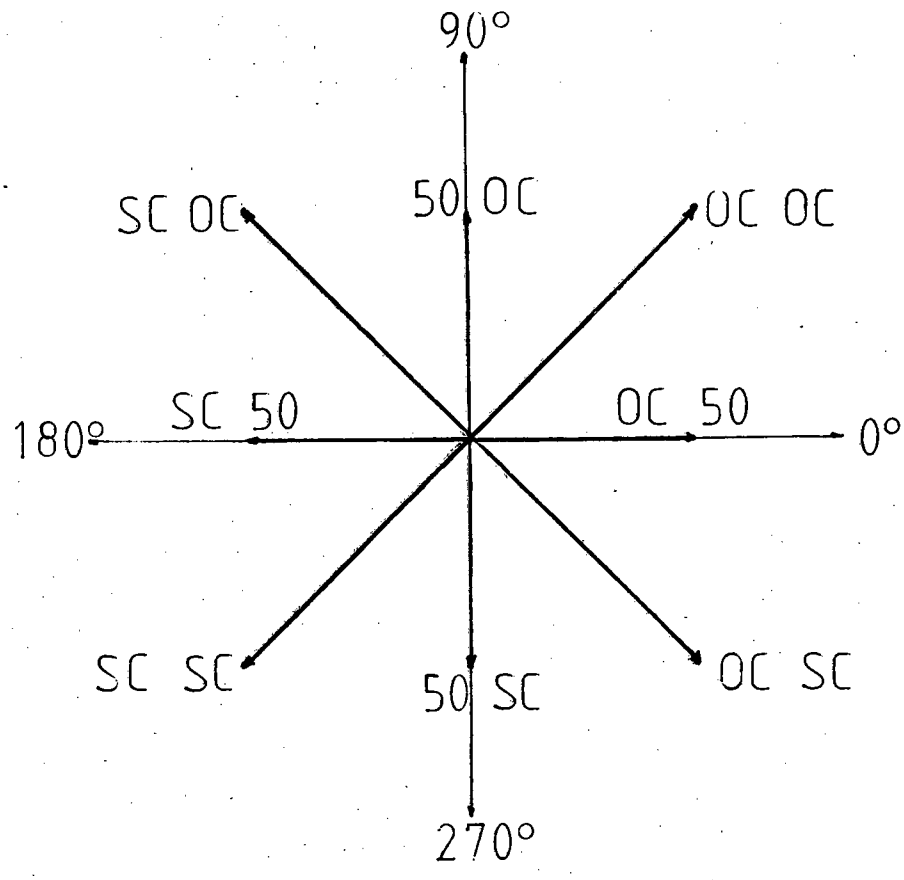

Figure 8.12 The phase shifts with the corresponding terminations applied to the couplers.

It can be seen that the phase shifts involving the 50 ohm terminations lie on the axes of the graph. These vectors are smaller in magnitude than the other four because only half of the signal that was originally split reaches the OUT port.

8.6 Discussion

The Switched Line Phase shifter does not readily lend itself to stepped phase shifting. If it is used in conjunction with a Schiffman differential phase shifter a bandwidth of an octave can be obtained [23]. The Reflection phase shifter is limited in bandwidth by the quadrature coupler used and the termination networks. The High-Pass Low-Pass phase shifter does not seem to have any major advantages in terms of bandwidth.

The best solution seems to be the Reflection phase shifter and power splitter as shown in figure 8.10. All the components which make up the system are instrumental in the overall operation which allows no redundancies to occur. The diode switches switch in either an open circuit, a short circuit or a matching load which is easily obtainable over a large frequency range. Thus the bandwidth is mainly determined by the quadrature coupler. If a microstrip Lange Coupler or Stripline Overlay Coupler is used then a bandwidth far greater than the previously mentioned phase shifters is possible.

9. THE PHASE SHIFTER CONSISTING OF REFLECTION PHASE SHIFTERS AND A POWER SPLITTER

This Phase Shifter was chosen to undergo further investigation mainly due to the broader bandwidth which can be achieved as well as the unique design.

The phase shifter consists of three basic components;

i) the power splitter
ii) the quadrature coupler
iii) the PIN diode termination switch.

All these components are analysed and developed seperately.

9.1 The power splitter

The power splitter as shown in figure 9.1 divides the signal equally into two branches but does not alter the phase. Any power that is reflected back due to mismatches further on is absorbed in the 100 ohm resistor. This gives a good match for all the ports. The operation is reversable ie. it can operate as a power divider as well as a power combiner.

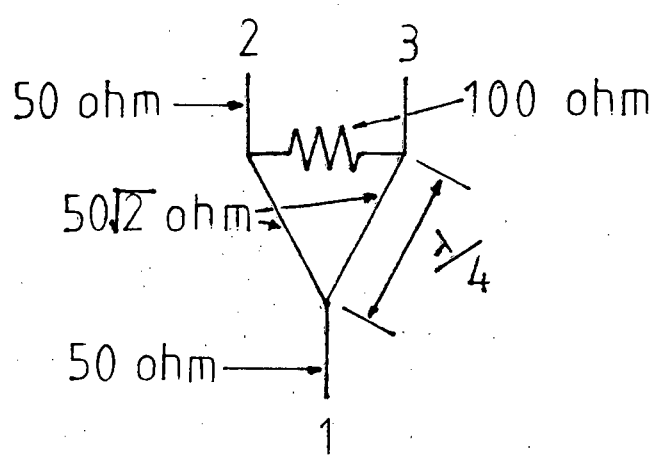

Figure 9.1 The Power Splitter

The circuit was modelled on TOUCHSTONE, the results of which can be seen in figure 9.2. The 3 dB split can be easily observed. If more matching sections are used then a further broadening of the return loss (S11) bandwidth results.

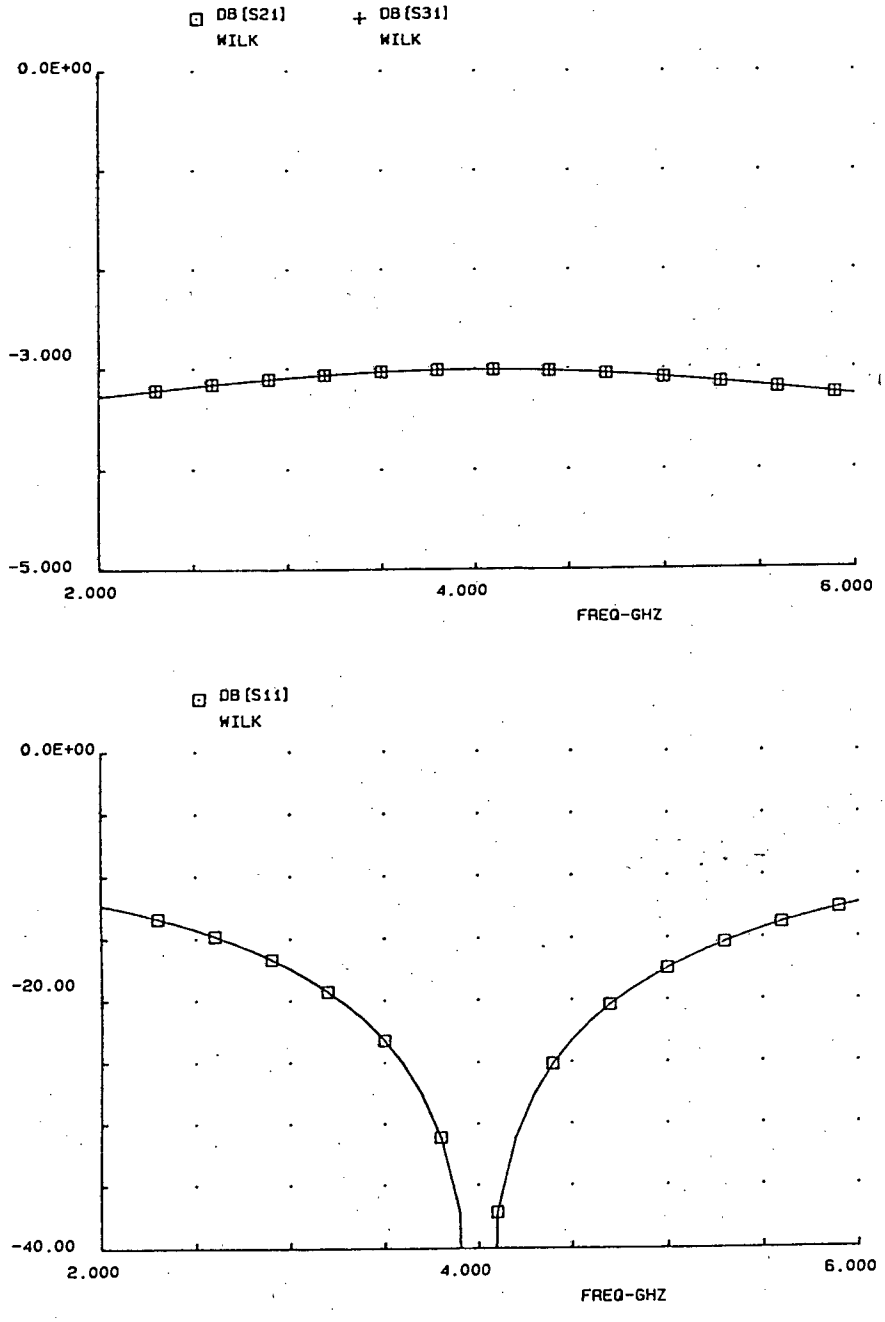

Figure 9.2 The response of the power splitter

9.2 The Simulation of the Phase Shifter on TOUCHSTONE

The entire circuit was modelled on TOUCHSTONE to see how the overall phase error is effected by the different parameters of the couplers. This allows a specification for the characteristics of the coupler to be generated for the final implementation stage.

Ideal coupled lines were used to implement the quadrature coupler and as it is represented in TOUCHSTONE can be considered as a Backward Wave coupler. The influence of the Even and Odd mode impedances on the phase error was initially investigated. Ideal terminations were applied to the coupler ports to generate the different phases. When Zoo and Zoe were set at 20 ohms and 125 ohms respectively the error was less than five degrees between 2.4 GHz and 5.6 GHz. Figure 9.3 illustrates how the phase shift is effected by changing these impedances. (See Program 21 Appendix A).

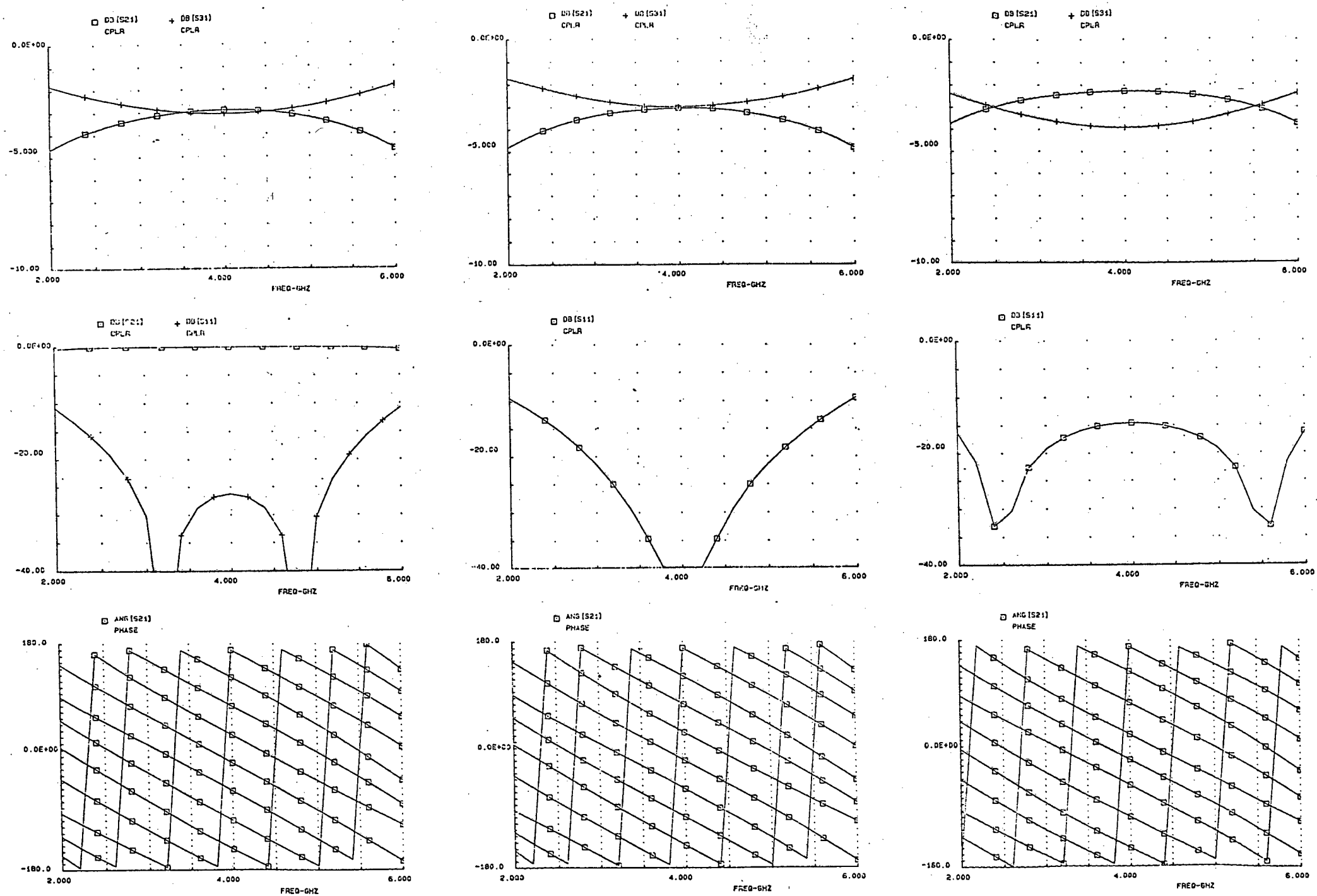

Figure 9.3 The Influence of the Even and Odd Mode Impedances

Z_{0o}=20 Z_{0e}=125

Z_{0o}=20.8 Z_{0e}=120.1923

Z_{0o}=18.0 Z_{0e}=138.8889

The plots at the top of the columns demonstrate the amount of coupling in the ideal coupled lines for the even and odd mode impedances stated at the bottom of the columns. The one trace is the direct paths (S31) and the other trace is the coupled path (S21). This gives an idea of the bandwidth of single section coupled lines. If more sections were used (say three sections) then a broader bandwidth would be achieved.

The middle plots in the columns demonstrates the return loss of a single coupler when either an open circuit or a short circuit is applied to the ports. The curves for the two cases lie exactly over one another.

The bottom plots were generated by changing the impedances on the coupler in the entire phase shifter configuration as shown in section 8.5 and plotting the resulting phase shift. The best return loss occurs where the coupling is close to the 3 dB line. If the spacings between the angular plots are carefully observed the least errors occur where the return loss (S11 plot) is better than 20 dB. The next two columns demonstrate how the phase error is influenced by the characteristics of the coupled lines.

For the phase errors to be minimized over 360° there must be an evenly placed distribution of the phase shift lines. If one line is displaced by 10 degrees (say) it effects the phase shift error before and after that particular phase line.

9.3 The realization of the Phase Shifter

The phase shifter consists of three identical couplers, two of which are used to switch between -90°, +90° and no output. The third adds the outputs from the two. Therefore the quadrature couplers are the main constituents of the overall phase shifter.

A stripline three section 3 dB Overlay coupler [30] was used to fabricate a complete phase shifter (the dimensions of the coupler are shown in Appendix E). The layout of the entire system is shown in Figure 9.4. Figure 9.4 b) and c) are the overlays for the circuit shown in a). The cross hatch represents the thin (.127 mm) dielectric sheet which is placed between the two overlays in the final construction. A thin brass tab had to be inserted through the dielectric sheet at point A to connect two couplers. The entire structure was then sandwiched between two thicker sheets (1.575 mm) of dielectric clad by aluminium. The stripline circuit was then screwed together.

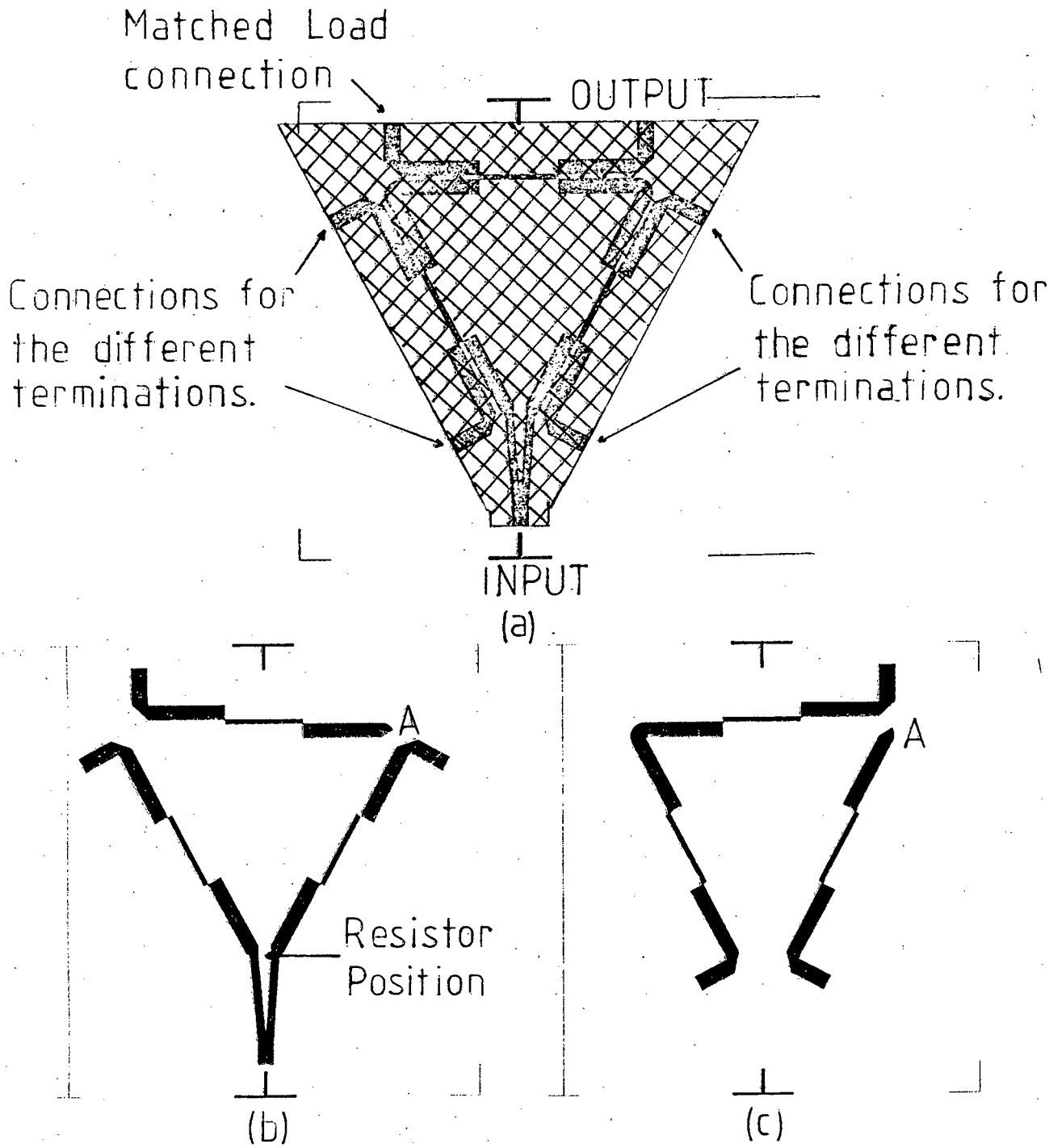

Figure 9.4 The layout of the Phase Shifter that was fabricated

Shorting tabs made from brass foil were clamped into place by tabless launchers to facilitate the short circuit terminations.

The open circuit condition was implemented by removing the launchers completely. The 50 ohm matched load was established by screwing on the wide tab launchers which were connected to 50 ohm screw on terminations.

Large errors were observed. The 135° trace fluctuated by 30° and the 180° fluctuated by 45°. The reasons for these large errors could be due to the terminations or the couplers.

The S-parameters of a single coupler was measured on the test set and a file was created to allow TOUCHSTONE to use these measurements. The coupled lines as shown in Program 21 (CLIN statement) was replaced by the S-parameter file. Large errors were found which corresponded to the measured case. The coupler had to undergo further investigation. Figure 9.5 a) illustrates the measured coupling and figure 9.5 b) shows the return loss when the coupler has short circuit terminations.

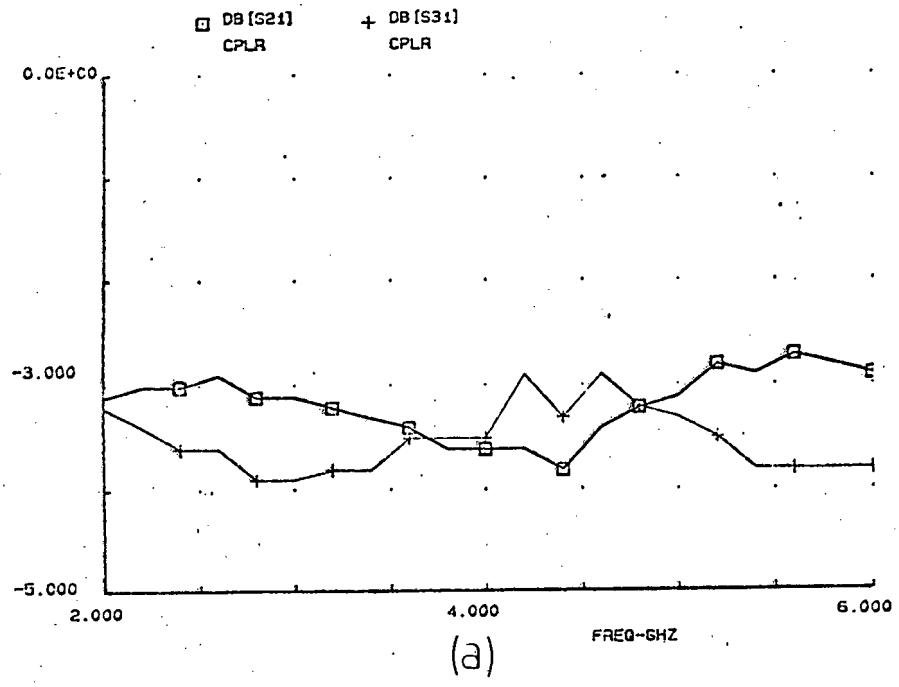

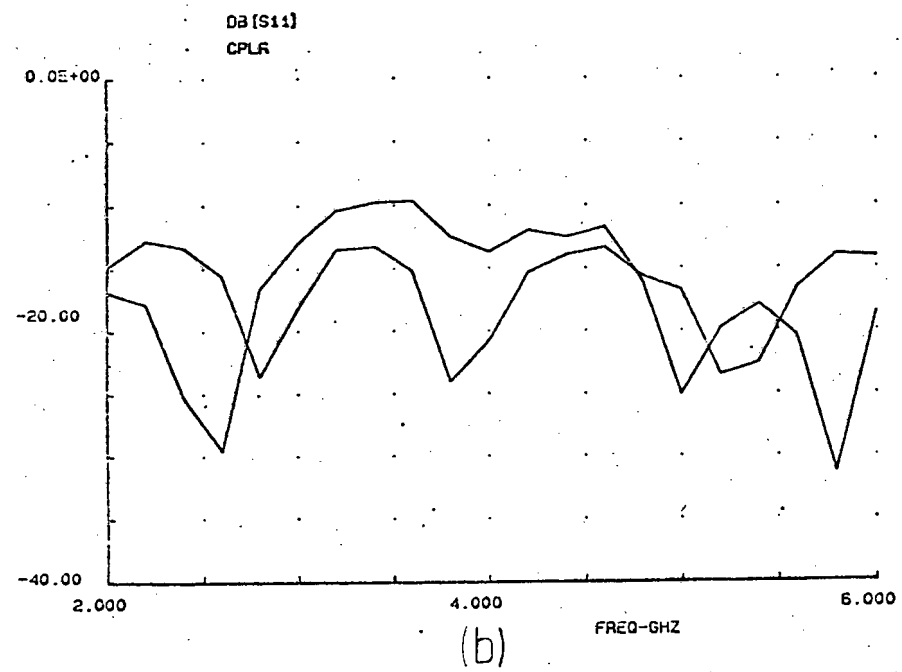

Figure 9.5 Measurements taken on D M Rachman's Overlay coupler

The coupling is almost 3 dB over the entire frequency range but the return loss falls to 10 dB in places. The isolation (matched loads on Ports 3 and 4 figure 2.8) varies between 13 dB and 26 dB. It is less than 20 dB between 2 GHz and 5 GHz which corresponds to where the largest errors take place in the overall phase shifter. The following table shows the phase differences between the open circuit and short circuit terminations that were measured.

Frequency (GHz)	Phase difference (Degrees)	Phase shift Error Degrees
2.0	161.7	18.3
2.2	201.0	21.0
2.4	201.4	21.5
2.6	199.8	19.2
2.8	165.7	14.3
3.0	170.0	10.0
3.2	179.0	0.0
3.4	187.7	7.7
3.6	195.7	15.7
3.8	157.3	22.7
4.0	154.6	25.4
4.2	157.1	22.9
4.4	155.0	25.0
4.6	201.7	21.7
4.8	194.4	14.4
5.0	188.5	8.5
5.2	183.5	3.5
5.4	176.8	3.2
5.6	178.8	1.2
5.8	179.5	0.5
6.0	176.4	3.6

Table 3 Phase shift for D M Rachman's Overlay coupler

These results suggest that for low phase errors the couplers used must have good matching for the short circuit and open circuit cases, there must be 3 dB coupling for the coupled path and the direct path and there must be good isolation. A single section coupler was investigated to establish what factors effect the errors.

9.4 The investigation of a Single Section Overlay coupler

Program 20 was used to generate the width of the conducting strips and the Even and Odd mode impedances for given dielectric heights.

For the total height of the dielectric (B) = 1.7018 mm and the height of the dielectric between conductors (S) = .127 mm.

Odd mode impedance	= 18.75 ohms
Even mode impedance	= 133.3 ohms
Width of conducting strip	= .6565 mm

The exact dimensions are shown in appendix E. In general as B increases the Even mode impedance increases and the width of the conducting strips increases. As S increases the Even mode impedance decreases and the width of the conducting strips increases. (Refer to figure 2.10).

For the Even and Odd mode impedances calculated above the plots shown in figure 9.6 are generated. The last plot is the phase shift of the entire phase shifter.

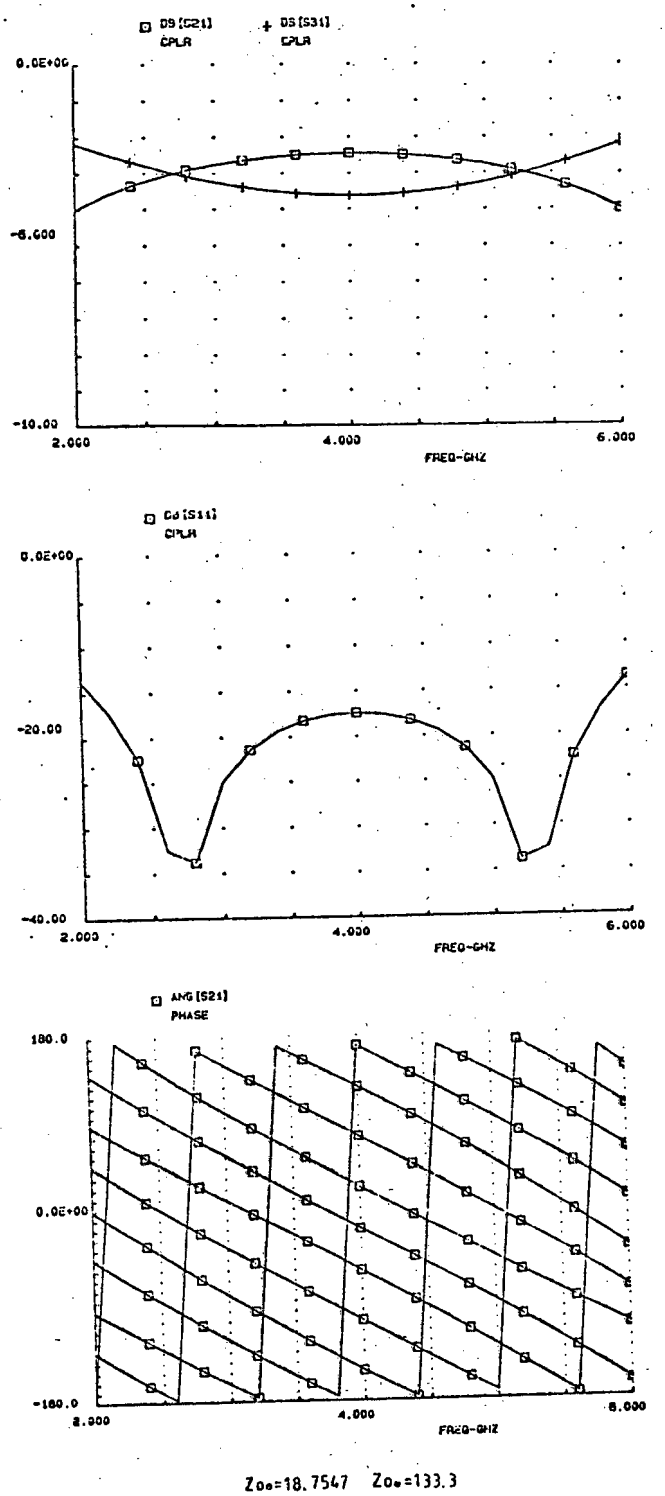

Figure 9.6 The theoretical characteristics of the Single Section Overlay coupler

It can be seen that these impedances theoretically lead to low phase errors. The phase difference between a single short circuit and open circuit terminated coupler is exactly 180 degrees. The isolation is minus infinity.

9.4.1 The fabrication of the single section Overlay coupler

The coupler as designed in section 9.3 was built and tested. The measurements are shown in figure 9.7. Figure 9.7 a) shows the direct and coupled path couplings. Figure 9.7 b) shows the isolation which is a vast improvement over the isolation in D M Rachman's coupler. The response showing the coupler short circuited and open circuited falls to almost 10 dB in the middle of the range.

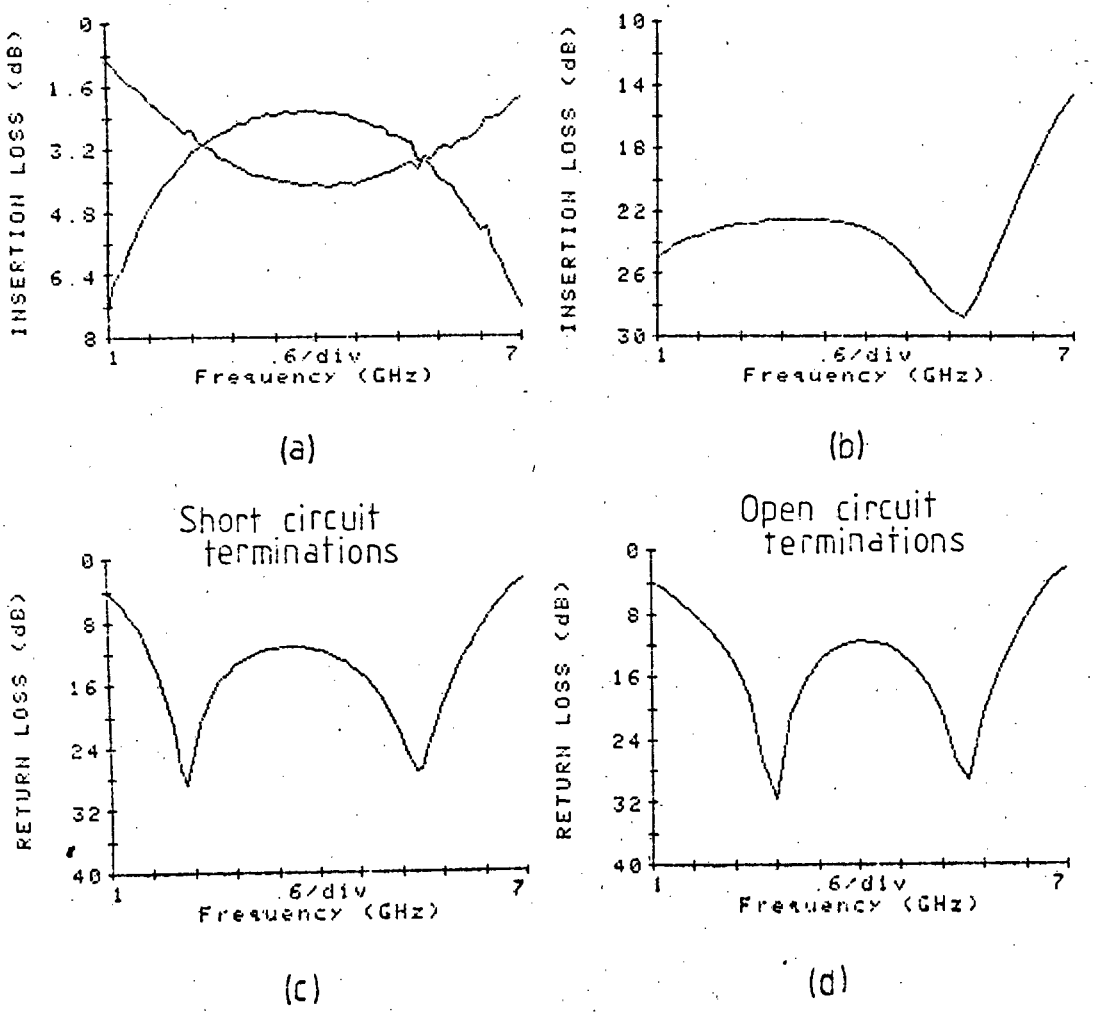

Figure 9.7 The measured response of the single section coupler

The difference between the phases of the measured open circuited and short circuited terminated coupler is shown in the table 4.

Frequency (GHz)	Phase difference (degrees)	Phase shift error (degrees)
2.0	173	7
2.2	171	9
2.4	168	12
2.6	169	11
2.8	170	10
3.0	170	10
3.2	168	12
3.4	173	7
3.6	171	9
3.8	172	8
4.0	174	6
4.2	178	2
4.4	176	4
4.6	179	1
4.8	176	4
5.0	178	2
5.2	174	6
5.4	167	13
5.6	169	11
5.8	161	19
6.0	167	13

Table 4 Phase shift for the single section Overlay coupler

It is very important that the metal tabs that are clamped onto the side of the coupler to facilitate the short circuit performs as a good short circuit. ie. Has a low resistance and reactance. The measure of the performance of this termination is seen by observing the display as shown in figure 9.7 c). The return loss decreases at any frequency where there is a poor short circuit termination.

The error is lower than in D M Rachman's coupler. A comparison of the characteristics indicate that the isolation for the single section coupler is a vast improvement over the coupler in reference [30] but the latter has better 3 dB coupling over the frequency range.

9.5 The Lange Coupler

The overlay coupler displays phase shift errors which causes the error in the complete Phase Shifter configuration to be compounded. A 3 dB 2 GHz to 6 GHz Lange coupler supplied by the CSIR was then investigated. Appendix F shows the measured s-parameters which were entered into a four port s-parameter file where it was assumed that the circuit was totally symmetrical ie

$$|S14|\angle S14 \equiv |S41|\angle S41 \equiv |S23|\angle S23 \equiv |S32|\angle S32$$

This might not be strictly true in practice.

The phase difference between the coupler open circuited and short circuited is shown in table 5. Large errors are observed between 3 GHz to 3.4 GHz and 5.4 GHz to 6 GHz. This corresponds to when the isolation (S41) falls below 19.5dB.

Frequency (GHz)	Phase Shift (degrees)	Phase Shift Error (degrees)
2.0	188.3	8.3
2.2	166.9	10.1
2.4	170.1	9.9
2.6	179.8	0.2
2.8	166.0	14.0
3.0	153.8	26.2
3.2	149.7	30.3
3.4	157.7	22.3
3.6	190.6	10.6
3.8	180.2	0.2
4.0	176.8	3.2
4.2	179.9	0.1
4.4	177.4	2.6
4.6	176.9	3.1
4.8	180.4	0.4
5.0	176.9	3.1
5.2	171.4	8.6
5.4	161.8	18.2
5.6	154.7	25.3
5.8	153.5	26.5
6.0	162.9	17.1

Table 5 Phase shift for the Lange Coupler

When the isolation is artificially improved by increasing |S41|, |S14|, |S23| and |S32| to 25 dB then the error decreases. When the isolation is increased to 30 dB then the 30 degree error at 3.2 GHz decreases to 20 degrees and when it is set at 60 dB then this error decreases to 16 degrees. Other parameters obviously effect the phase error.

The following parameters were artificially altered to see which one has the most influence on the error of a single coupler over the entire frequency range.

i) The coupling was split ie. instead of a 3dB coupling the direct path was set at 2 dB and the coupled path 4 dB.

S12 = S21 = S34 = S43 = 4 dB

S13 = S31 = S24 = S42 = 2 dB

ii) A small amount of loss was added to a 3 dB coupler

S12=S21=S34=S43=S13=S31=S24=S42=3.5 dB

iii) A small amount of loss was added to a split coupling

S12 = S21 = S34 = S43 = 5 dB

S13 = S31 = S24 = S42 = 3 dB

iv) The return loss of the input and output ports were altered.

S11 = S44 = 30 dB

v) The return loss of the terminated ports were altered.

S22 = S33 = 30 dB

vi) The lengths of the paths as shown in figure 9.8 were changed.

It was found that only the condition in (v) altered the error significantly. Different combinations of the changes were tried and it was found that only the isolation and the return loss has any major influence on the error.

9.6 The investigation of the different parameters which effect the phase error.

9.6.1 Isolation

Figure 9.8 shows the quadrature coupler as displayed previously but an additional path is added. This signal path (the isolation path) does not exist in the theoretical model of coupled lines but is very much a part of the characteristics of a real coupler in whatever form.

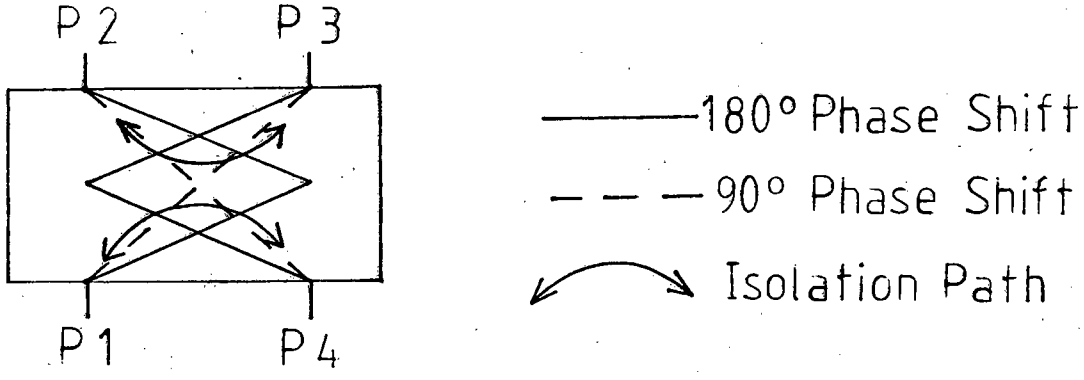

Figure 9.8 The phase shift paths of an ideal coupler with the addition of the Isolation path.

Theoretically the paths P1→P2→P4 and P1→P3→P4 add to 270° in length. When an open circuit is applied to P2 and P3 all the signals at these ports are reflected without any additional phase change onto port 4. The two signals from the two paths are then vectorially added at P4.

When a short circuit is applied to P2 and P3 then an additional 180° is introduced into the path but there is still total reflection at these ports. Therefore the difference between the open circuit and short circuit cases is 180 degrees as shown in figure 9.9 a).

When a leakage path is present between P1 and P4 represented by the vector at zero degrees then a small amount of signal is also vectorially added to the two paths previously mentioned. This causes the two vectors as shown in figure 9.9 a) to have less than a 180 degree seperation. This is illustrated in figure 9.9 b) and c).

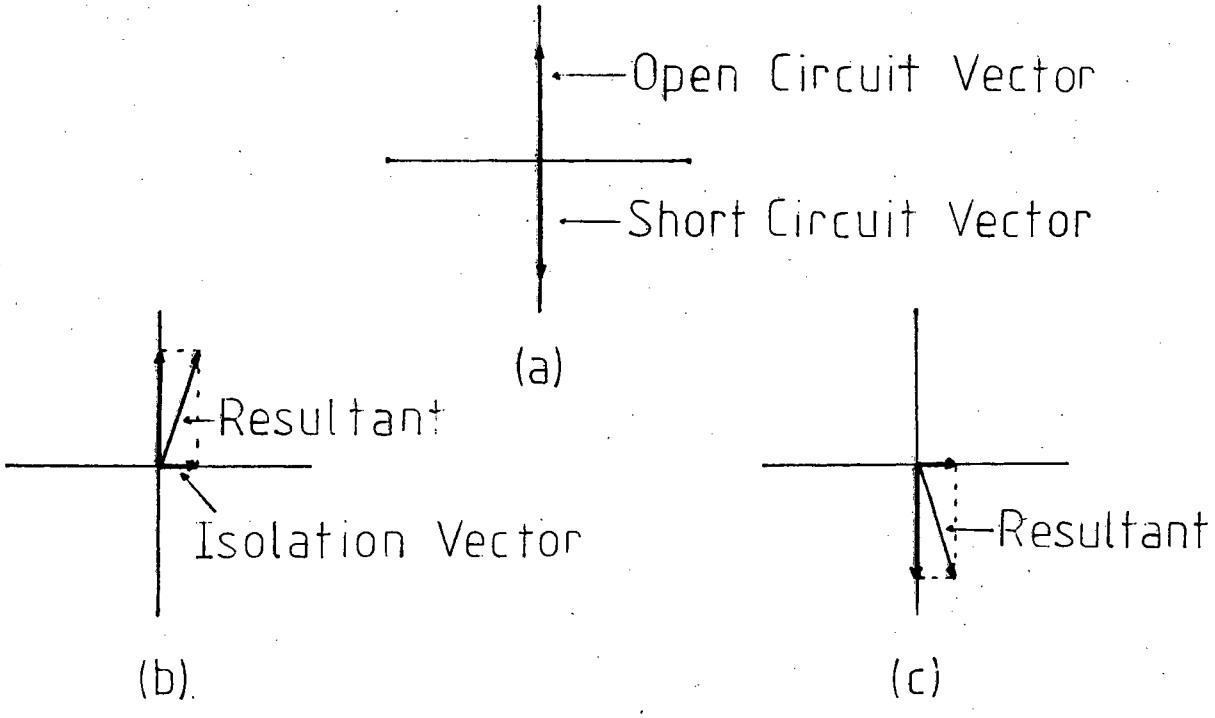

Figure 9.9 The effect of Isolation on the Open circuit and short circuit conditions.

If this isolation vector is either small or lies along the open or short circuit vector then its effect will be negligible. The following tables demonstrate this, where the s-parameters from TOUCHSTONES ideal coupled lines were modified. The

isolation was set at 20 dB and the angle was changed between zero degrees and 90 degrees. The coupling was set at 3 dB.

Freq. (GHz)	Short Circuit (Degrees)	Open Circuit (Degrees)	Difference between Open Circuit and Short Circuit
2	-19.0	156.9	175.9
3	-53.6	116.8	170.4
4	-84.4	84.3	168.7
5	-116.8	53.5	170.3
6	-157.0	19.0	176.0

Table 6 (a) Phase Shift with the isolation angle set at Zero degrees

Freq. (GHz)	Short Circuit (Degrees)	Open Circuit (Degrees)	Difference between Open Circuit and Short Circuit
2	-9.6	149.0	158.6
3	-54.7	119.1	173.8
4	-90.0	89.9	180.0
5	-129.0	63.3	167.7
6	-170.0	30.8	159.2

Table 6 (b) Phase Shift with the isolation angle set at 90 degrees

At 4 GHz it is clearly seen how the vector at the two angles effect the phase error. The isolation angle cannot be controlled to lie on the open circuit or short circuit vector, therefore the only alternative is to ensure that it is small in magnitude. An Isolation approaching 30 dB is thus required.

9.6.2 Return loss of the terminated ports

After the isolation was increased to 60 dB the difference between the open circuit and the short circuit cases was still not 180 degrees. It was found that only when the return losses (S22 and S33) was increased to 30 dB was the phase shift errors less than 4 degrees, which is acceptable.

The return loss at each port is a measure of the match to 50 ohms of that port. Even if the port is not a good match it should not make a difference to the reflection if that port is short circuited or open circuited.

The conclusion that was drawn is that TOUCHSTONE does include this return loss measurement in its calculation when the different terminations are applied which is not true for the physical circuit. Therefore TOUCHSTONE assumes that a four port network is to be inserted into a position where all the ports are connected to 50 ohm lines. To artificially increase the return loss at the coupler ports that are to have the different terminations applied, is a better representation of the physical model.

9.7 PIN diode switches for switching in the open circuit short circuit and 50 ohm matched load.

The objective of the switch is to either absorb power (50 ohm match) or to reflect power with a phase difference of 180 degrees from the two modes of reflection (ie open circuit and short circuit). It is important for the switches to present low phase errors because an error introduced at this point will cause a large deviation from the required phase shifts.

A simple switch that would perform this operation is shown in figure 9.10. Table 7 shows the diode conditions for the different terminations.

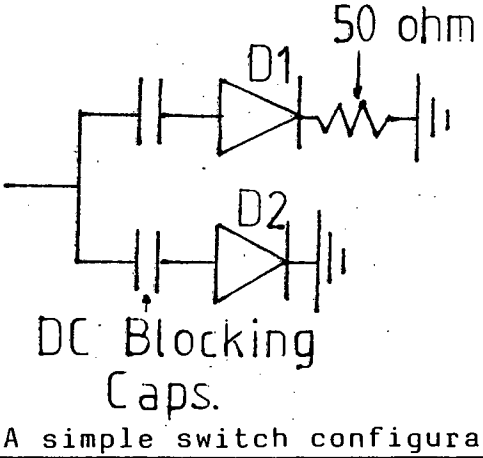

Figure 9.10. A simple switch configuration.

D1	D2	Termination switched in
OFF	OFF	OPEN CIRCUIT
ON	OFF	50 ohm
OFF	ON	SHORT CIRCUIT

Table 7 Resulting terminations for the different diode conditions.

At microwave frequencies care has to be taken to ensure a good short circuit to ground. At frequencies up to 3 GHz, a short wire bonded to the microstrip and ground plane and passed through an unmetallized hole in the substrate provides a good short circuit. As frequencies increase beyond approximately 3 GHz the reactance associated with such a wire becomes significant. The equivalent reactance is frequency dependent and thus different effective lengths of the microstrip line are associated with the same structure at different frequencies.

It has been established that holes containing a brass rod or merely metallized around their cylindrical surface (through hole plated) obtain identical results. A 1.52mm diameter hole results in a reactance which is less than jo.5 ohm over the frequency range 4 GHz to 18 GHz [4] page 106. The short circuit was constructed by screwing an 8BA brass bolt through the substrate into the aluminium ground plane.

The layout as shown in figure 9.10 was constructed in microstrip as shown in figure 9.11. A Ferrite bead with a length of thin wire was used for biasing and the diodes were biased at approximately 15 milli-Amps.

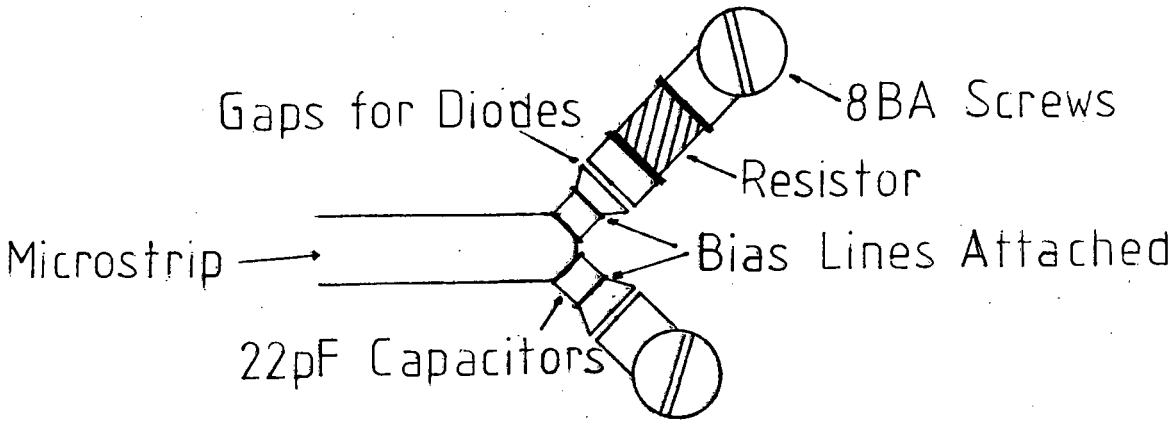

Figure 9.11. The microstrip layout of the switch

The resistor used is a 47 ohm chip resistor intended for UHF-VHF thick film technology. When the diodes were switched accordingly the different terminations were not met, ie the reflection in both cases were 3 dB and large phase errors resulted between the open circuit and the short circuit cases. The 50 ohm match approaches 8 dB over certain frequencies.

It was first suspected that these errors are due to the bias lines being connected very close to the diodes which meant that the lower impedance bias lines are connected in shunt to the high impedance reverse biased diode which results in a lower overall impedance.

A test was carried out where a bias line was connected at increasing spacings away from an open circuit on a 50 ohm line. As the line moves away from the open circuit the response looks more like the ideal open circuit. This trend continued until the distance became more than a quarter wavelength away from the open circuit. This is illustrated in figure 9.12. It was concluded that a bias line must be connected to a low impedance point along the line.

The 47 ohm resistor was placed between a 50 ohm transmission line and a short to ground. The measurement is shown in figure 9.13. It is evident that the resistor does not present a good match. A microwave 50 ohm chip resistor is required.

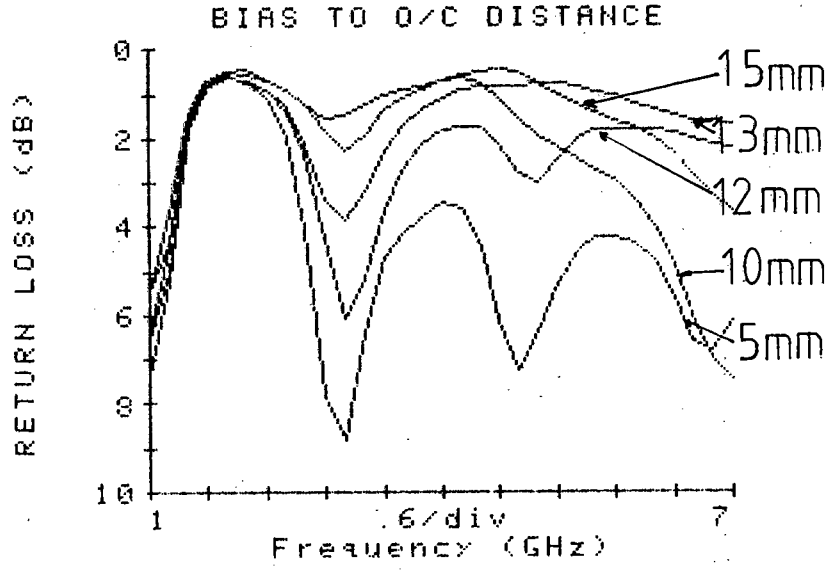

Figure 9.12. The effect of increasing the distance between an Open circuit and a bias line.

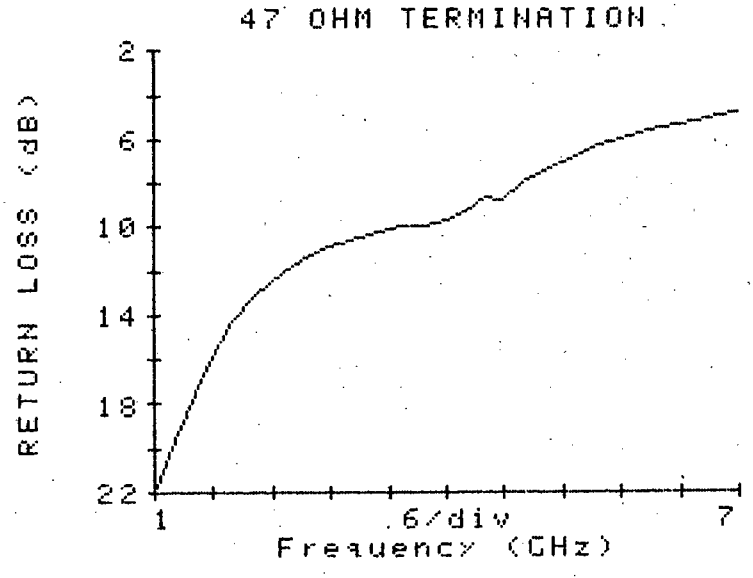

Figure 9.13. The response of the 47 ohm resistor

The bias network consisting of a quarter wavelength at 4 GHz length of thin wire grounded via a 22 pF capacitor was used for all further tests. This gave far better results.

A number of circuits as shown in figure 9.14 were analysed, which allowed the bias lines to be attached a quarter wavelength away from the open circuit. It was found that it is very important for low phase errors that the line lengths that are switched in when the different terminations are activated are the same in length.

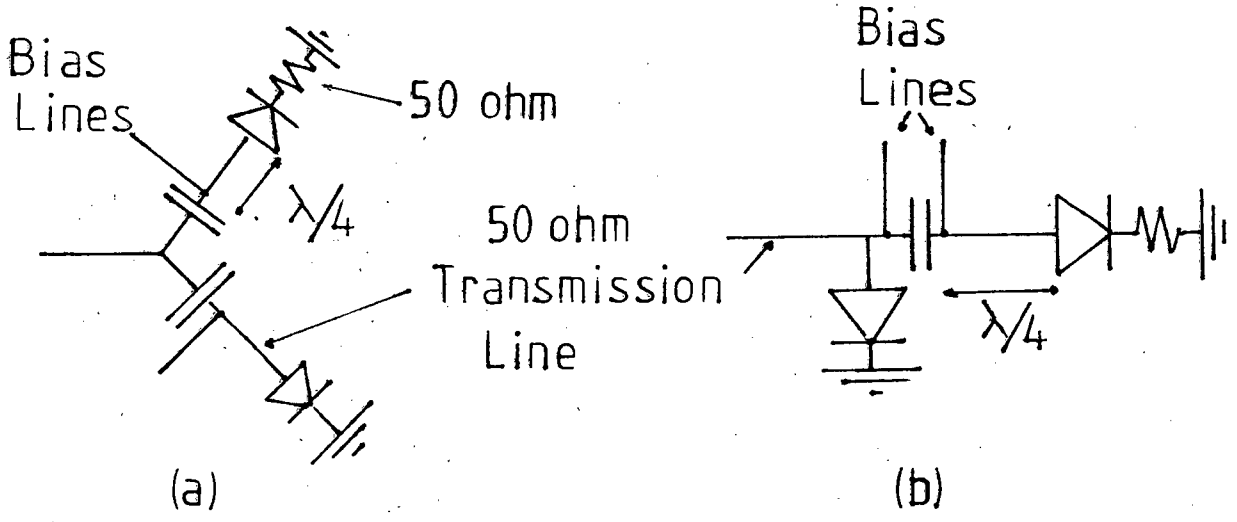

Figure 9.14 Different switch configurations that were analysed.

The circuit in 9.14 a) has the problem that when the 50 ohm resistor is switched in there is an open circuited stub approximately a quarter wavelength in length.

The following circuit as shown in figure 9.15 was devised which allows the short circuit to be physically close to the open circuit on a length of line. The positive and negative biasing voltages with the specific diode orientation allows this to be possible.

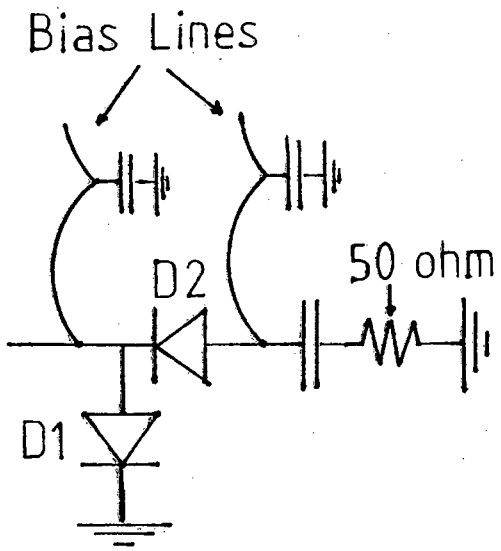

Figure 9.15 The Termination switch

The following table shows the bias voltage polarity on 1 and 2 for the respective terminations required.

BIAS 1	BIAS 2	Resulting Termination
-	-	Open circuit
+	-	Short circuit
+	-	50 ohm

Table 8 The resulting terminations for the different bias voltage polarity.

TOUCHSTONE predicted that the phase difference between the open circuit and the short circuit case is $180^{o} \pm 4.3^{o}$.

One of the first tests that was performed was to solder one diode (D1 in figure 9.15) to an earthing screw and to leave a gap (where D2 is) in the 50 ohm line for the open circuit condition. The errors increased with frequency up to 40 degrees. When D2 was soldered into place the phase error did not change significantly.

When the open circuit and the short circuit was observed on the display it was seen that the open circuit deviates from a straight line at the lower frequencies and the short circuit deviates at the high frequencies. This is shown in figure 9.16. This test was possible by extending the reference plane in the s-parameter test set.

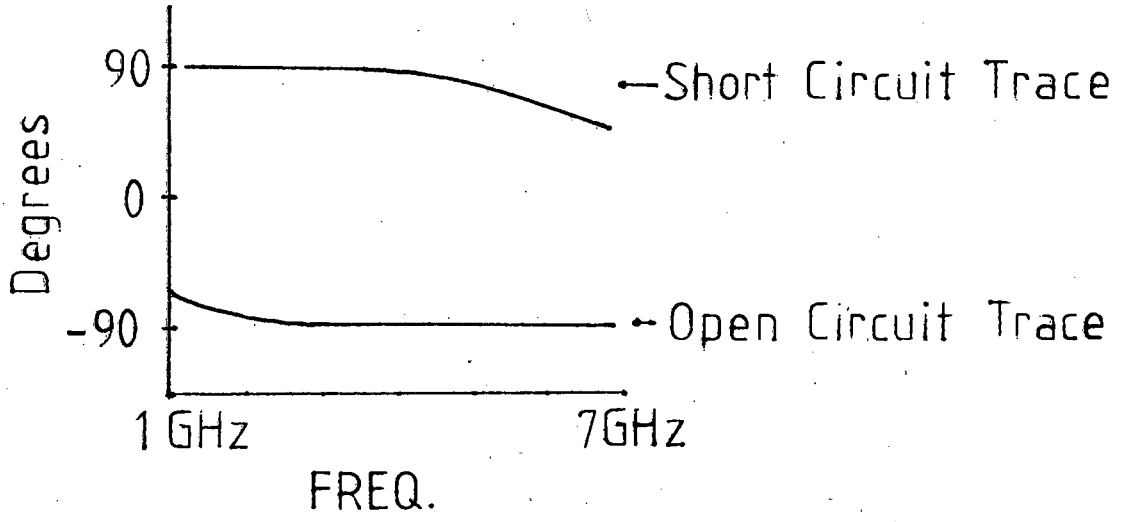

Figure 9.16 The phase display of the open circuit and short circuit conditions.

There was no region where the phase shift difference was 180 degrees. It was evident that the short circuit condition needed to be improved. This was accomplished by soldering an additional diode onto an earthing screw on the other side of the microstrip line as shown in figure 9.17.

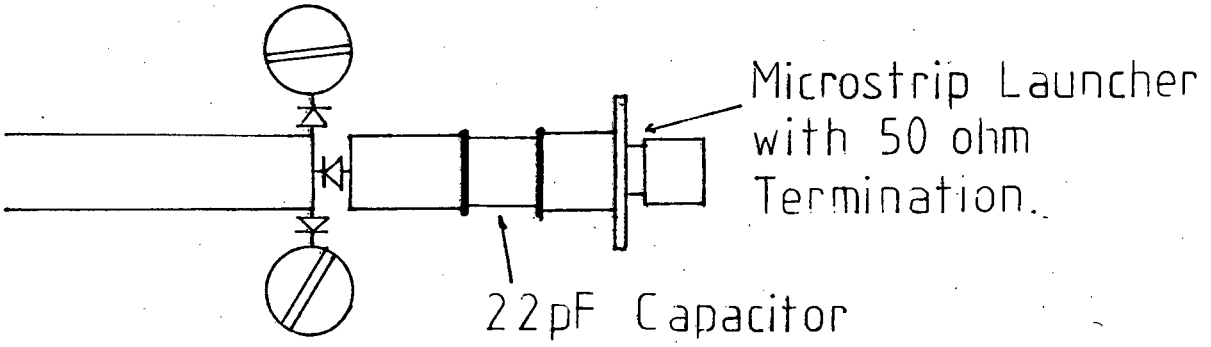

Figure 9.17 The Termination switch with two diodes connected directly to ground.

Figure 9.18 illustrates the return loss for the two conditions and table 9 shows the phase difference between the open and short circuited conditions.

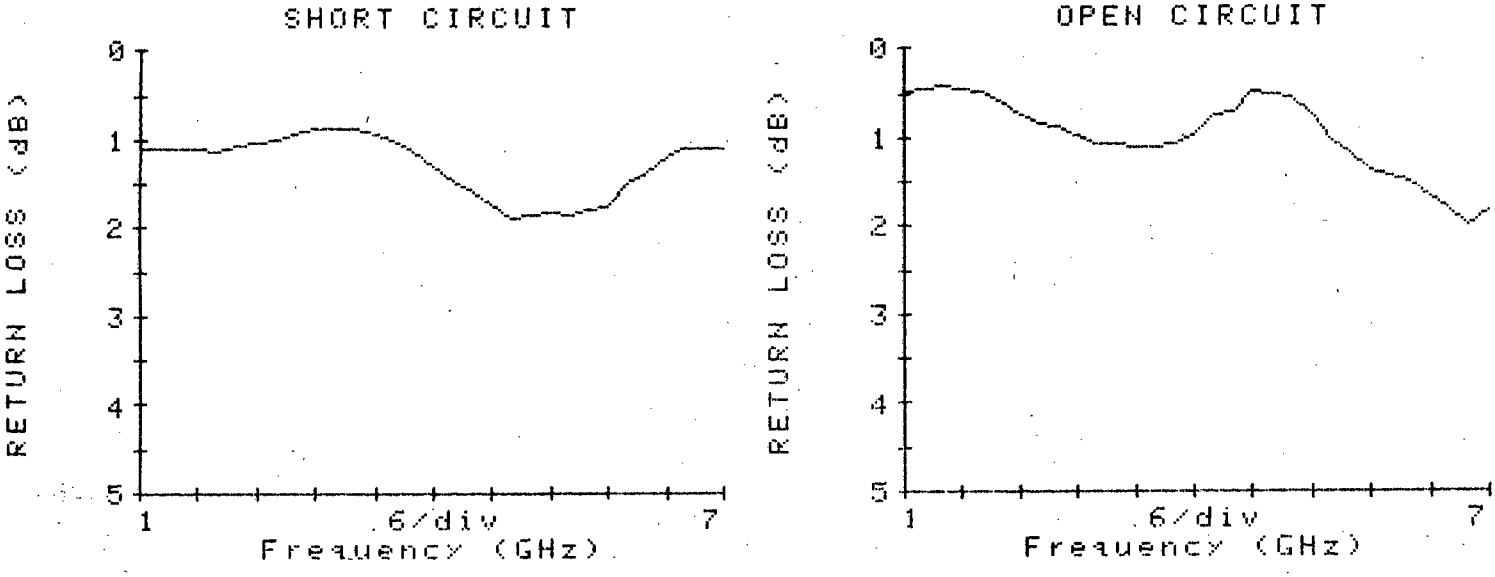

Figure 9.18 Return loss for the two impedance states for the circuit shown in figure 9.17.

Frequency (GHz)	Open circuit phase shift minus short circuit phase shift (Degrees)
2.0	184
2.2	174
2.4	174
2.6	178
2.8	173
3.0	175
3.2	176
3.4	178
3.6	179
3.8	179
4.0	180
4.2	179
4.4	182
4.6	184
4.8	187
5.0	189
5.2	191
5.4	193
5.6	193
5.8	190
6.0	191

Table 9 The phase difference between the open circuit and short circuit conditions.

When the 50 ohm matched load was switched in the return loss was better than 20 dB.

An s-parameter file of the measured short and open circuited condition was created in TOUCHSTONE. (The measurements are shown in appendix F). The different terminations were then applied to the phase shifter consisting of ideal coupled lines as shown in program 21. Figure 9.19 shows the plot of the response at the different frequencies. A $\pm$ 10 degrees line was drawn at every 45 degree step to give an indication of the error incurred. The response falls out of the $\pm$ 10 degree error band at the higher frequencies at 135 degrees and 270 degrees but overall the error is low.

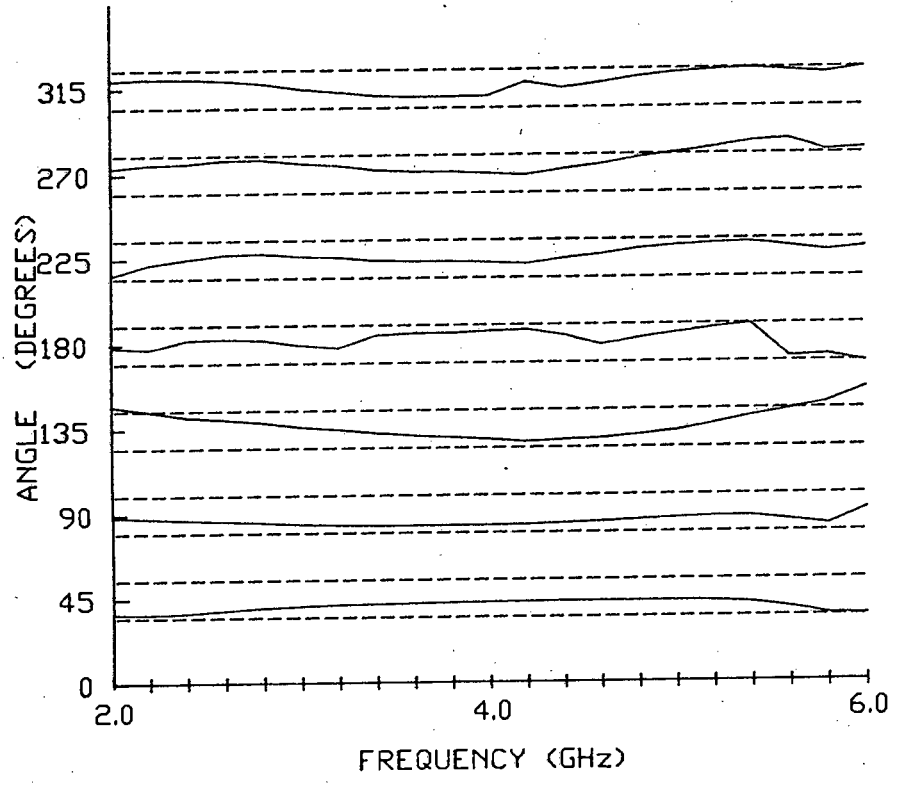

Figure 9.19 The phase shift using the measured parameters of the termination switch.

It must be kept in mind that all the results are referenced to the calculated zero degree line. ie the 135 degree response is actually 135 degree minus zero degrees to obtain a straight line.

9.8 The effect of the imperfect components on the overall phase shifter

The Lange coupler measurements obtained from the CSIR was artificially improved slightly by modifying the s-parameter file. The isolation was increased to 30 dB and the return loss in the terminated ports were also increased to 30 dB. Figure 9.20 shows the phase shift versus frequency using ideal terminations. The errors are less than $\pm$ 10 degrees at all the different steps with three exceptions. A small deviation at the 225 degree, 270 degree and 315 degree lines.

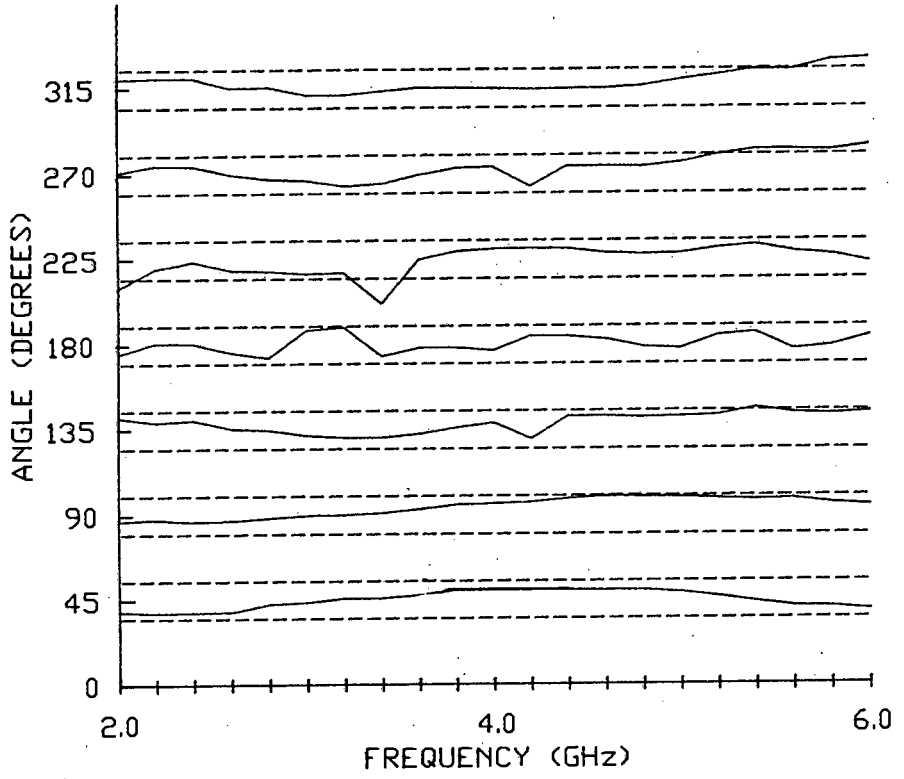

Figure 9.20 The phase shift using ideal terminations and a slightly improved Lange coupler

The Lange coupler on its own with the above mentioned modifications results in errors between the open circuit and short circuit cases of less than 7 degrees. The highest errors were found to be at 3.2 GHz and above 5.4 GHz.

The phase shift of the Lange coupler was then tested with applying the measured s-parameters of the termination switch as developed in section 9.7. The phase difference between the open circuit and short circuit terminated coupler is shown in table 10.

Frequency GHz	Open circuited minus short circuited (degrees)	Error (degrees)
2.0	193.8	13.8
2.2	168.5	11.5
2.4	168.9	11.1
2.6	189.7	9.7
2.8	192.2	12.2
3.0	198.3	18.3
3.2	151.7	28.3
3.4	147.4	32.6
3.6	213.4	33.4
3.8	212.4	32.4
4.0	148.7	31.3
4.2	147.9	32.1
4.4	148.2	31.8
4.6	210.6	30.6
4.8	209.4	29.4
5.0	149.9	30.1
5.2	148.1	31.9
5.4	143.7	36.3
5.6	222.1	42.1
5.8	221.6	41.6
6.0	141.2	38.8

Table 10. The phase difference between the open circuit and short circuit terminated coupler.

It can be seen that large errors are present. When this coupler with the measured terminations were tested in the entire phase shifter configuration then the following plots result.

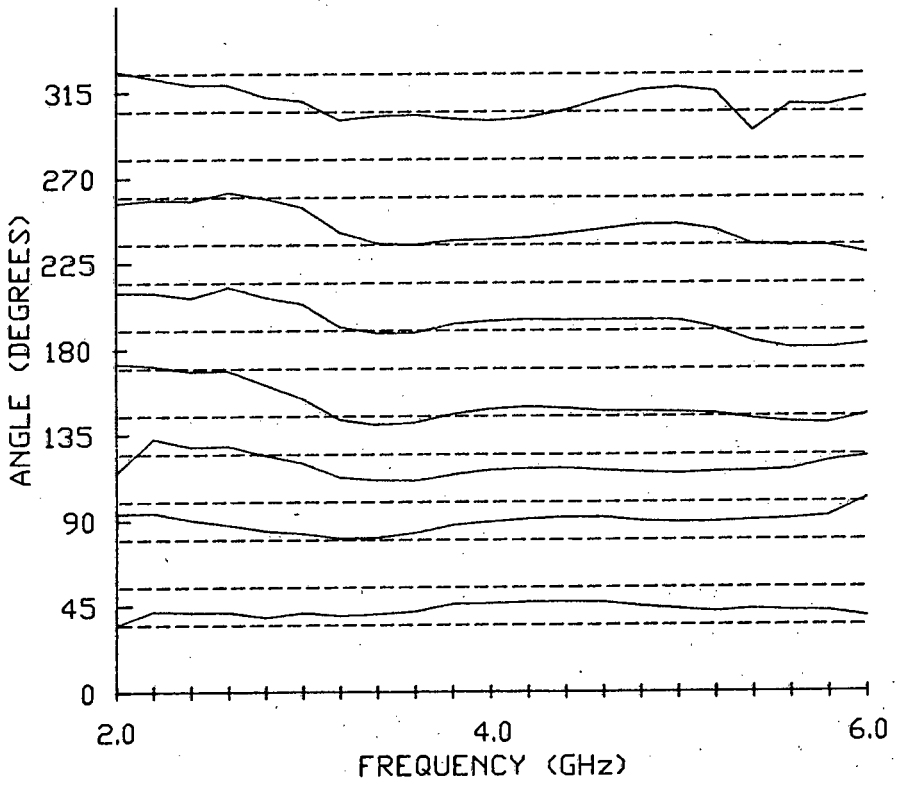

Figure 9.21 The phase shifter using the real terminations and a slightly improved Lange Coupler

It can be seen that the errors are compounded at only some of the phase shifts. The worst case being the 225 degree line which lies totally out of the $\pm$ 10 degree band and extends into the 180 degree area. There is still approximately 45 degrees between the 180 degree and the 225 degree shifts but relative to the zero degree shift errors of up to 40 degrees are encountered.

When the errors are observed when consulting Figure 8.12 Section 8.5 it is noted that the phase shifts which involve short circuits result in the largest deviations. But the major problem which still remains is to develop a quadrature coupler which presents an isolation in the region of 30 dB.

9.9 Conclusion

It was found that when the constructed PIN diode termination switch was used to switch the different phases of a physical quadrature coupler large errors were produced. The demands made by this phase shifter configuration on the elements were not met in practice and no further development was undertaken. A switch that switches between zero and 180 degrees (or $\pm$ 90 degrees) which presents low phase shift errors over a large bandwidth is needed for this system to be successful.

It has been reported in the literature [2] that a phase shifter with the same basic configuration replaces couplers 1 and 2 in figure 8.10 with a non-reflective switch and a coupler which switches only between zero degrees and 180 degrees. An incremental phase change of 45 degrees $\pm$ 7 degrees from 6 GHz to 18 GHz was obtained.

10. CONCLUSION

The basic Single Pole Double Throw switch using shunt mounted PIN diodes was found to have a maximum bandwidth of just over one octave. (2 GHz to 5.1 GHz). The switch consisting of series mounted diodes is inherently much broader in bandwidth, the limiting factor only being determined by the parasitic components of the PIN diodes used. Differing number of throws of a switch in the series mounted case does not change any design feature or parameter. The main disadvantage of the series mounted diode is the low power handling capability.

To increase the isolation of the basic switch additional diodes have to be inserted in each branch. Different combinations of shunt and series mounted diodes were investigated. It was found that if a shunt mounted diode was placed directly after the series mounted diode a high isolation can be achieved without affecting the bandwidth, but this was not possible in practice. Three series mounted diodes with a separation of 10 mm along the length of the microstrip was found to be a good compromise. In addition the circuit has to be enclosed in an evanescent waveguide system to prevent radiation effects from degrading the isolation. For further miniturization of the circuit a thinner dielectric substrate (.127 mm) can be used which would result in a narrower 50 ohm transmission line which in turn allows a smaller waveguide system.

Only after experience was gained in the use of TOUCHSTONE was its full potential utilized. Care has to be taken to which statement is most accurate in specifying microstrip TEE junctions and CROSS junctions. Generally to avoid large errors in the software the line lengths of microstrip stubs and sections must be longer than the widths by at least a factor of two. For the theoretical model to be an accurate representation of the physical circuit an understanding of how the software takes all the parameters into account is essential.

The phase shifter consisting of three quadrature couplers and a power splitter works well in theory but couplers and termination switches still have to be developed which comply with the demands made on them by this particular configuration.

All the circuits fabricated made use of the bias networks that were developed. It was found that the ferrite bead with two turns of thin wire does not perform well if it is used in circuits that have discontinuities. The bias system consisting of a grounded capacitor and a short length of thin wire gives the best results overall.

A P P E N D I X A

Computer Programs

PROGRAM 1

```
tlhilo.ckt    01-01-80  00:57:49

!THIS CCT USES IDEAL TRANS. LINES TO DEVELOP A HIGH IMP. LOW IMP. SECTION
CKT
  TLIN 1 2 Z=50 E=360 F=4
  TLIN 2 3 Z=50 E=360 F=4
  TLIN 2 4 Z=148 E#70 107.62540 140 F=5
  TLOC 4 0 Z=30 E=110 F=5
  TLIN 4 5 Z=148 E#100 136.81580 140 F=5
  TLOC 5 0 Z=30 E=76 F=2.5
  DEF2P 1 3 BIAS
OUT
  BIAS DB[S11] GR1
FREQ
  SWEEP 1 7 .1
OPT
  RANGE 2 6
  BIAS DB[S11] < -20
GRID
  RANGE 1 7 .5
  GR1 -40 0 5
```

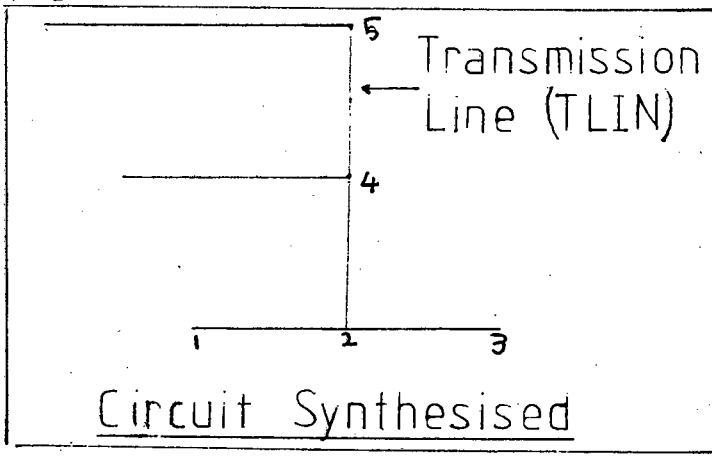

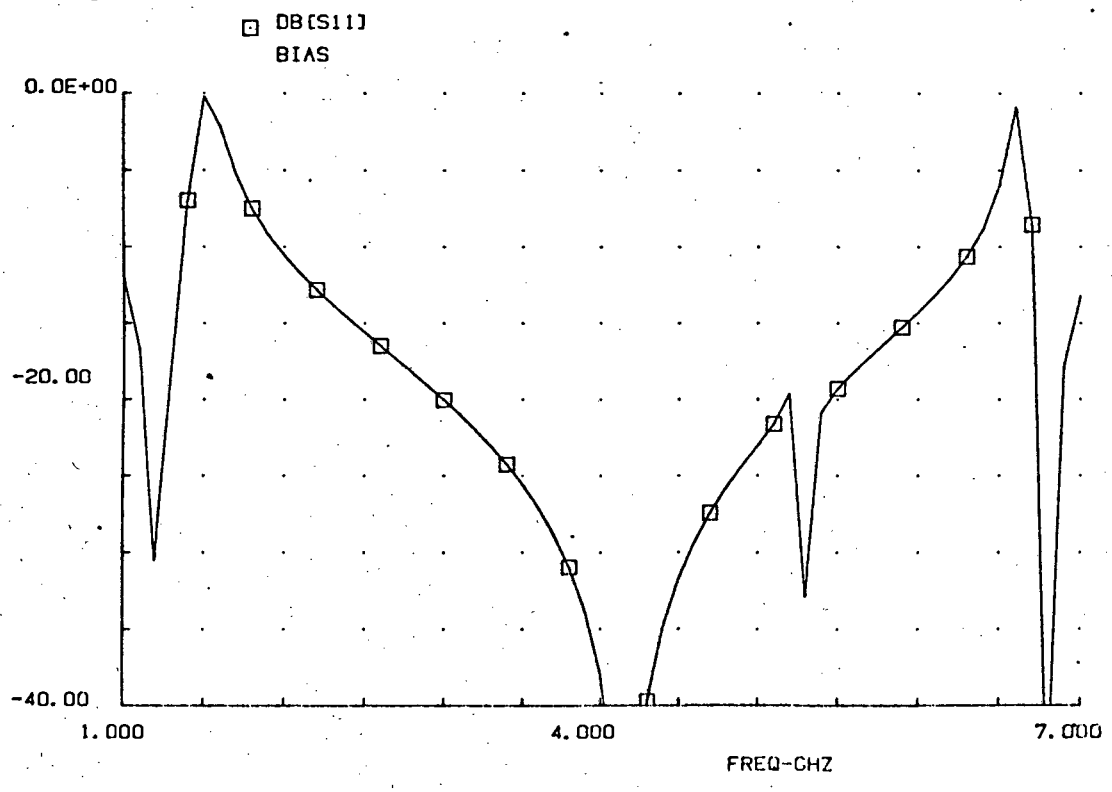

Touchstone (TM)
H.ckt

PROGRAM 2

```
!HIGH IMP. LOW IMP. SECTION FOR BIAS NETWORK
DIM
  LNG MM
VAR
  WH=.6                          !WIDTH OF HIGH IMP. SECTION
  WL1=4                          !WIDTH OF FIRST LOW IMP. SECTION
  WL2\3.16199                        !WIDTH OF SECOND LOW IMPEDANCE
CKT
  MSUB ER=2.2 H=.7874 T=.034 RHO=.7066 RGH=0
  MLIN 1 3 W=2.46 L=53.79
  MLIN 4 2 W=2.46 L=53.79
  MLIN 5 6 W^WH L\17.25064
  MLIN 7 9 W^WH L\3.80948
  MTEE 3 4 5 W1=2.46 W2=2.46 W3^WH
  MTEE 10 11 9 W1^WL2 W2^WL2 W3^WH
  MTEE 6 7 8 W1^WH W2^WH W3^WL1
  MLOC 8 W^WL1 L\11.48134
  MLOC 10 W^WL2 L\11.33318
  MLOC 11 W^WL2 L=0
  DEF2P 1 2 BIAS
OUT
  BIAS DB[S11] GR1
FREQ
  SWEEP 1 7 .1
OPT
! RANGE 4.0 5.5
  RANGE 2.0 6.0
  BIAS DB[S11] < -20
GRID
  RANGE 1 7 .5
  GR1 -40 0 5
```

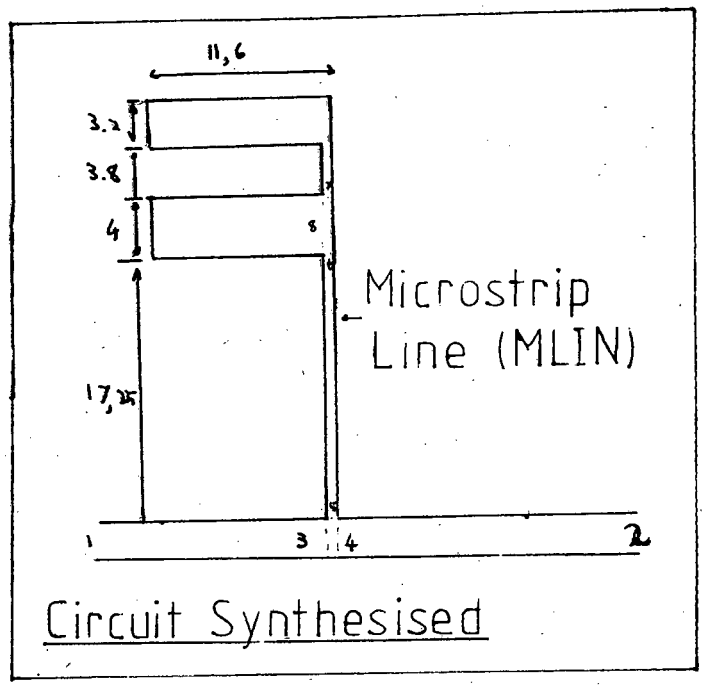

Circuit Synthesised

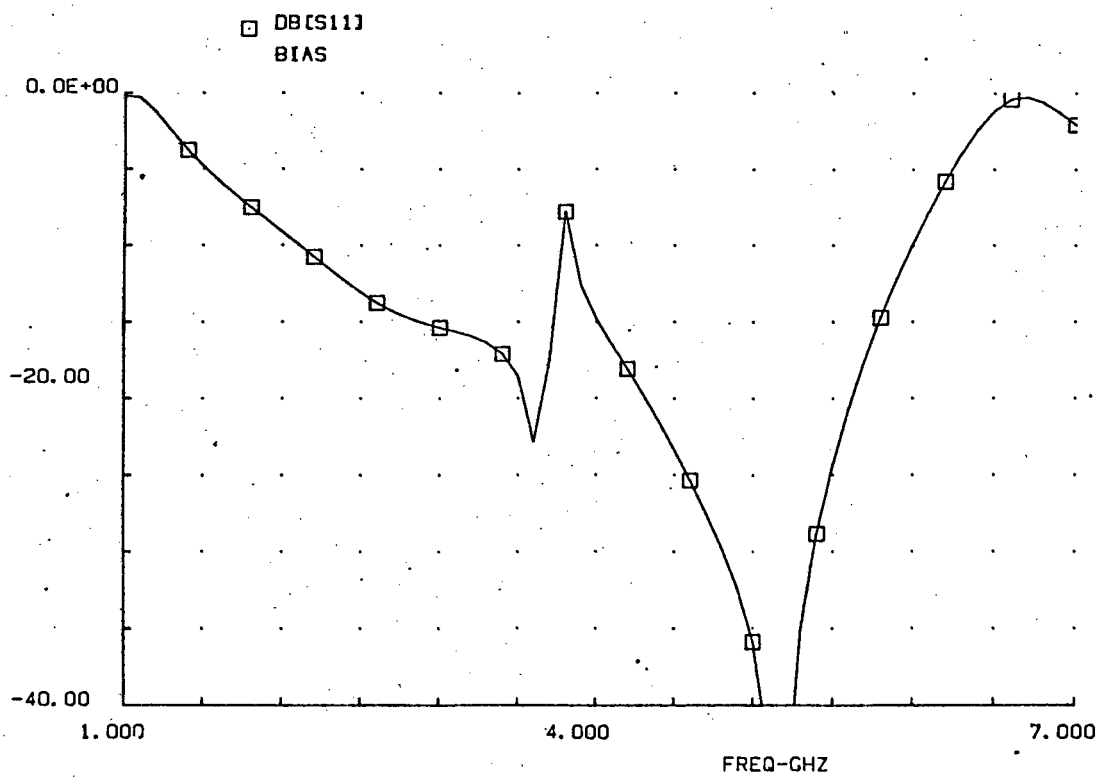

PROGRAM 3

A BASIC Program to calculate Resonant Frequency and pad dimensions for a Rectangular Pad Elliptic Filter.

```
10  INPUT"L="; I, "CA="; A, "CB="; B, "CC="; C
20  INPUT"WIDTH PORT 1="; W, "WIDTH PORT 2="; X
30  INPUT"WIDTH="; G
40  L=7.874E-4*(A+B)/(2.2*8.854E-12*G)
50  M=B/SQRT(2*(A*B+A*C+B*C))
60  N=-A/SQRT(2*(A*B+A*C+B*C))
70  P=(L/PI)*ACS(-M*PI*W/(2*L*SIN(PI*W/(2*L))))
80  Q=(L/PI)*ACS(N*PI*X/(2*L*SIN(PI*X/(2*L))))
90  F=(I*(C+A*B/(A+B)))^-.5/(2*PI)
100 PRINT "RES FREQ="; F
110 PRINT "LENGTH="; L
120 PRINT "P1="; P
130 PRINT "P2="; Q
140 END
```

PROGRAM 4

```
*****  052985    ********  SPICE 2E.0 (18JAN78)  ********  104028  *

     TWO SECTION BIAS FILTER

      INPUT LISTING                          TEMPERATURE =   27.000 DEG C

*******************************************************************************


VIN  0  1  AC  1
V1  2  3  AC  0
V2  6  5  AC  0
FS  1  2  V1  1
R1  6  0  1
TL1  3  0  4  0  Z0=1  F=4GHZ  NL=1
TL2  4  0  5  0  Z0=1  F=4GHZ  NL=1
TL3  15  0  7  0  Z0=1.4  F=3GHZ  NL=.3215
TL6  4  0  15  0  Z0=1.4  F=4.2GHZ  NL=.25
TL5  15  0  16  0  Z0=.6  F=4.2GHZ  NL=.25
CA  7  0  1PF
CB  8  0  1PF
CC  7  8  .04FF
LC  7  8  5.6NH
TL4  8  0  14  0  Z0=1.4  F=3GHZ  NL=.125
R2  14  0  1000MEG
R7  16  0  1000MEG
G1  9  0  3  0  1
F1  9  0  V1  1
R3  9  0  1
G2  10  0  6  0  1
F2  10  0  V2  1
R4  10  0  1
G3  11  0  3  0  1
F3  0  11  V1  1
R5  11  0  1
G4  12  0  6  0  1
F4  0  12  V2  1
R6  12  0  1
.AC  LIN  100  2GHZ  6GHZ
.PLOT  AC  VDB(11)
.PLOT  AC  VDB(12)
.END
```

PROGRAM 5

biashilo.ckt

```
!HI IMP. LOW IMP. SECTION WITH ELLIPTIC FILTER PAD FOR BIAS NETWORK
DIM
  LNG MM
VAR
  WC1=1.400          !WIDTH OF CONNECTION FROM 50 OHM LINE TO LOW IMP
  WC2=1.400          !WIDTH OF CONNECTION FROM LOW IMP. TO ELLIPTIC
  WLI=11.40000           !WIDTH OF LOW IMP. SECTION
  WP=8.00000               !WIDTH OF ELLIPTIC FILTER PAD
  WS=1.400           !WIDTH OF STUB
CKT
  MSUB ER=2.2 H=.7874 T=.034 RHO=.7066 RGH=0
  MTEE 3 4 5 W1=2.46 W2=2.46 W3^WC1
  MTEE 6 7 8 W1^WC1 W2^WC2 W3^WLI
  MTEE 9 10 11 W1^WP W2^WP W3^WC2
  MTEE 12 13 14 W1^WP W2^WP W3^WS
  MLIN 5 6 W^WC1 L=18.50000
  MLIN 7 11 W^WC2 L=14.9000
  MLIN 9 12 W^WP L=11.000
  MLOC 8 W^WLI L\21.70000
  MLOC 10 W^WP L=4.80000
  MLOC 13 W^WP L=3.60000
  MLOC 14 W^WS L=9.00000
  MLIN 1 3 W=2.46 L=53.79
  MLIN 4 2 W=2.46 L=53.79
  DEF2P 1 2 BIAS
OUT
  BIAS DB[S11] GR1
```

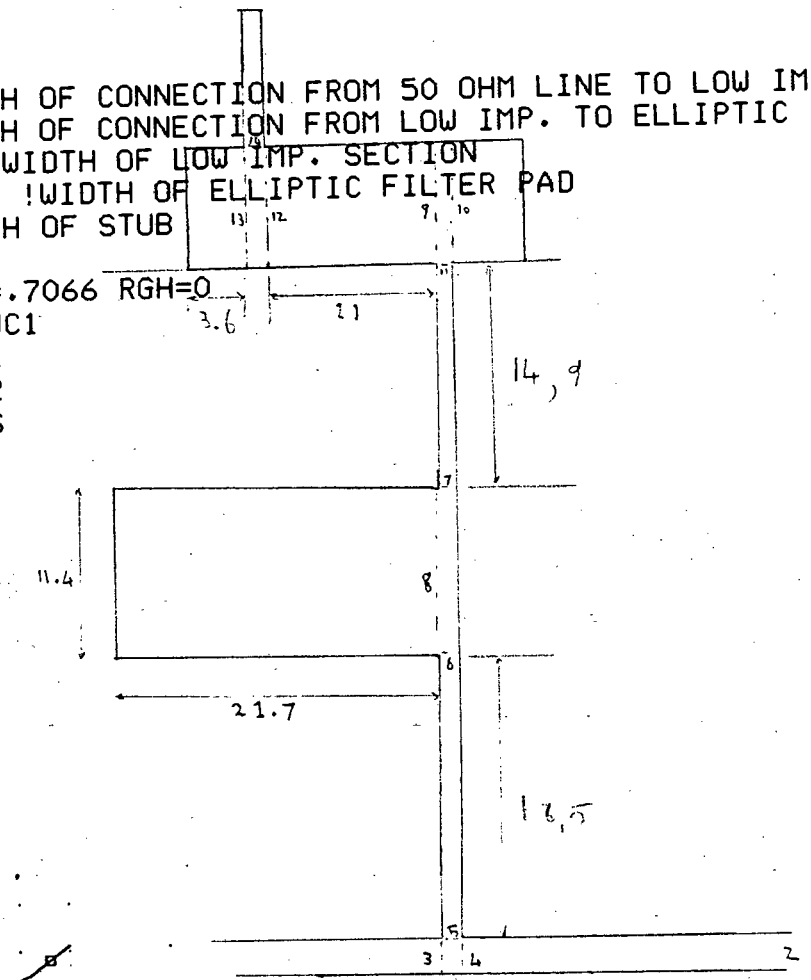

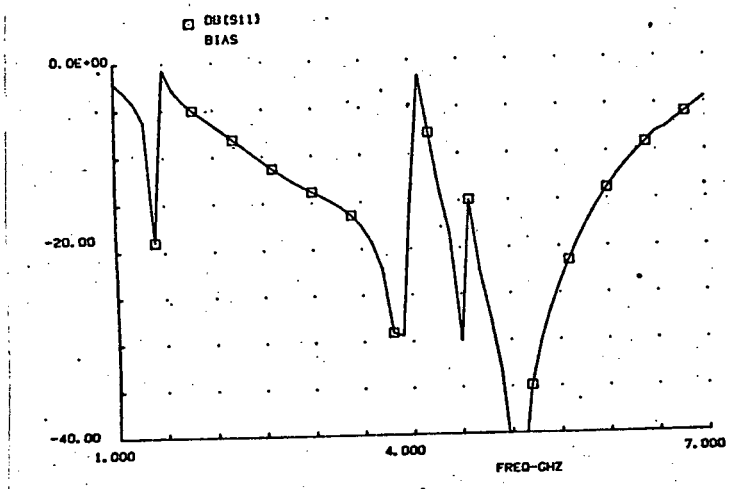

```
            bias2.ckt    01-01-80  01:02:08

!TWO SECTION ELLIPTIC FILTER USED IN BIAS NETWORK
DIM
  LNG  MM
VAR
  WP=8                                          !WIDTH OF FIRST FILTER PAD
  WS=0.89407                                     !WIDTH OF STUB
  WH\0.60000                                          !WIDTH OF CONNECTION TO 50
  WF=2.40000                                      !WIDTH OF SECOND FILTER PAD
CKT
  MSUB ER=2.2 H=.7874 T=.034 RHO=.7066 RGH=0
  MTEE 1 2 3 W1^WP W2^WP W3^WF
  MTEE 4 5 6 W1^WP W2^WP W3^WH
  MLOC 1 W^WP L=8.91428
  MLOC 5 W^WP L=1.17792
  MLIN 2 4 W^WP L=5.56185
  MLOC 14 W^WS L=6.55433                                !STUB
  MLIN 6 9 W^WH L\12.95236                !HALF WAVELENGTH
  MTEE 7 8 9 W1=2.46 W2=2.46 W3^WH
  MLIN 7 10 W=2.46 L=53.79
  MLIN 8 11 W=2.46 L=53.79
  MTEE 12 13 14 W1^WF W2^WF W3^WS
  MLIN 3 12 W^WF L=9.05217
  MLOC 13 W^WF L=0.91117
  DEF2P 10 11 BIAS
OUT
  BIAS DB[S11] GR1
```

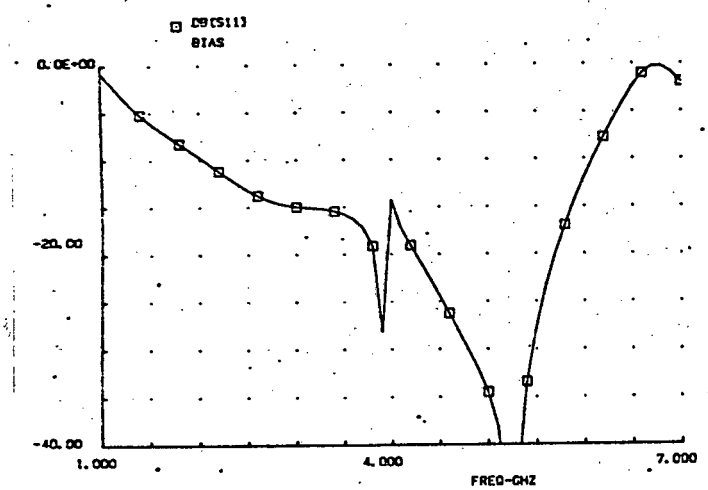

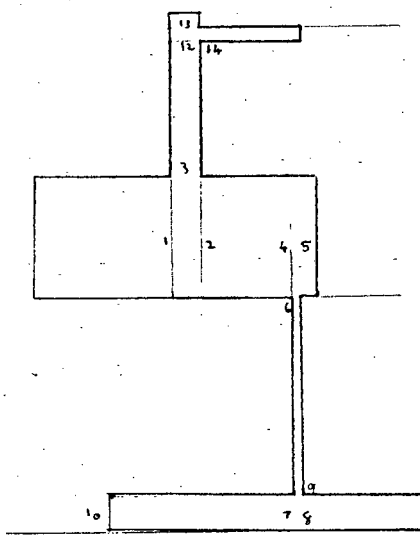

PROGRAM 7


```
!HIGH IMP. LOW IMP. SECTION FOR BIAS NETWORK
DIM
  LNG MM
VAR
  WH=1                                  !WIDTH OF HIGH IMP. SECTION
  WL=5                                  !WIDTH OF LOW IMP. SECTION
CKT
  MSUB ER=2.2 H=.7874 T=.034 RHO=.7066 RGH=0
  MLIN 1 3 W=2.46 L=53.79
  MLIN 4 2 W=2.46 L=53.79
  MLIN 5 8 W^WH L=4
  MTEE 3 4 5 W1=2.46 W2=2.46 W3^WH
  MTEE 6 7 8 W1^WL W2^WL W3^WH
  MLOC 6 W^WL L=2.00
  MLOC 7 W^WL L=0.00
  WIRE 8 9 D=.6 L=60 RHO=.7066
  SHOR 9
  DEF2P 1 2 BIAS
OUT
  BIAS DB[S11] GR1
FREQ
  SWEEP 1 7 .1
OPT
  RANGE 2 6
  BIAS DB[S11] < -20
GRID
  RANGE 1 7 .5
  GR1 -40 0 5
```

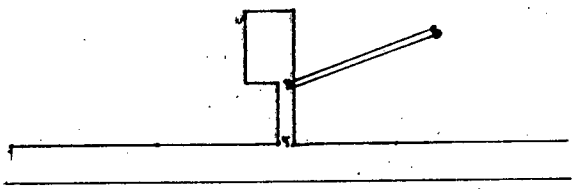

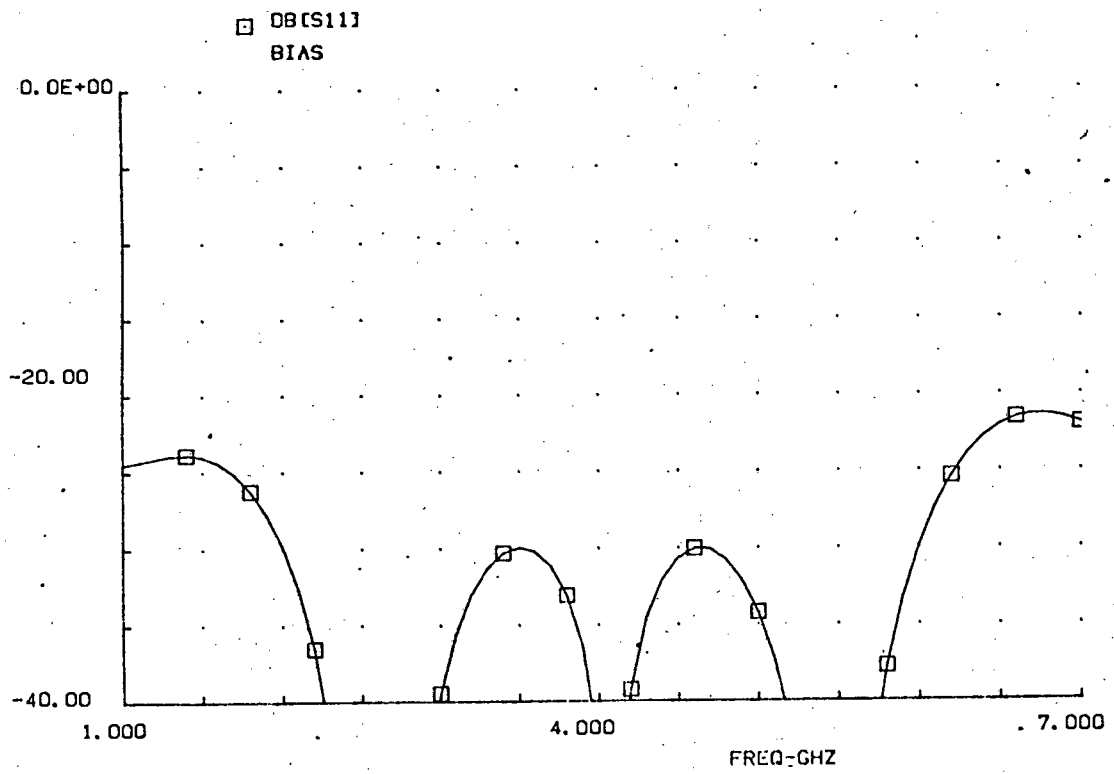

PINFOR.ckt

```
!THIS PROGRAM GENERATES THE S-PARAMETER FILE OF THE THEORETICAL MODEL
!OF THE FORWARD BIASED SERIES MOUNTED PIN DIODE. (TYPE DSG6474)
CKT
  SRL 1 2 R=4 L=.3
  CAP 1 2 C=.05
  DEF2P 1 2 PINFOR SPINFOR
OUT
  PINFOR MAG[S11]
  PINFOR ANG[S11]
  PINFOR MAG[S21]
  PINFOR ANG[S21]
  PINFOR MAG[S12]
  PINFOR ANG[S12]
  PINFOR MAG[S22]
  PINFOR ANG[S22]
FREQ
  SWEEP 1 7 .2
```

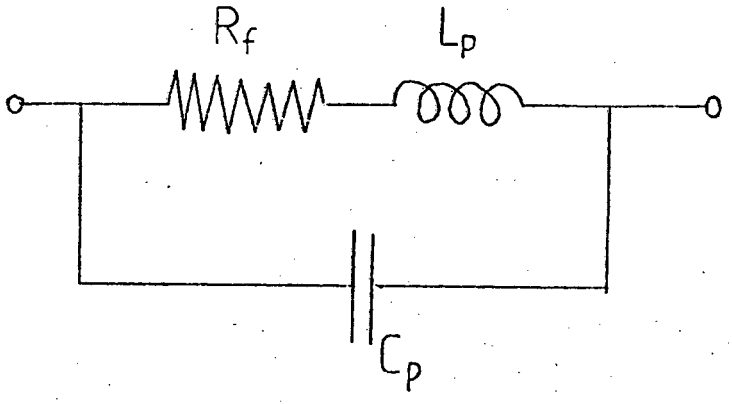

Forward biased series mounted PIN diode

PINREV.ckt

```
!THIS PROGRAM GENERATES THE S-PARAMETER FILE OF THE THEORETICAL MODEL
!OF THE REVERSE BIASED SERIES MOUNTED PIN DIODE. (TYPE DSG6474)
CKT
  SRLC 1 2 R=1000 L=.3 C=.05
  CAP 1 2 C=.05
  DEF2P 1 2 PINREV SPINREV
OUT
  PINREV MAG[S11]
  PINREV ANG[S11]
  PINREV MAG[S21]
  PINREV ANG[S21]
  PINREV MAG[S12]
  PINREV ANG[S12]
  PINREV MAG[S22]
  PINREV ANG[S22]
FREQ
  SWEEP 1 7 .2
```

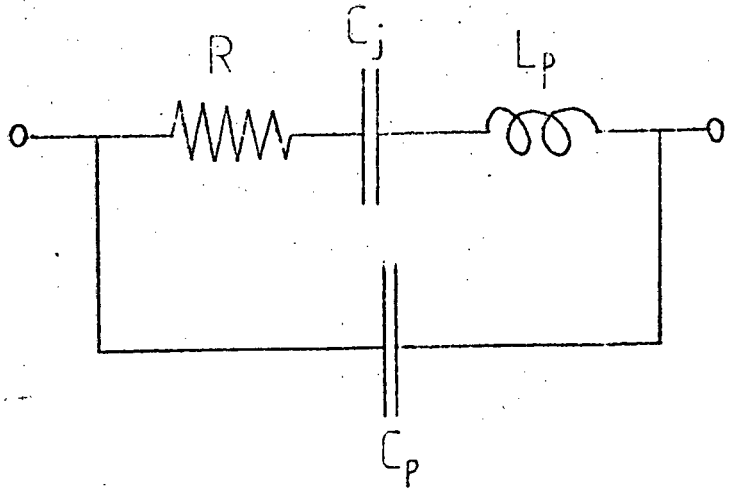

Reverse biased series mounted PIN diode

PROGRAM 9

MICRSPDT.ckt

```
!MICROSTRIP SPDT SWITCH USING A SHORT AND THRU LINE AS PIN DIODES FORWARD
!AND REVERSE BIASED AND NO CAPACITORS. THIS IS EXACTLY AS IT WAS CONSTRUCTED.
DIM
  LNG MM
VAR
  WL=2.46                    !WIDTH OF 50 OHM LINE
  WM=4                       !WIDTH OF QUARTER WAVELENGTH MATCHING SECTIONS
  LM=13.28                   !LENGTH OF QUARTER WAVELENGTH MATCHING SECTIONS
CKT
  MSUB ER=2.2 H=.7874 T=.034 RHO=.7066 RGH=0
  MLIN 1 2 W^WL L=10
  MLIN 4 5 W^WL L=10
  MLIN 7 8 W^WL L=10
  MLIN 3 12 W^WM L^LM
  MLIN 6 10 W^WM L=11.28
  MLIN 9 11 W^WM L=11.28
  MTEE 10 11 12 W1^WM W2^WM W3^WM
  MSTEP 2 3 W1^WL W2^WM
  MSTEP 5 6 W1^WL W2^WM
  MSTEP 8 9 W1^WL W2^WM
  SHOR 8
  DEF2P 1 4 SPDT
OUT
  SPDT DB[S11] GR1
  SPDT DB[S21] GR2
FREQ
  SWEEP 2 6 .1
GRID
  RANGE 2 6 .5
  GR1 -40 0 5
  GR2 -20 0 5
```

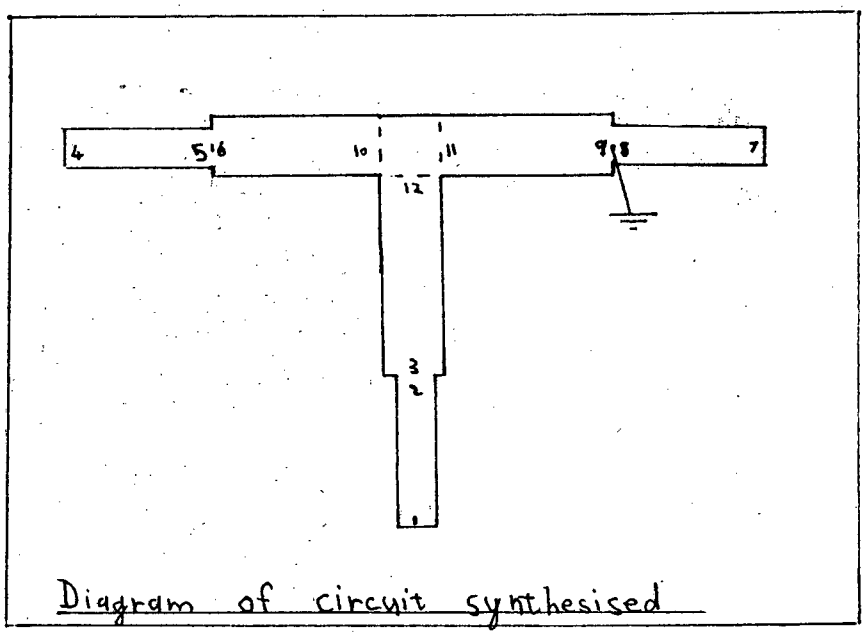

Diagram of circuit synthesised

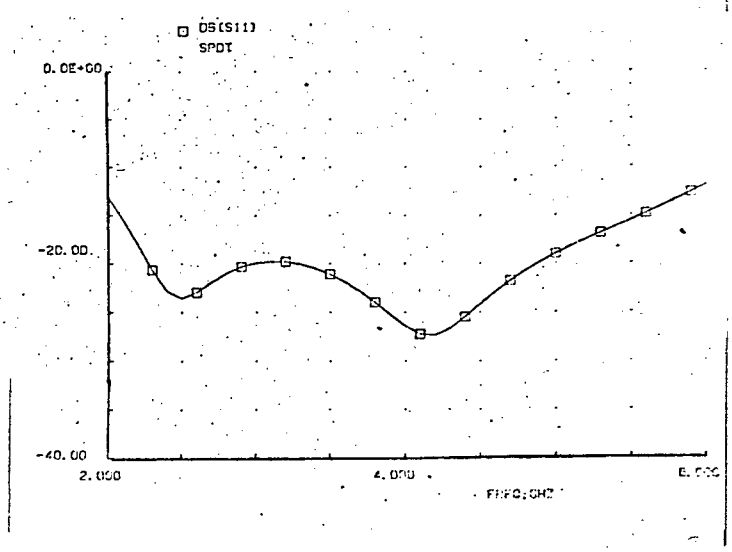

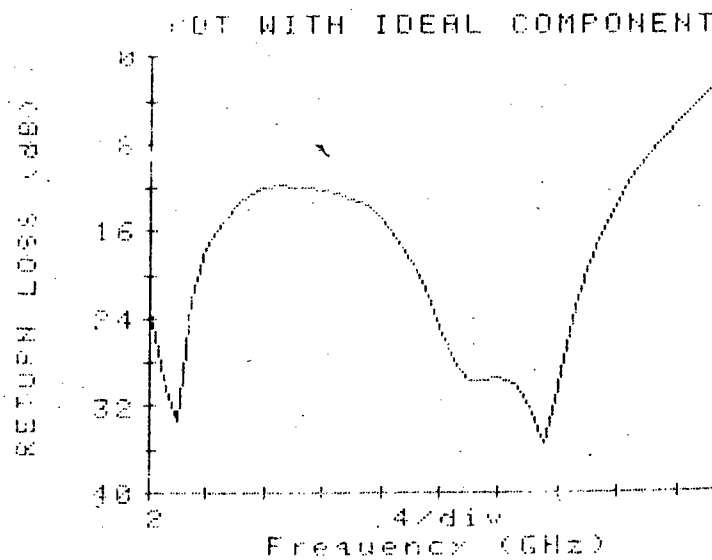

PROGRAM 10

MICRSPDT.ckt 01-01-80 02:23:19

```
!MICROSTRIP SPDT SWITCH WITH ONE PIN DIODE WHICH IS FORWARD BIASED. THERE ARE
!NO CAPACITORS.
DIM
  LNG MM
VAR
  WL=2.46                    !WIDTH OF 50 OHM LINE
  WM=4                       !WIDTH OF QUARTER WAVELENGTH MATCHING SECTIONS
  LM=13.28                   !LENGTH OF QUARTER WAVELENGTH MATCHING SECTION
CKT
  MSUB ER=2.2 H=.7874 T=.034 RHO=.7066 RGH=0
  MLIN 1 2 W^WL L=10
  MLIN 4 5 W^WL L=10
  MLIN 7 8 W^WL L=10
  MLIN 3 12 W^WM L^LM
  MLIN 6 10 W^WM L=11.28
  MLIN 9 11 W^WM L=11.28
  MTEE 10 11 12 W1^WM W2^WM W3^WM
  MSTEP 2 3 W1^WL W2^WM
  MSTEP 5 6 W1^WL W2^WM
  S2PA 8 9 0 PINON
  DEF2P 1 4 SPDT
OUT
  SPDT DB[S11] GR1
  SPDT DB[S21] GR2
FREQ
  SWEEP 2 6 .1
GRID
  RANGE 2 6 .5
  GR1 -20 0 5
  GR2 -20 0 5
```

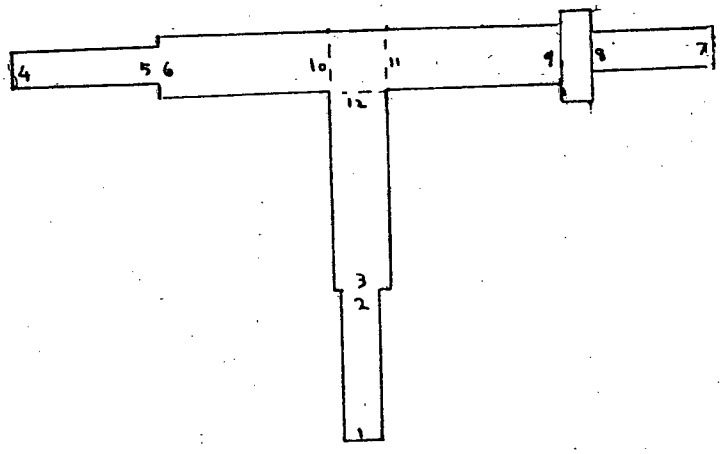

Diagram of the circuit synthesised by this program. (Double size)

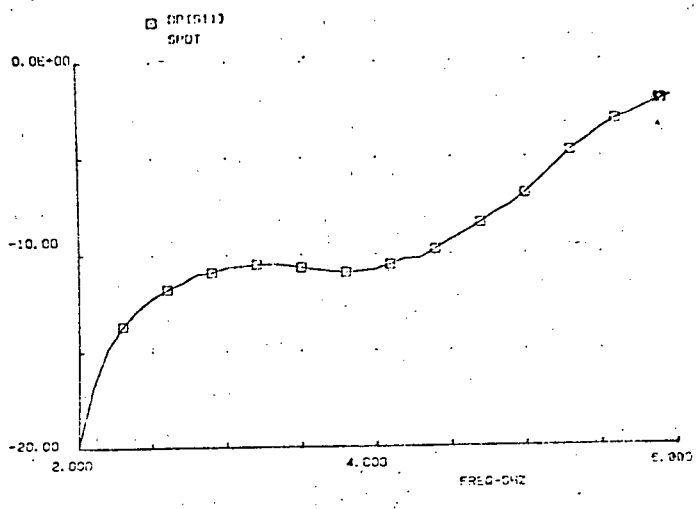

SPDT WITH 1 PIN & NO CAPS

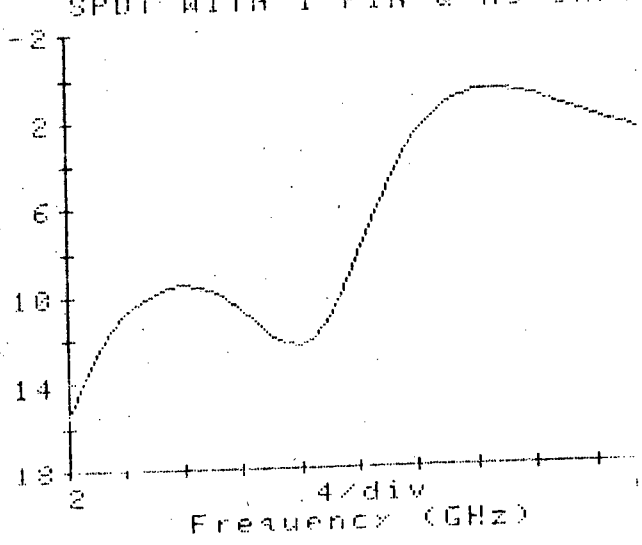

PROGRAM 11

SPDT2.ckt 01-01-80 01:25:00

```
!SPDT SWITCH WITH IDEAL TRANSMISSION LINES AND PIN DIODE MODELS IN
!FORWARD AND REVERSE BIAS.
VAR
  ZO\47.45506                    !IMPEDANCE OF SPDT BRANCHES (PIN)
  Z1\41.17668                    !IMPEDANCE OF SPDT BRANCH FEED
  LO\59.13683                    !LENGTH OF SPDT BRANCHES
  L1\87.28701                    !LENGTH OF SPDT BRANCH FEED
CKT
  TLIN 1 2 Z=50 E=360 F=4
  TLIN 6 7 Z=50 E=360 F=4
  TLIN 2 10 Z=50 E=29.819 F=4    !
  TLIN 3 11 Z=50 E=29.819 F=4    !
  IND 10 12 L=.2                 !        REVERSE BIASED PIN
  IND 11 12 L=.2                 !
  SRC 12 0 R=400 C=.14           !
  TLIN 3 4 Z^ZO E^LO F=4
  TLIN 5 4 Z^ZO E^LO F=4
  TLIN 5 13 Z=50 E=25.753 F=4    !
  TLIN 6 14 Z=50 E=25.753 F=4    !
  IND 13 15 L=.15                !        FORWARD BIASED PIN
  IND 14 15 L=.15                !
  SRL 15 0 R=.8 L=.02            !
  TLIN 4 8 Z^Z1 E^L1 F=4
  TLIN 8 9 Z=50 E=360 F=4
  MATCH 7
  DEF2P 1 9 SPDT
OUT
  SPDT DB[S11] GR1
  SPDT DB[S21] GR2
FREQ
  SWEEP 2 6 .1
OPT
  RANGE 2 6
  SPDT DB[S11] < -20
GRID
  RANGE 2 6 .5
  GR1 -40 0 5
  GR2 -20 0 5
```

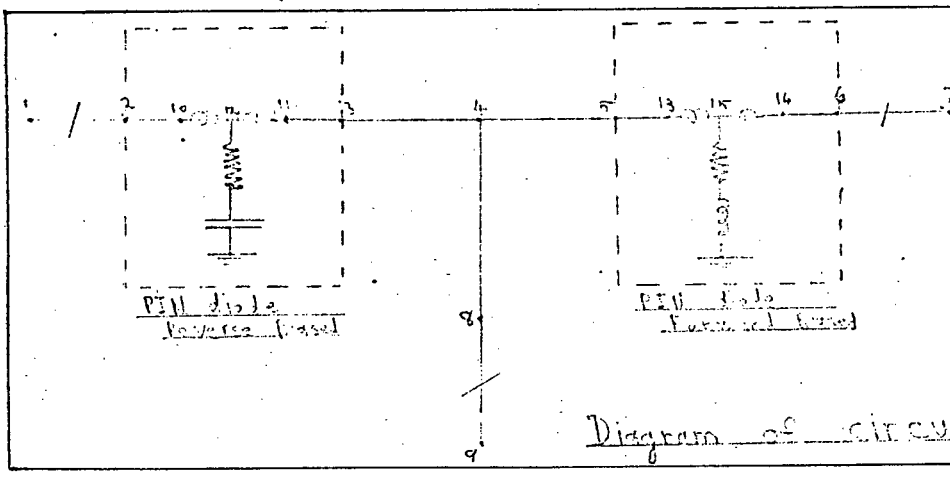

Diagram of ckt sw

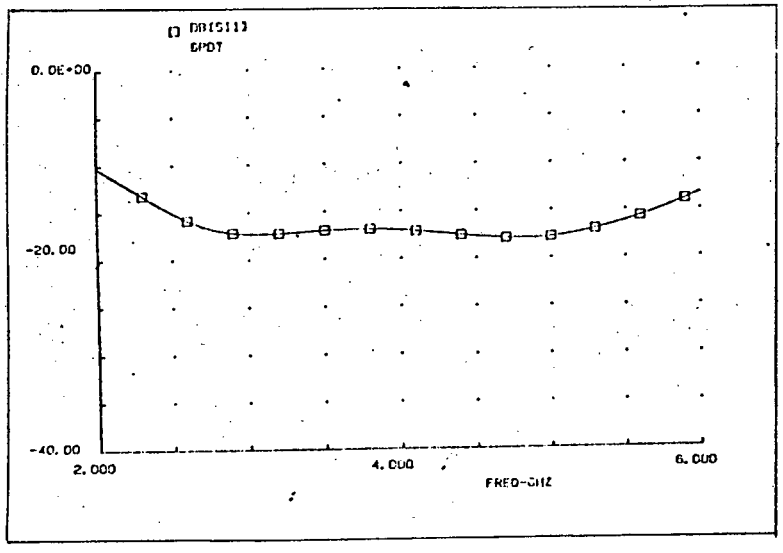

PROGRAM 12

SPDT2.ckt 01-01-80 03:39:27

```
!SPDT SWITCH WITH IDEAL TRANSMISSION LINES AND PIN DIODE MODELS IN
!FORWARD AND REVERSE BIAS. MATCHING STUBS ARE PLACED ON THE BRANCHES
!NEXT TO THE PIN DIODES.
VAR
  ZO=45                                  !IMPEDANCE OF SPDT BRANCHES (PIN)
  Z1=38                                  !IMPEDANCE OF SPDT BRANCH FEED
  LO\51                                  !LENGTH OF SPDT BRANCHES
  L1\87                                  !LENGTH OF SPDT BRANCH FEED
  ZS1=62                                 !IMPEDANCE OF MATCHING STUB
  LS1\25                                 !LENGTH OF MATCHING STUB
CKT
  TLIN 1 2 Z=50 E=360 F=4
  TLIN 6 7 Z=50 E=360 F=4
  TLIN 2 10 Z=50 E=29.819 F=4            !
  TLIN 3 11 Z=50 E=29.819 F=4            !
  IND 10 12 L=.2                         !       REVERSE BIASED PIN
  IND 11 12 L=.2                         !
  SRC 12 0 R=400 C=.14                   !
  TLIN 3 4 Z^ZO E^LO F=4
  TLIN 5 4 Z^ZO E^LO F=4
  TLIN 5 13 Z=50 E=25.753 F=4            !
  TLIN 6 14 Z=50 E=25.753 F=4            !
  IND 13 15 L=.15                        !       FORWARD BIASED PIN
  IND 14 15 L=.15                        !
  SRL 15 0 R=.8 L=.02                    !
  TLIN 4 8 Z^Z1 E^L1 F=4
  TLIN 8 9 Z=50 E=360 F=4
  TLOC 5 0 Z^ZS1 E^LS1 F=4
  TLOC 3 0 Z^ZS1 E^LS1 F=4
  MATCH 7
  DEF2P 1 9 SPDT
OUT
  SPDT DB[S11] GR1
  SPDT DB[S21] GR2
FREQ
  SWEEP 2 6 .1
OPT
  RANGE 2 6
  SPDT DB[S11] < -20
GRID
  RANGE 2 6 .5
```

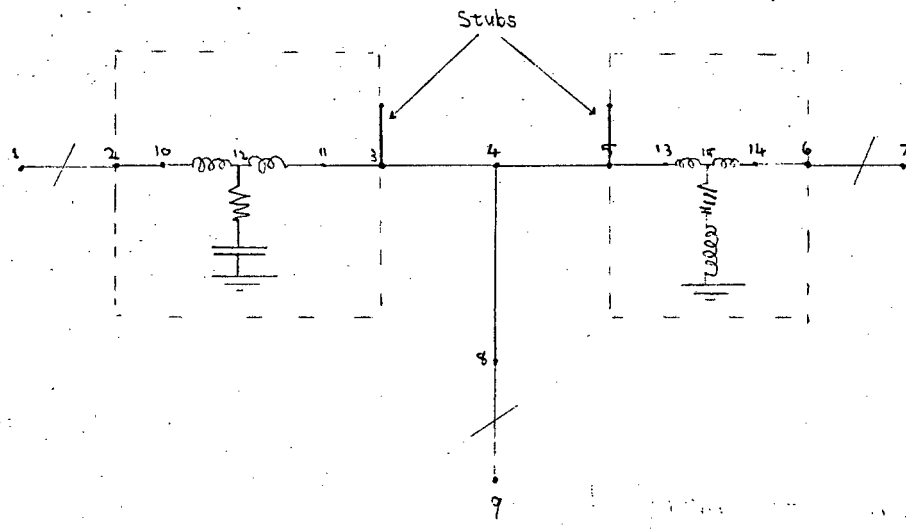

PROGRAM 13

```
SPDT2.CKT   01-01-80  02:51:26

!SPDT SWITCH WITH IDEAL TRANSMISSION LINES AND PIN DIODE MODELS IN
!FORWARD AND REVERSE BIAS. MATCHING STUBS ARE PLACED ON BOTH SIDES
!OF THE PIN DIODES.
VAR
  ZO=40                          !IMPEDANCE OF SPDT BRANCHES (PIN)
  Z1=35                          !IMPEDANCE OF SPDT BRANCH FEED
  LO=50                          !LENGTH OF SPDT BRANCHES
  L1=90                          !LENGTH OF SPDT BRANCH FEED
  ZS1=84                         !IMPEDANCE OF MATCHING STUB
  LS1=35                         !LENGTH OF MATCHING STUB
  ZS2\84                         !IMPEDANCE OF SECOND MATCHING STUB
  LS2\10                         !LENGTH OF SECOND MATCHING STUB
CKT
  TLIN 1 2 Z=50 E=360 F=4
  TLIN 6 7 Z=50 E=360 F=4
  TLIN 2 10 Z=50 E=29.819 F=4          !
  TLIN 3 11 Z=50 E=29.819 F=4          !
  IND 10 12 L=.2                       !       REVERSE BIASED PIN
  IND 11 12 L=.2                       !
  SRC 12 0 R=400 C=.14                 !
  TLIN 3 4 Z^ZO E^LO F=4
  TLIN 5 4 Z^ZO E^LO F=4
  TLIN 5 13 Z=50 E=25.753 F=4          !
  TLIN 6 14 Z=50 E=25.753 F=4          !
  IND 13 15 L=.15                      !       FORWARD BIASED PIN
  IND 14 15 L=.15                      !
  SRL 15 0 R=.8 L=.02                  !
  TLIN 4 8 Z^Z1 E^L1 F=4
  TLIN 8 9 Z=50 E=360 F=4
  TLOC 5 0 Z^ZS1 E^LS1 F=4
  TLOC 3 0 Z^ZS1 E^LS1 F=4
  TLOC 2 0 Z^ZS2 E^LS2 F=4
  TLOC 6 0 Z^ZS2 E^LS2 F=4
  MATCH 7
  DEF2P 1 9 SPDT
OUT
  SPDT DB[S11] GR1
  SPDT DB[S21] GR2
FREQ
  SWEEP 2 6 .1
OPT
  RANGE 2 6
  SPDT DB[S11] < -20
GRID
  RANGE 2 6 .5
  GR1 -40 0 5
  GR2 -20 0 5
```

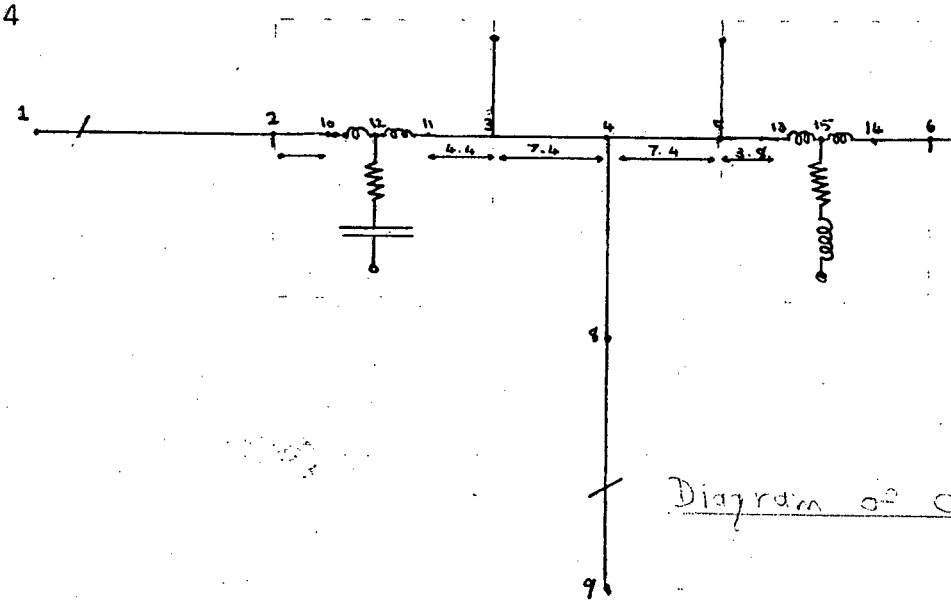

Diagram of C

PROGRAM 14

SPDT2.ckt 01-01-80 03:04:27

```
!SPDT SWITCH WITH IDEAL TRANSMISSION LINES AND PIN DIODE MODELS IN
!FORWARD AND REVERSE BIAS. A SECTION OF TRANSMISSION LINE IS INSERTED
!TO IMPROVE THE RESPONSE. THESE VALUES WHERE GENERATED USING THE OPTIMI
!FACILITY.
VAR
  ZO\52                          !IMPEDANCE OF SPDT BRANCHES (PIN)
  Z1\36                          !IMPEDANCE OF SPDT BRANCH FEED
  LO=33                          !LENGTH OF SPDT BRANCHES
  L1=83                          !LENGTH OF SPDT BRANCH FEED
  ZS\30                          !IMPEDANCE OF MATCHING SECTION
  LS=25                          !LENGTH OF MATCHING SECTION
CKT
  TLIN 1 2 Z=50 E=360 F=4
  TLIN 6 7 Z=50 E=360 F=4
  TLIN 2 10 Z=50 E=29.819 F=4          !
  TLIN 3 11 Z=50 E=29.819 F=4          !
  IND 10 12 L=.2                       !       REVERSE BIASED PIN
  IND 11 12 L=.2                       !
  SRC 12 0 R=400 C=.14                 !
  TLIN 20 4 Z^ZO E^LO F=4
  TLIN 21 4 Z^ZO E^LO F=4
  TLIN 5 13 Z=50 E=25.753 F=4          !
  TLIN 6 14 Z=50 E=25.753 F=4          !
  IND 13 15 L=.15                      !       FORWARD BIASED PIN
  IND 14 15 L=.15                      !
  SRL 15 0 R=.8 L=.02                  !
  TLIN 4 8 Z^Z1 E^L1 F=4
  TLIN 8 9 Z=50 E=360 F=4
  TLIN 3 20 Z^ZS E^LS F=4
  TLIN 5 21 Z^ZS E^LS F=4
  MATCH 7
  DEF2P 1 9 SPDT
OUT
  SPDT DB[S11] GR1
  SPDT DB[S21] GR2
FREQ
  SWEEP 2 6 .1
OPT
  RANGE 2 6
  SPDT DB[S11] < -20
GRID
  RANGE 2 6 .5
```

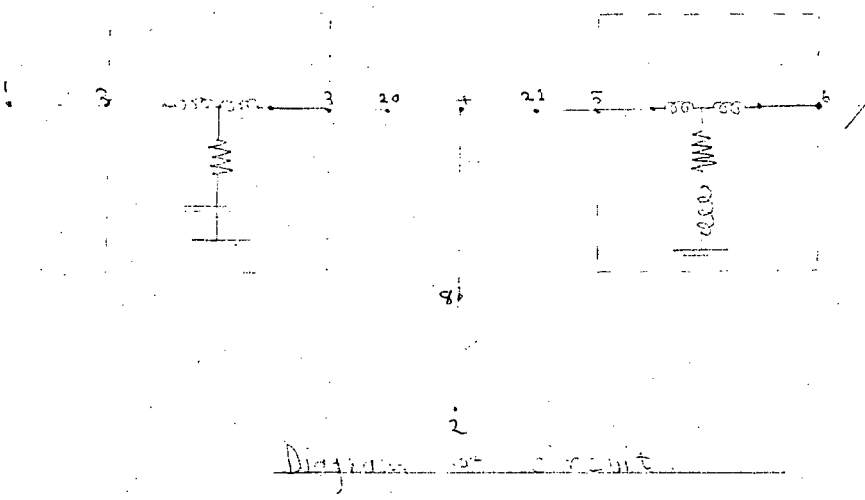

Diagram of circuit

PROGRAM 15

```
          MICRSPDT.ckt    01-01-80  02:12:00

!MICROSTRIP SPDT SWITCH WITH MODELS OF FORWARD AND REVERSE BIASED PIN DIODES
! OPEN CIRCUIT STUBS ARE USED TO IMPROVE THE RESPONSE.
DIM
  LNG MM
VAR
  WL=2.46                    !WIDTH OF 50 OHM LINE
  WM=3.8                     !WIDTH OF SPDT BRANCH FEED
  WB=1.8                     !WIDTH OF BRANCHES
  WS=3.36                    !WIDTH OF MATCHING STUBS
  LM=13.6                    !LENGTH OF SPDT BRANCH FEED
  LB1=.2                     !LENGTH OF LINE BETWEEN STUB AND PIN
  LB2=6                      !LENGTH OF LINE BETWEEN TEE AND STUB
  LS=2.95                    !LENGTH OF STUB
CKT
  MSUB ER=2.2 H=.7874 T=.034 RHO=.7066 RGH=0
  MLIN 1 2 W^WL L=10
  MLIN 4 5 W^WL L=10
  MLIN 7 8 W^WL L=10
  TLIN 5 19 Z=50 E=29.819 F=4          !
  TLIN 6 20 Z=50 E=29.819 F=4          !
  IND 19 21 L=.2                       !   MODEL OF REVERSE BIASED PIN DIODE
  IND 20 21 L=.2                       !
  SRC 21 0 R=400 C=.14                 !
  MLIN 3 12 W^WM L^LM
  MLIN 6 13 W^WB L^LB1
  MLIN 14 10 W^WB L^LB2
  MLIN 9 17 W^WB L^LB1
  MLIN 11 16 W^WB L^LB2
  TLIN 8 22 Z=50 E=25.753 F=4          !
  TLIN 9 23 Z=50 E=25.753 F=4          !
  IND 22 24 L=.15                      !   MODEL OF FORWARD BIASED PIN DIODE
  IND 23 24 L=.15                      !
  SRL 24 0 R=.8 L=.02                  !
  MTEE 10 11 12 W1^WB W2^WB W3^WM
  MTEE 13 14 15 W1^WB W2^WB W3^WS
  MTEE 16 17 18 W1^WB W2^WB W3^WS
  MSTEP 2 3 W1^WL W2^WM
  MLOC 15 W^WS L^LS
  MLOC 18 W^WS L^LS
  DEF3P 1 4 7 SPDT
OUT
  SPDT DB[S11] GR1
  SPDT DB[S21] GR2
  SPDT DB[S31] GR2
FREQ
  SWEEP 1 7 .2
GRID
  RANGE 1 7 .5
  GR1 -40 0 5
  GR2 -40 0 5
```

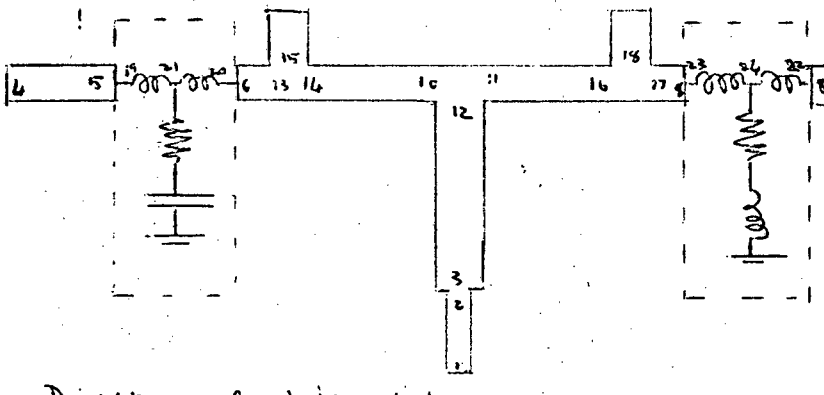

Diagram of microstrip circuit

PROGRAM 16

```
SP4TSPAR.ckt    01-01-80  01:35:02

!THIS SP4T SWITCH CONSISTS OF THREE SPDT SWITCHES. THE S-PARAMETER FILES
!WHERE OBTAINED FROM THE TOUCHSTONE PROGRAM "MICRSPDT" WHICH WAS USED
!TO DEVELOP  THE SPDT SWITCH.
DIM
  LNG MM
VAR
  LJ\5.83193              !LENGTH OF LINE JOINING THE SPDT SWITCHES
  WJ#1 1.64942 3           !WIDTH OF LINE JOINING THE SPDT SWITCHES
  LS#1 3.22625 8               !LENGTH OF MATCHING STUB
  WS#1 1.38448 4               !WIDTH OF MATCHING STUB
CKT
  MSUB ER=2.2 H=.7874 T=.034 RHO=.7066 RGH=0
  MLIN 1 2 W=2.46 L=10
  S3PA 2 3 4 SPDT
!
  MLIN 3 21 W^WJ L^LJ
  MLIN 5 20 W^WJ L^LJ
  MTEE 20 21 22 W1^WJ W2^WJ W3^WS
  MLOC 22 W^WS L^LS
!
  MLIN 4 23 W^WJ L^LJ
  MLIN 8 24 W^WJ L^LJ
  MTEE 23 24 25 W1^WJ W2^WJ W3^WS
  MLOC 25 W^WS L^LS
!
  S3PA 5 6 7 SPDT
  S3PB 8 9 10 SPDTON
  MLIN 6 13 W=2.46 L=10
  MLIN 7 14 W=2.46 L=10
  MLIN 9 12 W=2.46 L=10
  MLIN 10 11 W=2.46 L=10
  MATCH 12
  DEF4P 1 13 14 11 SP4T
OUT
  SP4T DB[S11] GR1
  SP4T DB[S21] GR2
  SP4T DB[S31] GR2
  SP4T DB[S41] GR2
FREQ
  SWEEP 1 8 .25
GRID
  RANGE 1 8 .5
  GR1 -40 0 5
  GR2 -70 0 5
OPT
  RANGE 2 7
  SP4T DB[S11] < -20
  SP4T DB[S41] < -60
```

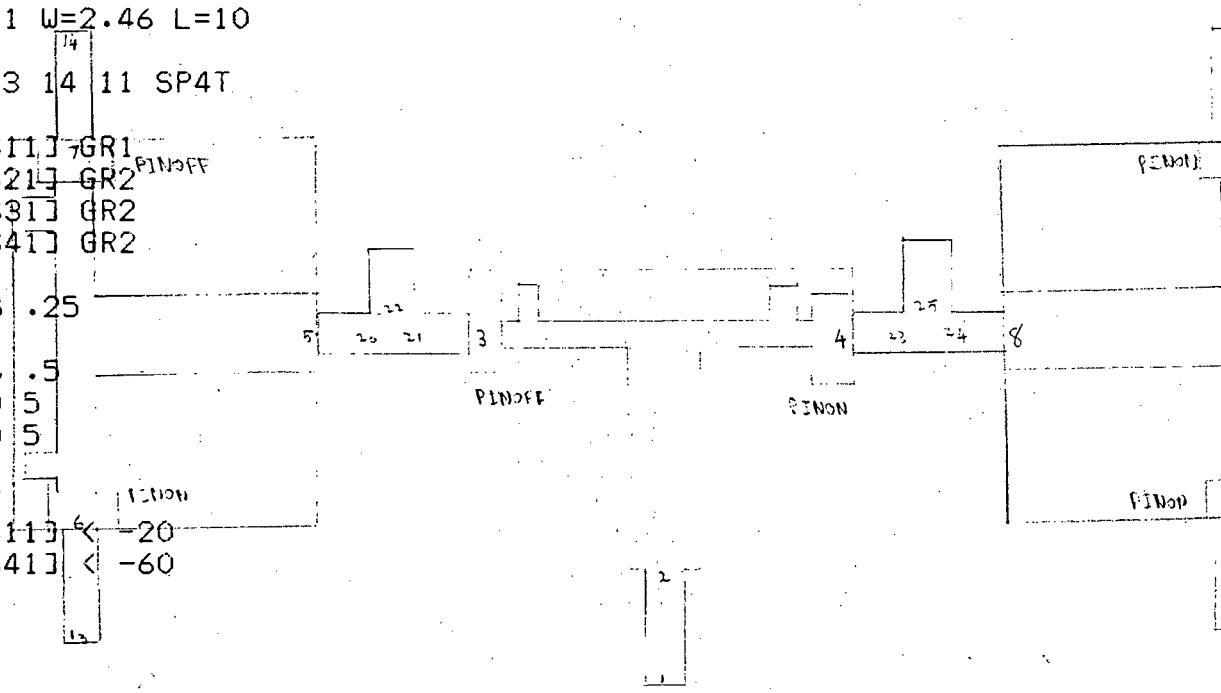

Diagram of SP4T switch with two switches used.

PROGRAM 17

```
SP4T.ckt    10-28-85  10:13:58

!THIS MICROSTRIP SP4T SWITCH USES THE EQUIVALENT CIRCUITS FOR THE FORWARD
!AND REVERSE BIASED SERIES MOUNTED PIN DIODE.
DIM
  LNG MM
CKT
  MSUB ER=2.2 H=.7874 T=.034 RHO=.7066 RGH=0
  MLIN 1 12 W=2.46 L=10
  MLIN 2 4 W=2.46 L=10
  MLIN 5 3 W=2.46 L=10
  MLIN 6 13 W=2.46 L=10
  MLIN 7 14 W=2.46 L=10
!
  SRL 4 12 R=4 L=.3                    ! MODEL OF FORWARD BIASED PIN DIODE
  CAP 4 12 C=.05
!
  SRLC 5 12 R=1000 L=.3 C=.05          ! MODEL OF REVERSE BIASED PIN DIODE
  CAP 5 12 C=.05
!
  SRLC 6 12 R=1000 L=.3 C=.05          ! MODEL OF REVERSE BIASED PIN DIODE
  CAP 6 12 C=.05
!
  SRLC 7 12 R=1000 L=.3 C=.05          ! MODEL OF REVERSE BIASED PIN DIODE
  CAP 7 12 C=.05
!
  MATCH 3
  MATCH 13
  MATCH 2
  DEF2P 1 14 SP4T
OUT
  SP4T DB[S11] GR1
  SP4T DB[S21] GR1
FREQ
  SWEEP 1 7 .2
GRID
  RANGE 1 7 .5
  GR1 -30 0 5
  GR2 -3 0 .5
```

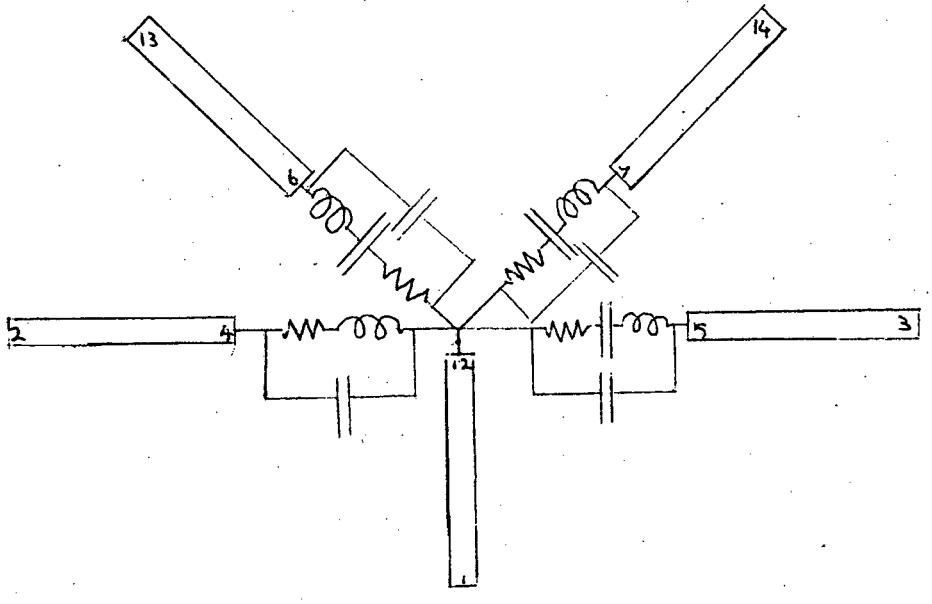

Layout of the circuit

PROGRAM 18

SSERSP4T.ckt 10-28-85 11:26:51

```
!THIS SP4T SWITCH USES A COMBINATION OF SERIES AND SHUNT MOUNTED PIN DIODES.
!THE THEORETICAL MODELS FOR FORWARD AND REVERSE BIASED DIODES ARE USED.
DIM
  LNG MM
VAR
  L=16.24                    !  LENGTH OF LINE BETWEEN PIN DIODES.
CKT
  MSUB ER=2.2 H=.7874 T=.034 RHO=.7066 RGH=0
  MLIN 1 12 W=2.46 L=10
  MLIN 2 15 W=2.46 L=10
  MLIN 18 3 W=2.46 L=10
  MLIN 19 13 W=2.46 L=10
  MLIN 22 14 W=2.46 L=10
  MLIN 16 4 W=2.46 L^L
  MLIN 6 20 W=2.46 L^L
  MLIN 7 21 W=2.46 L^L
  MLIN 5 17 W=2.46 L^L
!
  S2PA 4 12 0 SPINFOR              ! S-PARAMETERS FROM PINFOR PROGRAM
!
  TLIN 15 23 Z=50 E=29.819 F=4   !
  TLIN 25 16 Z=50 E=29.819 F=4   !
  IND 23 24 L=.2                 ! MODEL OF REVERSE BIASED SHUNT PIN DIODE
  IND 24 25 L=.2                 !
  SRC 24 0 R=400 C=.14           !
!
  S2PB 5 12 0 SPINREV              ! S-PARAMETERS FROM PINREV PROGRAM
!
  TLIN 17 32 Z=50 E=25.753 F=4   !
  TLIN 18 34 Z=50 E=25.753 F=4   !
  IND 32 33 L=.15                ! MODEL OF FORWARD BIASED SHUNT PIN DIODE
  IND 33 34 L=.15                !
  SRL 33 0 R=.8 L=.02            !
!
  S2PB 6 12 0 SPINREV              ! S-PARAMETERS FROM PINREV PROGRAM
!
  TLIN 19 26 Z=50 E=25.753 F=4   !
  TLIN 20 28 Z=50 E=25.753 F=4   !
  IND 26 27 L=.15                ! MODEL OF FORWARD BIASED SHUNT PIN DIODE
  IND 27 28 L=.15                !
  SRL 27 0 R=.8 L=.02            !
!
  S2PB 7 12 0 SPINREV              ! S-PARAMETERS FROM PINREV PROGRAM
!
  TLIN 21 29 Z=50 E=25.753 F=4   !
  TLIN 22 31 Z=50 E=25.753 F=4   !
  IND 29 30 L=.15                ! MODEL OF FORWARD BIASED SHUNT PIN DIODE
  IND 30 31 L=.15                !
  SRL 30 0 R=.8 L=.02            !
!
  MATCH 3
  DEF4P 1 2 13 14 SP4T
OUT
  SP4T DB[S11] GR1
  SP4T DB[S21] GR1
```

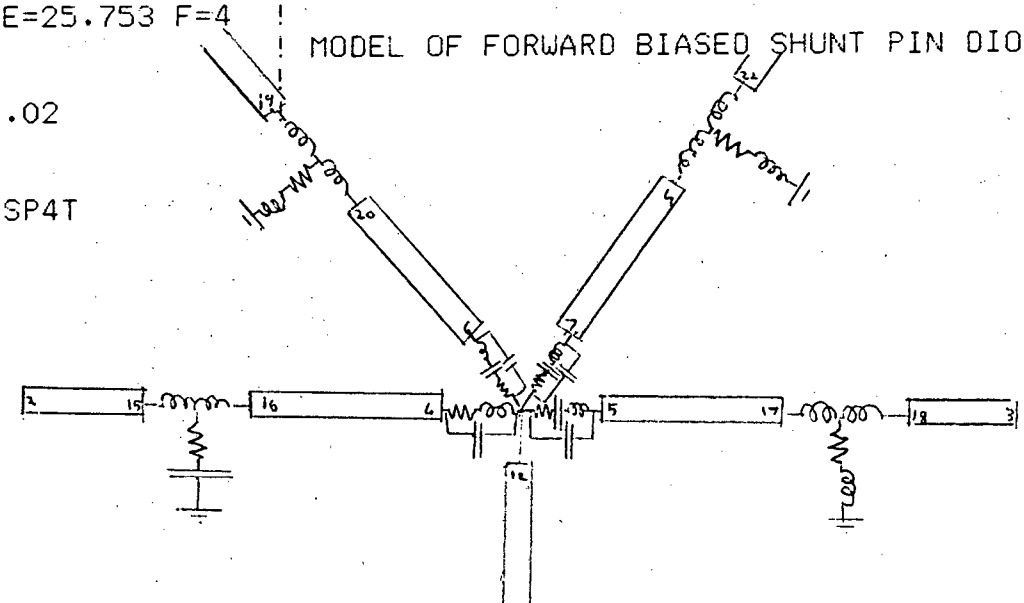

PROGRAM 19

SERSP4T.ckt

```
!THIS MICROSTRIP SP4T SWITCH USING THREE SERIES MOUNTED PIN DIODES IN
!EACH BRANCH TO INCREASE THE ISOLATION. THE S-PRAMETERS FOR THE THEORETICAL
!MODEL OF THE PIN DIODES ARE USED WHICH HAVE BEEN GENERATED BY THE PROGRAMS
!PINFOR AND PINREV.
DIM
  LNG MM
VAR
  L=10                    ! LENGTH OF LINE BETWEEN SERIES DIODES
  W=2.46                  ! WIDTH OF LINE BETWEEN PIN DIODES
CKT
  MSUB ER=2.2 H=.7874 T=.034 RHO=.7066 RGH=0
  MLIN 1 12 W=2.46 L=10
  MLIN 2 40 W=2.46 L=10
  MLIN 46 3 W=2.46 L=10
  MLIN 42 13 W=2.46 L=10
  MLIN 44 14 W=2.46 L=10
  MLIN 41 15 W=2.46 L^L
  MLIN 43 19 W=2.46 L^L
  MLIN 22 45 W=2.46 L^L
  MLIN 18 47 W=2.46 L^L
  MLIN 16 4 W^W L^L
  MLIN 6 20 W^W L^L
  MLIN 7 21 W^W L^L
  MLIN 5 17 W^W L^L
!
  S2PA 4 12 0 SPINFOR
  S2PA 15 16 0 SPINFOR
  S2PA 40 41 0 SPINFOR
  S2PB 5 12 0 SPINREV
  S2PB 17 18 0 SPINREV
  S2PB 46 47 0 SPINREV
  S2PB 6 12 0 SPINREV
  S2PB 19 20 0 SPINREV
  S2PB 44 45 0 SPINREV
  S2PB 7 12 0 SPINREV
  S2PB 21 22 0 SPINREV
  S2PB 42 43 0 SPINREV
!
  MATCH 3
  DEF4P 1 2 13 14 SP4T
OUT
  SP4T DB[S11] GR1
  SP4T DB[S21] GR2
  SP4T DB[S31] GR1
FREQ
  SWEEP 1 7 .2
GRID
  RANGE 1 7 .5
  GR1 -75  0 5
  GR2 -5 0 1
  GR3 -30 0 5
```

PROGRAM 20a

Flow Chart to calculate the Coupler width, Even mode impedance and Odd mode impedance given the height of the dielectric between ground planes and conductors, for a single section overlay Coupler.

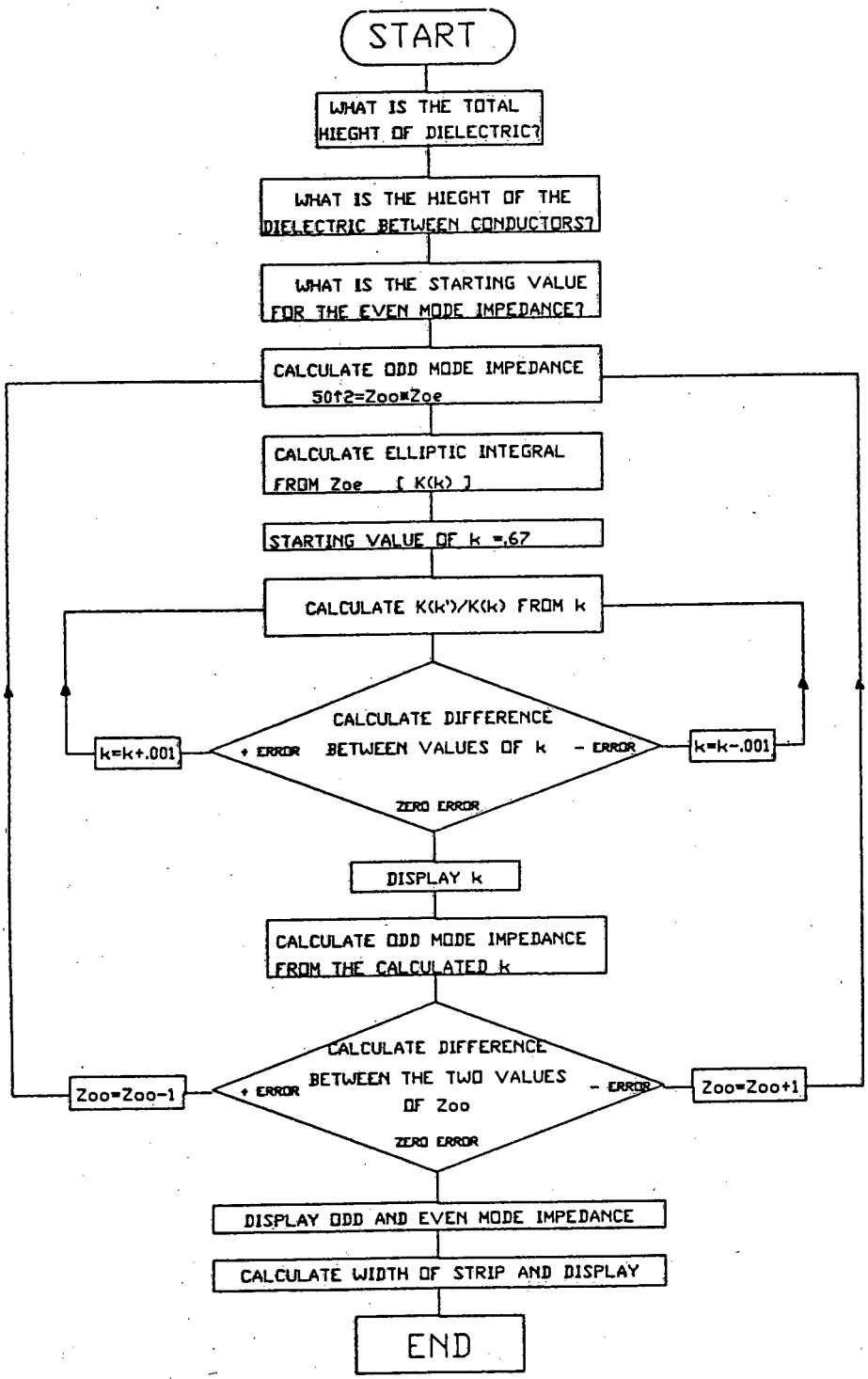

PROGRAM 20b

```
 10 REM  OVERLAY COUPLERS
 20 REM  ----------------
 30 DISP "A DIELECTRIC CONSTANT
     OF 2.2 IS ASSUMED"
 40 DISP "TOTAL HIEGHT OF DIELEC
    TRIC IN mm"
 50 INPUT B
 60 DISP "HIEGHT OF DIELECTRIC
    BETWEEN     CONDUCTORS="
 70 INPUT S
 80 DISP "EVEN MODE IMPEDANCE="
 90 INPUT E
100 O=2500/E
110 X=2.2^.5*E/188.3
120 REM ------------------------
130 REM  ELLIPTIC INTEGRALS OF
      THE FIRST KIND
140 K=.67
150 L=1+.5^2*(1-K^2)+.375^2*(1-K
    ^2)^2+.3125^2*(1-K^2)^3
160 M=1+.5^2*K^2+.375^2*K^4+.312
    5^2*K^6
170 N=L/M
180 Y=N-X
190 IF ABS(Y)<.001 THEN 250
200 IF Y>0 THEN 230
210 K=K-.001
220 GOTO 150
230 K=K+.001
240 GOTO 150
250 DISP "K=";K
260 REM ------------------------
    -
270 T=.5*LOG((1+K)/(1-K))
280 Z=296.1/(2.2^.5*B/S*T)
290 A=Z-O
300 DISP E,O,A
310 IF ABS(A)<.05 THEN 370
320 IF A>0 THEN 350
330 E=E+.1
340 GOTO 100
350 E=E-.1
360 GOTO 100
370 PRINT "ODD MODE IMPEDANCE";O
380 PRINT "EVEN MODE IMPEDANCE";
    E
390 REM ----------------------
400 P=(K*B/S-1)/(B/(K*S)-1)
410 Q=.5*LOG((1+SQR(P))/(1-SQR(P
    )))
420 R=.5*LOG((1+SQR(P)/K)/(1-SQR
    (P)/K))
430 W=2*B/PI*(Q-S*R/B)
440 PRINT "WIDTH OF STRIP IN mm"
    ,W
450 END
```

PROGRAM 21

IDEALPHA.ckt

```
!THE CIRCUIT CONSISTS OF A POWER SPLITTER WHICH FEEDS TWO 3DB COUPLERS.
VAR
   R1=1E4
   R2=0
   ZE=125
   ZO=20
CKT
   TLIN 1 2 Z=50 E=10 F=4
   TLIN 2 4 Z=70.7 E=90 F=4
   TLIN 2 3 Z=70.7 E=90 F=4
   RES 3 4 R=100
   CLIN 3 8 9 10 ZE^ZE ZO^ZO E=90 F=4
   CLIN 4 7 6 5 ZE^ZE ZO^ZO E=90 F=4
   CLIN 9 12 6 11 ZE^ZE ZO^ZO E=90 F=4
   MATCH 12
   RES 8 0 R^R1                    !
   RES 10 0 R^R1                   !       THESE VALUES ARE CHANGED TO ALTER
   RES 5 0 R^R2                    !       THE PHASE SHIFT.
   RES 7 0 R^R2                    !
   DEF2P 1 11 PHASE
OUT
   PHASE ANG[S21] GR1
   PHASE DB[S21] GR2
   PHASE DB[S11] GR2
FREQ
   SWEEP 2 6 .2
GRID
   RANGE 2 6 .5
   GR1 -180 180 20
   GR2 -20 0 1
```

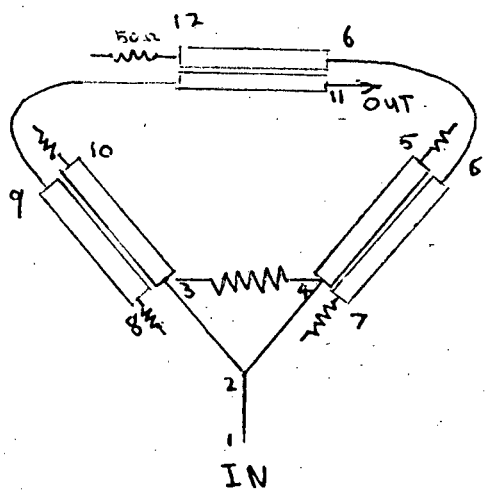

A P P E N D I X B

Specifications and Characteristics of Components

HEWLETT hp PACKARD
COMPONENTS

HERMETIC PIN DIODES FOR STRIPLINE/MICROSTRIP SWITCHES/ATTENUATORS 3 MHz - 12 GHz

5082-3140
5082-3141
5082-3170

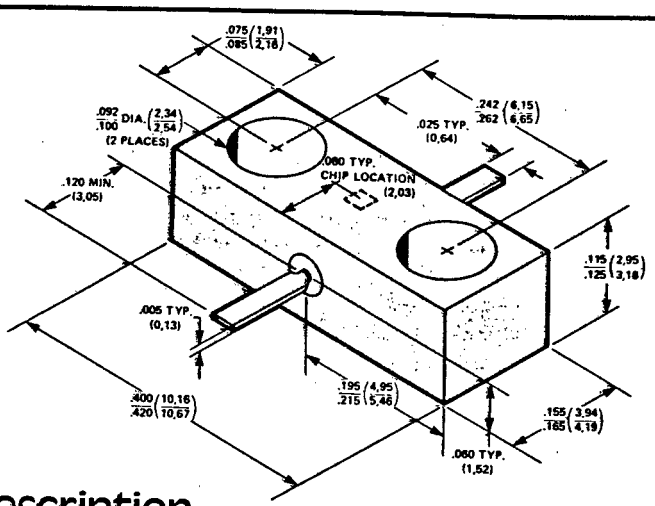

Features

- Broadband Operation
  - HF Through X-Band
- Low Insertion Loss
  - Less Than 0.5 dB to 10 GHz (5082-3140, 3170)
- High Isolation
  - Greater Than 20 dB to 10 GHz (5082-3140, 3170)
- Fast Switching/Modulating
  - 5 ns Typical (5082-3141)
- Low Drive Current Required
  - Less Than 20 mA for 20 dB Isolation (5082-3141)

Description

These Hewlett-Packard PIN diode switches/attenuators consist of specially processed silicon PIN diodes in shunt configuration within a 50 ohm hermetic package. They are optimized for good continuity of characteristic impedance, which allows a continuous transition when used in 50 ohm stripline or microstrip circuits. The HP package style 60 is a direct mechanical replacement for HP package style 61 with top cap. For most applications the 5082-3140, 3141, and 3170 are direct electrical replacements (with top cap in place) for the 5082-3040, 3041, and 3340, respectively. Because of a difference in chip location between packages 60 and 61, there will be a difference in the phase relationships between equivalent devices. When forward biased, the PIN diode will appear as a current variable resistor in shunt with the transmission line, its value being variable from less than 1 ohm at high forward bias to greater than 10,000 ohms at zero or reverse bias. The stripline package concept overcomes the limitations in insertion loss, isolation, and bandwidth that are imposed by the package parasitics of other discrete devices.

The PIN diode chips used in the 5082-3140 and 5082-3170 devices are of oxide passivated planar design; the chip used in the 5082-3141 is of oxide passivated mesa design. Passivation and package hermiticity ensures maximum stability and reliability.

Applications

These diodes are designed for applications in microwave and HF-UHF systems using stripline, or microstrip transmission line techniques.

Typical circuit functions consist of switching, duplexing, multiplexing, leveling, modulating, limiting or gain control functions as required in TR switches, pulse modulators, phase shifters, and amplitude modulators.

Near ideal transmission characteristics and low intermodulation products from HF through X-Band are provided by the 5082-3140. The 5082-3170 is a reverse polarity device with characteristics similar to the 5082-3140.

The 5082-3141 is recommended for applications requiring fast switching or high frequency modulation of microwave signals or where the lowest bias current for maximum attenuation is required.

More information is available in HP Application Notes 922 (Applications of PIN Diodes) and 929 (Fast Switching PIN Diodes). Special Information #5 discusses harmonic generation in PIN diodes.

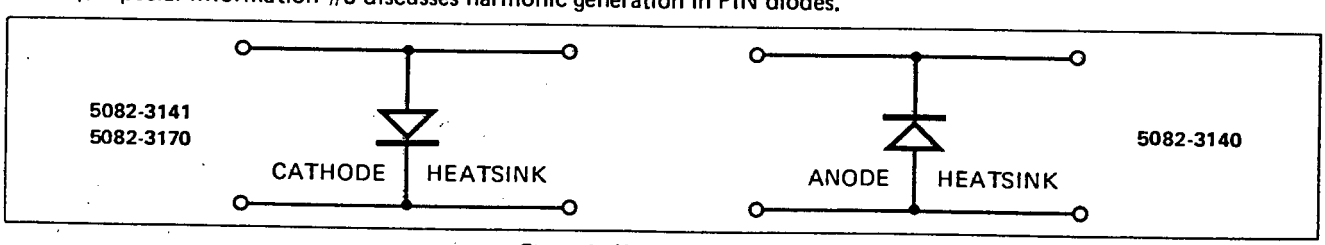

Figure 1. Heat Sink Polarities

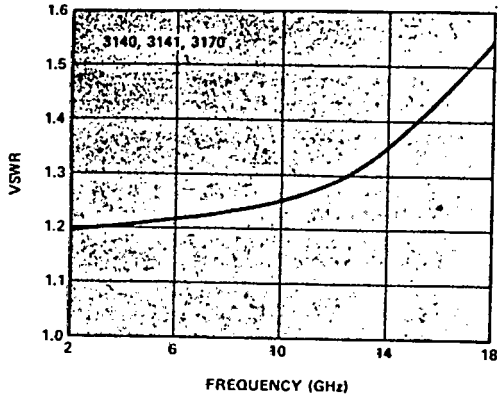

Figure 4. Typical VSWR vs. Frequency

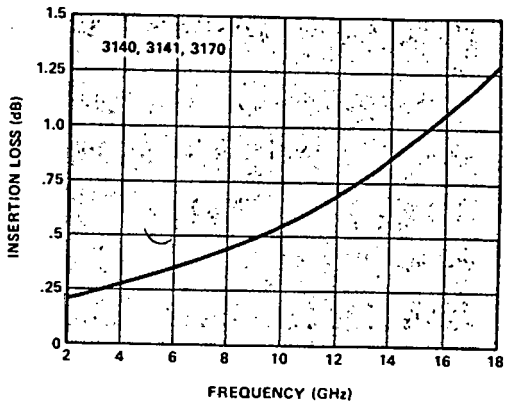

Figure 5. Typical Insertion Loss vs. Frequency

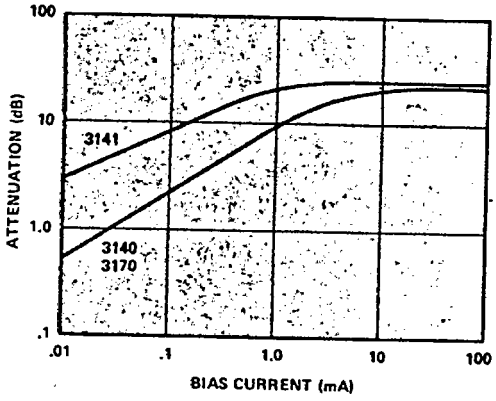

Figure 6. Typical Attenuation vs. Bias Current at f = 8 GHz

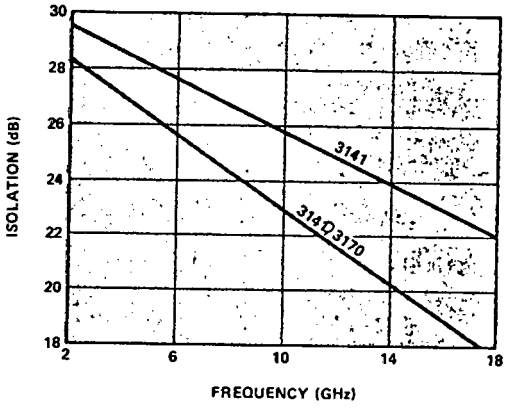

Figure 7. Typical Isolation vs. Frequency

Environmental Capabilities

The HP package style 60 is capable of passing the following environmental tests.

Characteristic	MIL-STD-750 Reference	Conditions
Moisture Resistance	1021	
Temperature, Storage	1031	–65°C to +150°C
Temperature, Operating	—	–65°C to +150°C
Solderability	2026	230°C as applicable
Temperature, Cycling	1051	5 cycles, –65°C to +150°C
Thermal Shock	1056	5 cycles, 0°C to +100°C
Shock	2016	5 blows, X_1, X_2, Y_1, Y_2, Z_1, Z_2 @ 1500 G
Vibration Fatigue	2046	32 hours, X, Y, Z @ 20 G
Vibration Variable Frequency	2056	Four 4-min. cycles, X, Y, Z, @ 20 G Min., 100 to 2000 Hz
Constant Acceleration	2006	20,000 G X_1, X_2, Y_1, Y_2, Z_1, Z_2
Terminal Strength	2036	Tension and Bending Stress
Barometric Pressure	1001	150,000 feet
Salt Atmosphere	1041	
Hermetic Seal	1071	Helium and Gross Leak

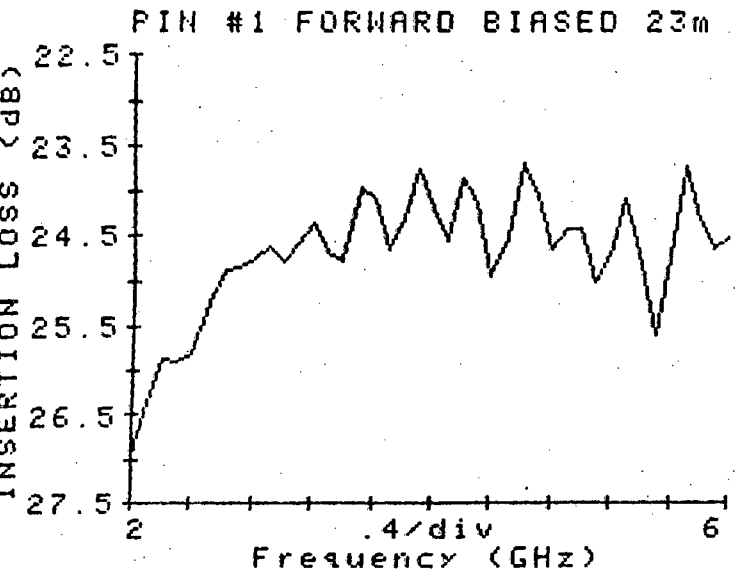

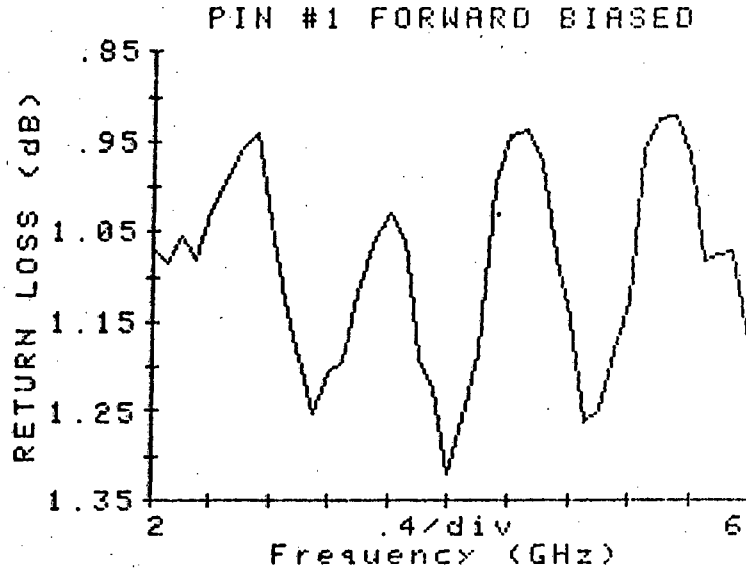

PIN #1 FORWARD BIASED 23mA (S21)

FREQUENCY GHz	INSERTION LOSS dB	Deg
2.000	27.0	30.
2.100	26.3	32.
2.200	25.9	30.
2.300	25.9	28.
2.400	25.8	30.
2.500	25.2	31.
2.600	24.9	28.
2.700	24.8	25.
2.800	24.7	26.
2.900	24.6	24.
3.000	24.8	24.
3.100	24.6	24.
3.200	24.4	23.
3.300	24.7	22.
3.400	24.8	25.
3.500	24.0	24.
3.600	24.1	19.
3.700	24.7	19.
3.800	24.3	23.
3.900	23.8	18.
4.000	24.2	16.
4.100	24.5	19.
4.200	23.9	20.
4.300	24.1	15.
4.400	24.9	16.
4.500	24.5	23.
4.600	23.7	19.
4.700	24.1	13.
4.800	24.7	13.
4.900	24.4	18.
5.000	24.4	15.
5.100	25.0	17.
5.200	24.7	20.
5.300	24.1	18.
5.400	24.7	14.
5.500	25.6	19.
5.600	24.8	25.
5.700	23.8	22.
5.800	24.3	16.
5.900	24.7	18.
6.000	24.5	21.

PIN #1 FORWARD BIASED (S11)

FREQUENCY GHz	RETURN LOSS dB	Deg
2.000	1.1	153.
2.100	1.1	151.
2.200	1.1	149.
2.300	1.1	148.
2.400	1.0	147.
2.500	1.0	146.
2.600	1.0	145.
2.700	0.9	144.
2.800	1.0	141.
2.900	1.1	140.
3.000	1.2	137.
3.100	1.3	135.
3.200	1.2	133.
3.300	1.2	131.
3.400	1.1	130.
3.500	1.1	129.
3.600	1.0	128.
3.700	1.1	126.
3.800	1.2	124.
3.900	1.2	122.
4.000	1.3	121.
4.100	1.3	119.
4.200	1.2	117.
4.300	1.0	118.
4.400	0.9	116.
4.500	0.9	114.
4.600	1.0	113.
4.700	1.1	112.
4.800	1.1	111.
4.900	1.3	111.
5.000	1.2	110.
5.100	1.2	108.
5.200	1.1	106.
5.300	1.0	104.
5.400	0.9	104.
5.500	0.9	103.
5.600	1.0	102.
5.700	1.1	103.
5.800	1.1	103.
5.900	1.1	103.
6.000	1.2	102.

Reference Plane Ext.= 28.35 cm

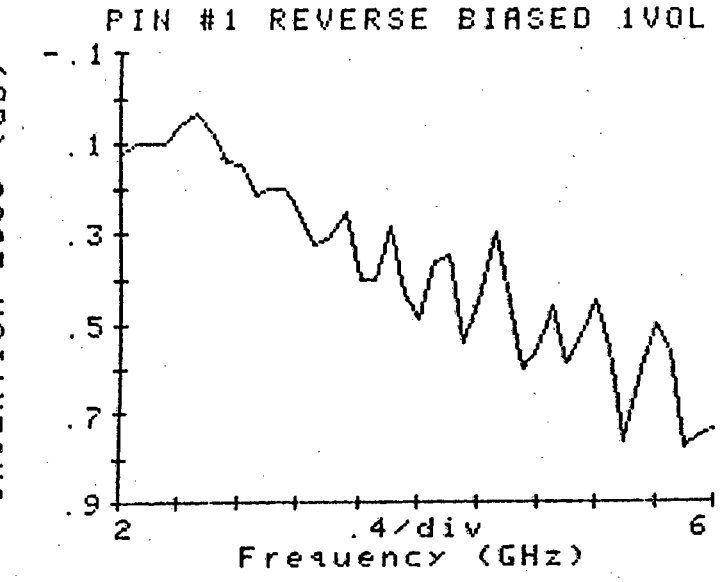

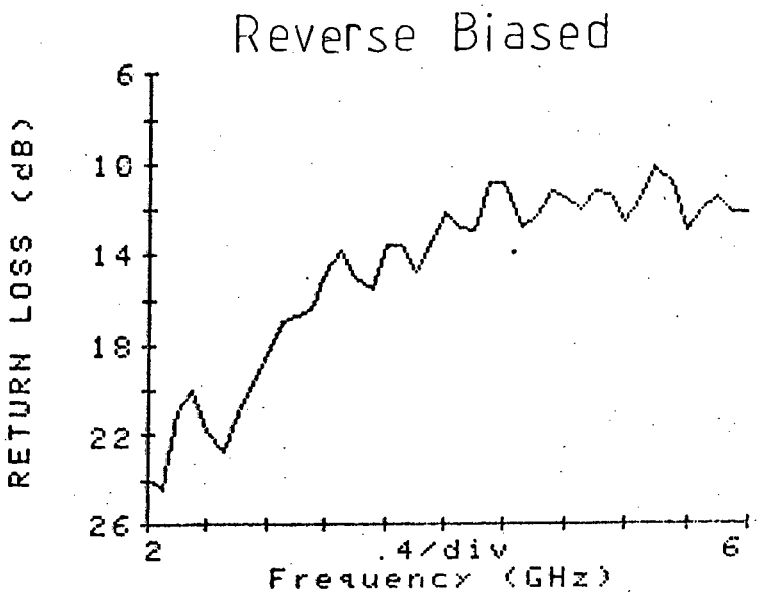

PIN #1 REVERSE BIASED 1VOLT (S21)

FREQUENCY GHz	INSERTION LOSS dB	Deg
2.000	0.1	-10.
2.100	0.1	-10.
2.200	0.1	-11.
2.300	0.1	-11.
2.400	0.1	-12.
2.500	0.0	-13.
2.600	0.1	-13.
2.700	0.1	-14.
2.800	0.2	-15.
2.900	0.2	-14.
3.000	0.2	-15.
3.100	0.2	-16.
3.200	0.3	-17.
3.300	0.3	-17.
3.400	0.3	-17.
3.500	0.3	-18.
3.600	0.4	-19.
3.700	0.4	-18.
3.800	0.3	-17.
3.900	0.4	-20.
4.000	0.5	-20.
4.100	0.4	-20.
4.200	0.4	-21.
4.300	0.5	-21.
4.400	0.5	-21.
4.500	0.3	-22.
4.600	0.5	-23.
4.700	0.6	-23.
4.800	0.6	-23.
4.900	0.5	-22.
5.000	0.6	-23.
5.100	0.5	-24.
5.200	0.5	-25.
5.300	0.6	-26.
5.400	0.8	-26.
5.500	0.6	-25.
5.600	0.5	-26.
5.700	0.6	-28.
5.800	0.8	-28.
5.900	0.8	-28.
6.000	0.7	-28.

FREQUENCY GHz	RETURN LOSS dB	Deg
2.000	23.9	39.
2.100	24.4	55.
2.200	20.9	64.
2.300	20.0	54.
2.400	21.8	51.
2.500	22.7	67.
2.600	21.0	70.
2.700	19.6	66.
2.800	18.2	58.
2.900	17.0	52.
3.000	16.7	46.
3.100	16.5	53.
3.200	14.7	58.
3.300	13.8	51.
3.400	15.0	47.
3.500	15.5	59.
3.600	13.6	60.
3.700	13.6	48.
3.800	14.8	49.
3.900	13.4	53.
4.000	12.1	45.
4.100	12.8	38.
4.200	12.9	50.
4.300	10.8	50.
4.400	10.9	40.
4.500	12.8	41.
4.600	12.2	55.
4.700	11.2	50.
4.800	11.5	43.
4.900	12.0	43.
5.000	11.2	41.
5.100	11.4	34.
5.200	12.5	35.
5.300	11.5	46.
5.400	10.1	42.
5.500	10.8	33.
5.600	12.9	39.
5.700	12.1	49.
5.800	11.5	45.
5.900	12.1	41.
6.000	12.2	42.

(S11)

Reference Plane Ext.= 28.35 cm

PIN #3 FORWARD BIAS=15mA

FREQUENCY GHz	IMPEDANCE R	+- JX
2.000	2.67	1.91
2.040	2.73	1.70
2.080	2.79	1.74
2.120	2.86	1.87
2.160	2.94	2.10
2.200	3.00	2.48
2.240	3.33	2.74
2.280	3.38	2.99
2.320	3.64	3.00
2.360	3.44	2.77
2.400	3.13	2.66
2.440	2.78	2.33
2.480	1.90	2.05
2.520	1.62	2.10
2.560	1.32	2.00
2.600	1.28	2.37
2.640	1.65	2.29
2.680	1.95	2.29
2.720	2.61	2.42
2.760	2.96	2.26
2.800	3.38	2.34
2.840	3.50	2.31
2.880	3.53	2.66
2.920	3.86	2.92
2.960	3.78	3.10
3.000	4.03	3.35
3.040	4.03	3.34
3.080	3.94	3.35
3.120	3.94	3.34
3.160	3.88	3.35
3.200	3.84	3.57
3.240	4.12	3.78
3.280	4.27	3.75
3.320	4.42	3.94
3.360	4.41	3.91
3.400	3.94	4.03
3.440	3.38	4.12
3.480	2.36	4.57
3.520	2.22	5.60
3.560	2.19	6.19
3.600	2.83	6.81
3.640	3.27	6.50
3.680	3.75	6.19
3.720	4.36	5.55
3.760	4.20	4.37
3.800	3.84	3.83
3.840	3.49	3.29
3.880	2.89	3.49
3.920	3.17	3.93
3.960	3.10	4.37
4.000	3.60	5.02
4.040	3.96	5.15
4.080	3.93	5.40
4.120	3.65	5.46
4.160	3.70	5.64
4.200	3.59	5.92
4.240	3.84	6.12
4.280	4.13	6.09
4.320	4.61	5.90
4.360	5.48	5.27
4.400	5.33	4.50
4.440	5.06	4.09
4.480	4.38	3.51
4.520	3.20	4.07
4.560	2.67	4.74
4.600	2.15	6.05
4.640	2.97	7.58
4.680	3.93	8.34
4.720	5.17	8.70
4.760	5.71	8.65
4.800	5.69	7.52
4.840	5.43	6.84
4.880	4.69	6.14
4.920	4.45	5.88
4.960	4.00	5.76
5.000	3.94	5.89
5.040	4.10	6.01
5.080	4.51	6.24
5.120	4.57	6.16
5.160	4.40	6.32
5.200	4.10	6.35
5.240	4.00	6.83
5.280	3.97	7.03
5.320	4.18	7.29
5.360	5.14	7.17
5.400	5.18	6.66
5.440	6.11	5.91
5.480	5.76	4.45
5.520	5.05	3.65
5.560	4.64	2.77
5.600	2.91	2.40
5.640	2.31	3.33
5.680	1.40	3.54
5.720	1.08	5.80
5.760	2.37	6.91
5.800	3.44	7.66
5.840	4.66	7.35
5.880	4.71	6.78
5.920	4.72	6.40
5.960	4.34	5.91
6.000	4.23	5.59

Reference Plane Ext.+-.2 cm

PIN #3 REVERSE BIAS=1V

FREQUENCY GHz	IMPEDANCE R	+- JX
2.000	53.33	-0.20
2.040	53.26	-0.19
2.080	52.64	-0.15
2.120	51.65	-0.11
2.160	51.46	-0.12
2.200	52.31	-0.24
2.240	53.12	-0.36
2.280	53.55	-0.44
2.320	53.70	-0.47
2.360	53.43	-0.41
2.400	52.12	-0.23
2.440	50.26	-0.03
2.480	48.54	0.14
2.520	47.45	0.24
2.560	46.82	0.29
2.600	46.81	0.28
2.640	47.35	0.23
2.680	48.18	0.16
2.720	49.08	0.08
2.760	50.22	-0.02
2.800	51.56	-0.17
2.840	52.84	-0.34
2.880	53.67	-0.48
2.920	54.44	-0.63
2.960	55.22	-0.79
3.000	55.56	-0.84
3.040	54.78	-0.70
3.080	53.53	-0.52
3.120	52.67	-0.42
3.160	52.38	-0.40
3.200	52.64	-0.48
3.240	53.47	-0.70
3.280	55.21	-1.13
3.320	57.03	-1.58
3.360	57.86	-1.73
3.400	57.06	-1.51
3.440	55.18	-1.09
3.480	52.68	-0.57
3.520	50.13	-0.03
3.560	48.52	0.35
3.600	48.29	0.42
3.640	48.99	0.25
3.680	49.81	0.05
3.720	50.36	-0.08
3.760	50.45	-0.09
3.800	50.07	-0.01
3.840	49.60	0.07
3.880	49.58	0.08
3.920	50.75	-0.17
3.960	52.92	-0.72
4.000	55.06	-1.32
4.040	56.59	-1.75
4.080	57.04	-1.81
4.120	55.85	-1.41
4.160	53.85	-0.69
4.200	50.34	-0.08
4.240	49.13	0.21
4.280	49.77	0.06
4.320	51.70	-0.47
4.360	54.13	-1.17
4.400	57.01	-1.97
4.440	59.13	-2.43
4.480	59.43	-2.29
4.520	57.51	-1.74
4.560	54.96	-1.20
4.600	53.38	-0.91
4.640	53.06	-0.91
4.680	53.22	-1.02
4.720	53.38	-1.09
4.760	53.36	-1.07
4.800	52.94	-0.91
4.840	52.35	-0.69
4.880	51.57	-0.45
4.920	50.95	-0.26
4.960	51.00	-0.28
5.000	52.17	-0.64
5.040	54.20	-1.28
5.080	56.10	-1.84
5.120	56.68	-1.94
5.160	56.16	-1.78
5.200	54.28	-1.11
5.240	51.56	-0.39
5.280	48.76	0.32
5.320	47.38	0.71
5.360	47.72	0.65
5.400	48.91	0.32
5.440	50.68	-0.20
5.480	52.67	-0.75
5.520	54.82	-1.25
5.560	54.98	-1.14
5.600	53.69	-0.77
5.640	51.77	-0.37
5.680	50.51	-0.12
5.720	50.86	-0.21
5.760	51.21	-0.32
5.800	51.79	-0.50
5.840	51.71	-0.47
5.880	51.77	-0.47
5.920	50.74	-0.19
5.960	49.73	0.07
6.000	49.42	0.15

Reference Plane Ext.+-.2 cm

PIN #5 FORWARD BIAS=15mA

FREQUENCY GHz	IMPEDANCE R	+- JX
2.000	2.53	-0.75
2.040	2.59	-0.92
2.080	2.55	-0.92
2.120	2.66	-0.82
2.160	2.62	-0.65
2.200	2.58	-0.28
2.240	2.82	-0.07
2.280	2.80	0.10
2.320	3.04	0.09
2.360	2.90	-0.21
2.400	2.64	-0.48
2.440	2.39	-0.91
2.480	1.62	-1.34
2.520	1.34	-1.33
2.560	1.09	-1.55
2.600	1.07	-1.29
2.640	1.51	-1.31
2.680	1.80	-1.27
2.720	2.36	-1.15
2.760	2.79	-1.34
2.800	3.21	-1.20
2.840	3.34	-1.24
2.880	3.19	-0.99
2.920	3.33	-0.59
2.960	3.33	-0.53
3.000	3.50	-0.39
3.040	3.46	-0.41
3.080	3.40	-0.47
3.120	3.14	-0.63
3.160	3.21	-0.57
3.200	3.19	-0.46
3.240	3.40	-0.26
3.280	3.54	-0.34
3.320	3.46	-0.21
3.360	3.51	-0.29
3.400	2.95	-0.33
3.440	2.22	-0.39
3.480	1.08	-0.14
3.520	0.70	0.75
3.560	0.45	1.24
3.600	0.93	1.78
3.640	1.48	1.49
3.680	2.01	1.10
3.720	2.92	0.48
3.760	3.21	-0.70
3.800	3.10	-1.40
3.840	3.00	-1.92
3.880	2.24	-1.81
3.920	2.40	-1.37
3.960	2.18	-1.01
4.000	2.25	-0.45
4.040	2.55	-0.24
4.080	2.41	-0.12
4.120	2.18	-0.05
4.160	2.00	-0.06
4.200	1.76	0.12
4.240	2.00	0.24
4.280	2.35	0.15
4.320	2.87	0.02
4.360	3.83	-0.49
4.400	4.16	-1.30
4.440	4.13	-1.79
4.480	3.66	-2.50
4.520	2.25	-2.26
4.560	1.42	-1.74
4.600	0.36	-0.58
4.640	0.29	0.98
4.680	0.77	1.86
4.720	1.77	2.30
4.760	2.49	1.75
4.800	2.74	1.03
4.840	2.94	0.13
4.880	2.67	-0.66
4.920	2.67	-1.10
4.960	2.29	-1.43
5.000	2.17	-1.30
5.040	2.24	-1.15
5.080	2.53	-0.94
5.120	2.51	-1.08
5.160	2.25	-1.06
5.200	2.00	-1.11
5.240	1.64	-0.81
5.280	1.59	-0.76
5.320	1.65	-0.53
5.360	2.56	-0.51
5.400	3.04	-1.05
5.440	4.25	-1.59
5.480	5.03	-3.09
5.520	4.93	-4.06
5.560	5.22	-5.05
5.600	3.83	-5.84
5.640	2.59	-5.38
5.680	1.54	-5.44
5.720	-0.11	-3.34
5.760	0.34	-2.06
5.800	0.79	-1.16
5.840	2.15	-1.27
5.880	2.59	-1.82
5.920	2.89	-2.35
5.960	2.94	-2.93
6.000	2.91	-3.49

Reference Plane Ext.= .2 cm

PIN #5 REVERSE BIAS 10VLT

FREQUENCY GHz	IMPEDANCE R	+- JX
2.000	51.87	-0.12
2.040	51.84	-0.11
2.080	51.26	-0.07
2.120	50.11	-0.01
2.160	49.49	0.04
2.200	49.91	0.01
2.240	50.42	-0.05
2.280	50.62	-0.07
2.320	50.68	-0.09
2.360	50.48	-0.06
2.400	49.44	0.06
2.440	47.80	0.21
2.480	46.19	0.33
2.520	45.15	0.39
2.560	44.55	0.41
2.600	44.53	0.40
2.640	44.99	0.37
2.680	45.76	0.32
2.720	46.47	0.28
2.760	47.30	0.24
2.800	48.30	0.17
2.840	49.17	0.09
2.880	49.62	0.05
2.920	50.00	-0.00
2.960	50.43	-0.06
3.000	50.74	-0.11
3.040	50.08	-0.01
3.080	48.84	0.16
3.120	47.75	0.33
3.160	47.14	0.44
3.200	46.94	0.51
3.240	47.27	0.50
3.280	48.20	0.36
3.320	49.62	0.08
3.360	50.38	-0.08
3.400	49.80	0.04
3.440	48.13	0.37
3.480	45.79	0.80
3.520	43.27	1.26
3.560	41.25	1.71
3.600	40.64	1.92
3.640	41.02	1.88
3.680	41.89	1.64
3.720	42.83	1.35
3.760	43.35	1.14
3.800	43.45	1.03
3.840	43.00	1.06
3.880	42.47	1.23
3.920	42.74	1.34
3.960	43.83	1.30
4.000	45.29	1.08
4.040	46.39	0.85
4.080	46.98	0.70
4.120	46.29	0.80
4.160	44.36	1.10
4.200	41.92	1.52
4.240	40.19	1.90
4.280	40.03	2.09
4.320	41.18	2.00
4.360	43.10	1.64
4.400	45.43	1.12
4.440	47.69	0.55
4.480	48.38	0.36
4.520	47.18	0.59
4.560	44.62	1.11
4.600	42.50	1.65
4.640	41.28	2.08
4.680	40.83	2.32
4.720	40.71	2.41
4.760	40.65	2.39
4.800	40.49	2.34
4.840	40.26	2.27
4.880	39.99	2.20
4.920	39.39	2.25
4.960	39.16	2.33
5.000	39.70	2.34
5.040	40.96	2.18
5.080	42.49	1.85
5.120	43.25	1.64
5.160	43.25	1.55
5.200	42.15	1.65
5.240	40.11	1.90
5.280	37.61	2.27
5.320	35.94	2.61
5.360	35.61	2.81
5.400	36.23	2.85
5.440	37.77	2.56
5.480	39.51	2.22
5.520	41.67	1.70
5.560	43.08	1.26
5.600	42.52	1.21
5.640	41.04	1.37
5.680	39.19	1.72
5.720	38.55	2.03
5.760	38.10	2.24
5.800	38.31	2.33
5.840	38.24	2.32
5.880	38.25	2.26
5.920	38.06	2.18
5.960	37.27	2.16
6.000	36.71	2.22

Reference Plane Ext.= .2 cm

Ground structure for the Transistor Test Fixture

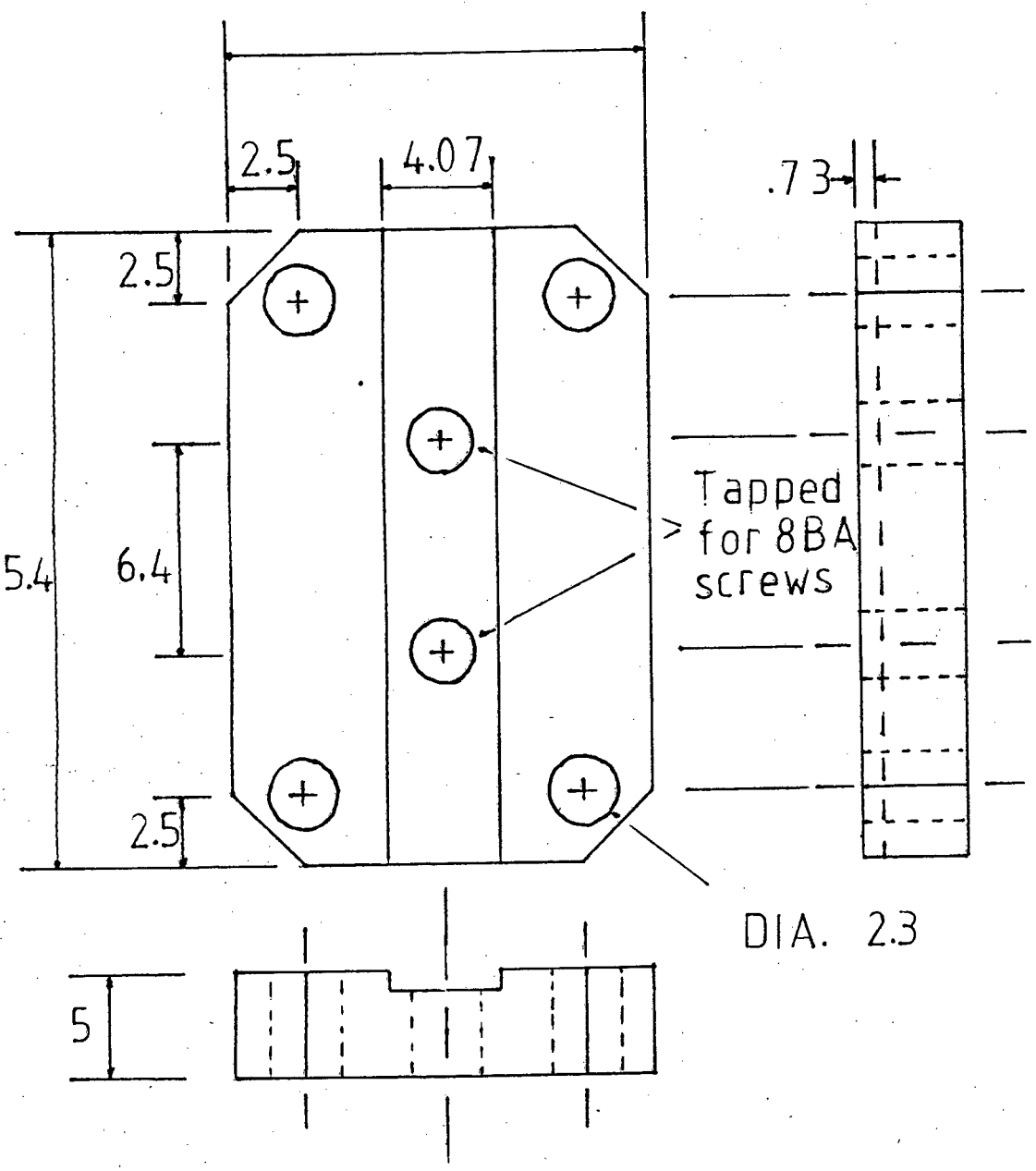

Not to scale

All dimensions in mm

Bulletin 4302

MA-47301

SILICON NITRIDE PASSIVATED BEAM LEAD PIN DIODE

DESCRIPTION

The MA-47301 PIN diode is constructed with beam leads for ease of assembly onto stripline or microwave integrated circuits. The surface orientated junction results in an extremely low junction capacitance for high speed switching. The silicon nitride passivation yields a device which is impervious to moisture allowing its use in environments which are not hermetically sealed.

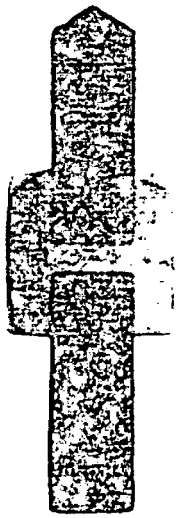

APPLICATIONS

The MA-47301 beam lead PIN is intended for use in broadband microwave stripline and integrated circuit control functions through Ku-band. Microwave signal processing functions consist of switching and attenuation in switches, phase shifters, limiters, duplexers, modulators and other similar applications.

FEATURES

- Silicon nitride passivated for use in non-hermetic containers
- Surface orientated for low parasitics and fast switching
- Special plating process for sturdy beams
- Low series resistance with 15 femtofarads reverse bias capacitance

SPECIFICATIONS @ T_A = 25°C

Specification	Symbol	Min.	Typ.	Max.	Units	Test Condition
Capacitance	C_{VR}	–	.015	0.02	pF	V_R = 50 Volts, f = 1.0 MHz
Series Resistance	R_s	–	6	8	ohms	I_F = 10 mA, f = 500 MHz
Breakdown Voltage	V_{BR}	50	75	–	Volts	I_R = 10 μA
Forward Current	I_F	10	–	–	mA	V_F = 1.0 Volt
Minority Carrier Lifetime	T_L	–	20	–	ns	I_F = 10 mA
RF Switching Time	t_{RF}	–	5	–	ns	V_R = 10V to I_F = 10 mA

MAXIMUM RATINGS

Total Power Dissipation 250 mW

Temperature:

Operating −65 to +175°C

Storage −65 to +200°C

OUTLINE DRAWING

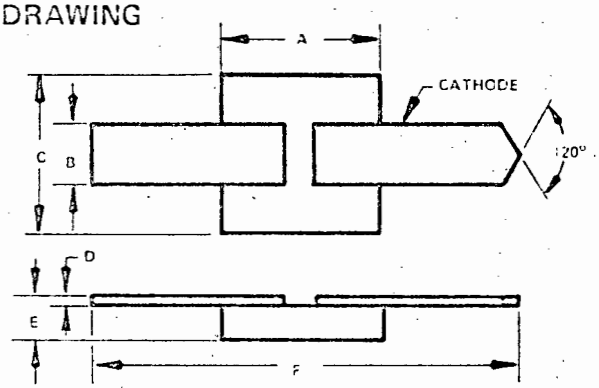

DIM.	INCHES MIN	INCHES MAX.	MM MIN.	MM MAX.
A	0.007	0.011	0.17	0.28
B	0.0045	0.0055	0.114	0.139
C	0.007	0.011	0.17	0.28
D	0.0004	0.0006	0.010	0.015
E	0.0020	0.0040	0.050	0.101
F	0.030	0.034	0.76	0.86

TYPICAL PERFORMANCE CURVE

MA47301 PIN BEAM LEAD

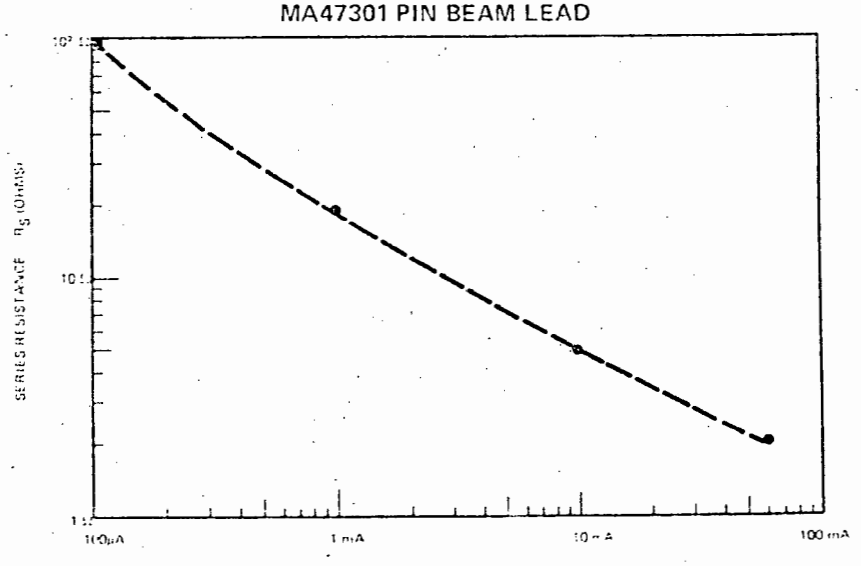

12/72 Printed in U.S.A.

Beam Lead PIN Diodes
DSG6470 and
DSG6474 Series

DATA SHEET
30300

ALPHA INDUSTRIES, INC.

FEATURES

- Low Capacitance .02 pF.
- Low Resistance 3.0 ohms
- Fast Switching 15 Nsec on, 25 Nsec off
- High Voltage 200 volts
- Oxide Passivated

DESCRIPTION

The DSG6470 and DSG6474 Series of silicon oxide passivated beam lead PIN diodes are designed for stripline and microstrip signal processing applications through 34 GHz. Extremely low junction capacitance combined with low series resistance makes these diodes ideal for circuits requiring high isolation from a series mounted diode, such as broadband multi-throw switches, and certain types of phase shifters, limiters, attenuators and modulators.

The DSG6470 and DSG6474 beam lead PIN diodes are constructed with a surface oriented junction and with plated gold beam leads for assembly onto stripline or microstrip microwave integrated circuits.

The silicon oxide passivation provides complete sealing of the junction, permitting use in nonsealed assemblies.

Alpha Industries has prepared an application note on suggested handling and bonding procedures for these diodes, which is available on request and which will assure optimum assembly into your circuit.

ABSOLUTE MAXIMUM RATINGS

Total Power Dissipation	250 mW
Reverse Working Voltage	200/100 Volts
Storage Temperature	175 Degrees C
Operating Temperature	150 Degrees C

169-001

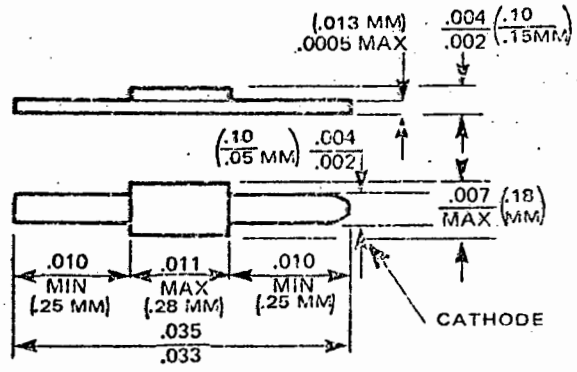

Note: Millimeters in parentheses.

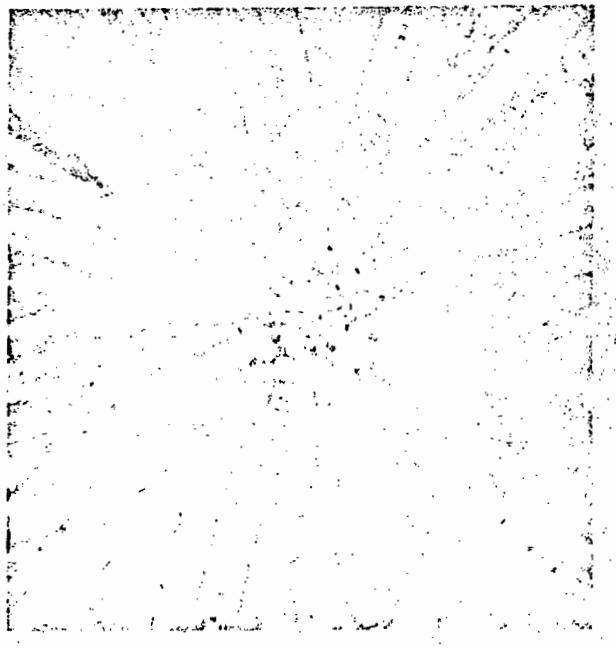

Typical Multi-Throw Switch with Beam Lead PIN Diodes

SPECIFICATIONS

Model Number	Min[1] V_B	Max Series[2] Resistance Rs (ohms)	Max Junction[3] Capacitance C_j (pf)	RF[4] Switching Time T_S (ns)	Minority[4] Carrier Lifetime Typ. (ns)
DSG6470A	200	5.5	.03	25	100
DSG6470B	200	4.0	.04	25	100
DSG6470C	200	3.0	.06	25	100
DSG6470D	200	5.5	.06	25	100
DSG6470E	200	4.0	.02	25	100
DSG6474A	100	5.5	.03	25	100
DSG6474B	100	4.0	.04	25	100
DSG6474C	100	3.0	.06	25	100
DSG6474D	100	5.5	.06	25	100
DSG6474E	100	4.0	.02	25	100

Notes:

1. Breakdown voltage measured at 10 μA.
2. Series resistance calculated from insertion loss at 3 GHz, 50 mA.
3. Total capacitance calculated from isolation at 9 GHz, zero bias. Series resistance and capacitance are measured at microwave frequencies on a sample basis from each lot. All diodes are characterized for capacitance at -50 volts, 1 MHz, and series resistance at 1 KHz, 50 mA, measurements which correlate well with microwave measurements.
4. Ts measured from RF transmission, 90% to 10%, in series configuration. Refer to section on RF Switching.

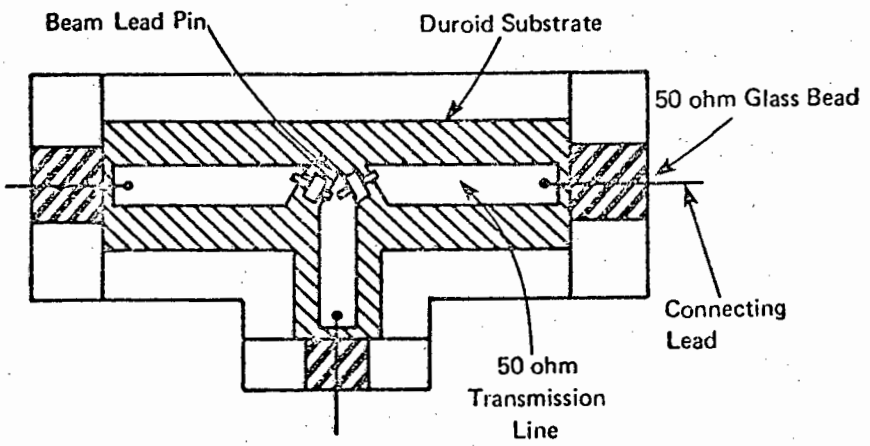

Figure 1a. Typical SPDT Circuit Arrangement

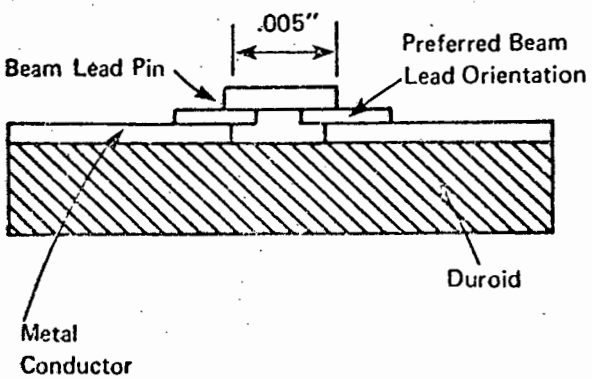

Figure 1b. Typical Beam Lead Mounting

PLICATIONS

ypical application of beam lead PIN diodes is shown Figure 1, a single pole double throw 1–18 GHz switch. e diodes are mounted on alumina, Duroid, or Teflon-erglass 50 ohm microstrip circuits. Typical bonding thods include thermal-compression bonding, parallel welding and soldering.

DT isolation curves are shown in Figure 2 and inser-n loss in Figures 3 and 4. With proper transitions d bias circuits, VSWR is better than 2.0 to 1 through GHz.

ITCHING CONSIDERATIONS

e typical minority carrier lifetime of the DSG6470 d DSG6474 diodes is 100 nanosec. With suitable vers the individual diodes can be switched from high pedance (off) to low Rs (on) in about 10 nano-conds. Switching in the opposite direction is slower, e to the need to extract stored charge (carriers) ich ve diffused away from the junction. Typically, high reverse bias voltage, say -20 volts, this requires out 20-50 nanoseconds. With a reverse bias of -1V, ich is the maximum available in simple SPDT without dividual biasing circuits, the switching time is on the der of 100 nanosec.

POWER HANDLING

Due to a high internal thermal impedance of about 300 degrees C/watt beamlead diodes are not suitable for high power operation.

With maximum CW power dissipation of 250 mW the DSG6470 and DSG6474 diodes are normally rated at 2 Watt CW with linear derating between 25°C and 150°C. Figure 5 presents data on CW power handling as a function of bias and frequency.

For pulsed operation the total RF plus bias voltage must not exceed the rated breakdown. Alpha has made high power tests at 1 GHz with 1 microsec pulses, .001 duty, with 200 volt diodes. With 50 mA forward bias there is no increase in insertion loss over the 0 dBm level with a peak power input of 50 watts. In the "open" state reverse bias voltage is required to keep the diode from "rectifying", with resultant decrease in isolation and possible failure. Figure 6 shows allowed peak power versus reverse bias at 1 GHz.

At this frequency the required reverse voltage is almost equal to the peak RF voltage; at high frequency the bias can be reduced somewhat. Experimentation is necessary.

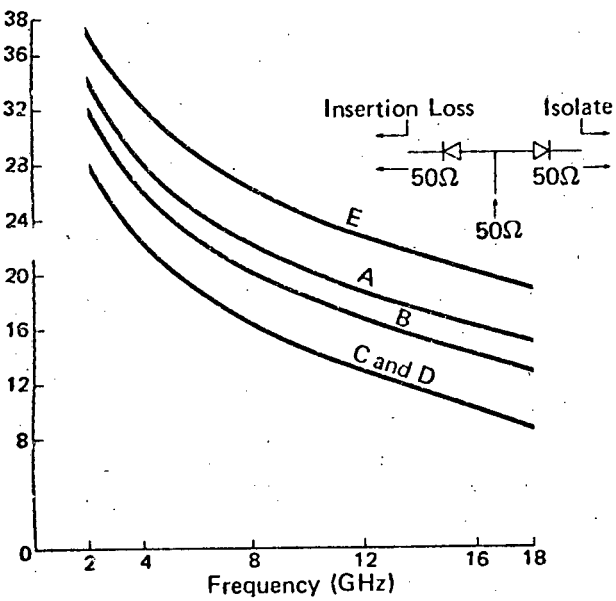

Figure 2. Isolation vs Frequency, SPDT
DSG6470, DSG6474 Series

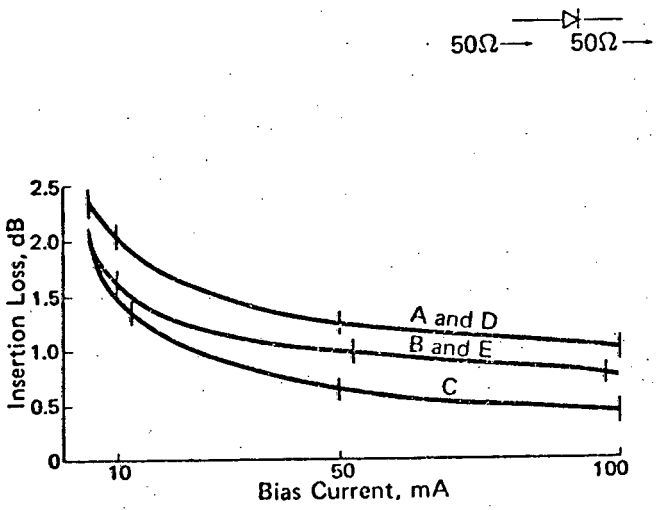

Figure 3. Diode Insertion Loss vs Bias
SPST, 18 GHz
DSG6470, DSG6474 Series

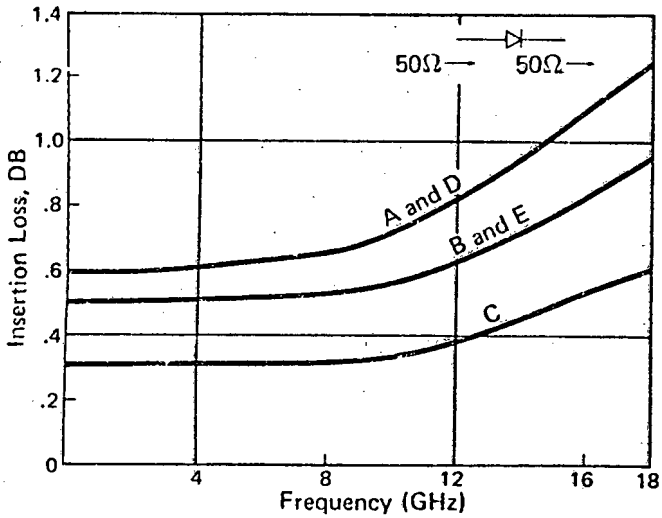

Figure 4. Diode Insertion Loss vs Frequency SPST, 50mA Bias DSG6470, DSG6474 Series

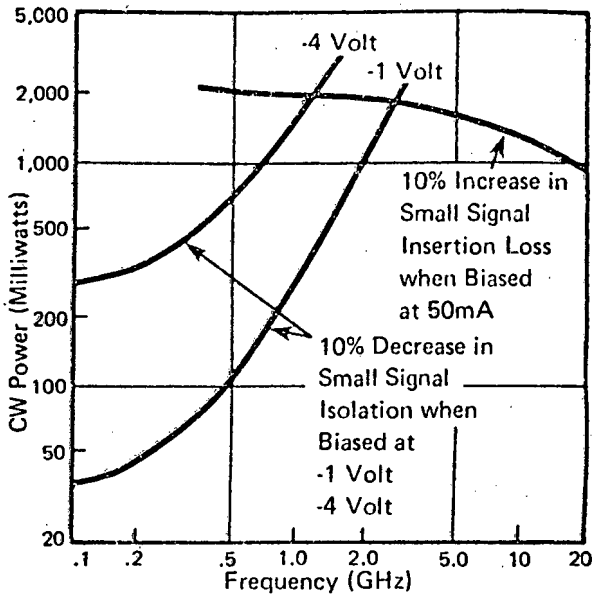

Figure 5. Typical Series Switch Behavior at Room Temperature and Biased at 50 mA/1 volt/4 volt DSG 6470, DSG 6474 Series.

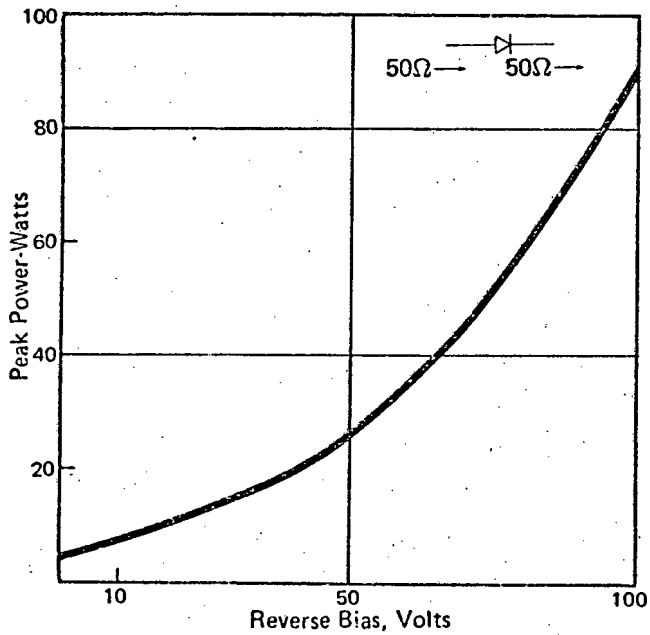

Figure 6. Peak power Handling, SPST, 1 GHz DSG6470, DSG6474 Series

A P P E N D I X C

Single Pole Double Throw Switch Microstrip Layouts and Microwave Capacitors

SPDT Switch Test Board 1

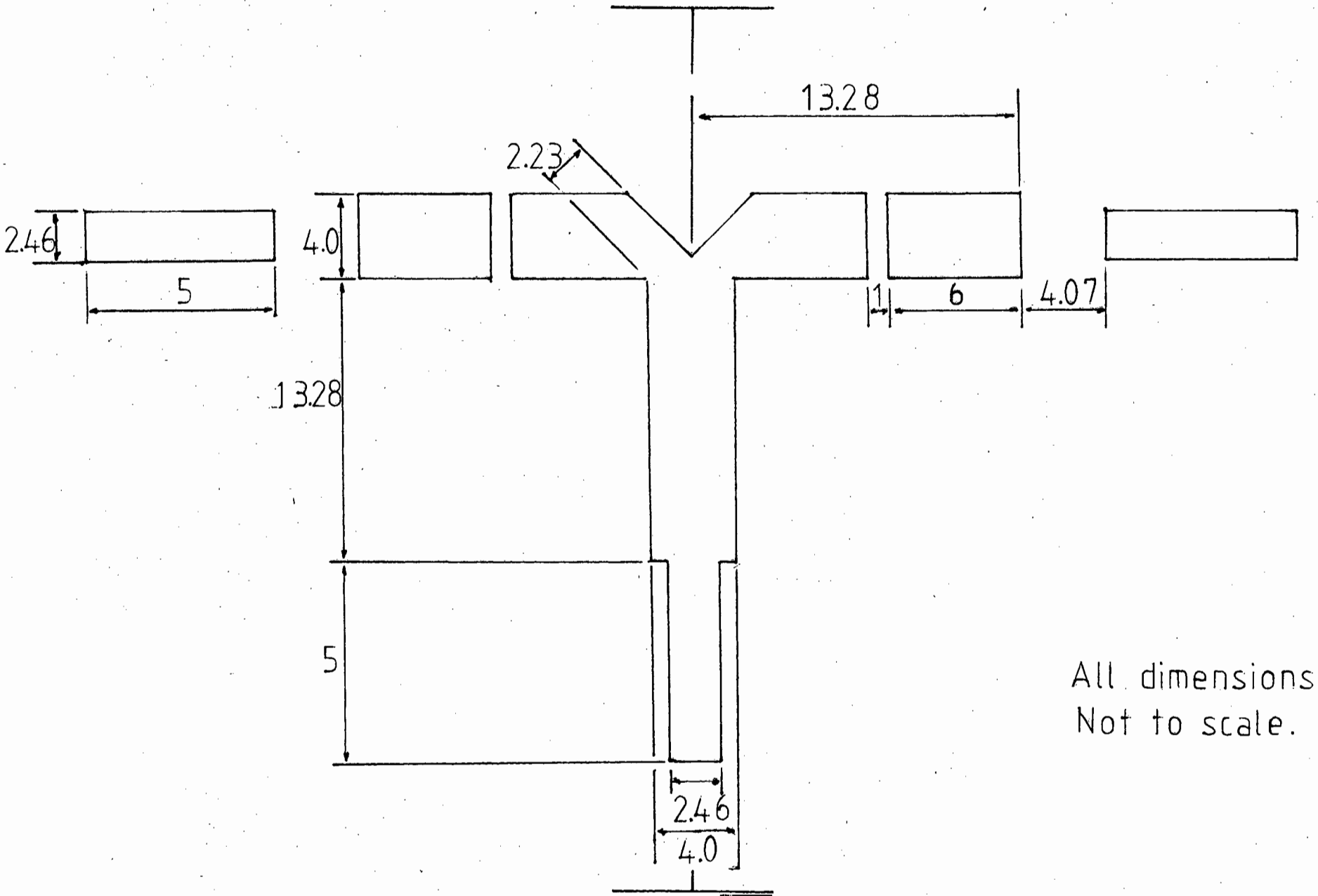

All dimensions in mm.
Not to scale.

SPDT Switch Test Board 2

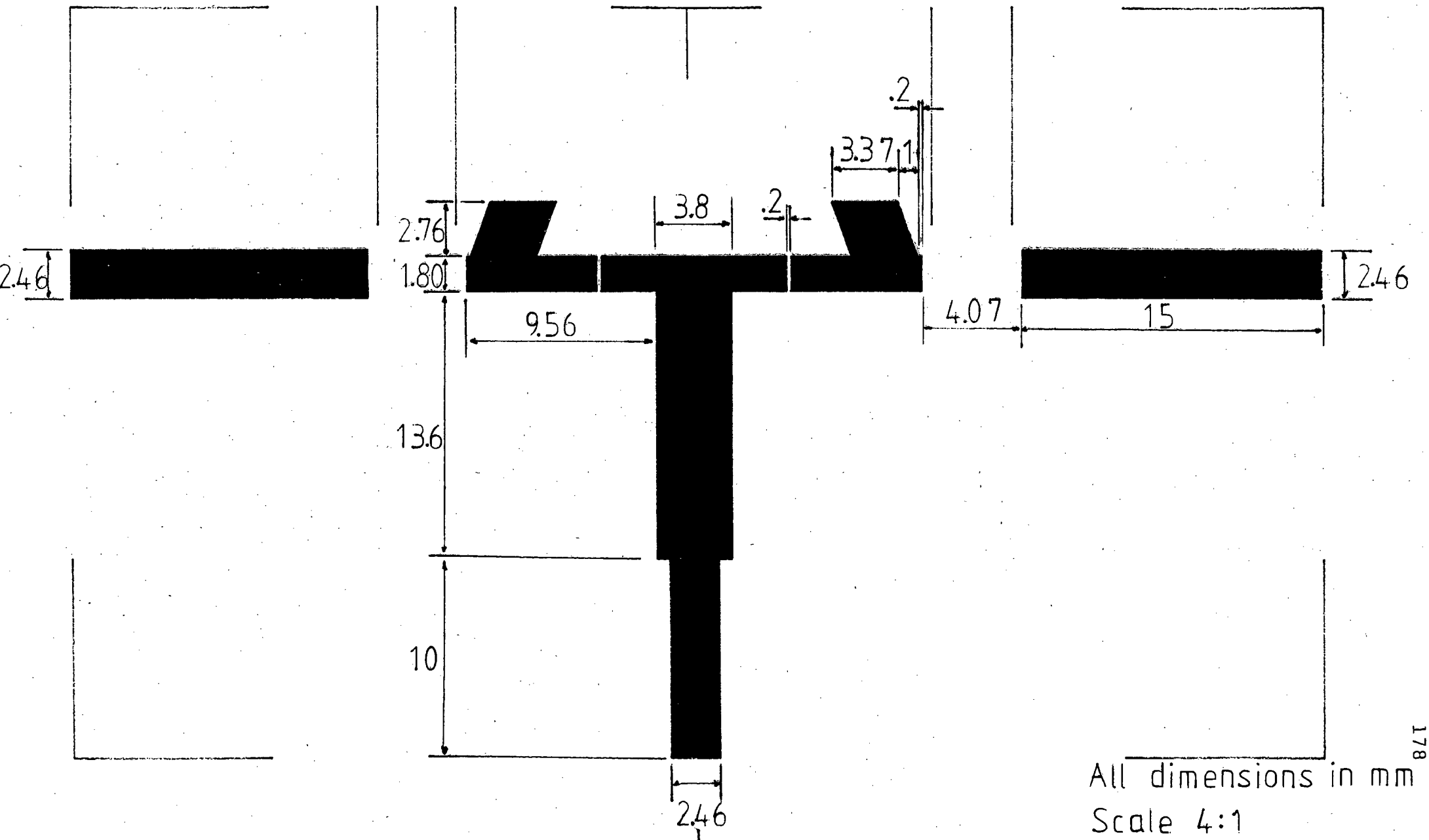

All dimensions in mm

Scale 4:1

SPDT Switch Test Board 3

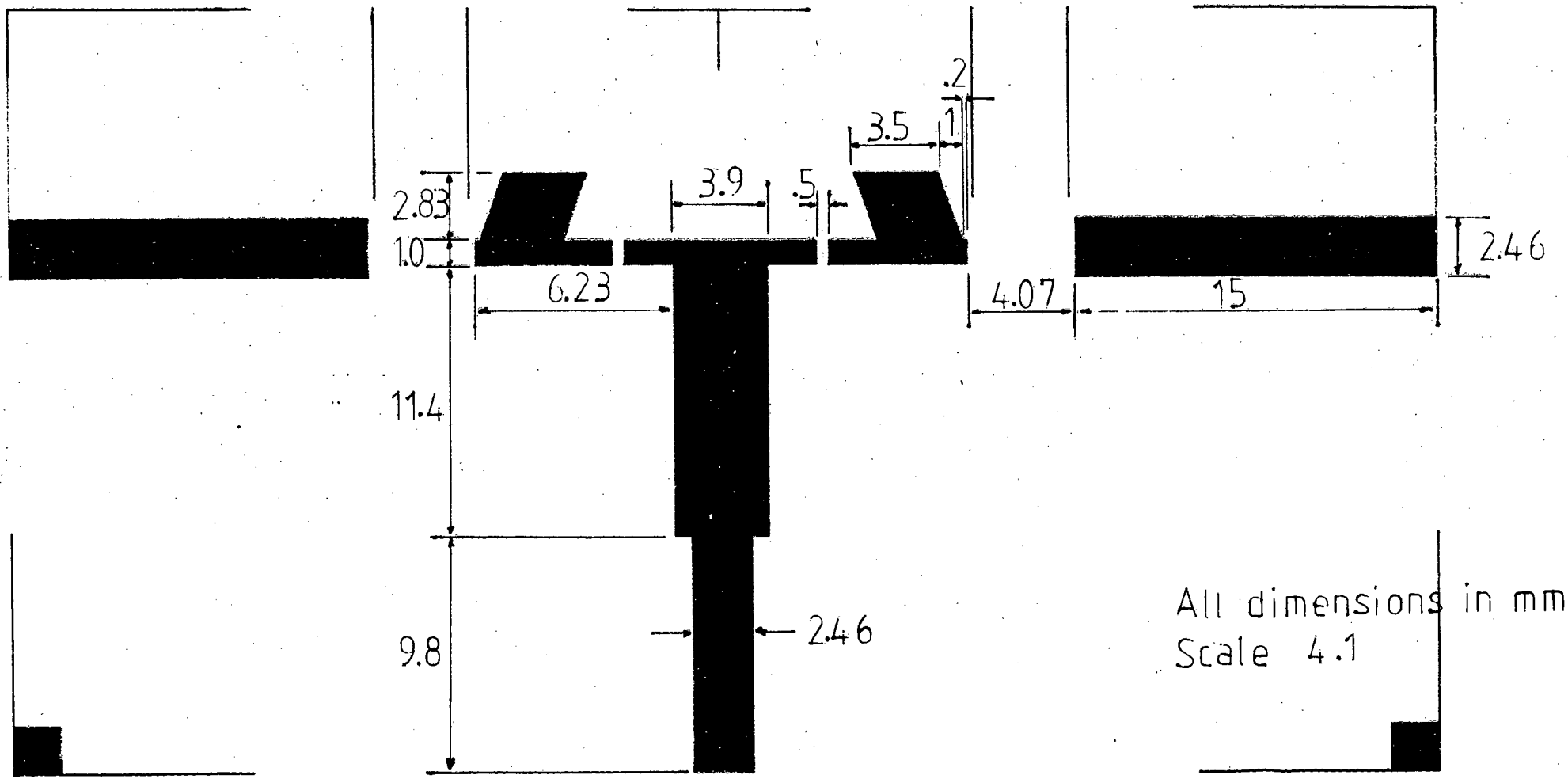

All dimensions in mm
Scale 4.1

gap - cap

microwave/millimeterwave
ceramic capacitors

CAZENOVIA, NY 13035

dielectric laboratories inc.

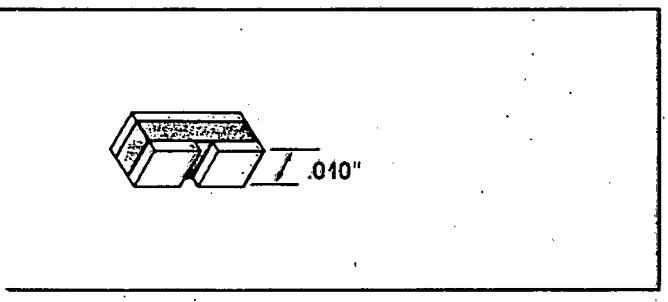

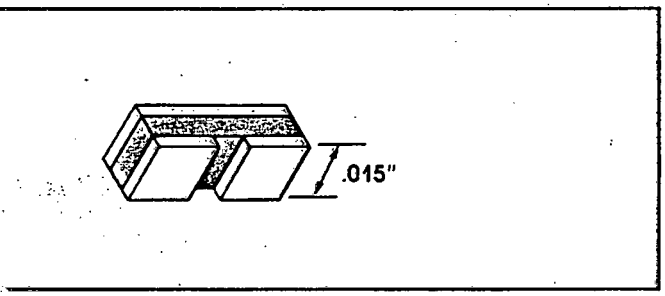

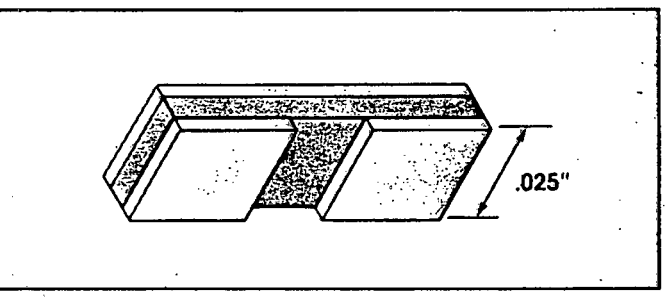

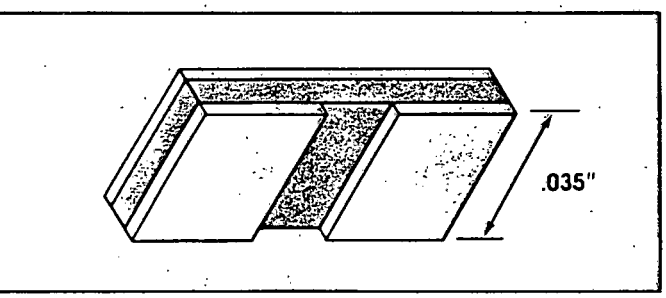

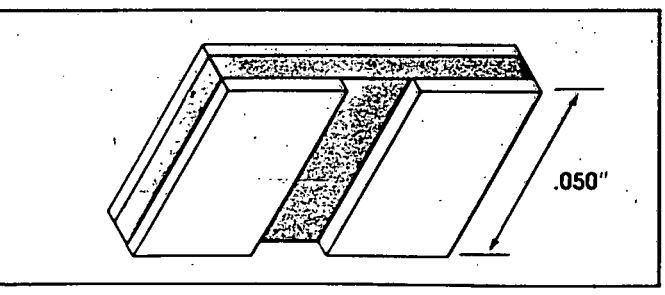

The Ultimate in Capacitor Design!

- Lowest insertion loss
- Lowest self inductance
- Lowest series resistance
- Easy to mount
- Matches stripline width

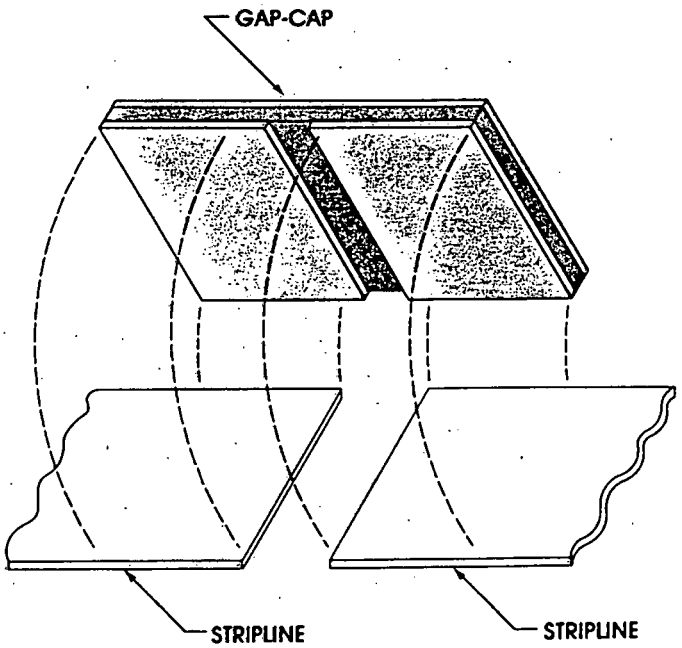

gap - cap

microwave/millimeterwave ceramic capacitors

dielectric laboratories inc.

G10 G15 G20 G25 G30 G35 G50

*Chips shown larger than actual size.

Environmental Parameters

Parameters	-MIL-STD-202- Method	Condition
Thermal Shock	107	A
Immersion	104	B
Moisture Resistance	106	—
Solderability	208	—
Resistance to Solder Heat	210	C
Burn In	108	A
Barometric Pressure	105	B
Shock	213	I
Vibration	204	G

Mechanical Parameters

Bond Strength	Exceeds MIL-STD-883, Method 2011
Shear Strength	Exceeds MIL-STD-883, Method 2019
Breaking Strength	10 times greater than MOS capacitors
Metalization	Gold, 100 μ in. standard thickness
Hermeticity	Impervious to moisture and solvents

High Reliability Testing

Dielectric Laboratories performs the following tests:

(A) **According to MIL-C-55681:**

Group A—100 hours burn-in plus 100% screening

Group B—Group A testing plus temperature coefficient and solderability

Group C—Group A and B testing plus 2000 hours life

(B) Special tests to provide the highest quality assurance.

Note: gap-caps are space approved.

Temperature Coefficient Designators Performance Characteristics

Dielec. Matrl.	T.C. Desig.	T.C. (−55 to +125°C) PPM/°C	Max. D.F. 1 MGHz (%)	I.R. 25°C	DWV
Class I	CF	0±15	.6	$>10^6$	
	CG	0±30	.7	$>10^6$	
	NR	N1500±500	.25	$>10^6$	2.5x
	NS	N2400±500	.5	$>10^6$	Rated
	NU	N3700±1000	1.5	$>10^5$	Volt-
	NV	N4700±1000	1.2	$>10^6$	age
Class II	BG	±10%	2.0	$>10^4$	
	BH	±15%	2.5	$>10^5$	
	BU	+22%, −70%	2.5	$>10^6$	

Note: Class I materials do not age

Dimensions

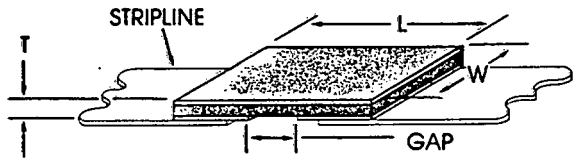

Capacitor width is designed to match stripline width.

Dimensions and Capacitance Ranges

Style	W	L Max 25V	L Max 50V	Gap Width Max.	T 25V	T 50V	Maximum Capacitance 25V	Maximum Capacitance 50V
		(Inches)						
G10	.010±.003	.030	.030	.005	.004±.001	.006±.001	17pF	12pF
G15	.015±.003	.040	.040	.008	.004±.001	.006±.001	30pF	22pF
G20	.020±.003	.050	.050	.010	.004±.001	.006±.001	51pF	33pF
G25	.025±.003	.060	.080	.020	.004±.001	.006±.001	62pF	62pF
G30	.030±.003	.060	.080	.020	.004±.001	.006±.001	82pF	82pF
G35	.035±.005	.060	.080	.020	.004±.001	.006±.001	100pF	100pF
G50	.050±.010	—	.080	.020	—	.006±.001	—	150pF
		(Millimeters)						
G10	.254±.076	.762	.762	.127	.102±.025	.152±.025	17pF	12pF
G15	.381±.076	1.016	1.016	.203	.102±.025	.152±.025	30pF	22pF
G20	.508±.076	1.270	1.270	.254	.102±.025	.152±.025	51pF	33pF
G25	.635±.076	1.524	2.032	.508	.102±.025	.152±.025	62pF	62pF
G30	.762±.076	1.524	2.032	.508	.102±.025	.152±.025	82pF	82pF
G35	.889±.127	1.524	2.032	.508	.102±.025	.152±.025	100pF	100pF
G50	1.270±.254	—	2.032	.508	—	.152±.025		150pF

Larger styles available.

Packaging

Waffle Pack—Max. 400 capacitors/pack

Part Number Structure

G 15 BH 100 M 2 P X 08

- Style
- Case Size
- T.C. Designator
- Capacitance Code
- Capacitance Tolerance
- WVDC
- Gold Termination
- High Reliability Testing
- Gap Width Designator

gap - cap

microwave/millimeterwave
ceramic capacitors

dielectric laboratories inc.

PARALLEL PLATE

Precision Shaped Ceramic Capacitors
Recommended For Applications up to 40 GHz

PART NUMBERS AND ORDERING INFORMATION

		50 VOLTS						
Dielectric	Series Cap. Value	G10	G15	G20	G25	G30	G35	G50
Class I	.05pF	G10CFR05_5P** ***	G15CFR05_5P** ***	G20CFR05_5P** ***	G25CFR05_5P** ***	G30CFR05_5P** ***		
	.06pF		G15CFR06_5P_ _ _	G20CFR06_5P_ _ _	G25CFR06_5P_ _ _	G30CFR06_5P_ _ _	G35CFR06_5P** ***	G50CFR06_5P** ***
	.08pF	G10CGR08_5P_ _ _	G15CFR08_5P_ _ _	G20CFR08_5P_ _ _	G25CFR08_5P_ _ _	G30CFR08_5P_ _ _	G35CFR08_5P_ _ _	G50CFR08_5P_ _ _
	.1pF	G10CG0R1_5P_ _ _		G20CF0R1_5P_ _ _	G25CF0R1_5P_ _ _	G30CF0R1_5P_ _ _	G35CF0R1_5P_ _ _	G50CF0R1_5P_ _ _
	.2pF	G10NR0R2_5P_ _ _	G15CG0R2_5P_ _ _	G20CG0R2_5P_ _ _	G25CF0R2_5P_ _ _	G30CF0R2_5P_ _ _	G35CF0R2_5P_ _ _	G50CF0R2_5P_ _ _
	.3pF	G10NR0R3_5P_ _ _		G20CG0R3_5P_ _ _	G25CG0R3_5P_ _ _	G30CF0R3_5P_ _ _	G35CF0R3_5P_ _ _	G50CF0R3_5P_ _ _
	.4pF	G10NS0R4_5P_ _ _	G15NR0R4_5P_ _ _	G20CG0R4_5P_ _ _	G25CG0R4_5P_ _ _	G30CG0R4_5P_ _ _	G35CF0R4_5P_ _ _	G50CF0R4_5P_ _ _
	.5pF	G10NS0R5_5P_ _ _	G15NR0R5_5P_ _ _	G20NR0R5_5P_ _ _	G25CG0R5_5P_ _ _	G30CG0R5_5P_ _ _	G35CG0R5_5P_ _ _	G50CF0R5_5P_ _ _
	.6pF	G10NS0R6_5P_ _ _	G15NR0R6_5P_ _ _	G20NR0R6_5P_ _ _	G25CG0R6_5P_ _ _	G30CG0R6_5P_ _ _	G35CG0R6_5P_ _ _	G50CF0R6_5P_ _ _
	.8pF	G10NU0R8_5P_ _ _	G15NS0R8_5P_ _ _	G20NR0R8_5P_ _ _	G25CG0R8_5P_ _ _	G30CG0R8_5P_ _ _	G35CG0R8_5P_ _ _	G50CG0R8_5P_ _ _
	1.0pF	G10NU1R0_5P_ _ _	G15NS1R0_5P_ _ _	G20NR1R0_5P_ _ _	G25NR1R0_5P_ _ _	G30CG1R0_5P_ _ _	G35CG1R0_5P_ _ _	G50CG1R0_5P_ _ _
	1.2pF	G10NU1R2_5P_ _ _	G15NS1R2_5P_ _ _	G20NS1R2_5P_ _ _	G25NR1R2_5P_ _ _	G30NR1R2_5P_ _ _	G35CG1R2_5P_ _ _	G50CG1R2_5P_ _ _
	1.5pF	G10NU1R5_5P_ _ _	G15NU1R5_5P_ _ _	G20NS1R5_5P_ _ _	G25NR1R5_5P_ _ _	G30NR1R5_5P_ _ _	G35NR1R5_5P_ _ _	G50CG1R5_5P_ _ _
	1.8pF	G10NV1R8_5P_ _ _	G15NU1R8_5P_ _ _	G20NS1R8_5P_ _ _	G25NR1R8_5P_ _ _	G30NR1R8_5P_ _ _	G35NR1R8_5P_ _ _	G50CG1R8_5P_ _ _
	2.2pF	G10NV2R2_5P_ _ _	G15NU2R2_5P_ _ _	G20NS2R2_5P_ _ _	G25NS2R2_5P_ _ _	G30NR2R2_5P_ _ _	G35NR2R2_5P_ _ _	G50CG2R2_5P_ _ _
	2.7pF		G15NU2R7_5P_ _ _	G20NU2R7_5P_ _ _	G25NS2R7_5P_ _ _	G30NS2R7_5P_ _ _	G35NR2R7_5P_ _ _	G50NR2R7_5P_ _ _
	3.3pF		G15NV3R3_5P_ _ _	G20NU3R3_5P_ _ _	G25NS3R3_5P_ _ _	G30NS3R3_5P_ _ _	G35NS3R3_5P_ _ _	G50NR3R3_5P_ _ _
	3.9pF		G15NV3R9_5P_ _ _	G20NU3R9_5P_ _ _	G25NS3R9_5P_ _ _	G30NS3R9_5P_ _ _	G35NS3R9_5P_ _ _	G50NR3R9_5P_ _ _
	4.7pF			G20NU4R7_5P_ _ _	G25NU4R7_5P_ _ _	G30NS4R7_5P_ _ _	G35NS4R7_5P_ _ _	G50NR4R7_5P_ _ _
	5.6pF			G20NU5R6_5P_ _ _	G25NU5R6_5P_ _ _	G30NU5R6_5P_ _ _	G35NS5R6_5P_ _ _	G50NS5R6_5P_ _ _
	6.8pF			G20NV6R8_5P_ _ _	G25NU6R8_5P_ _ _	G30NU6R8_5P_ _ _	G35NU6R8_5P_ _ _	G50NS6R8_5P_ _ _
	8.2pF				G25NU8R2_5P_ _ _	G30NU8R2_5P_ _ _	G35NU8R2_5P_ _ _	G50NS8R2_5P_ _ _
	10pF				G25NU100_5P_ _ _	G30NU100_5P_ _ _	G35NU100_5P_ _ _	G50NS100_5P_ _ _
	12pF				G25NV120_5P_ _ _	G30NV120_5P_ _ _	G35NU120_5P_ _ _	G50NU120_5P_ _ _
	15pF				G25NV150_5P_ _ _	G30NV150_5P_ _ _	G35NU150_5P_ _ _	G50NU150_5P_ _ _
	18pF					G30NV180_5P_ _ _	G35NV180_5P_ _ _	G50NU180_5P_ _ _
	20pF						G35NV200_5P_ _ _	G50NU200_5P_ _ _
	22pF						G35NV220_5P_ _ _	G50NU220_5P_ _ _
	27pF							G50NV270_5P_ _ _
	33pF							G50NV330_5P_ _ _
Class II	1.0pF	G10BG1R0_5P_ _ _						
	1.2 pF	G10BG1R2_5P_ _ _						
	1.5pF	G10BG1R5_5P_ _ _						
	1.8pF	G10BG1R8_5P_ _ _						
	2.2pF	G10BG2R2_5P_ _ _	G15BG2R2_5P_ _ _					
	2.7pF	G10BG2R7_5P_ _ _	G15BG2R7_5P_ _ _					
	3.3pF	G10BH3R3_5P_ _ _	G15BG3R3_5P_ _ _	G20BG3R3_5P_ _ _				
	3.9pF	G10BH3R9_5P_ _ _	G15BG3R9_5P_ _ _	G20BG3R9_5P_ _ _				
	4.7pF	G10BH4R7_5P_ _ _	G15BG4R7_5P_ _ _	G20BG4R7_5P_ _ _	G25BG4R7_5P_ _ _			
	5.6pF	G10BH5R6_5P_ _ _	G15BH5R6_5P_ _ _	G20BG5R6_5P_ _ _	G25BG5R6_5P_ _ _	G30BG5R6_5P_ _ _		
	6.8pF	G10BU6R8_5P_ _ _	G15BH6R8_5P_ _ _	G20BG6R8_5P_ _ _	G25BG6R8_5P_ _ _	G30BG6R8_5P_ _ _		
	8.2pF	G10BU8R2_5P_ _ _	G15BH8R2_5P_ _ _	G20BG8R2_5P_ _ _	G25BG8R2_5P_ _ _	G30BG8R2_5P_ _ _	G35BG8R2_5P_ _ _	
	10pF	G10BU100_5P_ _ _	G15BH100_5P_ _ _	G20BH100_5P_ _ _	G25BG100_5P_ _ _	G30BG100_5P_ _ _	G35BG100_5P_ _ _	G50BG100_5P_ _ _
	12pF	G10BU120_5P_ _ _	G15BU120_5P_ _ _	G20BH120_5P_ _ _	G25BG120_5P_ _ _	G30BG120_5P_ _ _	G35BG120_5P_ _ _	G50BG120_5P_ _ _
	15pF		G15BU150_5P_ _ _	G20BH150_5P_ _ _	G25BG150_5P_ _ _	G30BG150_5P_ _ _	G35BG150_5P_ _ _	G50BG150_5P_ _ _
	18pF		G15BU180_5P_ _ _	G20BH180_5P_ _ _	G25BH180_5P_ _ _	G30BG180_5P_ _ _	G35BG180_5P_ _ _	G50BG180_5P_ _ _
	20pF		G15BU200_5P_ _ _	G20BU200_5P_ _ _	G25BH200_5P_ _ _	G30BH200_5P_ _ _	G35BG200_5P_ _ _	G50BG200_5P_ _ _
	22pF		G15BU220_5P_ _ _	G20BU220_5P_ _ _	G25BH220_5P_ _ _	G30BH220_5P_ _ _	G35BG220_5P_ _ _	G50BG220_5P_ _ _
	27pF			G20BU270_5P_ _ _	G25BH270_5P_ _ _	G30BH270_5P_ _ _	G35BH270_5P_ _ _	G50BG270_5P_ _ _
	33pF			G20BU330_5P_ _ _	G25BH330_5P_ _ _	G30BH330_5P_ _ _	G35BH330_5P_ _ _	G50BG330_5P_ _ _
	39pF				G25BU390_5P_ _ _	G30BH390_5P_ _ _	G35BH390_5P_ _ _	G50BG390_5P_ _ _
	47pF				G25BU470_5P_ _ _	G30BU470_5P_ _ _	G35BH470_5P_ _ _	G50BH470_5P_ _ _
	51pF				G25BU510_5P_ _ _	G30BU510_5P_ _ _	G35BH510_5P_ _ _	G50BH510_5P_ _ _
	56pF				G25BU560_5P_ _ _	G30BU560_5P_ _ _	G35BU560_5P_ _ _	G50BH560_5P_ _ _
	62pF				G25BU620_5P_ _ _	G30BU620_5P_ _ _	G35BU620_5P_ _ _	G50BH620_5P_ _ _
	82pF					G30BU820_5P_ _ _	G35BU820_5P_ _ _	G50BU820_5P_ _ _
	100pF						G35BU101_5P_ _ _	G50BU101_5P_ _ _
	120pF							G50BU121_5P_ _ _
	150pF							G50BU151_5P_ _ _

*Insert letter for tolerance (≥ ±20%):

A = ±.05 pF
B = ±.1 pF
C = ±.25 pF
D = ±.5 pF
M = ±20%
Z = +80% −20%

**Insert letter for high reliability testing:

X = not applicable, commercial part
A = Group A as per MIL-C-55681
B = Group A and B as per MIL-C-55681
C = Group A, B and C as per MIL-C-55681
D = Special, agreed upon testing

***Insert numbers for gap width:

05 = .005" gap for styles G10 thru G50
08 = .008" gap for styles G15 thru G50
10 = .010" gap for styles G20 thru G50
15 = .015" gap for styles G25 thru G50
20 = .020" gap for styles G25 thru G50

Notes: (a) A popular gap width is .010".
(b) Other gap widths are available from .002" to .060".

gap - cap

microwave/millimeterwave
ceramic capacitors

dielectric laboratories inc.

Mounting Methods

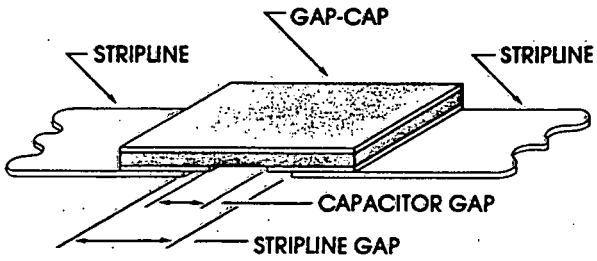

Control Gap With Gap-Cap
to Achieve Tightest Capacitance

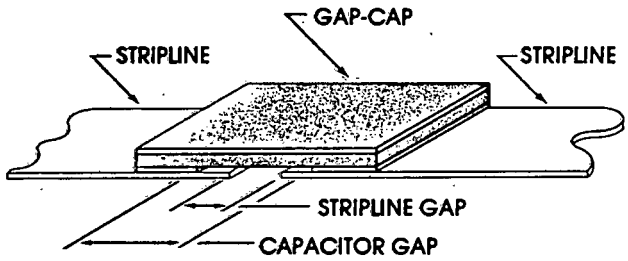

Stripline Gap Control
For Design Purposes

Die Attachment: Eutectics
Conductive Epoxy
Solder (Sn62)

SERIES RESONANCE CURVE

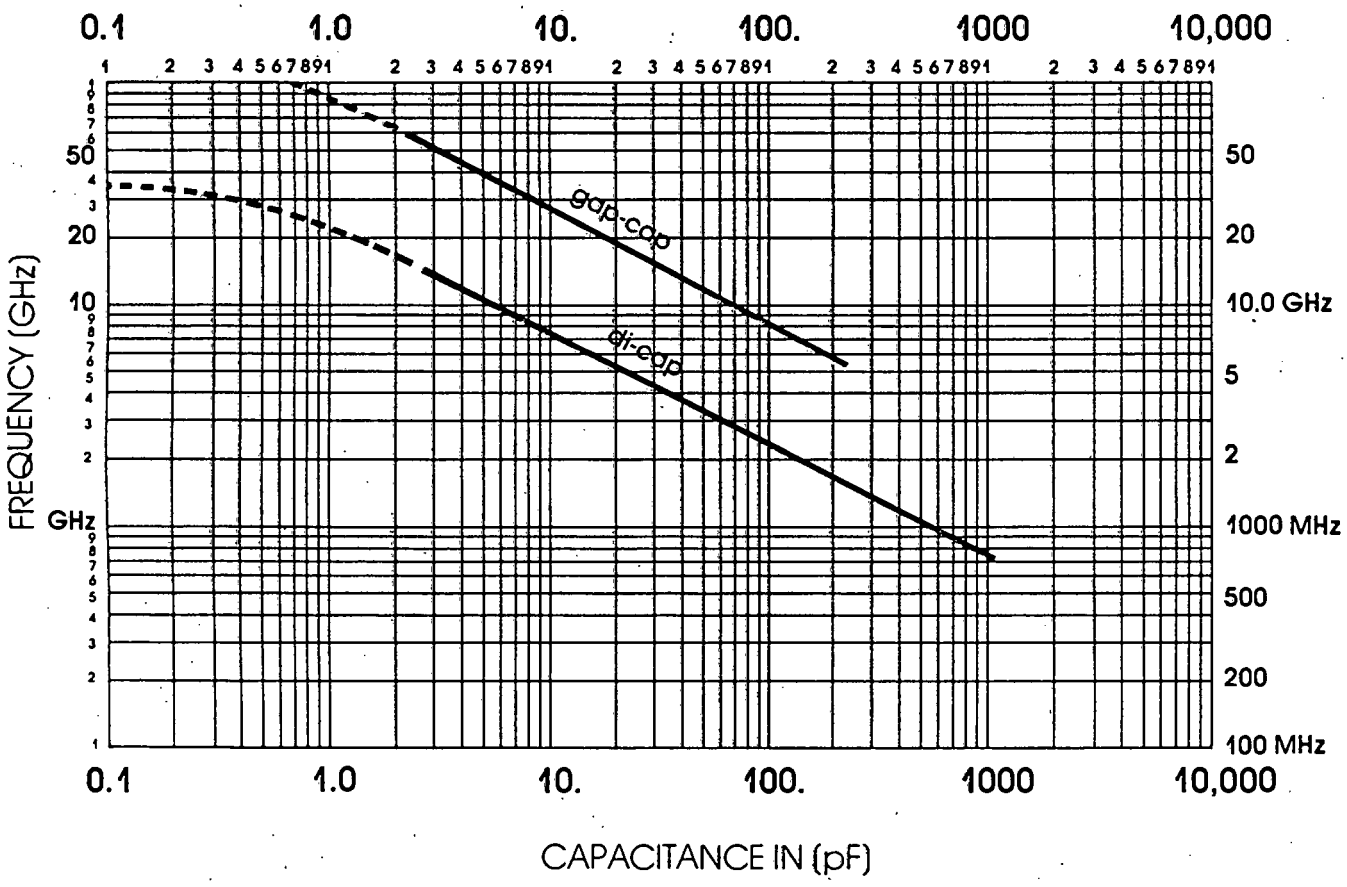

A P P E N D I X D

Specifications and Measurements of the Enclosed SP4T Switch

Specifications for the inclosed SP4T switch which uses series mounted PIN diodes.

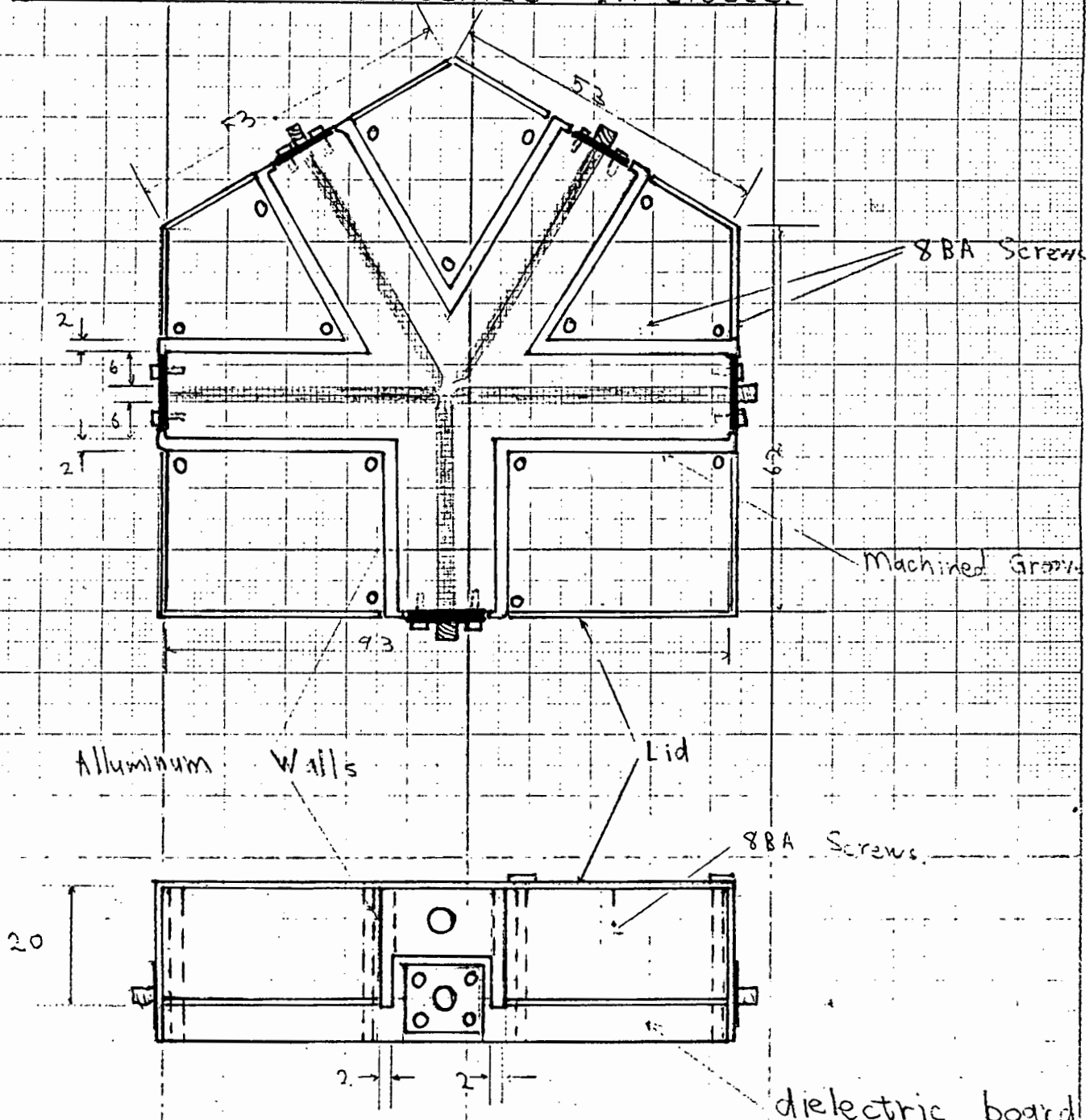

Note All grooves machined are 2mm wide and are deep enough for the aluminum walls to come into contact with the aluminum of the dielectric board.

Aluminium Walls

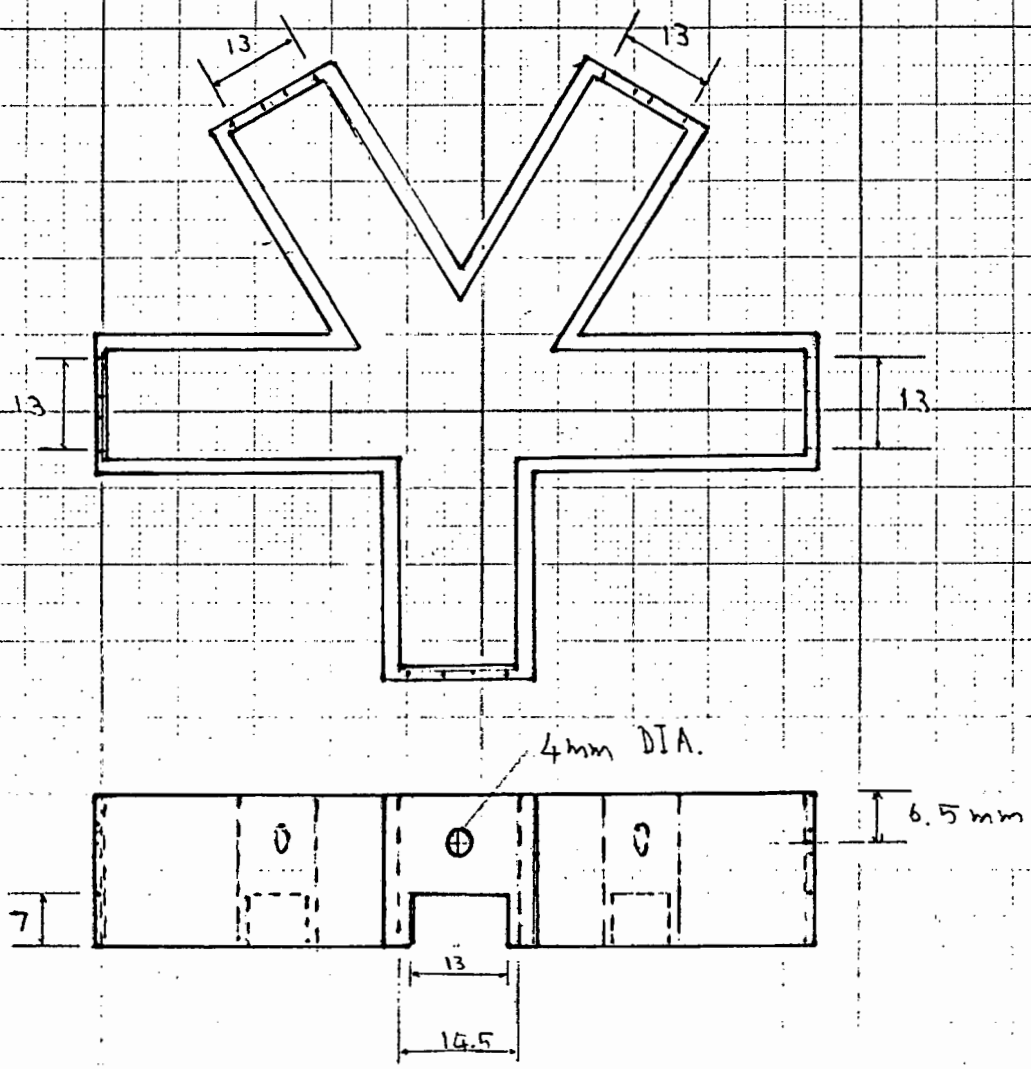

Lid

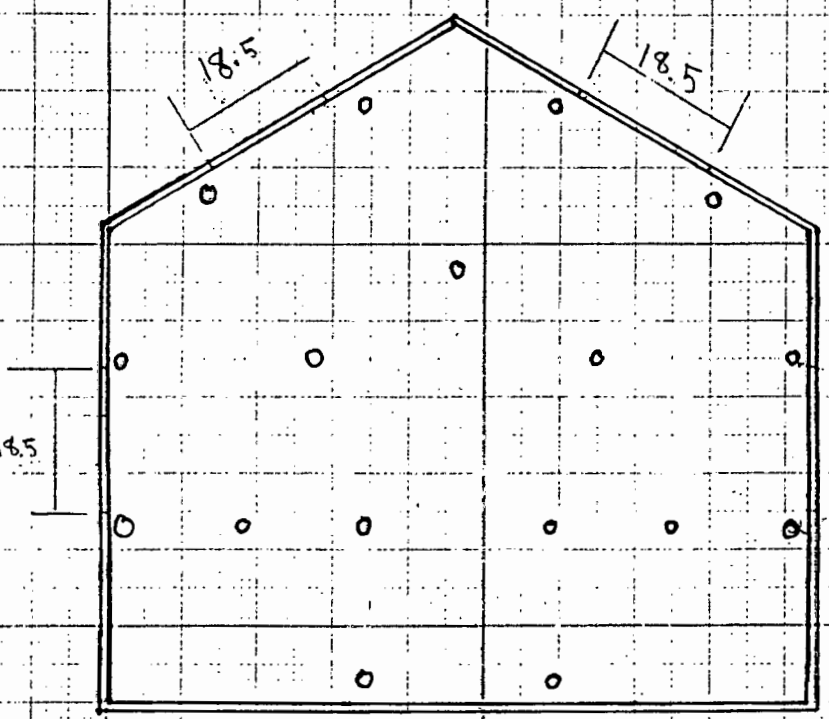

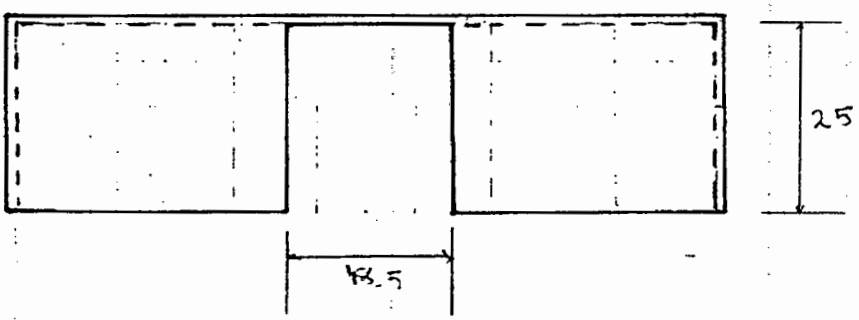

Measurements taken on the SP4T Switch.

TRANS. PORT 1

FREQUENCY GHz	RETURN LOSS dB	Deg
1.000	18.7	-159.
1.200	16.4	141.
1.400	15.6	99.
1.600	15.8	63.
1.800	16.7	27.
2.000	18.2	-7.
2.200	19.8	-39.
2.400	21.5	-68.
2.600	22.9	-91.
2.800	23.3	-109.
3.000	22.7	-123.
3.200	21.6	-141.
3.400	20.6	-160.
3.600	19.8	-180.
3.800	19.4	160.
4.000	19.6	141.
4.200	20.2	122.
4.400	21.0	104.
4.600	21.7	88.
4.800	22.5	69.
5.000	23.6	51.
5.200	21.4	20.
5.400	20.1	-30.
5.600	17.9	-81.
5.800	15.3	-127.
6.000	13.1	-166.
6.200	11.7	157.
6.400	11.2	123.
6.600	12.3	114.
6.800	8.2	101.
7.000	6.0	18.

TRANSMISSION

FREQUENCY GHz	INSERTION LOSS dB	Deg
1.000	1.5	-117.
1.200	1.6	-157.
1.400	1.7	173.
1.600	1.9	142.
1.800	1.8	109.
2.000	1.9	78.
2.200	1.9	48.
2.400	1.9	18.
2.600	1.9	-13.
2.800	2.0	-44.
3.000	2.0	-74.
3.200	2.0	-103.
3.400	2.0	-133.
3.600	2.1	-165.
3.800	2.1	166.
4.000	2.2	137.
4.200	2.1	105.
4.400	2.2	75.
4.600	2.1	46.
4.800	2.3	15.
5.000	2.3	-13.
5.200	2.4	-45.
5.400	2.1	-75.
5.600	2.4	-103.
5.800	2.3	-138.
6.000	2.5	-170.
6.200	2.6	162.
6.400	2.9	130.
6.600	3.0	95.
6.800	4.8	49.
7.000	4.7	20.

ISOLATION

FREQUENCY GHz	INSERTION LOSS dB	Deg
1.000	65.0	-45.
1.200	64.7	13.
1.400	64.5	146.
1.600	64.2	-127.
1.800	64.0	-67.
2.000	63.9	57.
2.200	63.9	158.
2.400	63.9	-159.
2.600	63.8	-44.
2.800	63.7	83.
3.000	63.5	130.
3.200	63.5	-133.
3.400	63.4	24.
3.600	63.4	54.
3.800	63.3	137.
4.000	63.2	-51.
4.200	63.1	-13.
4.400	62.9	26.
4.600	62.9	-118.
4.800	62.8	-84.
5.000	62.8	-67.
5.200	62.9	172.
5.400	62.1	-140.
5.600	60.0	-150.
5.800	57.7	136.
6.000	62.5	167.
6.200	61.8	158.
6.400	55.5	167.
6.600	35.3	64.
6.800	41.8	37.
7.000	43.1	35.

A P P E N D I X E

Specifications for the Overlay Couplers

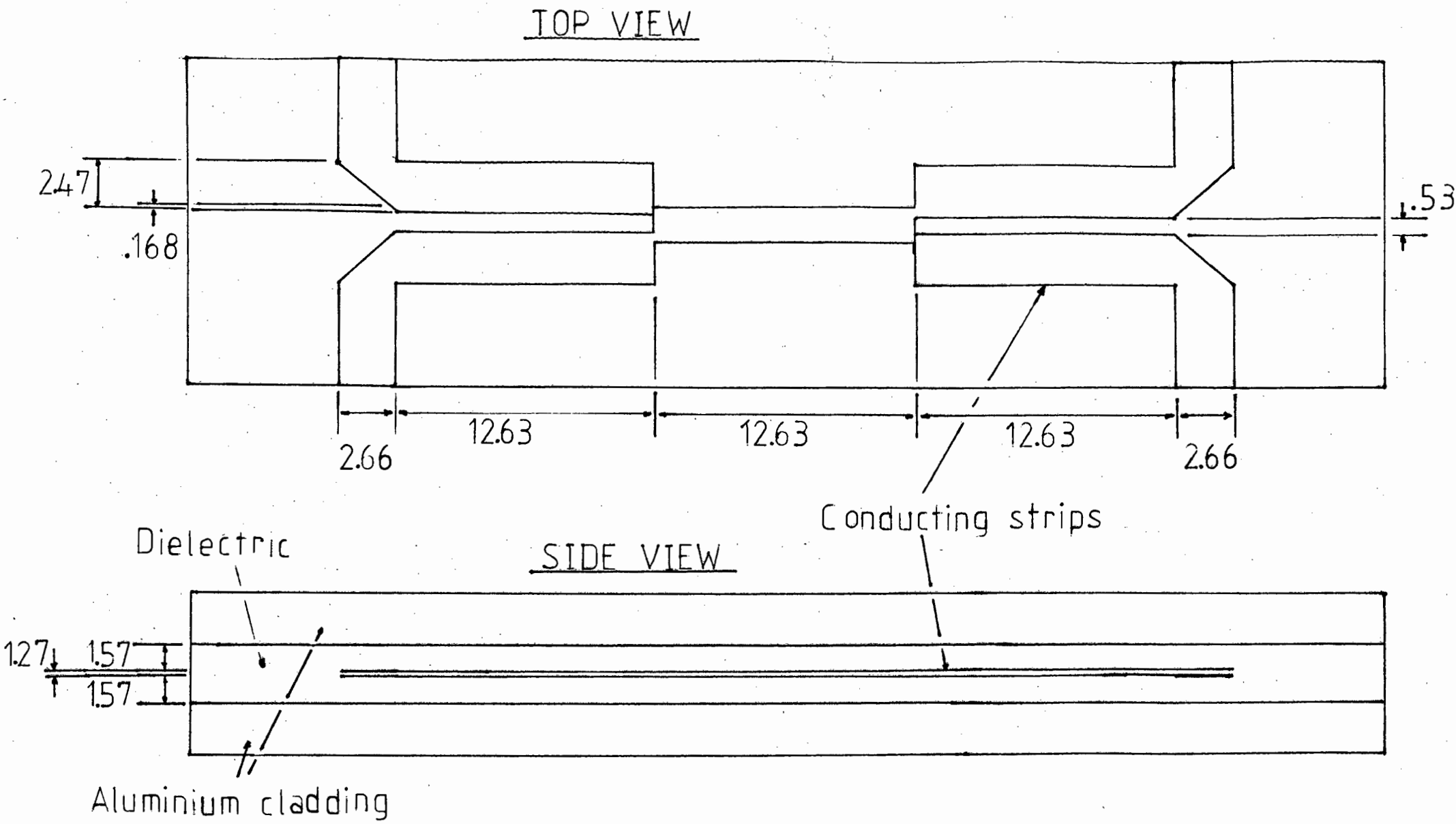

All dimensions in mm.
Not to scale.

190

Specifications for D M Rachman's Overlay coupler

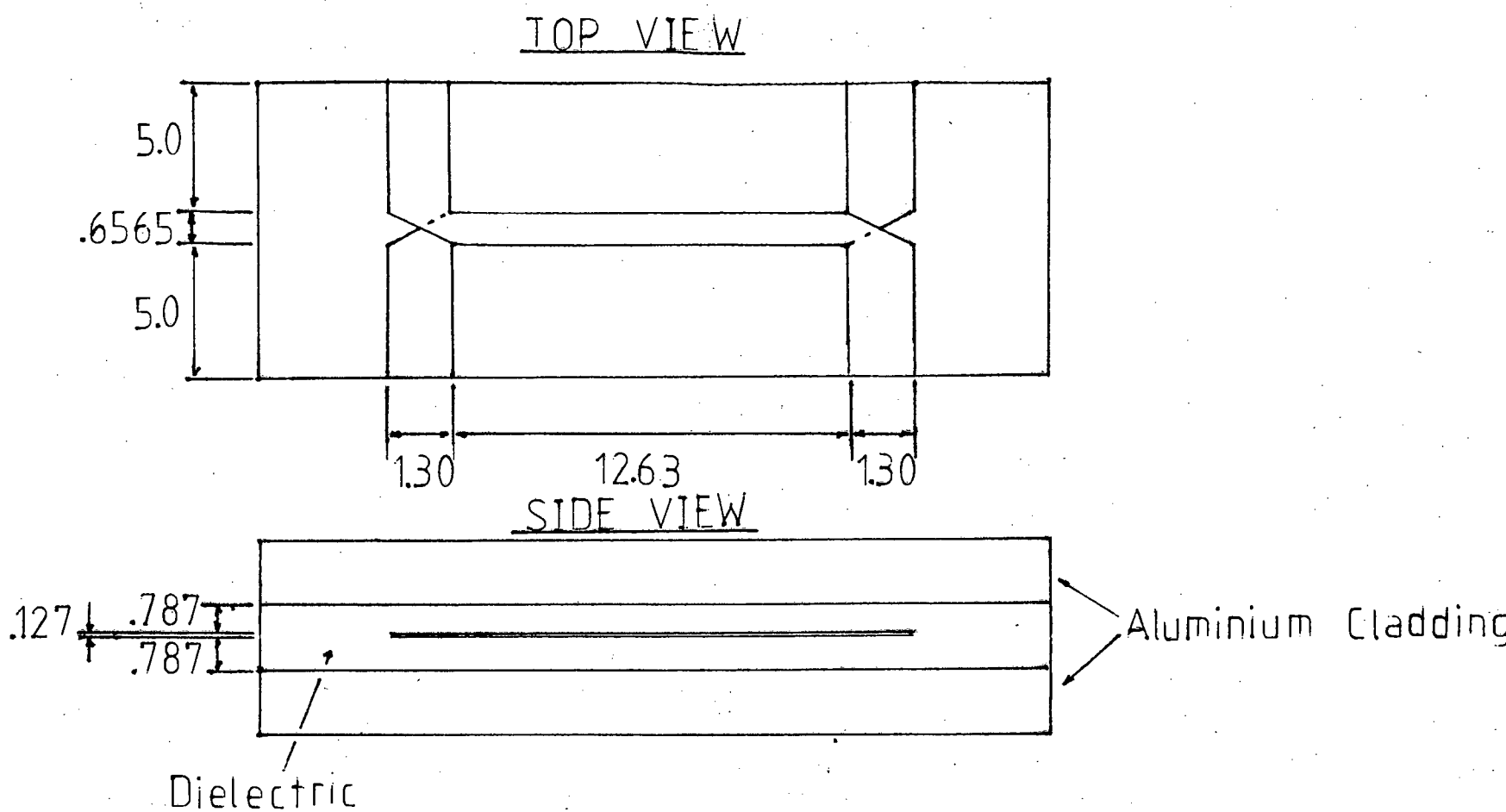

All dimensions in mm.
Not to scale.

Specifications for the single section Overlay Coupler

A P P E N D I X F

S-Parameter Measurements of the CSIR's Lange Coupler and the Termination Switch

S-parameter measurements of the Lange Coupler

1 to 3

1 to 3

FREQUENCY	RETURN LOSS-IN S11		LOSS-FORWARD S21		DELAY
MHz	DB	ANG	DB	ANG	u-SEC
2000	17.2	-31	2.4	64	0.0004
2100	16.8	-52	2.5	50	0.0004
2200	16.3	-74	2.7	36	0.0004
2300	16.2	-95	2.8	23	0.0004
2400	16.0	-116	3.0	9	0.0004
2500	15.9	-137	3.0	-4	0.0004
2600	15.9	-157	3.1	-18	0.0004
2700	16.1	-178	3.2	-31	0.0004
2800	16.2	161	3.3	-45	0.0004
2900	16.4	140	3.4	-59	0.0004
3000	16.7	120	3.4	-72	0.0004
3100	16.9	99	3.5	-86	0.0004
3200	17.2	78	3.7	-99	0.0004
3300	17.5	56	3.6	-113	0.0004
3400	17.9	35	3.6	-127	0.0004
3500	18.2	13	3.7	-141	0.0004
3600	18.5	-9	3.7	-154	0.0004
3700	18.8	-32	3.8	-168	0.0004
3800	19.1	-55	3.8	178	0.0004
3900	19.4	-78	3.8	164	0.0004
4000	19.6	-101	3.8	150	0.0004
4100	20.0	-125	3.8	137	0.0004
4200	20.4	-147	3.8	123	0.0004
4300	20.8	-170	3.9	109	0.0004
4400	21.3	168	3.8	95	0.0004
4500	21.9	146	3.8	82	0.0004
4600	22.5	125	3.8	68	0.0004
4700	23.2	105	3.7	55	0.0004
4800	23.7	88	3.7	41	0.0004
4900	24.3	72	3.7	27	0.0004
5000	24.3	58	3.7	13	0.0004
5100	23.9	43	3.6	-1	0.0004
5200	22.9	27	3.6	-15	0.0004
5300	21.9	8	3.4	-29	0.0004
5400	20.7	-13	3.5	-43	0.0004

5500	19.6	-36	3.3	-58	0.0004
5600	18.7	-59	3.3	-71	0.0004
5700	17.8	-83	3.2	-85	0.0004
5800	17.2	-107	3.1	-99	0.0004
5900	16.8	-131	3.1	-114	0.0004
6000	16.5	-154	3.0	-127	

1 TO 2

FREQUENCY	RETURN LOSS-IN S11		LOSS-FORWARD S21		DELAY
MHz	DB	ANG	DB	ANG	u-SEC
2000	17.6	-37	4.9	155	0.0004
2100	17.4	-57	4.7	141	0.0004
2200	17.3	-78	4.5	128	0.0004
2300	17.1	-97	4.4	114	0.0004
2400	17.0	-116	4.3	100	0.0004
2500	16.7	-135	4.1	87	0.0004
2600	16.5	-154	4.0	73	0.0004
2700	16.3	-174	3.9	60	0.0004
2800	16.2	166	3.9	46	0.0004
2900	16.1	145	3.7	32	0.0004
3000	16.2	124	3.6	20	0.0004
3100	16.2	102	3.5	6	0.0004
3200	16.4	80	3.6	-7	0.0004
3300	16.6	58	3.4	-21	0.0004
3400	16.9	34	3.4	-35	0.0004
3500	17.4	11	3.3	-49	0.0004
3600	17.9	-14	3.3	-62	0.0004
3700	18.5	-38	3.3	-76	0.0004
3800	19.1	-63	3.2	-89	0.0004
3900	19.8	-87	3.3	-103	0.0004
4000	20.6	-111	3.3	-117	0.0004
4100	21.3	-134	3.4	-130	0.0004
4200	22.1	-154	3.3	-144	0.0004
4300	22.8	-174	3.5	-157	0.0004
4400	23.4	168	3.5	-171	0.0004
4500	23.7	152	3.5	176	0.0004
4600	23.8	135	3.6	163	0.0003
4700	23.7	120	3.7	150	0.0004
4800	23.3	104	3.8	136	0.0004
4900	22.7	87	3.9	123	0.0004
5000	22.0	68	4.0	109	0.0004
5100	21.1	48	4.0	96	0.0004
5200	20.4	26	4.2	82	0.0004
5300	19.7	2	4.3	68	0.0004
5400	19.0	-22	4.5	54	0.0004
5500	18.6	-46	4.6	40	0.0004
5600	18.2	-71	4.7	27	0.0004
5700	17.9	-95	4.8	13	0.0004
5800	17.7	-118	5.1	-1	0.0004
5900	17.8	-140	5.3	-15	0.0004
6000	17.8	-160	5.5	-29	

1 TO 4

FREQUENCY	RETURN LOSS-IN S11		LOSS-FORWARD S21		DELAY
MHz	DB	ANG	DB	ANG	u-SEC
2000	16.9	-32	21.1	-152	0.0005
2100	16.5	-54	20.7	-171	0.0006
2200	16.0	-75	20.4	169	0.0006
2300	15.9	-97	20.1	149	0.0006
2400	15.8	-118	19.9	128	0.0005
2500	15.7	-139	19.6	109	0.0006
2600	15.7	-159	19.5	88	0.0006
2700	15.9	179	19.3	68	0.0006
2800	16.0	158	19.3	47	0.0006
2900	16.3	137	19.2	27	0.0005
3000	16.7	116	19.2	7	0.0006
3100	17.2	94	19.2	-14	0.0006
3200	17.7	73	19.3	-34	0.0006
3300	18.3	52	19.3	-54	0.0006
3400	18.9	31	19.4	-74	0.0006
3500	19.7	10	19.5	-95	0.0005
3600	20.3	-11	19.7	-114	0.0005
3700	20.9	-32	19.8	-134	0.0005
3800	21.4	-52	20.0	-153	0.0005
3900	21.8	-72	20.1	-172	0.0005
4000	22.0	-92	20.3	169	0.0005
4100	22.0	-112	20.5	151	0.0005
4200	22.0	-133	20.6	132	0.0005
4300	21.8	-153	20.8	114	0.0005
4400	21.5	-174	20.8	97	0.0005
4500	21.2	165	20.9	79	0.0005
4600	21.1	143	20.9	62	0.0005
4700	20.9	122	20.8	45	0.0005
4800	20.6	101	20.7	28	0.0005
4900	20.3	79	20.6	10	0.0005
5000	20.0	58	20.4	-8	0.0005
5100	19.7	36	20.1	-26	0.0005
5200	19.3	13	19.9	-45	0.0005
5300	19.1	-10	19.5	-64	0.0005
5400	18.7	-33	19.3	-83	0.0005
5500	18.6	-56	19.0	-102	0.0005
5600	18.4	-78	18.8	-122	0.0006
5700	18.3	-100	18.4	-143	0.0006
5800	18.2	-121	18.3	-163	0.0006
5900	18.1	-141	18.1	176	0.0006
6000	18.2	-160	18.0	155	

Measured response of the Termination Switch as shown in Figure 9.18

SHORT CIRCUIT			OPEN CIRCUIT		
FREQUENCY GHz	RETURN LOSS dB	Deg	FREQUENCY GHz	RETURN LOSS dB	Deg
1.000	1.1	96.	1.000	0.5	-51.
1.200	1.1	79.	1.200	0.4	-80.
1.400	1.1	61.	1.400	0.4	-107.
1.600	1.1	44.	1.600	0.4	-132.
1.800	1.1	26.	1.800	0.5	-154.
2.000	1.1	8.	2.000	0.6	-176.
2.200	1.1	-11.	2.200	0.7	163.
2.400	1.0	-30.	2.400	0.8	144.
2.600	0.9	-49.	2.600	0.9	124.
2.800	0.9	-68.	2.800	1.0	105.
3.000	0.9	-88.	3.000	1.1	87.
3.200	0.9	-108.	3.200	1.1	68.
3.400	0.9	-128.	3.400	1.1	50.
3.600	1.0	-148.	3.600	1.1	31.
3.800	1.2	-166.	3.800	1.1	13.
4.000	1.3	174.	4.000	1.0	-6.
4.200	1.5	155.	4.200	0.8	-24.
4.400	1.6	138.	4.400	0.7	-44.
4.600	1.7	120.	4.600	0.5	-64.
4.800	1.9	102.	4.800	0.5	-85.
5.000	1.9	84.	5.000	0.5	-105.
5.200	1.8	66.	5.200	0.7	-125.
5.400	1.9	48.	5.400	1.0	-145.
5.600	1.8	30.	5.600	1.2	-163.
5.800	1.8	11.	5.800	1.4	179.
6.000	1.5	-8.	6.000	1.4	161.
6.200	1.4	-27.	6.200	1.5	143.
6.400	1.2	-46.	6.400	1.7	124.
6.600	1.1	-67.	6.600	1.8	105.
6.800	1.1	-87.	6.800	2.0	87.
7.000	1.1	-108.	7.000	1.8	68.

REFERENCES

1. White, J.F., Diode Phase Shifters for Array Antennas, IEEE Trans. Microwave Theory Tech., Vol. MTT - 22, No. 6 June 1974, pp 658-674.

2. Topi, M., An Eight-Phase Broadband Serrodyne Modulator, IEEE MTT-S DIGEST, 1983, pp 432-434.

3. Kraus, J.D. and Carver, K.R., Electromagnetics, McGraw-Hill, Inc, 1973.

4. Edwards, T.C.,Foundations for Microstrip Circuit Design, John Wiley and Sons Ltd, 1981.

5. Gupta, K.C., Garg, R., Chadha, R., Computer Aided Design of Microwave Circuits, Artech House, Inc. 1981.

6. Wheeler, H.A., Transmission-Line Properties of a Strip Line Between Parallel Planes, IEEE Trans. on Microwave Theory and Tech., Vol. MTT 26, November 1978, pp 866-876.

7. Osmani, R.M., Synthesis of Lange Couplers, IEEE Trans. on Microwave Theory and Tech., Vol MTT 29, No.2, February 1981, pp 168-170.

8. Rizzoli, V. and Lipparini, A., The Design of Inter-digitated Couplers for MIC Applications, IEEE Trans. on Microwave Theory and Tech., Vol. MTT 26, No. 1, January 1978, pp 7-15.

9. Kemp, G., Hobdell, J., Biggin, J.W., Ultra-Wideband Quadrature Coupler, Electronics Letters, Vol. 19, No. 6, March 1983, pp 197-199.

10. Cohn, S.B., Shielded Coupled- Strip Transmission Lines, IRE Microwave Theory and Tech. Vol. MTT-3, No. 5, October 1955, pp 29-38.

11. Cohn, S.B., Characteristic Impedances of Broadside-Coupled Strip Transmission Lines, IRE Trans. on Microwave Theory and tech., Vol. MTT-8, No. 6, November 1960, pp 633-637.

12. Syrett, B.A., A Broad-band Element for Microstrip Bias or Tuning Circuits, IEEE Trans. on Microwave Theory and Tech., Vol. 28, No. 8, August 1980, pp 925-927.

13. Wolff, I., Knoppik, N., Microstrip Ring Resonators and Dispersion Measurements on Microstrip Lines, Electronics Letters, Vol. 7, No. 26, December 1971 pp 779-781.

14. Liao, S.Y., Microwave Devices and Circuits, Prentice-Hall, Inc, 1980.

15. Giannina, F., Salerno, M., Design of Low-Pass Elliptic Filters by Means of Cascaded Microstrip Rectangular Elements, IEEE Trans. on Microwave Theory and Tech. Vol. MTT - 30, No. 9, September 1982, pp 1348-1353.

16. Mehran, R., Computer-Aided Design of Microstrip Filters Considering Disperson, Loss and Discontinuity Effects, IEEE Trans. on Microwave Theory and Tech., Vol. MTT - 27, No. 3, March 1979, pp 239-245.

17. D'Inzeo, G., Giannini, F., sorrentino, R., Novel Microwave Integrated Lowpass Filters, Electronics Letters, Vol. 15, No. 9, April 1979, pp 258-260.

18. Kovacs, K.F., High Frequency Application of Semi-conductor Devices, Elsevier Scientific, 1981.

19. Microwave Associates PIN Diode Designer's Guide Catalogue No. 4013.

20. Broadbanding the Shunt PIN diode SPDT switch, Hewlett Packard Application Note 957-1.

21. Garver, R.V., Broad-band Diode Phase Shifters, IEEE Trans. on Microwave Theory and Tech. Vol. MTT - 20, No. 5, May 1972, pp 314-323.

22. Shiffman, B.M., A New Class of Broad-Band Microwave 90-Degree Phase Shifters, IRE Trans. on Microwave Theory and Tech. Vol. 6, No. 2, April 1958 pp 232-237.

23. Coats, R.P., An Octave-Band Switched-Line Microstrip 3-b Diode Phase Shifter, IEEE Trans. on Microwave Theory and Tech. Vol. MTT - 21, No. 7, July 1973, pp 444-449.

24. Lynes, G.D. et al, Design of a Broad-Band 4 Bit Loaded Switched-Line Phase Shifter, IEEE Trans. on Microwave Theory and Tech. Vol. MTT - 22, No. 6, June 1974, pp 693-697.

25. Bahl, I.J., Gupta, K.C., Design of Loaded-Line PIN diode Phase Shifter Circuits, IEEE Trans. on Microwave Theory and Tech. Vol. MTT - 28, No. 3, March 1980, pp 219-224.

26. Davis, W.A., Design Equations and Bandwidth of Loaded-Line Phase Shifters, IEEE Trans. on Microwave Theory and Tech. Vol. 22, May 1974, pp 561-563.

27. Atwater, H.A., Reflection Coefficient Transformations for Phase-Shift Circuits, IEEE Trans. on Microwave Theory and Tech. Vol. MTT - 28, No. 6, June 1980, pp 563-568.

28. Wahi, P., Gupta, K.C., Effect of Diode Parameters on Reflection-Type Phase Shifters, IEEE Trans. on Microwave Theory and Tech. Vol. MTT - 24, September 1976, pp 619-621.

29. Johan Pretorius. Private Communication.

30. Rachman, D.M., A Three Section Overlay Coupler, Private Communication.

BIBLIOGRAPHY

Aitchison, C.S. et al, Lumped-Circuit Elements at Microwave Frequencies, IEEE Trans. on Microwave Theory and Tech. Vol. MTT-19, No. 12, December 1971, pp 928-937.

Bahl, I.J., Use Exact Methods For Microstrip Design, Microwaves, Vol. 17, No. 12, December 1978 pp 61-62.

Lee, F., Achieve High Isolation in Series Applications with a Low Capacitance Beam Lead PIN, Microwave Journal, February 1983 pp 143-146.

Lev, J.J., Synthesize and analyse microstrip lines, Microwaves and RF, Vol. 24, No. 1, January 1985, pp 111-116.

March, S., Microstrip Packaging : Watch The Last Step, Microwaves, December 1981, pp 83-94.

Owens, R.P., Accurate Analytic Determination of Quasi-Static Microstrip Line Parameters, Radio and Electronic Engineer, Vol. 46, No. 7, July 1976, pp 360-364.

Wolf, I., Knoppik, N., Rectangular and Circular Microstrip Disk Capacitors and Resonators, IEEE Trans. on Microwave Theory and Tech. Vol. MTT-22, No. 10, October 1974, pp 857-864.